

Immunological studies on Swine Influenza Virus in pigs: from gene to epitopes

Massimiliano Baratelli

PhD in immunology

Centre de Recerca en Sanitat Animal (CReSA)

Doctoral thesis – 2015

Department of Cellular Biology, Physiology and Immunology

Universitat Autònoma de Barcelona

Author:

Director:

Tutor:

Massimiliano Baratelli

**Dra. Maria Montoya
González
IRTA, CReSA**

**Dra. Mercè Martí Ripoll
Department of Cellular
Biology, Physiology and
Immunology UAB
IBB**

Dr. Maria Montoya González, group leader at “Centre de Recerca en Sanitat Animal (CReSA)”

CERTIFIES

That the thesis titled “Immunological studies on Swine Influenza Virus in pigs: from gene to epitopes” has been made by Massimiliano Baratelli under her supervision.

In Bellaterra on of of 2015

Dr. Maria Montoya González

PhD studies of Massimiliano Baratelli were founded by the grant “Formación de Personal Investigador (FPI)” of Spanish Minister of Economy and Competitiveness.

This work was funded by the project AGL2010-22200-C02-01 from the Spanish Minister; the work was also partially funded by the EU Network of Animal Disease Infectiology Research Facilities (NADIR) and The Pirbright Institute.

Printing of this thesis was funded by the “Institut de Recerca i Tecnologia Agroalimentaria (IRTA)”.

Table of Contents

ACKNOWLEDGMENTS	1
ABSTRACT	5
RESUMEN	9
LIST OF ABBREVIATIONS	13
INTRODUCTION	19
OVERVIEW ON INFLUENZA A VIRUS	21
<i>GENETIC AND STRUCTURAL CHARACTERISTICS</i>	21
<i>REPLICATION CYCLE</i>	23
<i>IAV EVOLUTION</i>	26
SWINE INFLUENZA VIRUS	27
<i>INFECTION</i>	27
<i>EVOLUTION AND EPIDEMIOLOGY</i>	28
<i>ZOONOTIC THREAT</i>	31
IMMUNE RESPONSE TO IAV INFECTION	33
<i>INNATE RESPONSE</i>	34
<i>CHIMERA CELL, HALF INNATE AND HALF ADAPTIVE.</i>	35
<i>ANTIGEN PRESENTATION AND TRIGGERING OF THE ADAPTIVE IMMUNE RESPONSE.</i>	36
<i>ADAPTIVE RESPONSE</i>	40
<i>SWIV IMMUNE RESPONSE. WHAT IS KNOWN IN PIGS.</i>	45
RATIONAL DESIGN OF VACCINES AGAINST IAV– REVERSE VACCINOLOGY FOR THE RATIONAL DESIGN OF PIGS	
VACCINES	47
<i>IAV VACCINES</i>	47
<i>RATIONAL DESIGN OF VACCINES</i>	49
<i>BIOINFORMATICS IN REVERSE VACCINOLOGY – ANTIGEN PREDICTION FOR T CELLS RESPONSE.</i>	50
<i>MHC-I EPITOPES BINDING ASSAYS</i>	52
<i>TRANSLATION OF RV TECHNOLOGIES IN PIGS.</i>	52
<i>INFLUENZA VACCINES AND THEIR RATIONAL DESIGN IN PIGS</i>	55
GENERAL OBJECTIVES	57
CHAPTER I: AN UPDATE ON SWINE INFLUENZA EPIDEMIOLOGY IN SPAIN	61
MATERIALS AND METHODS	63

RESULTS	65
<i>H₁N₁ SUBTYPE</i>	68
<i>H₃N₂ SUBTYPES</i>	68
<i>H₁N₂ SUBTYPES</i>	69
<i>MOLECULAR CHARACTERIZATION</i>	71
<u>CHAPTER II: GENERATION OF AN <i>IN VITRO</i> ASSAY TO CHARACTERIZE BINDING PROPERTIES OF PEPTIDES TO SLA-I</u>	<u>73</u>
MATERIALS AND METHODS	76
RESULTS	78
<i>OPTIMIZATION OF SLA RECONSTITUTION ASSAY.</i>	78
<i>GENERATION OF C1R EXPRESSING SLA-I ALLELES.</i>	79
<i>OPTIMIZATION OF THE SLA-I RECONSTITUTION ASSAY</i>	81
<u>CHAPTER III: IDENTIFICATION OF SWINE INFLUENZA VIRUS T CELLS EPITOPES IN INBRED PIGS</u>	<u>85</u>
MATERIALS AND METHODS	87
RESULTS	96
<i>CANDIDATE T CELL EPITOPES</i>	96
<i>PRIMING OF IMMUNE RESPONSE IN BABRAHAM PIGS</i>	97
<i>IDENTIFICATION OF T CELLS EPITOPE.</i>	98
<i>CELLS INVOLVED IN EPITOPE RECOGNITION</i>	106
<i>CHARACTERISTICS OF IDENTIFIED EPITOPES</i>	115
<u>CHAPTER IV: IDENTIFICATION OF SWINE INFLUENZA VIRUS CLASS I T CELLS EPITOPES IN A SLA-I DEFINED PIG HERD</u>	<u>119</u>
MATERIALS AND METHODS	121
RESULTS	125
<i>IN SILICO PREDICTION</i>	125
<i>IN VITRO TEST</i>	126
<i>IN VIVO TEST</i>	127
<i>CONSERVATION ANALYSIS OF THE IMMUNODOMINANT EPITOPE</i>	130
DISCUSSION	131
UPDATING THE EPIDEMIOLOGY OF SWIV IN SPAIN FOR RDV (CHAPTER I).	133
REVERSE VACCINOLOGY: FROM GENE TO EPITOPE.	136
<i>PROVIDING NEW IN VITRO TOOLS TO RV. DEVELOPMENT OF A CELL BASED SLA BINDING ASSAY (CHAPTER II)</i>	137
<i>RV VS. CONVENTIONAL METHODS. (CHAPTER III AND CHAPTER IV)</i>	140
T CELLS SUBSETS INVOLVED IN SWIV IMMUNE RESPONSE. (CHAPTER III AND IV)	146

SWIV T CELLS EPITOPES. (CHAPTER III AND CHAPTER IV)	149
CONCLUSIONS	153
REFERENCES	157
SUPPLEMENTARY FILES	175
CHAPTER I	177
CHAPTER II	186
CHAPTER III	187
CHAPTER IV	195
PUBLICATIONS	197

Acknowledgments

Durante cinco años pasan muchas cosas; estos son los años que dedique a hacer la tesis. Mucha gente estuvo a mi lado animándome, confortándome y haciéndome feliz. Primero de todo agradezco a mi familia por estar siempre conmigo nonostante los 1200km que nos separan. Agradezco también a mi novia "Peperoncino" que me ha acompañado en la fase más dura de la tesis y me acompañara por muchos más años felices. Agradezco a mis amigos de Italia Aldo, Andrea, Rocky, Veronica que siempre me tuvieron en su corazón nonostante la distancia. Luego agradezco a mis amigos Fer "el guapera", Guille "el chef" y marco "el abuelo gruñón". Agradezco también otros compañeros como Salva, Feng, Juliana, Paula "la gallega" y Paula "la colombiana", Beatriz Vidaña y Beatriz Gracia, Karlita, Alexandra, Sara, Almejo, SantaMaria. Agradezco mis compañeras de grupo Elisa, Tufaria y Pamela, y a María que me cogieron bajo sus alas y me enseñaron a volar☺. También agradezco a todo el personal del CreSA que me ayudaron con mucho cariño en hacer la tesis. Durante estos años estuve haciendo estancia en institutos al extranjero; ahí encontré personas fantásticas que también me acogieron con todo el cariño del mundo y me enseñaron muchas cosas bonitas de ciencias como de sus culturas. Agradezco a Eric, Jean-Remy, Jens, Bryan, Sophie, Hanneke y Gennaro.

Gracias a todooooos

Abstract

Swine Influenza Virus (SwIV) is an important pathogen in veterinary field with a great zoonotic potential and thus it is considered also a potential threat for public health. Surveillance and control of this pathogen in pigs is therefore crucial. Current methods of control are based on prophylaxis; in particular they are based on vaccines eliciting humoral response. Escaping capacity and high variability of SwIV make that the efficacy of those can be compromised; thus vaccines need to be periodically updated. This problem is shared in human health and thus rationally designed vaccines are being developed. Those are being designed to enhance T cell response against Influenza A Virus (IAV). T cell responses showed to be related with protection against IAV infection, targeting the highly conserved internal protein of the virus. This would solve the problems above cited. T cell epitopes of SwIV in pigs are just few and related to class I Swine Leucocytes Antigens (SLA). Reverse vaccinology is used in human health to identify T cells epitope; however, in pigs this has just recently been introduced and thus just few tools were available.

The main aim of this work was to identify T cells epitopes in SwIV to be used in rationally designed vaccines. For this purpose, the following studies were performed.

Surveillance of SwIV is fundamental to design a proper control. The epidemiological situation of SwIV in Spain needed to be updated and more genetic data were required to allow the use of reverse vaccinology. The study showed that the epidemiological situation of Spain was similar to other European countries in which circulating strains were closely related and evolving in the same way. However, some exceptions were found; one strain evolved divergently in Spain. Genetic shift has been suggested as a recent event in the evolution of those strains.

In vitro assays to determine binding affinities of epitopes to class I SLA (SLA-I) available were few and based on recombinant molecules. Therefore, in a first instance an *in vitro* tool based on native forms of SLA-I was attempted. MHC reconstitution assay for SLA-I was designed and almost entirely developed. C1R cells expressing the Babraham pigs allele SLA-1*es11 were generated. Finally, the denaturalization step of the assay was set-up.

Reverse vaccinology was then applied to identify T cells epitopes. Epitopes of the virus selected as target were predicted *in silico* by *NetMHCpan* on Babraham SLA-I alleles (SLA-1*es11 and SLA-2*es22) and tested by *ex vivo* functional assays (IFN γ and proliferation responses) using cells from immunised Babraham inbred pigs. Unfortunately, this approach did not give any positive epitope.

Additionally, T cells epitopes were empirically identified. Proteins M1 and NP of a human IAV were selected as target and thus dissected by using overlapping peptides and functional methods (IFN γ and proliferation responses) until finding T cells epitopes. The tests were performed using cells from IAV immunised Babraham inbred pigs. Two overlapping SLA-II epitope were found, NP₄₀₅₋₄₁₆ and NP₄₀₇₋₄₂₀.

In another attempt, a more complex strategy of reverse vaccinology was used. This was previously used by other authors and it is based on a combination of methods: *in silico* prediction of epitopes by *NetMHCpan* and validation of results by using *in vitro* binding preferences of the selected SLA-I allele , an *in vitro* test binding assay and *in vivo* test by tetramers. Peptides were identified in animals infected and challenged with two heterologous SwIV. This strategy showed to be highly accurate and thus one immunodominant epitope (NA₁₇₁₋₁₈₀) was identified.

Overall, these data pave the way for rational design of vaccine against SwIV as well as providing new insight into pig responses to infection or immunization with IAV.

Resumen

El virus de la gripe porcina (VGP) es un patógeno importante en el sector veterinario con un gran potencial zoonótico, y por lo tanto se considera también una amenaza potencial para la salud pública. La vigilancia y el control de este patógeno en cerdos es por lo tanto crucial. Los métodos actuales de control se basan en la profilaxis, en particular, en vacunas que suscitan una respuesta de tipo humoral. La capacidad de escape y la alta variabilidad de VGP hacen que la eficacia de estas vacunas pueda verse comprometida; por tanto, deben ser actualizadas periódicamente. El mismo problema se plantea en la salud humana donde se están desarrollando vacunas diseñadas racionalmente con tal de solventarlo. Estas vacunas están siendo diseñadas para potenciar la respuesta de células T contra el virus de la gripe A (VGA). La respuesta de células T esta relacionada con la protección contra la infección por el VGA, centrándose en las proteínas internas y altamente conservadas del virus. Esto permitiría resolver los problemas anteriormente citados. Los epítomos de células T de VGP conocidos en cerdos son sólo unos pocos y están relacionados con el Complejo Mayor de Histocompatibilidad porcino de clase I (CMHpo-I). La vacunología inversa se utiliza en sanidad humana para identificar los epítomos de células T; sin embargo, en cerdos este concepto se ha sido introducido recientemente y por lo tanto se dispone de pocas herramientas. El objetivo principal de este trabajo era identificar epítomos de células T para diseñar racionalmente vacunas contra VGP. Para este propósito, se abordaron las siguientes estrategias.

La vigilancia de VGP es fundamental para un control adecuado. La situación epidemiológica de VGP en España debía ser actualizada y se necesitaban más datos genéticos para permitir el uso de la vacunología inversa. El estudio realizado mostró que la situación epidemiológica de España era similar a la de otros países europeos; las cepas circulantes estaban estrechamente relacionadas y evolucionaron de la misma manera. Sin embargo, también se encontraron excepciones; una cepa evolucionó de forma divergente en España. Se sugiere que el cambio genético pueda ser un evento reciente en la evolución de esas cepas.

Los ensayos *in vitro* para determinar la afinidad de unión de epítomos a CMHpo-I disponibles actualmente son pocos y están basados en moléculas recombinantes. Por lo tanto, en primera instancia se intentó generar una herramienta *in vitro* basada en la forma nativa del CMHpo-I. Para ello se diseñó y desarrolló casi por completo un ensayo de reconstitución de MHC aplicado a CMHpo-I, para el cual se generaron células C1R que expresaran el alelo SLA-1*es11 de los cerdos singénicos Babraham. Por último se puso a punto el ensayo de desnaturalización.

A continuación, se aplicó la vacunología inversa para identificar epítomos de células T. Se predijeron epítomos del VGP *in silico* mediante *NetMHCpan* para los alelos CMHpo-I de los cerdos singénicos Babraham (SLA-1*es11 y SLA-2*es22); estos epítomos se probaron mediante ensayos funcionales *ex vivo* (IFN γ y respuesta de proliferación) usando células de cerdos Babraham inmunizados. Desafortunadamente, este enfoque no dio ningun epítomo positivo.

Los epítomos de células T fueron también identificados empíricamente. Las proteínas M1 y NP de un VGA humano fueron seleccionadas como diana, se estudiaron mediante el uso de péptidos solapantes y métodos funcionales (IFN γ y respuestas de proliferación) hasta encontrar epítomos de células T. Los epítomos fueron analizados con células procedentes de cerdos Babraham inmunizados con VGA. Se encontraron dos epítomos CMHpo de clase II solapados, NP₄₀₅₋₄₁₆ y NP₄₀₇₋₄₂₀.

En otro intento, se utilizó una estrategia más compleja de vacunología inversa. Esta había sido utilizada anteriormente por otros autores y comprende una combinación de métodos: predicción de epítomos *in silico* mediante *NetMHCpan* y validación de los resultados utilizando las preferencias de unión del alelo CMHpo determinadas *in vitro*, analisis *in vitro* mediante un ensayo de unión y analisis *in vivo* mediante tetrámeros. Los péptidos fueron identificados en animales infectados y expuestos a dos VGP heterólogos. Esta estrategia demostró ser muy precisa y así se identificó un epítomo inmunodominante (NA₁₇₁₋₁₈₀).

En general, estos datos allanan el camino para el diseño racional de una vacuna contra la SwIV a parte de proporcionar una nueva visión de la respuesta de los cerdos a la infección o inmunización con VGA.

List of Abbreviations

A

ADCC: Antibody Dependent Cell Cytotoxicity

APC: Antigen Presenting Cells

B

BALc: Broncho Alveolar Lavage cells

C

CDSs: Coding Sequences

CFSE: Carboxylfluorescein Succinimidyl Ester

CMI: Cellular Mediated Immune

Con A: Concanavalin A

CSF: Classical Swine fever

CTL: Cytolytic T Lymphocytes

Cpm: counts per minute

D

DCs: Dendritic Cells

DIVA: Differentiation of Infected from Vaccinated Animals

DNA: Deoxyribonucleic Acid

DMSO: Dimetil Sulfoxid

E

ELISA: Enzyme Linked Immunosorbent Assay

ER: Endoplasmic Reticulum

F

FCS: Foetal Calf serum

G

GC: Germinal Centre

H

HA: Hemagglutinin

HLA: Human Leucocyte Antigen

I

IAV: Influenza A Virus

iBALTs: inducible Bronchus-Associated Lymphoid Tissue

ICS: Intracellular Cytokine Staining

IFN: Interferon

IL: Interleukin

ISC: IFN γ secreting cells

L

LN: Lymph Nodes

M

MDCKs: Madin-Darby Canine Kidney
MHC: Mayor Histocompatibility Complex
MHC-I: MHC class I
MHC-II: MHC class II
mLN: mediastinal LNs
moDC: monocyte derived Dendritic Cells
mRNA: messenger RNA
M1: Matrix protein 1
M2: Matrix protein 2

N

NA: Neuraminidase
NEP: Nuclear Export Protein
NLS: Nuclear Localization Signals
NLRP3: NOD-LRR and Pyrin domain containing 3
NK: Natural Killer
NP: Nucleoprotein
NS1: Non structural protein 1
NS2: Non structural protein 2

O

ORF: Open Reading Frame
OWOH: One World One Health

P

PA: Polymerase Acid protein

PAMPs: Pathogen-Associated Molecular Patterns

PBMCs: Peripheral Blood Mononuclear Cells

PBS: Phosphate Buffered Saline

PB1: Polymerase Basic protein 1

PB2: Polymerase Basic protein 2

pDCs: plasmacytoid Dendritic Cells

pdmH₁N₁: pandemic H₁N₁ 2009 IAV

pMHC: peptide –MHC complex

PRMs: Pattern Recognition Molecules

PRR: Pattern Recognition Receptors

PSCPL: Positional Scanning Combinatorial Peptide Libraries

p-SLA: peptide-SLA complex

PWM: Pokeweed mitogen

R

RBC: Red Blood Cells

RDV: Rational Designed Vaccines

RIG-I: Retinoic acid-Inducible Gene I

RNA: Ribonucleic Acid

RT-PCR: Reverse Trancription-Polymersase Chain Reaction

RV: Reverse vaccinology

S

Sd: Standard deviation

SA: sialic acids

SLA: Swine Leucocyte Antigen

SLA_{hc}: SLA heavy chain

SLA-I: class I SLA

SLA-II: class II SLA

SwIV: Swine Influenza Virus

T

TAP: Transporter Associated with antigen Processing

T_{CM}: Central Memory T cells

TCR: T Cells Receptor

T_{EM}: Effector Memory T cells

T_{Eff} : Effector T cells

TGF β : Transforming Growth Factor β

Th: T helper cells

TLRs: Toll Like Receptors

TNF α : Tumor Necrosis Factor α

TRAIL: TNF α -Related Apoptosis Inducing Ligand

T_{RM}: Resident Memory T cells

T_{SCM}: Stem Cell Memory T cells

U

UTRs: Untranslated Regions

W

WHO: World Health Organization

Others

β 2m: β -2-microglobulin

Introduction

Overview on Influenza A virus

Influenza A virus (IAV) is thought to have emerged from aquatic birds and bats. Its peculiar evolution characteristics allowed it to cross barrier species and therefore spread to mammals and domestic poultry ¹. It has caused several pandemic outbreaks in the human population during the last century, being the 1918 (The Spanish Flu) the most devastating one. In veterinary, mostly in poultry, it causes great economic losses. Any available prophylactic or therapeutic tool has been demonstrated ineffective due to the peculiar escaping characteristics of the virus. The general characteristics of IAV and its evolution are briefly reviewed here.

Genetic and structural characteristics

Orthomyxoviridae have a negative-sense, single-stranded, and segmented ribonucleic acid (RNA) genome. They are classified into 5 different genera in which IAV is found. IAV genome is constituted by 8 segments named from 1 to 8 (Figure 1) or as PB2 (2341pb), PB1 (2341pb), PA (2233pb), HA (1778pb), NP (1565pb), NA (1413pb), M (1027pb), NS (890pb); each of those is constituted by a central coding region flanked by two short Untranslated Regions (UTRs) located at the 5' and 3' extremes. The UTRs play important roles as a packaging signal ², polyadenylation ³, or signals for genomic replication ⁴. Notwithstanding, even when there are just 8 genomic segments, their central regions codify for at least 18 known proteins due to the fact that different molecular mechanisms provide expression of multiple proteins from some of them. These mechanisms are schematically represented for each segment in figure 1 and they include alternative splicing of viral mRNAs as well as non-canonical translation, such as leaky ribosomal scanning, non-AUG initiation, re-initiation, and even ribosomal frameshifting ^{5,6}. Viral translated proteins undergo a variety of post translational modifications including glycosylation ⁷, acylation ⁸ and proteolytic cleavage ⁹ that contribute to formation of the mature proteins constituting the viral particle.

The IAV particle (represented in figure 2) could be described from an immunological point of view into two parts. The surface part of the virus, which is exposed to the humoral response of hosts and it is constituted by three glycoproteins: Hemagglutinin (HA), Neuraminidase (NA) and Matrix protein 2 (M2). Those proteins are inserted into a phospholipid bilayer membrane that masks the proteins of the inner part of IAV from the interaction with the cited immune response. Secondly, Ribonucleoproteins (RNPs) complexes surrounded by the protein of the

Matrix (M1) constitute the inner part of the virus. The RNPs complexes constitute the core of the virus and each of them contains: a genomic segment, Nucleoprotein (NP), Polymerase Basic proteins 1 and 2 (PB1 and PB2) and Polymerase Acidic protein (PA).

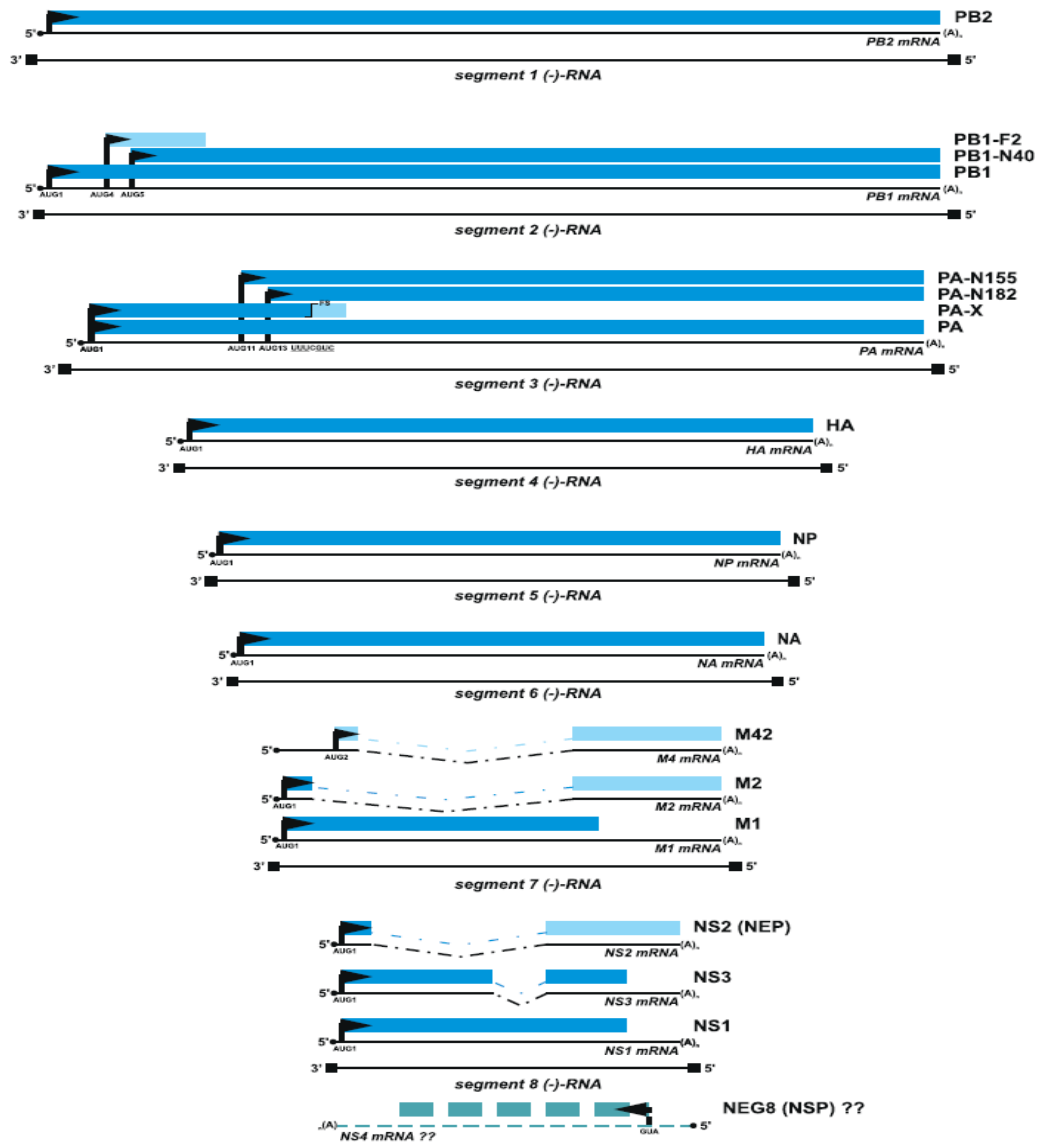


Figure 1. The proteome of influenza A viruses. The organization of the protein-coding Open Reading Frames (ORF) in viral mRNAs transcribed from IAV genome segments is shown. The (-)-RNA genome segments are indicated by square-ended black lines. Non-spliced and spliced viral mRNAs are shown as black lines, where the 5'-cap structures are shown as black circles and the poly A tails are depicted as (A)_n. Spliced regions are shown as dotted lines. Black arrows indicate initiation of protein synthesis at the start codon (AUG) of an ORF. Proteins are shown as blue rectangles, alternative ORFs are shown in different shades of blue. FS – frameshifting event. The hypothetical NEG8 mRNA and protein are shown as dotted lines. Based on Vasin et al. 2014¹⁰.

The Non-Structural protein 2 (NS2), also known as Nuclear Export Protein (NEP), it is associated with M1 in the internal part of IAV ¹¹. Finally, there are other known factors constituting the proteome of the virus; however, those are non-structural and are involved the replication cycle.

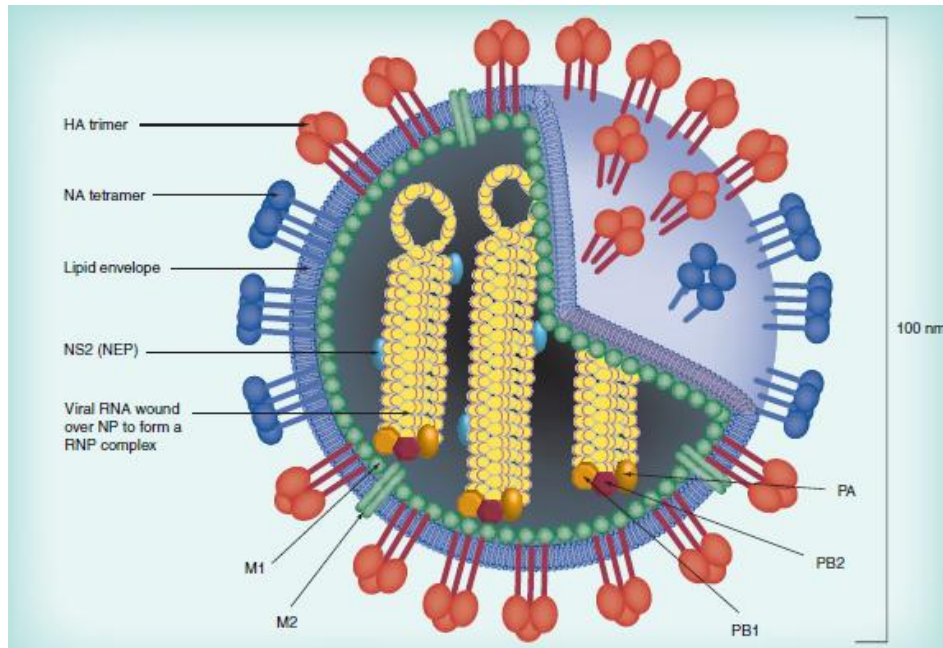


Figure 2. Structure of IAVs. IAV is about a 100 nm particle. HA, NA and M2 proteins are encased in a phospholipid membrane surrounding the internal part of IAVs. The latter is constituted by M1 protein and RNP complexes. RNP complexes are in turn constituted by PA, PB1, PB2 and NP proteins. Each of IAV genomic segments is wound by NP proteins; thus viral particles host 8 RNP complexes. Based on Epstein et al. 2010 ¹².

Replication cycle

IAV is an intracellular pathogen whose cycle is the result of a complex network of interactions of viral and cellular factors. The most relevant ones are here described. The replication cycle could be divided into several steps ¹³ which are summarized in figure 3. IAV is adsorbed on cell surface membranes by the binding of its HA with terminal sialic acids. Cellular endocytic processes internalize and traffic the viral particle up to the endosome compartments, through which viral RNPs complexes are released into the cytoplasmic compartment. The characteristic low pH of mature endosome compartment triggers conformational changes of the M2 and HA proteins. Activated M2 alters the curvature of the viral membrane and acidify the virion interior, leading respectively to fragmentation of filamentous virions into spherical particles

and dissociation of the M1 from the RNPs. The new conformation of the HA exposes a fusion peptide which inserts into the endosomal membrane and, by another conformational change, forces the cell membrane to fuse with the viral one; thus, viral contents (the uncoated RNP complex and the M1) are released into the cytoplasm. Replication of IAV genome takes place in the nucleus of cells. The uncoated RNPs complexes are transported there from cytoplasm through the nuclear membrane and then dissociated. Nuclear Localization Signals (NLS) allow the importation process. All proteins of the RNP complex bear those signals; however, NP NLS cover a major role in the importation process. The negative sense viral RNA ((-)vRNA) is transcribed into the nucleus to complementary positive sense RNA ((+)cRNA) which in turn is the template for generation of new (-)vRNA. The trimeric viral RNA-dependent RNA polymerase, consisting of PB1, PB2 and PA subunits, is responsible of that process. However, NP is also involved¹⁴. (-)vRNA is also used for transcription of viral mRNA by the activity of the cellular RNA polymerase II. Cap-snatching is fundamental in that process as it permits the initiation using the host pre-mRNA 5' end Cap. The primer is generated by the endonuclease activity encompassed within the trimeric viral RNA-dependent RNA polymerase¹⁴. Viral mRNAs undergo maturation and they are used in the cytoplasm for translation of new structural and non-structural proteins. New RNPs are ensembled in the nucleus and then they are transported in the cytoplasm. One of the most known viral factors involved in the exportation process and bearing the needed signals (Nuclear Export Signals, NES) is NEP. The internal part of the virus (constituted by the RNP, M1 and NEP) is assembled with HA, NA and M2 glycoproteins, already expressed on the membrane of the cellular surface; finally, the new virion is realised by budding. Several proteins contribute to the budding process and in particular HA, M1, M2 and NP are known to be part of it. IAV is pleomorphic and it can be found as spherical virions as well as filamentous virions. Mutation in the M1, M2 or NP proteins seems to influence the budding process and thus the resulting form of the virions¹⁵⁻¹⁷. NA enzymatically removes terminal sialic acid linkages, facilitating release of virus from cells during budding¹⁸. Moreover, it also removes decoy receptors and mucins from cells surface to aid IAV particle entry¹⁹.

Role of some other IAV proteins is not yet clear. PB1-F2 and Non Structural protein 1 (NS1) are multifunctional proteins involved in virulence or viral cycle. However, they are also well known to modulate host innate immune response^{20,21}. PB1-F2 and NS1 are known to act on the cellular sensing pathway; thus, cells do not detect IAVs presence as a threat. In that way, those factors limit the Type I Interferons (IFN) response, which triggers the immune response. NS1 is

also able to act post-transcriptionally; it limits the available cellular mRNA and thus it reduces the translated Type I IFNs. The high mutation rate of IAV genome generates different phenotypes of those proteins with enhanced or decreased functions or changing the mechanisms of action. One paradox example is that PB1-F2 protein of some strain has the opposite function than the described; therefore it is not limiting but in contrast it is exacerbating Type I IFN production²². The rest of IAV proteins have been recently discovered and their function is being studied; they are mostly involved in complementation of lacking function of other viral proteins¹⁰.

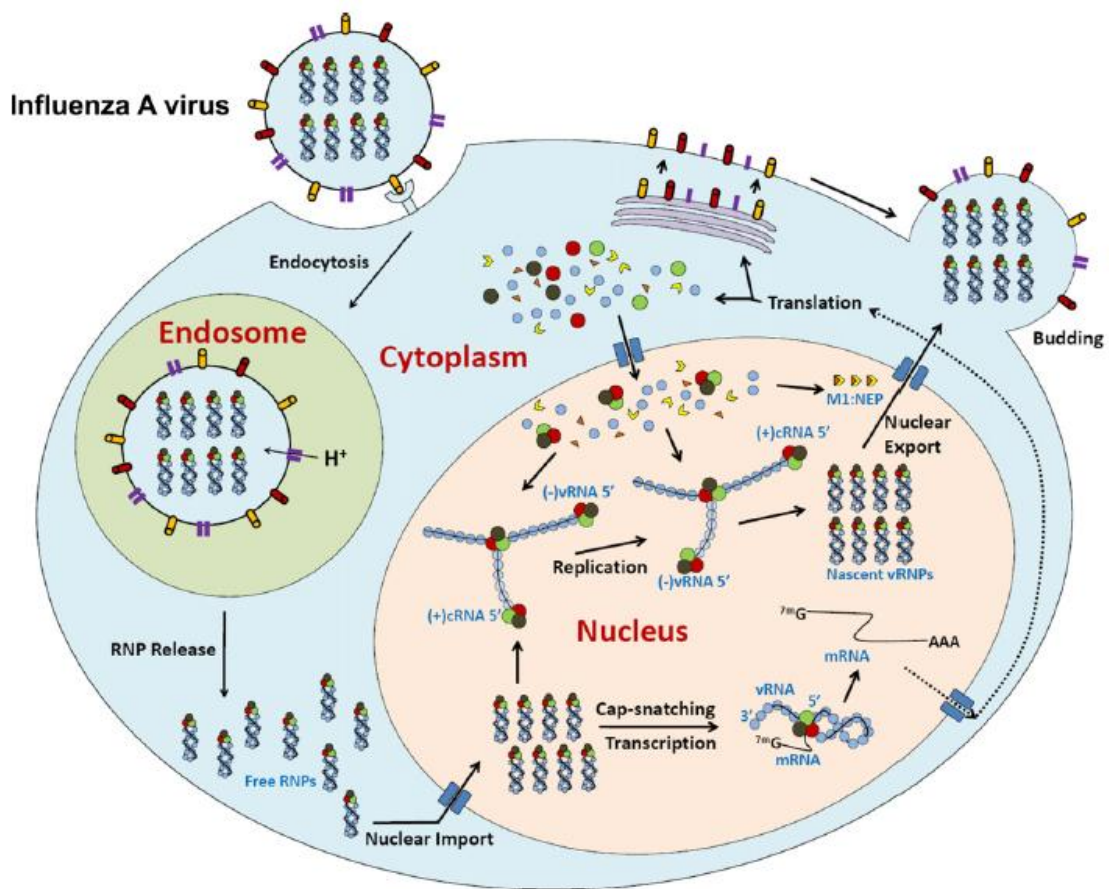


Figure 3. IAV life cycle. IAV is absorbed to the cell surface through interaction of its HA with salicylate receptor. Viral particle is then transported to the ER where low pH triggers release of the RNP complexes into the cytoplasmic compartment. Those are transported to the nucleus where the replication process of the viral genome is taking place. The (-)vRNA are here transcribed and in turn re-transcribed by viral polymerases complexes into mRNA and new viral genomes; the first are used to translate new viral proteins which are transported into the nucleus (Polymerases, NP, M1 and NEP) to be assembled with viral genomes into new RNP complexes. New RNP complexes are transported into cytoplasm and then assembled with the rest of new proteins (HA, NA, M2 ad M1) to compose the IAV particle. Finally the nascent particle is released by budding processes. Polymerases: red, green and black circles; NP: blue circles; M1: yellow; NEP: red triangle; HA and NA: yellow and red cylinder; M2: cyan bars. Based on Zheng et al. 2013²³.

IAV evolution

Understanding of viral evolution has fundamental importance into designing a good control strategy. A phenomenon named quasispecie evolution has had substantial negative impact on the development of a long lasting and efficient vaccine or drug for IAV. Viral quasispecies refer to the fact that RNA viral populations consist of mutant spectra (or mutant clouds) rather than genomes with the same nucleotide sequence. Mutant spectra and not individual genomes are the target of evolutionary events ²⁴. In IAV, there are two evolutionary events termed as genetic drift and shift. The first one consists in nucleotide misincorporation leading into mutation of the genome. The second one lies in reassortment of genomic segment to form a new combination. There is another factor that could contribute to IAV evolution; this is recombination. However, this seems to play little or no role in IAV evolution ²⁵. Those events could contribute to generate a great genetic diversity; however, negative selection also contributes to eliminate unfit genomes, like those loosing biological information ²⁴. Therefore, mutant spectra are the source of virus adaptability because they constitute dynamic (continuously changing) repositories of genotypic and phenotypic viral variants. Major events in the biology of RNA viruses, such as their capacity to change their cell tropism or host range or to overcome internal or external selective constraints (immune responses, antiviral agents, etc.) have their origin in the repertoire of variants present and arising in mutant spectra ²⁴.

IAV viruses are identified by the strain name that is unique and composed of A/Host/Place of isolation/Code/Year of isolation (Subtype). Selecting pressures are acting differently on the surface or internal proteins of the virus. As a result of strong selecting pressure, the surface glycoproteins HA and NA are divided, depending on antigenic characteristics, into various subtypes. So far there have been identified 18 HA (HA1-HA18) and 11 NA (NA1-NA11) types (the lasts subtypes have been just recently described by Tong S. *et al* 2013 ²⁶). In some subtypes, those proteins could be further classified. If an IAV has formed a stable lineage in one host and the surface glycoproteins have adapted to it, they could be classified with the name of the host; for example Human HA1 or Avian HA1. When the virus is being recently introduced in a new host, and thus the surface glycoproteins are not changed too much, they are classified as Human-Like HA1 or Avian-Like HA1 (fully established but sufficiently different to be distinguished from the original). Another further step of classification could be done depending on the phylogenetic clustering (e.g. EuroAsian, American or American α , β , γ clades). The internal proteins are less variable than the surface glycoproteins ²⁷. However,

specie specific types or clades (e.g. Eurasian, American) can be also distinguished. IAV variability is not just a matter of antigenicity. Several virulence determinants influencing traits like replication, host range or host immune responses have been described ²⁸. Other determinants have been involved in IAV resistance to antiviral drugs like Adamantane or Neuraminidase inhibitors ²⁹. Those determinants are often few point mutations into the amino acid sequence able to generate a great diversity in viral phenotype.

Swine Influenza Virus

Swine influenza virus (SwIV) causes economic losses for pig industry ³⁰ and more recently it has also been recognized as a threat for public health ³¹. It is involved in the Porcine Respiratory Complex Disease and it is considered a sensitization factor for other porcine pathogens ³². It causes outbreaks of respiratory illness, which may lead pigs to death. However, enzootic infections are also showed. SwIV has a worldwide distribution in which, due to geographical isolation, two to three main genetic lineages can be found. Those are the American, European and Asian lineages. In the latter region, there is a complex epidemiological situation in which some of the European or American lineages are established (sometime this lineage is referred as Eurasian). In this section the aspect of SwIV infection together with the epidemiological situation of European lineages are briefly discussed.

Infection

Infection of SwIV in pigs is a threat in both forms: acute and subclinical both of which are damaging porcine production due to death or growth retardation of animals or due to the zoonotic and epidemiologic implications respectively.

Natural acute IAV infections in pigs causes classical symptoms like coughing, sneezing, fever pyrexia, anorexia, lethargy and often growth retardation ^{33,34}. SwIV infection leads to high morbidity and low mortality ³⁵. However, factors like poor farming conditions or co-infection with multiple pathogens could exacerbate infections and even cause death ³². Infection is restricted to the respiratory ways and so are lesions like pneumonia, pleuritis, and edema ³⁶. In swine, IAV primarily infect the epithelial cells lining the surface of the respiratory tract, from nasal mucosa to alveoli, but virus also has been detected in the glandular epithelial cells associated with the larger airways ³⁷. Therefore, virus replicates in both upper and lower respiratory ways ³⁸. Shedding of IAV is generally lasting up to 7 days ³⁹. One infected pig can infect between 3 and 7 other animals. However, shedding and propagation potential can be

higher³⁶. Virus load in lungs generally peaks at day 3 and it is hold till day 5 post infection³⁹. Therefore, infection is generally solved after 5-7 days^{37,39}. As previously mentioned IAV is a high variable virus and so are its phenotypic characteristics. The grades of lesions change depending on the subtype. A recent pathological study demonstrated that Korean SwIV subtypes H₃N₂ induces more severe gross lesions than the other two circulating subtype (H₁N₁ and H₁N₂)⁴⁰. These correlate with the clinical signs observed by other authors for SwIV of the same subtypes⁴¹. Finally, SwIV can also lead to subclinical infection in farms, which usually pass unnoticed as none of the classical Influenza symptoms can be detected⁴². Those clinical conditions can be also reproduced in experimental settings in which the intranasal route usually leads to subclinical infection while the intratracheal route leads to acute infections⁴³. Inoculums titre is also influencing the infection outcome³⁹.

Evolution and Epidemiology

SwIV circulating in America, Asia and Europe have similar origins. However, events like interspecies transmission, genetic shift or drift and extinguishment of lineages lead to completely different epidemiological situations.

The most important driving force for IAV drift in humans is the immune response pressure^{44,45}. SwIV showed a drift evolution of surface glycoproteins as other IAV, although it is weak⁴⁶⁻⁴⁹. The cause of the weak selection pressure could be attributed to the management system of porcine production in Europe. This implies a short lifespan of pigs and often also a lack of vaccination; therefore immunologically naïve populations can be frequently found⁴⁶. Interspecies transmission is an important event in SwIV history being the frequency of human-pig transmission recently been analysed. It has been shown that human to pig introduction occurs frequently but transmission of human internal gene segments in swine is a comparatively rare event⁵⁰. Introduction of Avian IAV in swine population seems to be a more rare or an event difficult to be detected⁵¹⁻⁵³. Another important event is the genetic shift and which has been described to have a high rate between H₁N₁ and H₁N₂ SwIV subtypes in Europe⁵⁴. Multiplicity of infections by different IAV strains in the same farm, batch or even animal are frequently observed^{36,55} and again the porcine production system might be responsible⁵⁶. European porcine production is distributed in few regions and the most prevalent system is the intensive one⁵⁷. Those characteristics might facilitate farm to farm and batch to batch transmission leading to high multiplicity of infections and thus reassortment. Genetic drift and

shift contribute to generate a great diversity in SwIV although just few viruses successfully transmit and persist.

Three main SwIV subtypes have been circulating in swine population in Europe; those are H₁N₁, H₃N₂ and H₁N₂ (Figure 4). First data on SwIV circulation in Europe was based on few outbreaks records or case observations during 1930s. Those viruses were supposed to have seasonal human origin⁵⁸. However, recent findings suggest that Classical H₁N₁ SwIV could have been circulating in the same period⁵⁹. The first strain of SwIV to be isolated in Europe belonged to Classical H₁N₁ lineage and it was isolated in 1950. This lineage spread in several countries and definitely disappeared from Europe in the 1990s, when the last one was isolated. Since that time, Classical H₁N₁ lineage has no longer been detected in Europe notwithstanding it is persistent in America.

The Avian-Like H₁N₁ lineage was generated from interspecies transmission to pigs of all segments of an avian IAV and it was probably circulating since 1979⁶⁰. It has spread across several countries and it is fully establish in Europe. The Avian-Like H₁N₁ lineage is now endemic in several European countries and its seroprevalence in pigs vary considerably^{55,61}.

The Human-Like H₃N₂ lineage is another fully established lineage with several degrees of seroprevalence in pigs or even absence in some countries (UK, France)^{48,55,61}. The first strains of that lineage were isolated in the 1980s. The Human-Like H₃N₂ lineage was generated by interspecies transmission, HA and NA segments of the virus have origin in the human IAV lineage. However, the genetic shift played also an important role, thus all the internal gene segments of Human-Like H₃N₂ virus have origin in the Avian-Like H₁N₁ lineage⁴⁶.

The third main lineage circulating in pig in Europe is the Human-Like H₁N₂. Its seroprevalence in pigs is variable among European countries^{55,61}. The first strain of that lineage was firstly reported in 1995⁶². The origin of this lineage is a complex mix of interspecies transmission and genetic shift; HA and NA of Human-Like H₁N₂ have origin in H₁N₁ and H₃N₂ Human IAV while its internal genes have origin in the Avian-Like H₁N₁ or more probable in the Human-Like H₃N₂ lineage⁶³.

One last lineage has just recently been introduced from human and its persistency in European pig population should be still clarified. That lineage is the pandemic H₁N₁ 2009 (pdmH₁N₁). The virus contained two gene segments derived from avian strains of North American lineage, one gene from human influenza, three genes from classical swine viruses (still circulating in North American and Asian pigs) and significantly, two segments from a Eurasian swine lineage (NA and MP)⁶⁴. Since its introduction in pigs after the human pandemic outbreaks, it has been detected several times in swine herds across Europe⁶⁵⁻⁶⁸.

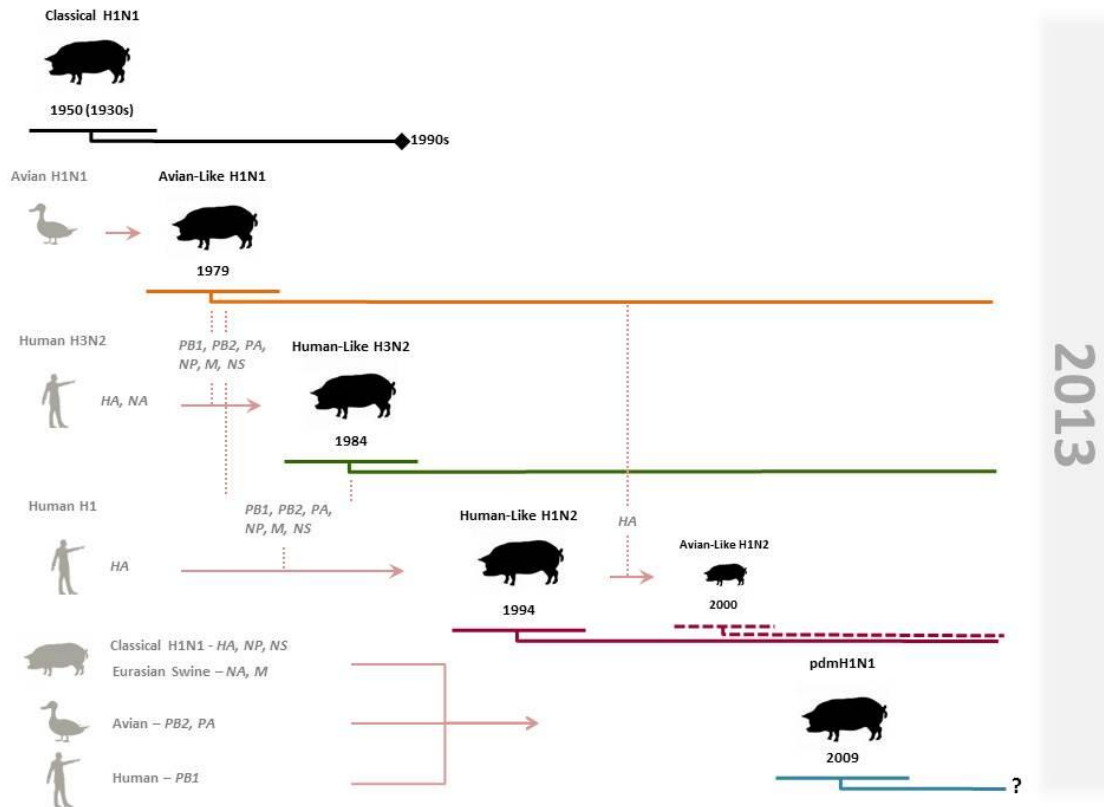


Figure 4. SwIV virus lineages circulating in Europe. SwIV main lineages were generated by interspecies transmission and genetic shift events (red lines) of avian, human and swine IAV. The Classical H_1N_1 SwIV was extinguished in Europe around 1990s. However, it has been perpetuated in America and that lineage contributed to the generation of the pdm H_1N_1 . The pdm H_1N_1 lineage is not yet clear if it is a stable in some countries. The Avian-Like H_1N_2 is a new recent reassortant generated from the Human-Like H_1N_2 and the Avian-Like H_1N_1 that is already established in few European countries. Based on Richt et al. 2013⁶⁹

Several new reassortants comprising the H_1N_2 subtypes of SwIV or the pdm H_1N_1 have been isolated recently in pigs in Europe^{47,66,70,71}. They mainly were generated from SwIV but also human IAV. Most of them have no longer been detected and therefore may have failed to persist. Just a few of them were showed to persist in specific European regions, like the Avian-Like H_1N_2 SwIV^{47,70}.

SwIV circulating in Spain

During 2001-2004, H_1N_1 , H_3N_2 and H_1N_2 SwIVs were reported as endemic in the pig population in Spain, with seroprevalences slightly lower than those described in other pig rearing areas in Europe^{61,72}. The three subtypes were reported to co-circulate in pigs in Spain, with sows often being seropositive to multiple subtypes at a time, probably as a result of multiple contacts during life^{55,72}. SwIVs described in the 2000s in Spain belonged to the Avian-Like H_1N_1 , the Human-Like H_3N_2 , and the Human-Like H_1N_2 lineages. Even though they were described at

subtype level using partial sequencing and antigenic procedures, a low number of complete genetic sequences of SwIVs in Spain were available for genetic comparison after that period. The three lineages showed to be maintained in Spain up to 2007^{48,55,72}. A new genetic lineage having an Avian-Like hemagglutinin gene related to the H₁N₁ strains circulating in Spain was also circulating in the same period^{73,74}. The epidemiological situation of SwIV in Spain was therefore incomplete, particularly from a genetic point of view.

Zoonotic threat

IAV has as natural reservoir in avian species, particularly waterfowl birds. However, during history it has spread and adapted to mammals and now IAV has reservoir in species like pigs, horses, bats, sea mammals, dogs and so more. Several pandemic outbreaks caused by IAV from other species occurred in humans⁷⁵ such as the one in 1918 when over twenty million deaths occurred worldwide. The viruses have been evolving divergently in each of those species with different strength; for example they can lose antibody cross reaction with viruses of the original lineage or capacity to spread to other species. The public threat for IAV resides in the novelty for humans and the ability to transmit within population. The virus that causes the pandemic outbreaks in 2009 exhibited these characteristics. pdmH₁N₁ showed a novel genetic and antigenic composition originated in other species than humans, from a complex mix of interspecies transmission and shift events. Novelty of the antigenic characteristics makes that no current vaccine was efficient and that previous exposition to seasonal IAV was not protective⁶⁴. Naïve human populations were available and therefore virus spread worldwide. pdmH₁N₁ 2009 is the lone documented pandemic virus to sustain transmission in humans and nowadays it has replaced the humans seasonal H₁N₁ viruses⁷⁶

One World One Health (OWOH) signals greater collaboration in the face of shared health risks that exist at the human, animal and environmental interfaces⁷⁷. This initiative was born before 2009 to face zoonotic problem. However, just after that date there has been a call for increased surveillance and research⁶⁸. The survey and control of IAV in other species rather than humans has significantly improved, as virus with pandemic potential can be detected and controlled. Great attention has been recently focused on avian viruses as they are considered the next potential source of pandemic threat. Therefore, a number of studies have been recently focused on determining factors influencing the host range of infection, replication and transmission of IAV in different species. However, the real pandemic potential of IAV is still unpredictable. Species barrier crossing and transmission is generally achieved by multiple

mutations in the IAV genome in which several viral proteins are involved^{78,79}. The most important and known host range determinant is the HA. Viral infectivity restriction is influenced by the type of sialic acids (SA) showed by the host and its body distribution. For example, it is of general assumption human IAV preferentially bind to α 2,6-linked SA receptors (α 2,6-SA) which are predominant on epithelial cells in the human upper respiratory tract, whereas avian IAV preferentially bind to α 2,3-linked SA (α 2,3-SA) receptors, which are abundantly present on epithelial cells in the intestinal tract of birds and in the lower respiratory tract of humans. Therefore, the infectivity of those viruses is restricted to members of the respective host species. Pigs are an exception of those rules; their respiratory tract showed both kinds of sialic acids and thus they can be virtually infected by IAV from mammals and avian. If that occurs, novel genetic reassortant IAV could be generated. The pdmH₁N₁ virus is the result of that concept and therefore, after the 2009 outbreaks, pig has been reassessed as “mixing vessel” for novel reassortant viruses⁸⁰.

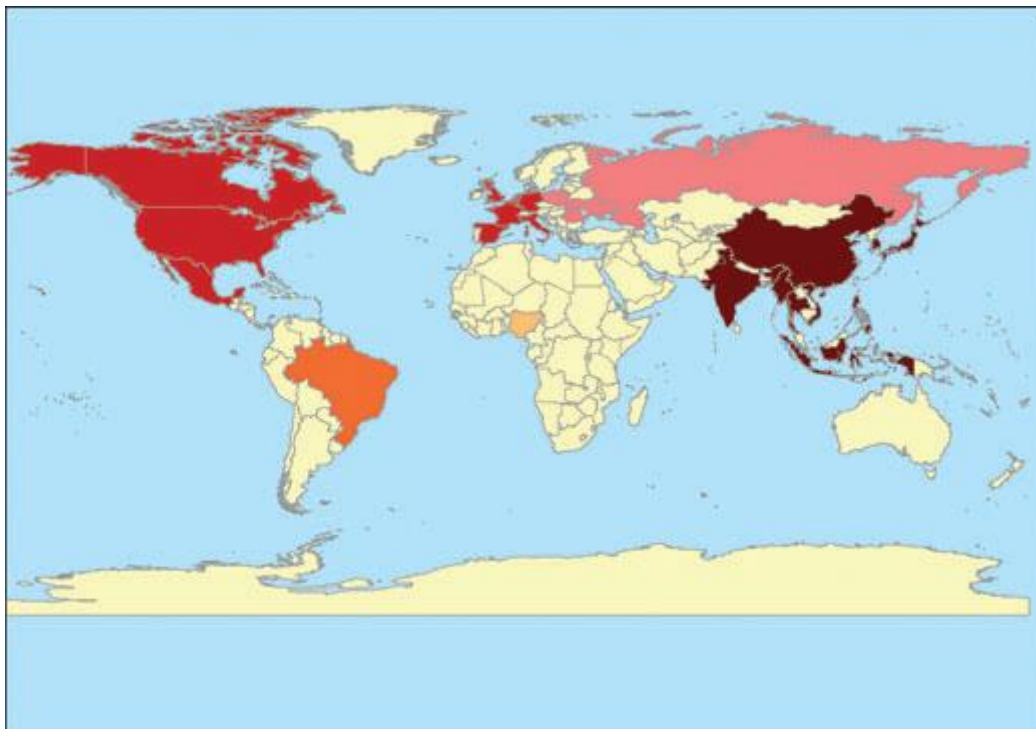


Figure 5. Countries with priority for targeted surveillance for (IAV evolution or circulation in swine. Brown, the highest priority for surveillance in swine is in countries of East and Southeast Asia due to higher rankings for spread and emergence of IAV in swine, with high population numbers of pig, poultry, and waterfowl, risk factors for outbreaks, and potential for reassortment between viruses circulating in pigs and birds due to husbandry methods. Red, Western Europe and North America have higher ranking with risk factors for outbreaks in pigs and continental and global spread through movement and export. Pink, countries of Eastern Europe are ranked for potential reassortment between viruses circulating in pigs and birds plus global spread. Light orange, Nigeria ranked for potential reassortment between viruses circulating in pigs and birds. Dark orange, Brazil ranked for outbreaks in pigs, but with lower risk

of global spread by export. This priority ranking does not imply that lower-ranked countries should not conduct IAV surveillance in swine, but emphasizes those regions that should receive priority focus. Based on Vincent et al. 2014⁶⁸.

Several pig to human transmission of SwIV have been reported⁸¹, this together with the “mixing vessel” theory of pigs and the fact that IAV can circulate unnoticed in this specie⁴² make that a great pandemic potential reside in pigs and SwIV. A recent study demonstrated that pigs can independently facilitate combinatorial genetic changes in the genesis of a potential human pandemic strain that has all gene segments of swine origin⁸².

Altogether, those findings emphasize the importance of continued monitoring and control of influenza viruses in pigs. Figure 5 summarizes those countries identified as being a high-priority for targeted surveillance for IAV in swine.

Immune response to IAV infection

Swine are considered one of the major animal species used in translational research. They are similar to humans in terms of anatomy, genetics and physiology. Swine has been used as model for a wide range of infection diseases including respiratory diseases. The respiratory ways of the pigs have some little anatomical differences, like the lobulation of the lungs. The similarities with humans in virology studies of IAV make pigs a good animal model to study that disease⁸³. Notwithstanding, the knowledge of porcine immune system is still limited. Recently, great advances have been done and paradoxically this is due to a change in direction of translation of knowledge and reagents, from humans and other animal models like pigs. The immune response to IAV is here briefly described. However, it mainly refers to what is known in humans and rodents as the knowledge in pigs is still incomplete.

The outcome of IAV infection depends on the capacity of the host to deal with pathogens. There are two main mechanism: the antiviral resistance reduces the viral burden and the antiviral tolerance reduces the negative impact of infection on host fitness⁸⁴. The same mechanism could be translated to swine in which IAV can induce different shades of clinical outcomes from acute to subclinical. Therefore, the clinical outcome depends on the interplay of viral resistance and tolerance. Susceptible animals that end to death are those not able to sufficiently provide one of such mechanisms.

Innate response

The first line of defence of the host organisms to pathogens infection is the innate immune system (Figure 6). The primary infection site of IAV is the respiratory ways, therefore the virus has first to get through mucus ⁸⁵ and counteract the effect of the humoral arm of innate response that includes members of the complement cascade and soluble pattern recognition molecules (PRMs) ⁸⁶. The host organism senses IAV by non soluble PRMs or Pattern Recognition Receptors (PRR) ⁸⁴, such as Toll Like Receptors (TLR3, TLR7 and TLR8), Retinoic acid-inducible gene (RIG-I), NOD-like Receptor family member NOD-LRR and pyrin domain containing 3 (NLRP3). PRRs differ in their capacity to recognize Pathogen-Associated Molecular Patterns (PAMPs) or in the signalling pathway, cellular localization and cell type expression. Those characteristics permit to differently sense pathogens and thus signalling out accordingly. The host organism response to sensing (signalling out) is wide too; it includes secretion of type I and III IFNs, proinflammatory cytokines, eicosanoids and chemokines ⁸⁴. Type I and III IFNs induce antiviral state in neighbour cells by activating IFN stimulated genes. Proinflammatory cytokines and eicosanoids cause local and systemic inflammation, induce fever and anorexia, and instruct the adaptive immune response to IAV. Chemokines recruit additional immune cells. In summary, lung resident cells (epithelial, endothelial, alveolar macrophages, dendritic cells) sense virus, activate and in turn recruit and activate more cells. Activation does not involve just signalling out, cells have also effector functions ⁸⁷⁻⁸⁹. Resident or recruited macrophages are involved in clearing pathogens, apoptotic cells and they are also involved in antigen presentation to T-cells ⁹⁰. Macrophages kill pathogens by phagocytosis and releasing of toxic compounds. The action of released compound goes beyond virus and thus also kills host organism cells. Cells debris is also cleared by phagocytosis process of macrophages. Neutrophils are recruited cells that once activated assist viral clearance by phagocytosis, extracellular release of toxic compounds and by trapping and killing them by the neutrophil extracellular traps. Toxic function of neutrophils is also non-specific and therefore leads to tissue damage. Natural Killer (NK) cells are resident or recruited cells that can recognize and kill IAV infected cells by two basic mechanisms: natural cytotoxicity and Antibody Dependent Cell Cytotoxicity (ADCC). NK cells are activated by PAMPs or by Type I IFNs and carry out their killing activity through releasing toxic compound or FAS-ligand induced apoptosis. ADCC mechanism permits to better restrict the cytotoxic activity to infected cells taking advantage of the specificity of antibodies to recognize pathogens.

In summary, the innate immune response is needed to recognize IAV during the first phase of infection. Innate immune responses are known to orchestrate adaptive immune response⁹¹. The effectiveness in clearing virus at this stage will influence the involvement of the adaptive response.

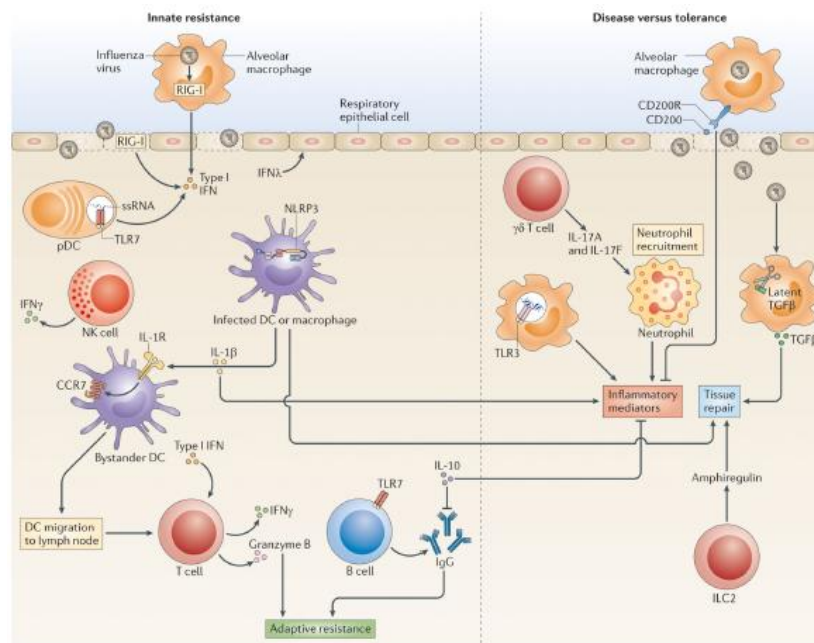


Figure 6. Mechanisms of resistance, disease and tolerance in mice. Innate resistance (left) is conferred by type I and type III IFNs that are secreted upon stimulation of RIG-I in infected cells and TLR7 in plasmacytoid dendritic cells (pDCs). Type I IFNs act on most cells, whereas type III IFN (IFN λ) acts on epithelial cells to block virus replication. DCs and macrophages that are infected with IAV release IL-1 β , which enables bystander DCs to upregulate CC-chemokine receptor 7 (CCR7) expression and migrate to the draining lymph nodes to stimulate T cells. NLRP3 signalling pathway also increases disease tolerance by promoting tissue repair. T cells and NK cells secrete IFN- γ to induce an antiviral state or induce the granzyme B-mediated lysis of virus infected cells, whereas B cells secrete antibodies to viral antigens to mediate adaptive immune protection of the host. The balance between these negative and positive regulators determines whether the host succumbs to disease or can enter a state of tolerance (right). ILC2, type 2 innate lymphoid cell; ssRNA, single-stranded RNA. Based on Iwasaki et al. 2014⁸⁴.

Chimera cell, half innate and half adaptive.

$\gamma\delta$ T cells play a great variety of roles in innate and adaptive immune responses due to their half way nature; those roles are briefly summarized in figure 7⁹². $\gamma\delta$ T cells, like the other cells of the innate immune system, can be activated through PRRs and/or cytokine receptors and respond without requirement of a prior extensive clonal expansion⁹³. However, their halfway nature with cells of the adaptive immune response permits them to be activated through the TCR too. Moreover, their capacity to be primed, expanded and even to generate memory like “conventional” adaptive Lymphocytes have been observed in some circumstances⁹⁴. The $\gamma\delta$

version of the TCR molecule seems to be able to recognize antigens in a MHC independent way including soluble or cell surface proteins, small peptides, phospholipids, prenily-pyrophosphates, and sulfatides ⁹². Their effector function in infection is based on releasing inflammatory and effector molecules by which they kill infected cells. Contribution of $\gamma\delta$ T cells to combat IAV infection is still partially unknown; however, it has been reported that they are able to kill some type of cells infected by IAV ⁸⁹.

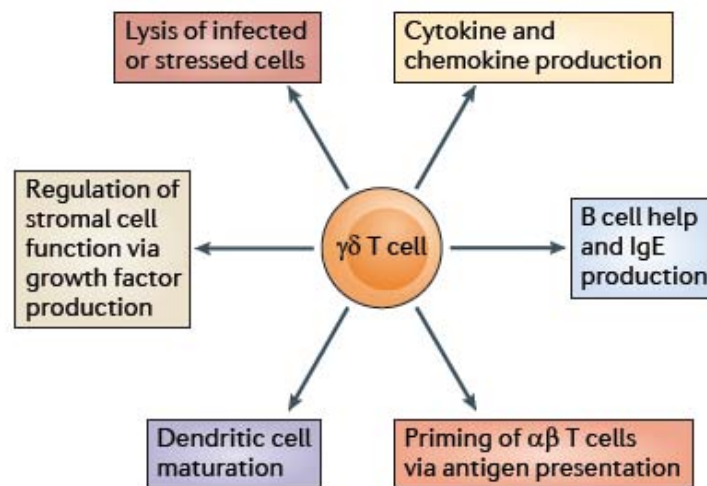


Figure 7. Six of the best $\gamma\delta$ T cell known functions ⁹². One, $\gamma\delta$ T cells can directly lyse and thereby eliminate infected or stressed cells through the production of granzyme. Two, they can produce a diversified set of cytokines and chemokines to regulate other immune and non-immune cells. Three, they can provide help for B cells and promote the production of IgE. Four, they can present antigens for $\alpha\beta$ T cell priming. Five, they can trigger DC maturation. And, six, they can regulate stoma cells function through the production of growth factors. Based on Vantourout et al. 2013 ⁹².

Antigen presentation and triggering of the adaptive immune response.

The ability to present antigens for triggering the adaptive immune system is restricted to certain cell types, called Antigen Presenting Cells (APC). Antigen presentation in APC has been generally studied in Dendritic cells (DCs) ⁹⁵; thus this process is here described referring to them. DCs play a key role in bridging innate and adaptive immune responses following IAV infection. The bridge nature of DCs lies on their ability to sense pathogen and signalling out (like the innate immune system cells) and to mount and regulate the adaptive immune response ⁹⁶. Dendritic cells are divided in different subset which distribution is tissue dependent⁹⁷. In lungs, two main DC types can be found: conventional DC and plasmacytoid DCs. In the first type, further subsets could be defined depending on the tissue localization;

those cells are specialized in process and present antigens. In contrast, pDCs are more specialised in sensing and producing cytokines. In inflammation conditions, this heterogeneity can be further enriched by recruited monocyte derived DCs. Draining Lymph Nodes (LN) migration of DCs is followed by activation. Adaptive immune response is mounted there through antigen presentation to T cells^{96,97}. However, it has been also recently demonstrated that B or T cells dependent immune responses can also be mounted in the site of infection and in particular in secondary lymphoid tissues induced by IAV⁹⁸; those are located in the lungs and have been named inducible Bronchus-Associated Lymphoid Tissue (iBALTs).

T cells differentiation requires three basics signals^{99,100}. Signal 1 is delivered through the T-cell receptor (TCR) when it recognizes an appropriate peptide–MHC complex (pMHC). Signal 2 is referred to as “co-stimulation” and it is mainly mediated through the CD28 when it engages CD80 and/or CD86. Signal 3 is mediated by ILs and factors like TGFβ. The first two signals are exposed on APC while the third signal is depending on the microenvironment to which the cells are exposed. The Major Histocompatibility Complex molecules class I (MHC-I) or class II (MHC-II) (which are part of the first signal) have epitope presenting functions and are differentially recognized by different T cells subsets. This discrimination depends on CD4 and CD8 receptors, which are TCR co-receptors differentially expressed by T cells; generally speaking, CD4⁺ T cells subsets are recognizing MHC-II molecules whereas CD8⁺ T cells subsets are recognizing MHC-I molecules. Those discriminations lead to different T cell responses to IAV infection or vaccination as described in the next sections. DC are likely to be the primary population responsible at least for the induction of IAV specific CD8⁺ T cells responses. However, the primary route of antigen uptake *in vivo* is still unclear¹⁰¹. Two mechanisms have been described: through direct infection with IAV or through phagocytosis of either dead or dying cells.

It is generally known that the route undertaken by the antigen will influence the class of the MHC by which it will be presented. Three main routes have been described (Figure 8)¹⁰²⁻¹⁰⁴. In the first route, antigens found at the cytoplasm compartment, usually expressed in the cytoplasm, undergoes proteasoma cleavage to generate peptides of different length; those are then further cleaved by peptidases at the endoplasmic reticulum (ER) compartment. Then, peptides are transported through specific proteins named Transporter Associated with antigen Processing (TAP). Peptide Loading Complex loads the generated peptides into the MHC-I and then those peptide-MHC complexes (pMHC) are transported to the surface. In the second pathway, antigens are coming from an extracellular source and they are uptaken by APC

through different processes. Antigens could enter the endosomal route, where they are degraded by proteases and loaded into MHC-II molecules for cell surface display. Intracellular antigens can also enter the normal class II pathway through a process called Autophagy¹⁰⁵. In the third route, antigens from extracellular source are uptaken by cells as the normal class II pathway does. However, the antigens in the late endosome are preserved or just partially cleaved by proteases; thus they are transported to the cytoplasm and processed through the classical class I pathway. This route is referred as Cross-presentation pathway¹⁰⁵.

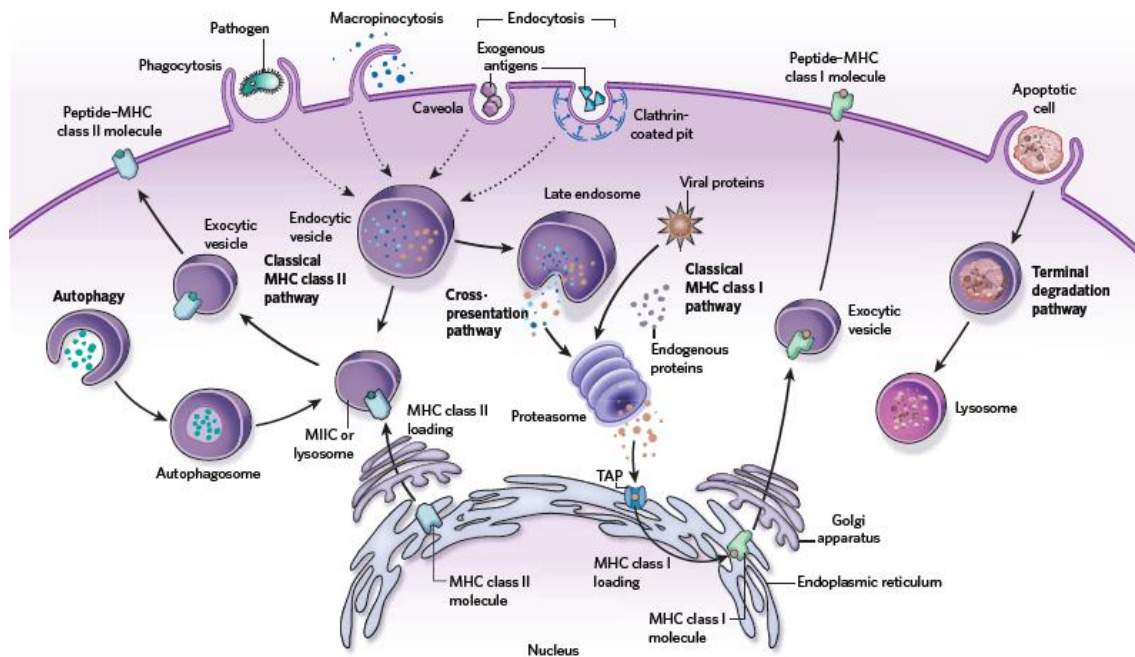


Figure 8. A simplified view of antigen presentation by DC (humans, mice). Left, exogenous particles, proteins or pathogens can be taken into the cell through various pathways, including phagocytosis (for particles $>1 \mu\text{m}$), macropinocytosis ($<1 \mu\text{m}$), and endocytosis from caveolae ($\sim 60 \text{ nm}$) or clathrin-coated pits ($\sim 120 \text{ nm}$). Exogenous antigens are then processed in endocytic vesicles. Processed antigen (peptide) is subsequently loaded onto MHC-II molecules (which have been assembled in the ER, transported through the Golgi apparatus and targeted to endocytic compartments) in a lysosome or MHC-II compartment (MIIC). The peptide–MHC-II complexes then move through exocytic vesicles to the cell surface, where antigen presentation occurs. MHC-II loading of endogenous antigen provided by autophagy can also occur, particularly when the cell is under stress. Right, antigen can be loaded onto MHC-I molecules through two main pathways. In the classical pathway, endogenous or viral proteins in the cytosol are processed through the proteasome, transported into the endoplasmic reticulum through the molecule TAP, loaded onto MHC-I molecules, and then transported through the Golgi apparatus and exocytic vesicles to the cell surface for presentation. In addition, exogenous antigens that have been phagocytosed, macropinocytosed or endocytosed can be cross-presented on MHC-I molecules by some subsets of DC. In this pathway, antigen either may be loaded in endocytic compartments (not shown) or may escape endosomes and arrive in the cytosol, where it is processed through the proteasome as usual, loaded onto MHC-I molecules and transported to the surface. Finally, terminal degradation pathways can occur (for example when apoptotic cells are internalized). Based on Hubbell et al. 2009¹⁰⁵.

Cleavage activities during antigen processing generate peptides of different length; however, each MHC class prefers peptides of specific length. This is due to structural differences of the MHCs, which can be appreciated in figure 9¹⁰⁶. It is generally accepted that MHC-I binds short peptides (9-10 aminoacids, but longer peptides have been observed) as its binding cleft is closed at the edges; in contrast, MHC-II has got open edges and thus the length of hosted peptide molecules can be larger.

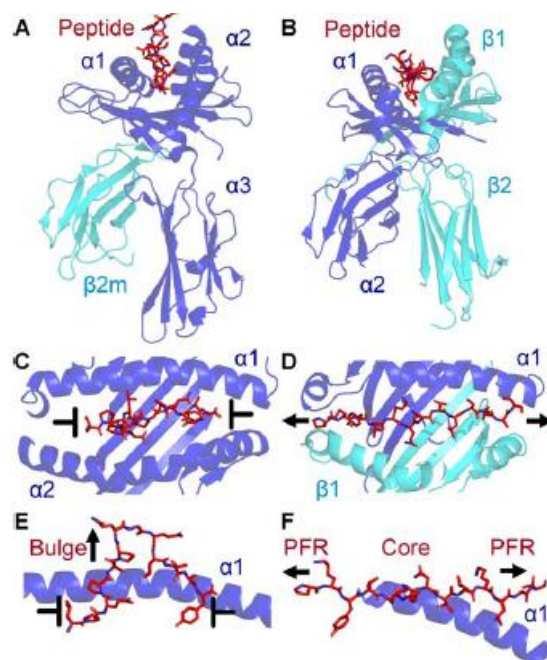


Figure 9. A structural comparison of MHC-I and MHC-II peptides complexes. Although the subunit compositions of (A) MHC-I (PDB: 2AK4) and (B) MHC-II (PDB: 3S4S) are different, the structural conformation they assume is very similar, illustrating their shared role in presenting antigenic peptides (red) to T-cells. (A) MHC-I is comprised of 3 α -chain domains ($\alpha 1$, $\alpha 2$, and $\alpha 3$ in blue), which constitute the heavy chain and β -2-microglobulin ($\beta 2m$) (cyan), whereas (B) MHC-II is comprised of $\alpha 2$ domain α -chain (blue) and $\alpha 2$ domain β -chain (cyan). (C) A top down view of the MHC-I binding cleft demonstrating the closed conformation of the cleft and (D) the MHC-II binding cleft demonstrating how the open cleft enables the peptide to extend from either end (colours as in A and B). (E) Side view of pMHC class I showing how the closed conformation of the cleft forces the central residues of the peptide up in a bulged conformation. (F) Side view of pMHC class II showing how the open ended peptide binding cleft enables the peptide to lie flat and extend. Based on Bhati et al. 2014¹⁰⁶.

Other cell types, a part from DCs, have been shown to be involved in antigen presentation and triggering of adaptive immune responses. Macrophages are cells carrying out various functions in the innate immune response; however, they also have antigen presenting functions and

thus they are thought to be implicated in generation of T cells response, in particular MHC-II related ^{107,108}. $\gamma\delta$ T Lymphocytes can promote indirectly antigen presentation providing help to other APC; however, they can also act as professional APC. Antigen presenting functions in $\gamma\delta$ T cells have been described in different species like mice, bovine and human ¹⁰⁹⁻¹¹¹. For example, in humans, the V γ 9/V δ 2 T cells have shown to capture antigen through endocytosis ¹¹² or phagocytosis ¹¹³, and to prime CD4⁺ or CD8⁺ T cells ^{110,114}. In V γ 9/V δ 2 T cells, antigens are thought to be uptaken from extracellular sources and to be processed through the normal pathway to be presented on MHC-II; in contrast, antigens presented by MHC-I are processed through the cross-presentation pathway ¹¹⁴. MHCs are not just used by APC to expand adaptive immune response; those molecules are also used to activate effector functions of T cells. MHC-I molecule is virtually expressed in all nucleated cells; this molecule alone permits to drive the effector function of T cells to those cells presenting epitopes recognised by their TCR ¹¹⁵. Therefore, cells infected by viruses are specifically targeted by CD8⁺ T cells. In contrast, MHC-II is preferentially expressed by APC cells allowing activation of effector functions of the CD4⁺ subsets of T cells ¹¹⁵.

Adaptive response

APC contribute to both humoral and cellular responses of the adaptive immune system. The generation of humoral response relies on the activity of B cells (Figure 10). Those are being primed, expand and differentiate into effectors cells named plasma cells and memory B cells, during IAV infection ¹¹⁶. The places where those events happen are the germinal centres (GC) of secondary lymphoid organs, including the iBALTs. Plasma cells showed different life span and thus different implication into the length of protection. Once generated, plasma cells reach specific niches in bone marrow and lungs in which they persist. IAV infection induces virus specific antibody response ^{117,118}. Protection to IAV infection relies on the neutralizing as well non-neutralizing antibodies ¹¹⁹. The first type of antibodies avoids infection of cells, while the second type can perform a larger variety of functions that are briefly summarized in figure 11. Moreover, two main antibody isotypes have been associated with protection to IAV infection. Those are IgG, which are found in blood and fluids (systemic) and IgA, whose secretory form is important for protection at the mucosal sites (local).

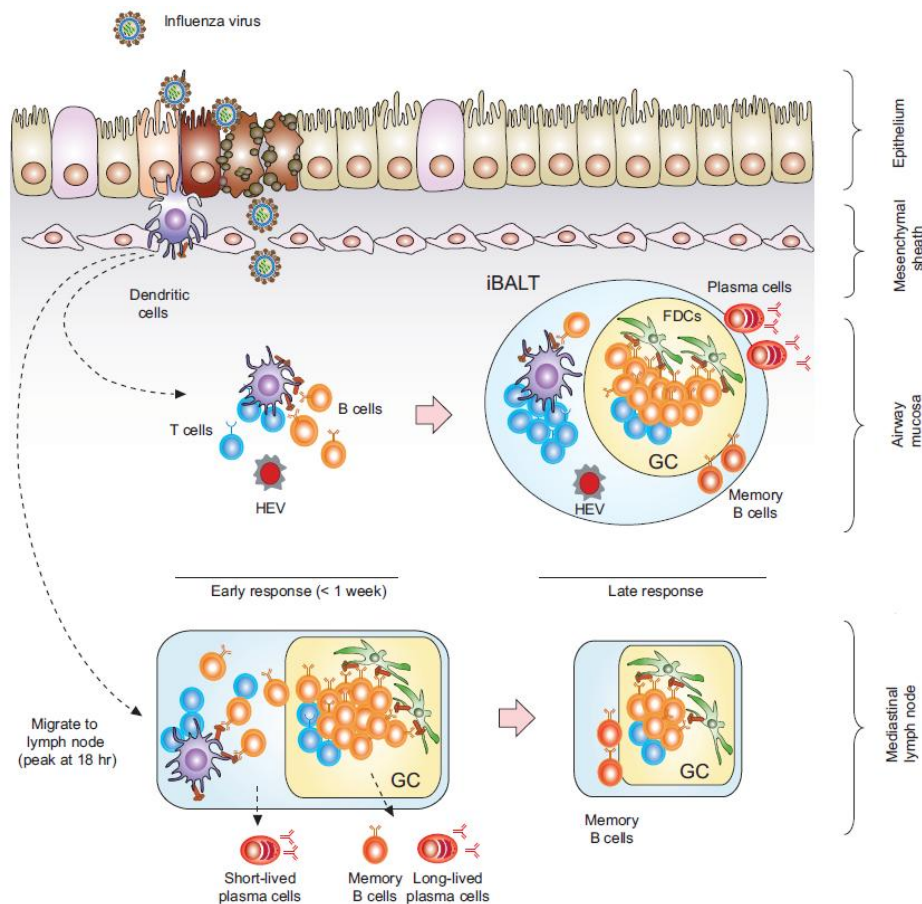


Figure 10. Primary B cell responses in lungs and Mediastinal LNs (mLN) following pulmonary influenza virus infection (mice). Infected DCs deliver viral antigen to mLN where initial priming of B and T cells and prompt supply of plasma cells takes place. mLNs also support the formation of GC which persist for a long period. One week after infection, iBALT begin to develop in inflamed lungs and support cellular niches for plasma cells and formation of GCs at the sites near virus replication. Based on Takahashi et al. 2012¹¹⁶.

Cellular Mediated Immune (CMI) response is constituted by T cells; those are a heterogeneous population of lymphocytes and so it is their response to IAV. T helper cells (Th) are the CD4⁺ fraction of the T cells. The microenvironment in which cells are found after antigen exposure, contributes to generate a great phenotypic variability of those cells¹²⁰. The classical view defined three subsets¹²¹: Th1, whose signature cytokine is IFN γ ; Th2 with IL-4; Th17 with IL-17. Those subsets polarize the immune response to be adapted to cope with intracellular microbes, helminths and venoms or finally extracellular bacteria and fungi respectively. However, a greater plasticity of Th subsets have been described (Figure 12)¹²²; thus different subsets have specialized effector functions which cooperation contributes to the above cited immune responses. The contribution to protection and mechanisms in IAV infection of the different subsets are not entirely clear¹²³. It has been reported that CD4⁺ T cells can provide protection through multiple pathways¹²⁴.

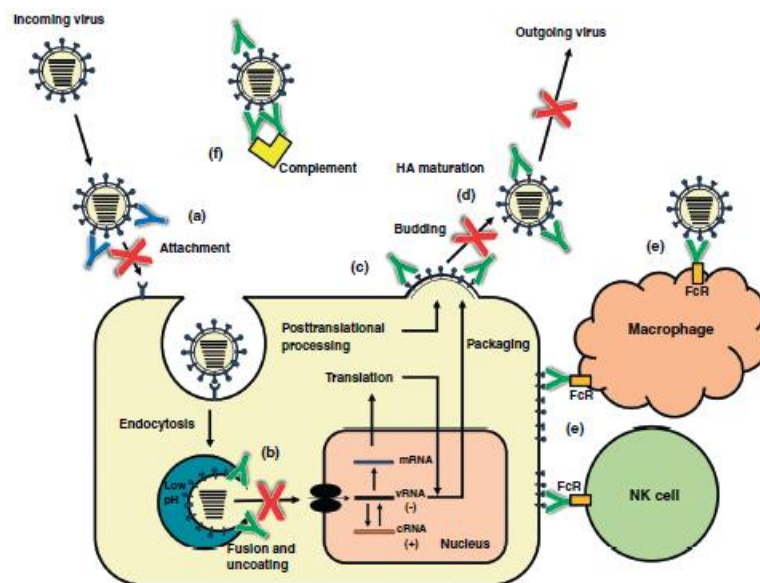


Figure 11. Alternative mechanisms of neutralization. (a) Classical HI active antibodies (in blue) neutralize by inhibiting attachment of the viral HA to sialylated host cell receptors and block entry at an early stage. (b) Stalk-reactive antibodies (green) bind to HA on the virus surface and may be taken up with the virus into the endosome. During acidification of the endosome they may prevent conformational change of the HA and inhibit release of the viral genome into the cytosol. (c) Broadly neutralizing antibodies may also inhibit viral egress. (d) Stalk-reactive antibodies may inhibit HA maturation by steric hindrance of the interaction of host proteases with the HA cleavage site. (e) Stalk-reactive antibodies may also work through ADCC, infected cells as well as viruses are killed/cleared by macrophages and NK cells. (f) Stalk-reactive antibodies have been shown to trigger complement mediated lysis of infected cells and could potentially also help to clear influenza virus particles. Based on Krammer et al. 2013¹²⁵.

Their antigen specific viral clearance function is largely dependent on IFN- γ and, to a lesser extent, perforin but this response alone is not sufficiently robust to clear high-challenge doses of virus. CD4⁺ T cells synergize with naïve B cells that act via secreting neutralizing antibodies to improve viral clearance. Finally, they synergize with CD8⁺ T cells during the phase of viral clearance and they promote CD8⁺ T cells memory. Cytolytic T Lymphocytes (CTL) are the CD8⁺ fraction of T cells bearing the $\alpha\beta$ TCR. CTL are important for viral clearance. Their effector functions against IAV infections include the ability to realize cytotoxic compounds such as perforin and granzymes, as well as being able to secrete chemokines and a variety of potent inflammatory cytokines. More IAV associated effector functions are the induction of Cell death pathways TNF α -related apoptosis inducing ligand (TRAIL) or FAS-FAS ligand¹²³. CTL can be classified into three different subsets depending on the cytokine production profile: Tc1 secreting IFN γ and TNF α ; Tc2 secreting IL-4, IL-5 and IL-13; finally, Tc17 secreting IL-17, IL-21 and IL-22. Each of those subsets is involved in protection^{126,127} against IAV infection although none of them seems to be essential¹²⁸.

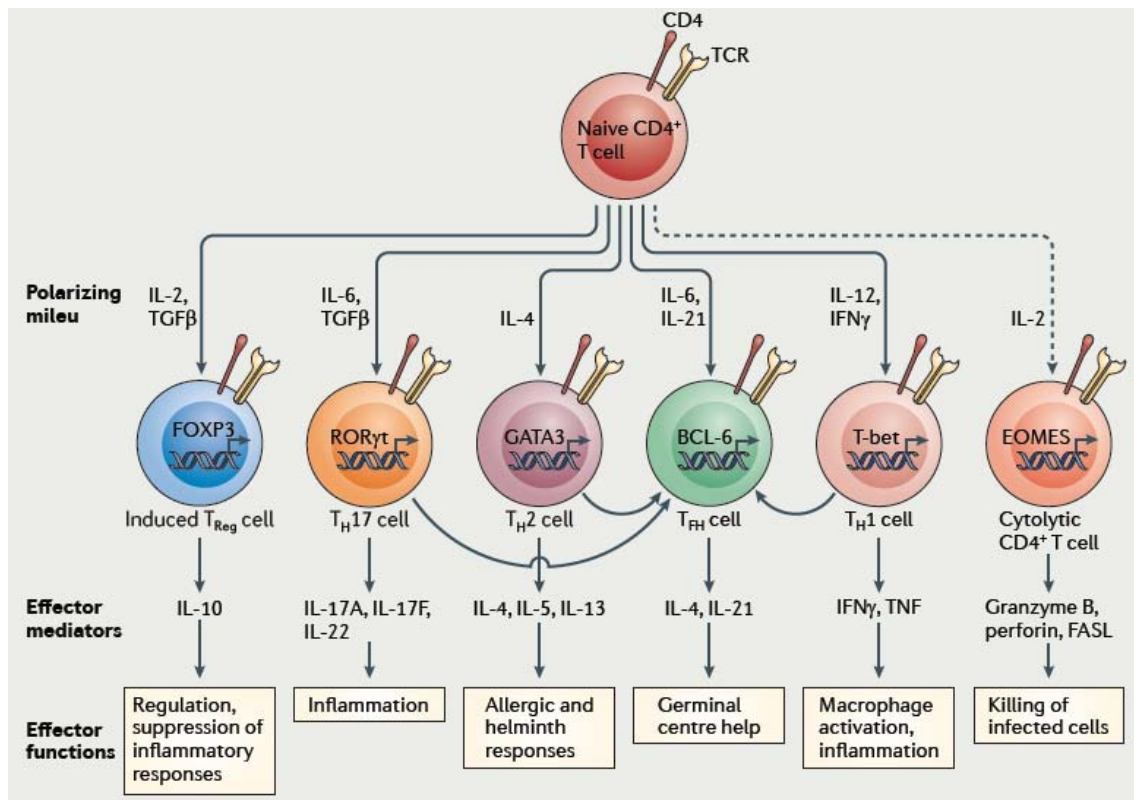


Figure 12. Subsetting $CD4^+$ T cell responses based on Th cell polarization. The polarizing milieu contributes to the polarization of Naive T cells. Differentiation of polarized effector T cells is controlled by unique sets of transcription factors (like *FOXP3*, *ROR γ δ* etc.), the expression of which is determined by multiple signals but particularly by soluble factors that act on responding $CD4^+$ T cells during their activation. Active T helper cells perform a great variety of effector function mediated by several factors (ILs, IFN, TNF etc.). Based on Swain et al. 2012¹²².

Effector functions of T lymphocytes are not just beneficial. Overwhelmed response to IAV could contribute to immunopathology. Both $CD4^+$ and $CD8^+$ could be involved; however, the exact mechanisms are not completely clear¹²⁹. As already mentioned, the immune response is a balance between antiviral and tolerance activities; in the adaptive immune system there are cells specialized in containing the immunopathology instead of the virus. Those are T regulatory cells (Figure 12) which have been demonstrated to suppress specific $CD8^+$ response to IAV through IL-10 and TGF- β ¹²⁹; therefore, limiting potential damage to the host. Effector Th and CTL cells have also be shown to have some regulatory proprieties through secretion of IL-10¹²⁹.

Presentation of antigens in the draining lymph nodes (or other peripheral lymphoid organs like spleen) contributes to priming, clonal expansion and differentiation of naive into effector T cells. The heterogeneity of subpopulation in each T cells subsets depends on the polarizing milieu. IAV effector T cells migrate to the site of infection where they perform their functions.

Here, re-stimulation by specific antigens is needed for optimal CD8⁺ T cells performance; although, for CD4⁺ T cells it is not completely clear¹⁰¹. Contraction of T cells is following viral clearance (Figure 13)¹³⁰. During that phase activated T-cell effectors die via apoptosis to leave a small but relatively stable population of memory cells; therefore, during contraction transition from effector to memory is occurring.

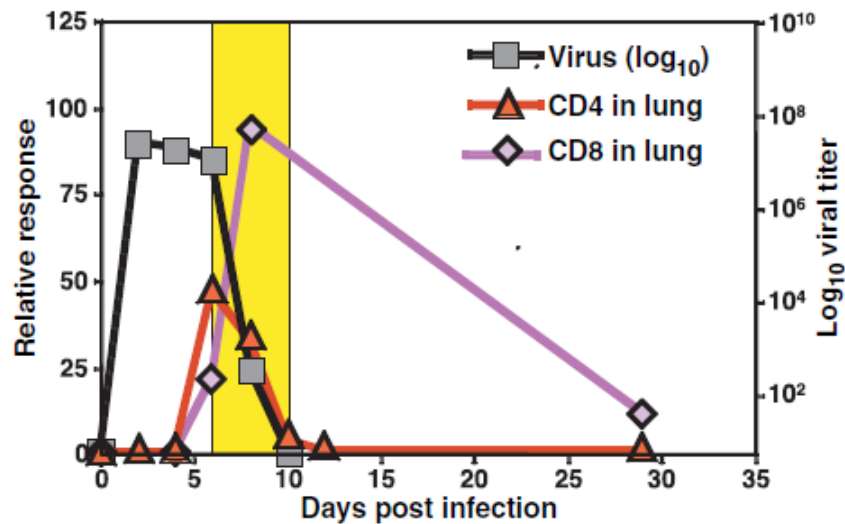


Figure 13. T-cell contraction following influenza infection (mice). Following maximal effector responses, an acute contraction phase (yellow highlighted) occurs in the lung; that is coincident with viral clearance. Based on McKinstry et al. 2010¹³⁰.

Memory T cells seem to be not lasting during all life span of an individual (at least in humans); therefore, there is a phase of: generation, homeostasis and then senescence; the maximum of protection is reached in the homeostasis phase¹³¹. Memory T cells are not a homogeneous population and thus differentiation stages can be distinguished. Recently, a model for memory generation in T cells has been proposed for human and it is reported in figure 14. T cells migrate with preference for specific tissues¹³¹; the stages from naive to Central Memory (T_{CM}) T cells have preference (this means they circulate among tissues of a specific type) for Lymphoid tissues while the Effector Memory (T_{EM}) and Effector (T_{Eff}) T cells have preference for peripheral tissues. Finally, a third stage is based on Resident Memory T cells (T_{RM}); those, in contrast to the previously described stages, persists at the site of the infection and thus does not circulate. The stages of memory differ more than just the tropism and thus difference in functionality has been described¹³¹; for example, T_{CM} proliferate more but secrete less cytokines like IFN- γ and TNF compared to T_{EM} cells.

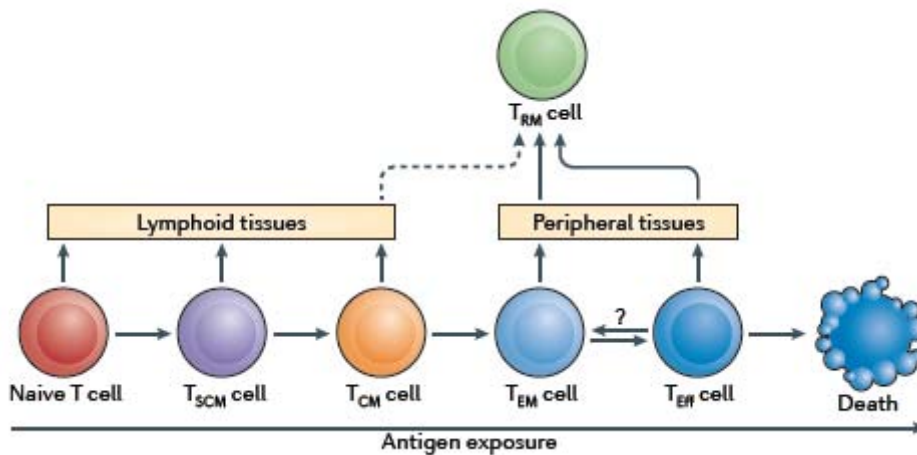


Figure 14. A model for the generation of human memory T cell subsets. The progressive differentiation of the three major circulating subsets — stem cell memory T (T_{SCM}) cells, T_{CM} cells and T_{EM} cells — from activated naive T cells is shown relative to the extent of antigen exposure. T_{Eff} cells represent terminally differentiated cells, and death is one outcome of increased antigen exposure and proliferation. Naive, T_{SCM} and T_{CM} cells circulate and migrate to lymphoid tissue, whereas T_{EM} and T_{Eff} cells are the subsets of T cells that have the capacity to traffic to peripheral tissues. T_{RM} cells in peripheral tissue sites may derive from either T_{EM} or T_{Eff} cells that migrate to these sites through tissue-specific factors. It is possible that T_{CM} cells could develop into T_{RM} cells in lymphoid sites (dashed arrow). T_{RM} cells in the peripheral compartments are probably terminally differentiated as they do not circulate or convert to other memory T cell subsets. Based on Farber et al. 2014¹³¹.

SwIV immune response. What is known in pigs.

Few studies have been studied the immune responses to IAV in pigs *in vitro* and even less have been studied this infection *in vivo*. Those were well reviewed by Crisci E. et al. 2013¹³² and briefly summarised below.

Innate Immune response

Responses of soluble PRMs have been described under SwIV infection. However, their direct implication in infection has been studied just for few of them. The previously described members of the innate cellular response have shown to be implicated in SwIV infection in pigs. Epithelial cells, DC and macrophages sense SwIV pathogen and respond with proinflammatory cytokines¹³³. However, just few PRR and pathways implicated in that process have been studied. Functionality of effector and APC (natural killer, macrophages and dendritic cells) during SwIV infection *in vivo* is still partial or it has not been described yet. However, some *in vitro* studies have analysed the interaction of porcine DC with IAV^{133,134}.

Adaptive immune response

IAV infection is inducing humoral responses in pigs similar to the observed in mice, as it can be appreciated in the model proposed by Crisci E. *et al.* 2013¹³² and reported in figure 15. B-cell clones are primed in lymphoid tissues and an antigen-specific and isotype-associated (IgM, IgG, IgA and even IgD and IgE) proliferation is induced¹³⁵. IgG and IgA are again the main protagonists due to their involvement in protection. Maternal derived antibodies also cover an important role in protection of piglets during the first weeks of life. Although they do not completely prevent infection, they reduce transmission of IAV¹³⁶.

Porcine $\alpha\beta$ T cells have been recently dissected and a model for memory and subsets, which is very similar to the human one, has been proposed¹³⁷. Studies on $\gamma\delta$ T cells are also recent in pigs. An ontogeny model has been proposed¹³⁸⁻¹⁴⁰ and phenotypes as well functional characteristics have been partially studied^{141,142}. CMI response dynamics to IAV infection in pigs¹³² resemble the one observed in other models like mice (Figure 13) in which infiltration of virus specific lymphocytes or cells of the CMI response in lungs corresponds with a drastic decrease of viral titre. This suggested the involvement of the CMI system in the response against IAV in pigs. However, no study has demonstrated their role in protection or viral clearance. Staining based on the CD3, CD4, CD8 and $\gamma\delta$ TCR showed the involvement of some population of lymphocytes in IAV infection responses¹⁴³⁻¹⁴⁵. Just few works were able to properly differentiate those populations showing that CTL, T helper, T regulatory and $\gamma\delta$ T cells were responding to IAV infection in periphery and/or in the site of infection^{135,146-148}. It has been showed that $\alpha\beta$ TCR cell response is oligoclonal and therefore antigen specific¹³⁵. The effector functions of the CMI responses to IAV have been associated with IFN- γ and proliferation^{146,149,150}. Recently, multifunctional CD4⁺ T cells have been identified in peripheral blood of infected pigs; those were double or triple producers of IFN γ , TNF α and IL-2¹⁴⁸. In the same study, CTL responses were also multifunctional involving mainly IFN γ and TNF α ¹⁴⁸. $\gamma\delta$ T cells, T helper cells and CTL cells have been also shown to be involved in IFN- γ response^{143,144,151}. However, none of them discriminate with accuracy T cells lymphocyte nature, T helper (CD4⁺CD8⁺) or CTL (CD8⁺) by CD3 staining. Interestingly, it has also been showed that $\gamma\delta$ T cells could also respond by IL-10 secretion to IAV infection¹⁴⁴ and therefore they could be involved in regulatory responses. In summary, the effector mechanisms and the subpopulations of the CMI responding to IAV infection remain a matter of further studies.

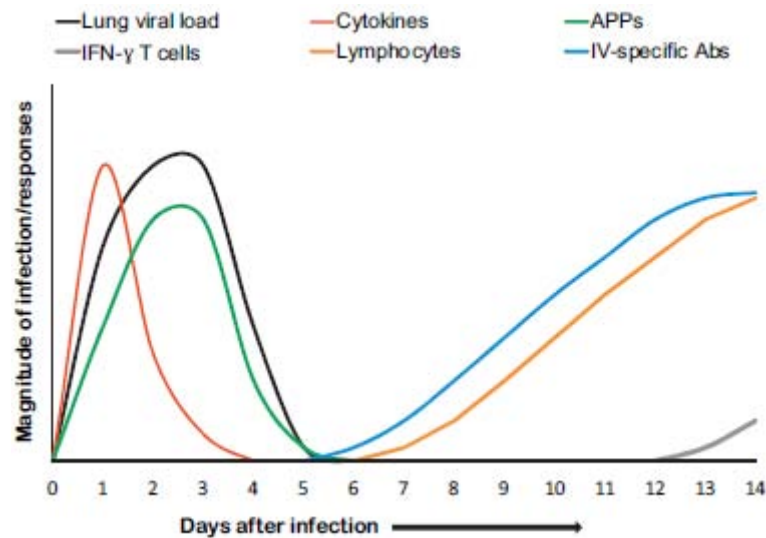


Figure 15. SwIV infection in pigs. General kinetics of lung viral load, acute phase proteins (APPs), cytokines (e.g. $TNF-\alpha$, $IL-6$, and $IL-8$) and different immune system components (lymphocyte, $IFN-\gamma$ producing cells and IAV specific antibodies (IV-specific Abs) during infection with different SwIV (H_1N_1 and H_3N_2) in pigs. The magnitude of responses is related to the days after infection (0–14). Based on Crisci et al. 2013¹³²

Rational design of vaccines against IAV– Reverse vaccinology for the rational design of pigs vaccines

IAV vaccines

Inactivated vaccines were the first to be developed for IAV and they are still largely used in humans. Current inactivated vaccines are composed by the whole killed virus, split virus (Split vaccine) and finally by just HA and/or NA proteins of the virus (subunit vaccine) (Figure 16). Another commercially available vaccine is constituted by an attenuated form of the IAV that is temperature sensitive and cold adapted; therefore, it is able to infect but it is not pathogenic. Novel vaccines reduce viral content to few parts of the virus but at the same time give relevance to more than HA and NA as immunogens. Those are coupled to adjuvant and/or proteins with carrier function (e.g. flagellin in subunit HA stalk vaccines) or delivery functions (e.g. viral vectors and plasmid based vaccines) (Figure 16). Novel vaccines are not yet commercially available for IAV. The main target of current inactivated vaccines is the generation of protecting humoral immune responses directed to HA. As previously mentioned, surface glycoproteins are highly variable; there are a lot of different subtypes and even subclades which usually induce a little or no cross reaction. Therefore, the major problem

related to current inactivated vaccines has been antigenic drifts and shifts of IAV which lead to a decrease of vaccine efficiency¹⁵².

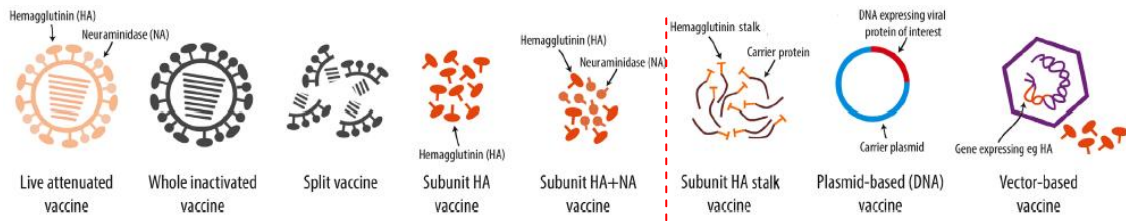


Figure 16. Range of current and new vaccine presentations against IAV¹⁵³. Current vaccines are showed on the left of red line, while novel vaccines are on the right hand side. Based on Reperant et al. 2014¹⁵³

Live attenuated influenza vaccines contain a defective virus, which replicates just in the upper respiratory ways without causing classical influenza illness. Those are able to generate specific IAV humoral and CMI response. However, they are only available for healthy individuals aged 2-49 years; the efficacy is controversial and it seems to be related with the age of the target population¹⁵⁴. Moreover, taking into account the cross reacting proprieties of the induced immune responses it needs to contain more than one virus subtype. IAV antigenic drifts and shifts force a periodical update of the strains contained in the vaccines. World Health Organization (WHO) analyses IAV surveillance data generated by the WHO Global Influenza Surveillance and Response System and issues recommendations on composition of vaccines for the following influenza season. Therefore, if circulating strains are matching the strain in the vaccine, this formulation would be kept for the next season. In contrast, if they are mismatched, a new reference strain would be introduced to keep vaccine efficacy standards. Figure 17 shows that some strains have been kept for long period during past IAV seasons (like in H₁N₁ subtype) while others have been changed yearly (like in H₃N₂ subtype). This system is quite efficient; however, lack of a complete knowledge of IAV and its unpredictability are the mayor pitfalls. pdmH₁N₁ is the clear example of system failing; the virus has been silently evolving in its animal reservoirs and suddenly jump to humans; therefore, it was not detectable by the normal surveillance system. Moreover, the current vaccines were not able to efficiently protect due to the novelty of the antigenic characteristics of the virus¹⁵⁵. Zoonotic characteristics of IAV are actually the mayor threat to this system; thus, recently surveillance of the virus in animals reservoirs, like pigs and chickens, has been taken into account into vaccine recommendations¹⁵⁶. Vaccines able to protect against different IAV lineages (with different subtypes, from different hosts and subclades) and thus able to give efficient cross protection, would cope with those problems.

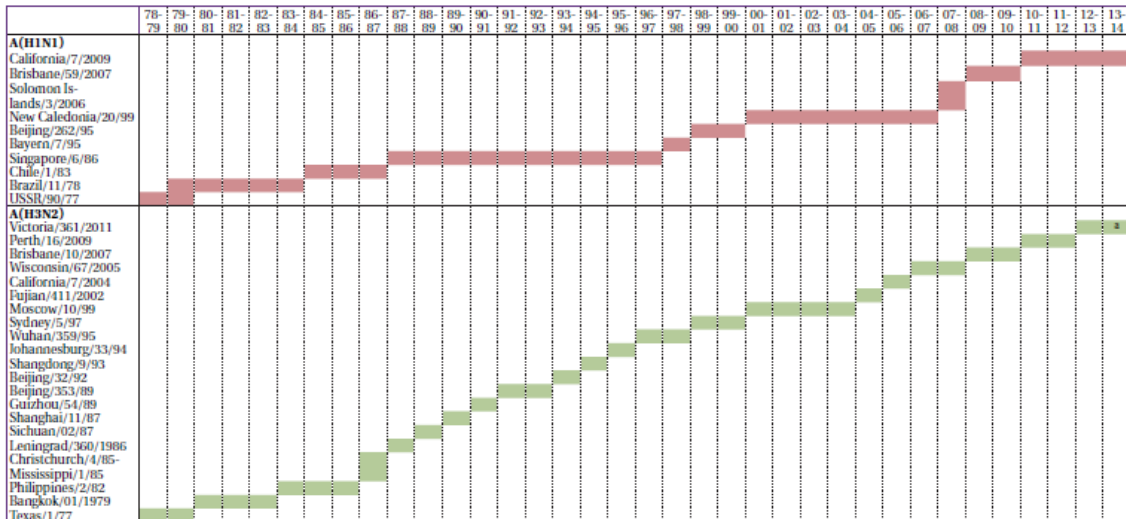


Figure 17. WHO recommendations on the composition of influenza vaccines from 1978-1979 to 2013-2014 for the northern hemisphere. The virus strains are periodically changed to match the antigenic characteristics of the circulating strains. Based on Noh et al 2014¹⁵⁴.

Rational design of vaccines

Empirically developed vaccines dominate the first era of vaccination and they are still widely used¹⁵⁷. However, they have safety and efficacy concerns, which are tried to be solved through rational design of vaccine (RDV). Figure 18 shows two examples of RDV applied to inactive or live pathogens¹⁵⁸.

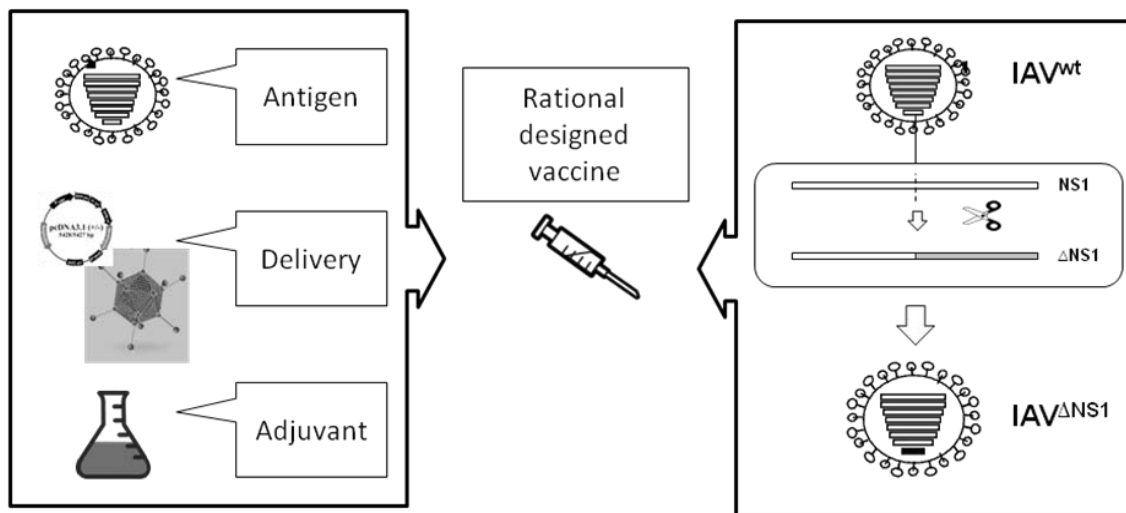


Figure 18. Example of rational designed vaccines. Left side: pathogens are reduced to antigens (subunit or peptides) and coupled to a delivery system (plasmids or viral vectors) and adjuvant. Right side: Virulence of the pathogen is reduced by deleting or editing specific factors; however, its infection abilities are maintained to generate a live attenuated virus. In the example (based on the work of Choi et al. 2015¹⁵⁹), NS1 of IAV is truncated.

In both cases, factors representing safety threats are removed and factors that could increase efficacy are coupled to pathogens antigens; in this case, a delivery system facilitating its transport and an adjuvant improving adaptive immune system responses are coupled.

Recombinant DNA and Reverse Vaccinology (RV) have been the motor of the development of the RDV¹⁶⁰. RV is a science in which knowledge of the genome leads to vaccines¹⁶¹. *In silico* mining has an important role permitting to narrow the laboratory work required for antigen identification.

The process starts from large databases that make available genomic sequences of pathogens; those are then used by bioinformatics softwares allowing to determinate a large range of proprieties including: predicted protein sequence, localization or predicted antigen sequence. Bioinformatics softwares have a great variety of function and their application depend just on the case studied. The identified antigens are then tested in laboratory.

Bioinformatics in reverse vaccinology – antigen prediction for T cells response.

Bioinformatics is already integrated in the process of RV. It is providing tools for data analysis and prediction which can be applied in multiple steps constituting the pipeline of vaccine discovery¹⁶¹. Prediction of immunogenicity is one of the pivotal roles of bioinformatics in RV, which looks for predictions in regions of the proteins from each pathogens that are recognized by the humoral or cellular adaptive immune response (epitopes). Correct identification of epitopes recognized by antibodies is crucial to design molecules that potentially mimic protective epitopes; unfortunately, the available tools for prediction are not accurate enough due to the complexity of the prediction¹⁶².

As previously mentioned, T cells epitopes have to be exposed on the cell surface by the MHC, in order to be recognized by the TCR. Prediction of the immunogenicity for T cells epitopes primary relies on the determination of the binding parameter of peptides to the MHC¹⁶³. Bioinformatics software predicts the sequences of possible MHC binders from the aminoacidic sequence of target proteins through the use of algorithms (Figure 19). The algorithms are used to train and generate prediction model (usually specific for one MHC) using experimental binding data. Depending on the nature of the data, the models can be mainly categorized into Quantitative Binding Affinity Models and Binding Pattern Recognition Models. The first uses quantitative experimental data of binding (affinities) to predict the binding strength of epitopes; the second uses qualitative experimental data (binary data: binder or no binder) to predict the binding propriety of epitopes. A third category of data is structure based; those are

3D structures from already determined peptide-MHC complexes (pMHC) that are used to generate the most recent modelling based algorithms.

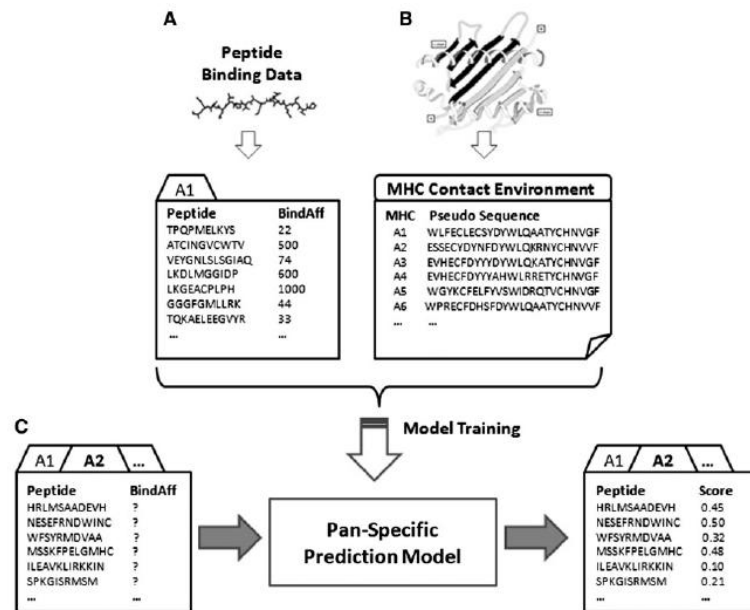


Figure 19. Schematic illustration of bioinformatics prediction by pan-specific methods. A) Peptide binding and B) MHC pseudosequence are two types of major data incorporated in training. C) It shows the trained model using binding data of A1, making predictions for a new A2 allele and other alleles. Based on Zhang et al. 2012¹⁶⁴

The models discussed are generally specific for each allele and experimental binding data is not always available. The *pan* methods of the Centre for Biological Sequence analysis (<http://www.cbs.dtu.dk/index.shtml>) allow solving this problem. Those methods allow predicting not just the binding characteristics of the epitopes to the MHC, but they predict even the binding preferences of virtually all MHC with known sequences (Figure 19)^{165,166}. This is because the prediction models are generated from both types of data, experimental epitopes binding data and pseudosequences of the MHC; being the latter the minimal position of the MHC that influence the epitope binding. Therefore, *pan* methods are useful for veterinary species in which the knowledge of MHC binding preferences is still incomplete.

MHC molecules of class I or class II have structural differences with functional implications in the binding propriety to peptides and also in the specificity to T cells subsets, as already explained in previous sections. Therefore, bioinformatics softwares offer the possibility to make predictions for one or the other class of MHC. Binding of epitopes to MHC is used as pivotal parameter for immunogenicity predictions; however, other factors could be crucial too. The processing pathways preceding the presentation to MHCs can influence the availability of some epitopes into the MHC charging process¹⁶⁷⁻¹⁶⁹; for examples, some epitopes could not be

formed during proteases cleavage but they could not be transported from the cytoplasm to the ER. Software for predicting the activity of factors like the Proteasome and TAP functions have therefore been developed and successively integrated into the MHC binding assays^{170,171}. In that way, just the epitopes that are made available to the MHC are taken into account for binding predictions and thus the performance are increased (Figure 20).

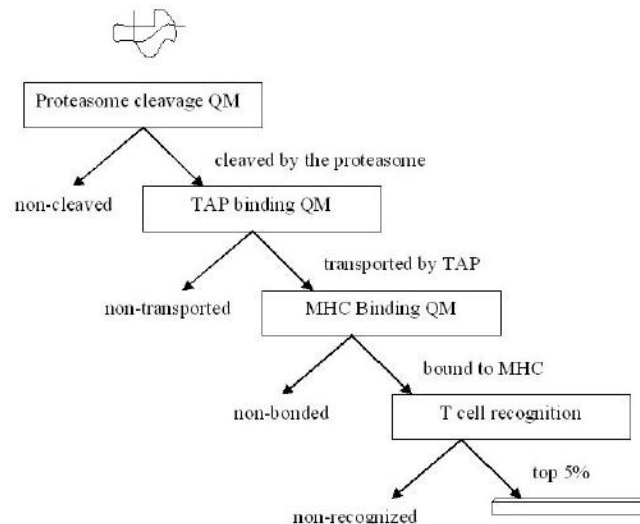


Figure 20. Pipeline of Epijen software analysis. This software integrate Proteasome cleavage and TAP binding preference to narrow the MHC binding prediction just to the peptide that have been made available after protein cleavage and transport to the ER. Based on Doytchinova et al. 2006¹⁷⁰.

MHC-I epitopes binding assays

The strength of binding (equilibrium dissociation constant, Kd) of peptides for MHC-I binding cleft is a predictor of CTL immunogenicity, as cited above. Assays characterising the affinity of peptides for the MHC (binding assays) can be used to generate prediction software or to validate predictions. The affinity is experimentally intended as the amount of peptide leading to the formation of 50% of the maximal p-MHC complexes; thus to obtain this value, the peptides must be titrated on MHC molecules.

Translation of RV technologies in pigs.

The recent advances in pig immunology allow a better understanding of host-pathogen interaction permitting to rationally design vaccines. Databases of pathogens genomes have been recently updated thanks to the recent lower cost of sequencing technologies. However, there is still lack of reliable tools for *in silico* prediction of antigen immunogenicity. This problem arises from the lack of experimental data without which, the prediction algorithms

cannot be generated. Looking at the Immune Epitope Database ¹⁷² we can observe that despite the large number of deposited T cells epitopes identified by functional methods (IFN- γ release or proliferation assays) in pigs, there is no MHC-II epitope and just few and recently published MHC-I epitopes characterized in MHC binding assays ¹⁷³⁻¹⁷⁵. There are few Swine Leucocyte Antigen (SLA) class I (SLA-I) binding assays available and no one class II (SLA-II). The first attempts to characterize binding propriety of peptides to SLA-I were done in similar ways by Oleksiewicz *et al.* 2002 and Gao *et al.* 2006 ^{176,177}. In those works, a recombinant form of SLA folded *in vitro* was used. It was constituted by the heavy chain of SLA (SLA_hc) fused by a linker to β 2m. Peptides (free or bound in turn to the SLA by a linker) able or not to bind the SLA were then identified through antibodies recognizing the p-SLA complex or by mass spectroscopy. Those qualitative assays were not used to characterize peptides in any other publications, probably because the difficulties to apply this techniques to different SLA alleles or because time and labour expensive. A second generation of *in vitro* SLA-I binding assay was then developed and expanded to different alleles ^{173,174}. In those assays, a recombinant form of SLA-I was again used, which was formed by a chimeric heavy chain composed of human α 1 and α 2 domains and porcine α 3 domain (where the binding cleft is located). The heavy chain was folded *in vitro* with free human β 2m and peptides to reconstitute the p-SLA complexes, which was then quantitatively detected through an Enzyme-Linked Immunosorbent Assay (ELISA). The absence of specific antibodies to detect all or at least the majority of known SLA-I alleles led to the decision of using a recombinant SLA form which can be easily detected by an anti Human Leucocyte Antigen (HLA) antibody. This decision did not influence the reliability of data, at least for the analyzed alleles. The use of Positional Scanning Combinatorial Peptide Libraries (PSCPL) permitted to characterize the binding preferences of the some SLA-I alleles ¹⁷⁴ and thus generated available data for the development of prediction algorithms. However, those data have just been recently generated and no SLA allele specific prediction tools have been developed.

The only available prediction tool applicable to SLAs of both classes are those using *pan* methods. NetMHC*pan* showed high accuracy of prediction for SLA-I ¹⁶⁵ and it has been recently used for the identification of epitopes in Foot and Mouth Disease Virus, Classical Swine Fever and even SwIV ^{173,178,179}. A pipeline for identification of class I epitopes in pigs allowing to have higher success rate is shown in figure 21.

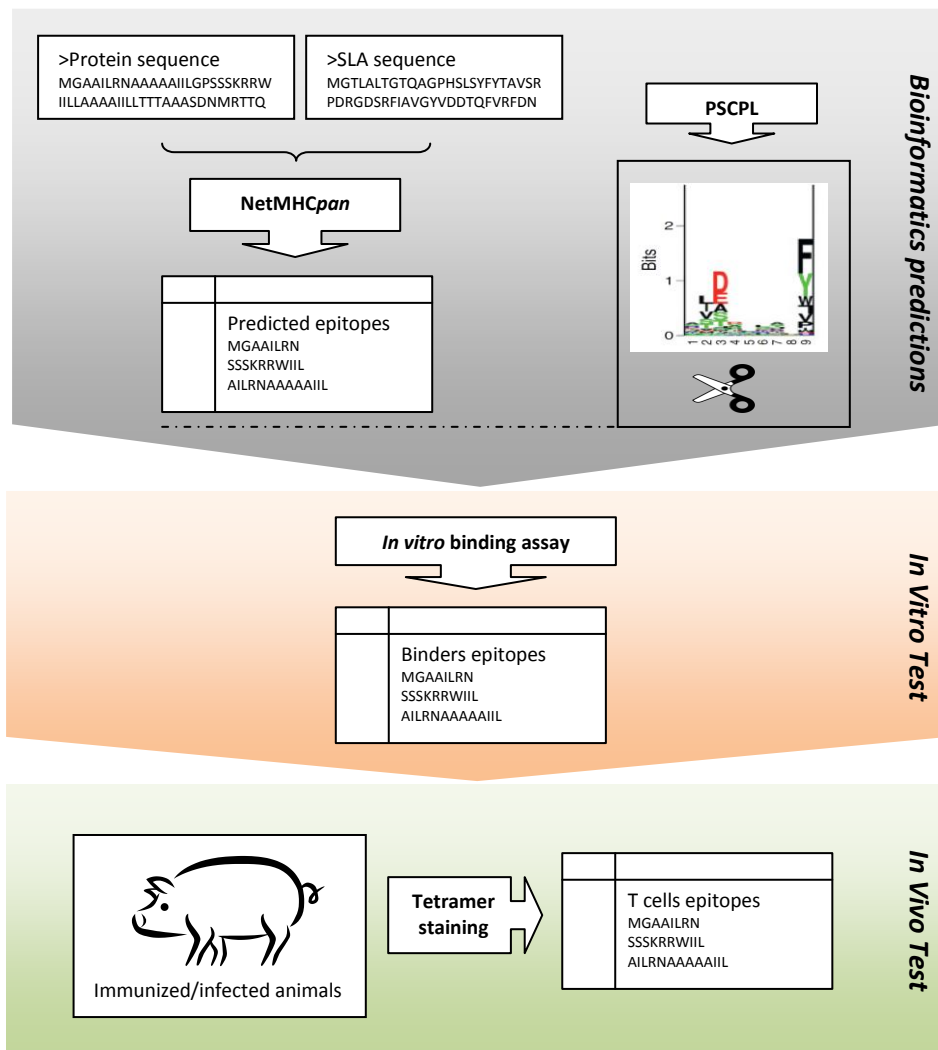


Figure 21. Pipeline for SLA-I T cells epitopes discovery. PSCPL are used to determine the binding preference of SLA. Those last are represented as LOGO; the example shows that SLA-1*0401 has binding preference for specific aminoacids at positions 2, 3 and 9¹⁷³. Those data are used as cut off on the predicted peptide; therefore, the peptides showing consistency between NetMHCpan and the PSCPL are then tested *in vitro*. Finally, those peptides that bind to the SLA are used to generate tetramers and thus they are tested *in vivo* on animals immunized or infected with the target pathogen. Based on Pedersen et al. 2014¹⁷⁸

This pipeline combines the predictions of NetMHCpan with the *in vitro* determined binding preference of the target SLA (determined by PSCPL). Candidate peptides are then characterized in an *in vitro* binding assay. This system drastically reduces the number of peptides to be tested *in vivo* or *ex vivo*. In this way, laborious and expensive but more accurate technologies like the tetramers can be applied. In summary, whereas SLA-I binding preference are being characterised *in silico* or *in vitro*, SLA-II are still uncharacterised due to the lack of both *in vitro* and *in silico* technologies. *In silico* pan method for SLA-II are available but they have not been yet tested nor used in pig.

Influenza vaccines and their rational design in pigs

Vaccines for pigs against IAV exhibit the same problems as their human counterparts. Antigenic drift for SwIV has been described, although it is weaker than human IAV. In contrast, there are a great variety of IAV lineages circulating in pigs, which are the result of recombination events, highlighting the importance of this event in that specie. However, the most important concern is the susceptibility of pigs to cross specie transmission of IAV. The available commercial vaccines are based on inactivated whole or split virus. The epidemiology situation of SwIV is directly influencing vaccines efficacy. For example, in USA SwIV have become increasingly diverse; updating strains in commercial vaccines has fallen behind and in response, autogenous (made by the exact strain circulating in the farm) vaccines have become common among USA swine producers¹⁸⁰. In Europe, the strains contained in vaccines have been updated with very less frequency, and just recently a trivalent vaccine has been commercialized to cope with the new circulating H₁N₂ subtype. A recent study showed that, although the virus is evolving, the old vaccines might be still efficient to cope with SwIV infection of circulating strains¹⁸¹. The efficacy of homologous or autogenous vaccines is unclear, probably due to the inconsistency of vaccines formulations and type of viruses used for challenges. Clinical signs and transmission are certainly reduced and sometimes they are even avoided. However, the immunity induced is not sterilizing and animals still show infection¹⁸¹⁻¹⁸⁴.

In a recent study, a mathematical model predicts that the most common vaccination strategies are ineffective in eliminating or even reducing IAV infection in a breeding herd, as the virus can still be found in piglets regardless of target population or vaccine type¹⁸⁵. The major problem of inactivated vaccines is still the protection against heterologous SwIV (protection against a different subtype or SwIV lineage or HA clustering). Inactivated vaccines can induce partial protection, which can reduce viral transmission^{182,183,185}, or no significant protection¹⁸⁴. In some cases, even vaccine-associated enhanced respiratory disease has been observed^{186,187}. The observed weak heterologous protection induced by inactivated SwIV vaccines could be derived from CMI responses as well as from cross reacting antibodies; however, this issues have not yet been fully addressed.

Influenza vaccines for pigs are adjuvated and therefore compared to humans vaccines, they might be better at boosting CMI responses. Inactivated vaccines are able to induce IFN γ secreting CMI response against homologous or heterologous SwIV, which has been associated

at least with the Th effector /memory cells^{188,189} and CTL cells¹⁸⁸. Proliferative response of CMI specific for SwIV has been detected too after vaccination with inactivated virus¹⁹⁰. A different study associated this response with Th effector/memory cells, but also with CD4⁺ and CD8⁺ T cells¹⁹¹. Analysis of CD25 (α chain of IL-2 receptor) confirms those results, showing up-regulation in T helper^{188,189}, but also in CD4⁺ T cells and CTL cells (CD8⁺ $\gamma\delta$)¹⁸⁸. Regulatory functions have been also associated with T helper cells after vaccination with inactivated SwIV, which showed IL-10 responses to homologous or heterologous virus recall^{188,189}. A very recent study showed that vaccines are able to induce SwIV specific T cells and several class I epitopes have been identified by tetramer technology¹⁷⁸. In addition, it was suggested that CTL subsets might possess multiple specificities as they could to be stained even by tetramers bearing epitopes mutated compared to the immunization strain. This means that CMI response, apart from recognizing conserved epitopes in the internal proteins of IAV, might possess a broader cross reactivity due to a TCR recognition flexibility, which permits recognizing epitopes even in case of mutations. Detection of SwIV specific CMI induced by vaccination sometimes is not detectable¹⁹². This might depend on the different vaccine formulation or strategy adopted. In a recent study, vaccination of pigs with adjuvated vaccines induced a better CMI response compared to the non adjuvated one¹⁹¹. The generation of a broadly protecting CMI response is not just a concept in pigs. Different platform of rational designed SwIV vaccines are being investigated, including Live attenuated, Subunit, DNA and vectored vaccines¹⁹³.

General objectives

The main objective of this thesis was to identify and characterize SwIV T cells epitopes in pigs that could be used in rational design of future vaccines against SwIV. This objective can only be informed by a deeper knowledge of immune responses during host-pathogen interaction. Thus, the following specific objectives were formulated:

- 1- To update the epidemiological situation of SwIV circulating in Spain, providing and analysing genetic information of current SwIV circulating strains.
- 2- To generate an *in vitro* cell assay to characterise peptides binding abilities to particular class I SLAs.
- 3- To identify SwIV T cells epitopes in inbred pigs.
- 4- To identify class I SwIV T cells epitopes in a SLA-I defined pig herd.

Chapter I: An update on Swine Influenza epidemiology in Spain

Deep knowledge of circulating IAV will enable future rational design of vaccines. The epidemiology of SwIV is fundamental to decide about vaccine formulations and in which situation would be more effective. That differs among different continents and countries. The epidemiological situation of SwIV strains circulating in Spain needed to be updated because all genetic information were few and old. Serological information is limited to the antigenic evolution of surface glycoproteins and their distribution. In contrast, genetic data gives more deep information about the evolution and distribution not only on the surface but also about internal proteins. This is very important considering the peculiarity of drift events in IAV.

The aim of this study was to complement the already available serological data of the pre-pandemic period 2006–2007 on circulating IAV, with genetic data.

Materials and methods

Virus isolation and subtype determination

Lungs were collected from freshly dead or euthanized pigs housed in 5 unrelated pig herds showing clinical signs of influenza at the time of sampling (Table 1). Virus isolation was attempted by inoculating the lung homogenates into the chorioallantoic sac of 9- to 11-day-old embryonated SPF chicken eggs. After 3-5 days of incubation at 37°C, the allantoic fluids were tested for the presence of influenza virus by Reverse Transcription-Polymerase Chain Reaction (RT-PCR)¹⁹⁴, and hemagglutination. Isolates were then tested by multiplex RT-PCR¹⁹⁵ and standard cross-hemagglutination inhibition to determine the virus subtype and lineage. Virus isolates were then propagated a maximum of 2 times on the Madin-Darby canine kidney (MDCK) cell line and stored at -80°C for further testing.

Virus	A/Swine/Spain/SF11131/2007 (H1N1)	Abbreviation: SF11131
Outbreak	Location: Alcarras (Lleida) Date: December 2007 Animals age ^a : 12 Mortality rate ^b : 3.28%	
Sampling date:	n/a	
Accession numbers:	HA: HF674888, NA: HF674889, PB2: HF674895, PB1: HF674894, PA: HF674893, NP: HF674891, M: HF674890, NS: HF674892	
Virus	A/Swine/Spain/SF32071/2007 (H3N2)	Abbreviation: SF32071
Outbreak	Location: Termens (Lleida) Date: July 2007 Animals age: 20 Mortality rate: 3.07%	
Sampling date:	September 2007	
Accession numbers:	HA: HE774666, NA: HE774670, PB2: HE774669, PB1: HE774671, PA: HE774668, NP: HE774667, M: HE774673, NS: HE774672	
Virus	A/Swine/Spain/80598LP1/2007 (H3N2)	Abbreviation: 80598LP1
Outbreak	Location: Torres de Segre (Lleida)	

	Date: August 2006 Animals age: 20 Mortality rate: 9.19%	
Sampling date:	May 2007	
Accession numbers:	HA: HF674896, NA: HF674897, PB2: HF674903, PB1: HF674902, PA: HF674901, NP: HF674899, M: HF674898, NS: HF674900	
Virus	A/Swine/Spain/ SF12091/2007 (H1N2)	Abbreviation: SF12091
Outbreak	Location: Binefar (Huesca) Date: August 2007 Animals age: 22-24 Mortality rate: 6.99%	
Sampling date:	n/a	
Accession numbers:	HA: HF674904, NA: HF674905, PB2: HF674911, PB1: HF674910, PA: HF674909, NP: HF674907, M: HF674906, NS: HF674908	
Virus	A/Swine/Spain/80598LP4/2007 (H1N2)	Abbreviation: 80598LP4
Outbreak	Location: Almenar (Lleida) Date: September 2006 Animals age: 10-12 Mortality rate: 6.98%	
Sampling date:	May 2007	
Accession numbers:	HA: HF674912, NA: HF674913, PB2: HF674919, PB1: HF674918, PA: HF674917, NP: HF674915, M: HF674914, NS: HF674916	

^a weeks of life

^b average mortality during the fattening period

Table 1. Data on the Spanish SwIV strains analyzed in this study.

Genome sequencing

Total RNA was extracted from the infected MDCK supernatants using the QIAamp Viral RNA Mini kit (Qiagen), according to the manufacturer's instructions. The full length coding sequences (CDS) of the 8 segments of the SwIV isolates was obtained using an RT-PCR method, which combines several approaches listed below. Primers from the World Health Organization¹⁹⁶ and from Chiapponi et al. (2003) were used. Additional primers were designed to obtain sequences of regions not amplified by the above cited sources (Table 1 in supplementary file). They were designed so they could be used under the same amplification conditions described in the WHO protocol. The AccessQuick master mix RT-PCR System (Promega) was used according to the conditions suggested by the WHO (detailed in Table 1 of Supplementary files). Amplification products were separated by standard agarose gel electrophoresis, and then purified using the NucleoSpin Extract II (Macherey-Nagel) purification kit as per manufacturer's instructions. Sequencing reactions were performed using the BigDye Terminator Cycle Sequencing kit v3.1 (Applied Biosystems), and resolved by using the ABI 3730 DNA automatic sequencer (Applied Biosystems). ChromasPro software was used to assemble and edit the overlapping fragments sequences (Technelysium Pty Ltd.).

Sequence analysis

BLAST sequence analysis¹⁹⁷ was used for assessing the greatest similarity for each gene. Publicly available nucleotide sequences of IAVs were collected from the Influenza Virus Resource database¹⁹⁸ and GenBank. Sequences were aligned using the ClustalW¹⁹⁹ tool implemented in the MEGA5 software²⁰⁰. A first phylogenetic tree for each CDS was constructed using all available sequences isolated in swine in Europe, with complete CDS. Then, for clarity, a second tree was constructed using only selected SwIV sequences representative of each cluster in the tree, along with all the existing sequences from Spanish isolates (available in the databases up to 14/03/2013). Phylogenetic trees of the eight CDS from SwIVs were constructed using MEGA5 software. The evolutionary history of SwIVs was inferred using the Neighbor-Joining method²⁰¹ with the Jukes-Cantor model²⁰², and bootstrapped 1000 times²⁰³. The reliability of the phylogenetic history was checked by comparing the phylograms generated with the above described method, and the phylograms generated with Maximum likelihood method based on the best DNA evolutionary model for each segment.

Screening for antigenic and glycosylation sites

The amino acid sequences of the hemagglutinin (HA) belonging to both Spanish field isolates, and strains in RESPIPORC FLU3/GRIPOVAC 3 (IDT Biologika GmbH, Merial S.A.S.) (Table 2 in supplementary file) were aligned and analysed for similarity (Figures 2 in supplementary files). The position of the antigenic sites Ca, Sa, Cb and Sb on the H1 type of the HA protein, were deduced from Brownlee 2001²⁰⁴. The glycosylation motifs were identified by NetNGlyc 1.0 server²⁰⁵.

Results

The five isolated viruses belonged to the subtypes H₁N₁ (n=2), H₁N₂ (n=1) and H₃N₂ (n=2). The phylogenetic trees constructed from the full coding regions of the eight viral genomic segments showed the same topology using either the Neighbor-Joining or the Maximum likelihood method (data not shown).

The internal genes (PB1, PB2, PA, NP, M and NS) CDSs of the isolated viruses belonged to the “Avian-Like” lineage and clustered together with SwIV strains isolated after 2004 (Table 2 and figure 1 of supplementary files), whereas the surface glycoproteins CDSs (HA and NA) belonged to different lineages depending on the subtype.

SF11131	Identity	Strain	Accession number
HA	98%	A/swine/Spain/53207/2004(H1N1)	CY010580.1
NA	99%	A/swine/Italy/65296/2004(H1N1)	EU045389.2
		A/swine/Italy/53949/2004(H1N1)	EU045388.2
		A/swine/Spain/53207/2004(H1N1)	CY010582.1
PB1 ^b	98%	A/swine/Spain/53207/2004(H1N1)	CY010586.1
		A/swine/Italy/71251/2005(H1N2)	JX843273.1
PB2	99%	A/swine/Gent/132/2005(H1N1)	CY116431.1
		A/swine/Spain/53207/2004(H1N1)	CY010587.1
		A/swine/Italy/50568/2005(H1N2)	HQ845023.1
PA	99%	A/swine/Spain/53207/2004(H1N1)	CY010585.1
		A/swine/Italy/50568/2005(H1N2)	HQ709221.1
NP ^b	99%	A/swine/Gent/132/2005(H1N1)	CY116435.1
		A/swine/Spain/53207/2004(H1N1)	CY010583.1
		A/swine/Hungary/13509/2007(H3N2)	FJ798771.1
M ^b	98%	A/swine/Greven/IDT2889/2004(H1N1)	GQ161157.1
		A/swine/Spain/53207/2004(H1N1)	CY010581.1
		A/swine/Ploufragan/0214/2006(H1N2)	CY116542.1
NS	99%	A/swine/Gent/132/2005(H1N1)	CY116437.1
		A/swine/Spain/53207/2004(H1N1)	CY010584.1
		A/swine/Italy/159870-2/2005(H1N1) ^a	CY116483.1
		A/swine/Hungary/13509/2007(H3N2) ^a	FJ798774.1
SF32071			
HA	99%	A/swine/Spain/82108/2007(H3N2)	CY116558.1
		A/swine/Hungary/13509/2007(H3N2)	FJ798772.1
		A/swine/Damme/IDT5673/2006(H3N2) ^a	GQ161147.1
		A/swine/Spain/54008/2004(H3N2)	CY010564.1
NA	99%	A/swine/Spain/82108/2007(H3N2)	CY116560.1
		A/swine/Gent/96/2007(H3N2)	CY116452.1
		A/swine/Hungary/13509/2007(H3N2) ^a	FJ798773.1
PB1 ^b	99%	A/swine/Gent/96/2007(H3N2) A/swine/Spain/82108/2007(H3N2)	CY116448.1
		A/swine/Spain/53207/2004(H1N1)	CY116556.1
			CY010586.1
PB2	99%	A/swine/Spain/82108/2007(H3N2)	CY116555.1
		A/swine/Gent/96/2007(H3N2)	CY116447.1
		A/swine/Hungary/13509/2007(H3N2) ^a	FJ798770.1
		A/swine/Spain/53207/2004(H1N1)	CY010587.1
PA	99%	A/swine/Spain/82108/2007(H3N2)	CY116557.1
		A/swine/Gent/96/2007(H3N2)	CY116449.1
		A/swine/Hungary/13509/2007(H3N2) ^a	FJ798775.1
NP	98%	A/swine/Spain/53207/2004(H1N1)	CY010585.1
		A/swine/Greven/IDT2889/2004(H1N1)	GQ161157.1
		A/swine/Spain/51915/2003(H1N1)	CY010575.1
M	99%	A/swine/Spain/53207/2004(H1N1)	CY010583.1
		A/swine/Spain/82108/2007(H3N2)	CY116561.1
		A/swine/Gent/96/2007(H3N2)	CY116453.1
NS	98%	A/swine/Ille et Vilaine/1455/1999(H1N1)	CY116383.1
		A/swine/Spain/82108/2007(H3N2) ^a	CY116562.1
		A/swine/Gent/96/2007(H3N2) ^a	CY116454.1
		A/swine/Hungary/13509/2007(H3N2) ^a	FJ798774.1
		A/swine/Spain/53207/2004(H1N1)	CY010584.1
80598LP1			
HA	98%	A/swine/Spain/54008/2004(H3N2)	CY010564.1
		A/swine/Gent/96/2007(H3N2)	CY116450.1
NA	97%	A/swine/Spain/54008/2004(H3N2)	CY010566.1
		A/swine/Damme/IDT5673/2006(H3N2)	GQ161148.1
PB1	98%	A/swine/Greven/IDT2889/2004(H1N1)	GQ161154.1
		A/swine/Spain/53207/2004(H1N1)	CY010586.1
PB2	99%	A/swine/Greven/IDT2889/2004(H1N1)	GQ161153.1
		A/swine/Spain/53207/2004(H1N1)	CY010587.1

PA	99%	A/swine/Greven/IDT2889/2004(H1N1)	GQ161155.1
		A/swine/Spain/53207/2004(H1N1)	CY010585.1
NP	98%	A/swine/Spain/42386/2002(H3N2)	CY020504.1
		A/swine/Ille et Vilaine/1455/1999(H1N1)	CY116381.1
		A/swine/Brno/00/2000(H1N1)	CY115882.1
M	99%	A/swine/Ploufragan/0214/2006(H1N2)	CY116542.1
		A/swine/Gent/132/2005(H1N1)	CY116437.1
		A/swine/Spain/53207/2004(H1N1)	CY010581.1
NS	98%	A/swine/Spain/54008/2004(H3N2)	CY010568.1
		A/swine/Spain/42386/2002(H3N2) ^a	CY020505.1
		A/swine/Cloppenburg/IDT4777/2005(H1N2)	EU053145.1
SF12091			
HA	99%	A/swine/Groitzsch/IDT6016-1/2007(H1N2) ^a	GQ161141.1
		A/swine/Kitzen/IDT6142/2007(H1N2)	GQ161145.1
		A/swine/Groitzsch/IDT6016-2/2007(H1N2) ^a	GQ161143.1
	98%	A/swine/Spain/40564/2002(H1N2)	CY116550.1
NA	99%	A/swine/Kitzen/IDT6142/2007(H1N2)	GQ161146.1
		A/swine/Groitzsch/IDT6016-1/2007(H1N2)	GQ161144.1
		A/swine/Groitzsch/IDT6016-2/2007(H1N2)	GQ161142.1
	98%	A/swine/Spain/40564/2002(H1N2)	CY116552.1
PB1	98%	A/swine/Spain/53207/2004(H1N1)	CY010586.1
		A/swine/Cloppenburg/IDT4777/2005(H1N2)	EU053139.1
		A/swine/Italy/71251/2005(H1N2)	JX843273.1
PB2	99%	A/swine/Gent/132/2005(H1N1)	CY116431.1
	98%	A/swine/Spain/53207/2004(H1N1)	CY010587.1
		A/swine/Italy/50568/2005(H1N2)	HQ845023.1
PA	99%	A/swine/Spain/53207/2004(H1N1)	CY010585.1
		A/swine/Italy/50568/2005(H1N2)	HQ709221.1
		A/swine/Italy/626-2/2006(H1N2)	HQ709222.1
NP	99%	A/swine/Gent/132/2005(H1N1)	CY116435.1
		A/swine/Spain/53207/2004(H1N1)	CY010583.1
M	99%	A/swine/Ploufragan/0214/2006(H1N2)	CY116542.1
		A/swine/Spain/51915/2003(H1N1)	CY010573.1
		A/swine/Gent/112/2007(H1N1)	CY116429.1
NS	99%	A/swine/Italy/159870-2/2005(H1N1) ^a	CY116483.1
	98%	A/swine/Spain/53207/2004(H1N1)	CY010584.1
80598LP4			
HA	94%	A/swine/England/690421/95(H1N2)	AF085415.1
		A/swine/Cotes d'Armor/790/1997(H1N2)	CY116410.1
		A/swine/Bakum/1832/2000(H1N2)	EU053148.1
NA ^b	96%	A/swine/England/88761/1997(H1N2)	CY116325.1
		A/swine/England/61605/1998(H1N2)	CY116246.1
	95%	A/swine/England/645913/1996(H1N2)	CY116262.1
PB1	98%	A/swine/Greven/IDT2889/2004(H1N1)	GQ161154.1
		A/swine/Spain/53207/2004(H1N1)	CY010586.1
PB2	99%	A/swine/Greven/IDT2889/2004(H1N1)	GQ161153.1
		A/swine/Spain/51915/2003(H1N1)	CY010579.1
PA	99%	A/swine/Greven/IDT2889/2004(H1N1)	GQ161155.1
	98%	A/swine/Spain/53207/2004(H1N1)	CY010585.1
NP	98%	A/swine/Spain/40564/2002(H1N2)	CY116551.1
		A/swine/Granstedt/IDT3475/2004(H1N2)	GQ161164.1
		A/swine/Haseluenne/IDT2617/2003(H1N1)	GQ161120.1
		A/swine/Spain/53207/2004(H1N1)	CY010583.1
M	99%	A/swine/Spain/51915/2003(H1N1)	CY010573.1
NS	99%	A/swine/Spain/51915/2003(H1N1)	CY010576.1

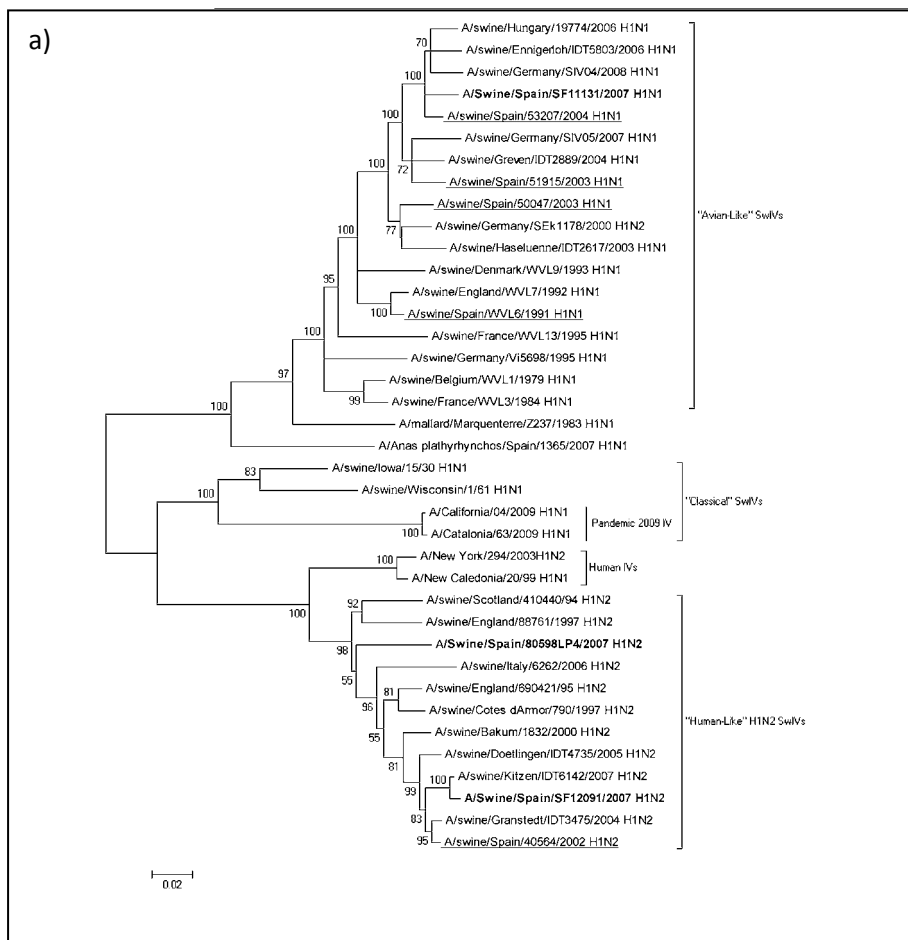
Table 2. The most homologous SwIV sequences for each segment analyzed in this study, according to BLASTn search (25/02/2013). ^aQuery coverage: 99%; ^bThe sequence of the virus isolated in this study showed degenerate nucleotide (multiple nucleotide have been found at particular positions).

H₁N₁ subtype

The phylogenetic analysis showed that all eight CDSs of the SwIV strain SF11131 belonged to the European “Avian-Like” lineage (Figures 22a, 23a and figures 1 a-f in supplementary file) and clustered together with the contemporary strains isolated after 2000. This isolate also showed high identity (Table 2) and close clustering of the HA and NA CDSs, with the Spanish strain A/Swine/Spain/53207/2004 (H₁N₁). This latter, in turn, showed similar relationship with other European strains like A/Swine/Hungary/19774/2006 (H₁N₁), and A/swine/Germany/SIV04/2008 (H₁N₁) for HA CDS and A/swine/Italy/53949/2004 (H₁N₁) and again A/Swine/Hungary/19774/2006 (H₁N₁) for the NA CDS.

H₃N₂ subtypes

The HA and NA CDSs of the isolates SF32071 and 80598LP1 clustered with the European strains of the “Human-Like” H₃N₂ SwIV subtype. Both isolates exhibited a close relationship with the Spanish strains A/Swine/Spain/54008/2004 (H₃N₂) and A/Swine/42386/2002 (H₃N₂), and clustered together with strains described in North-East Europe in 2006-2007.



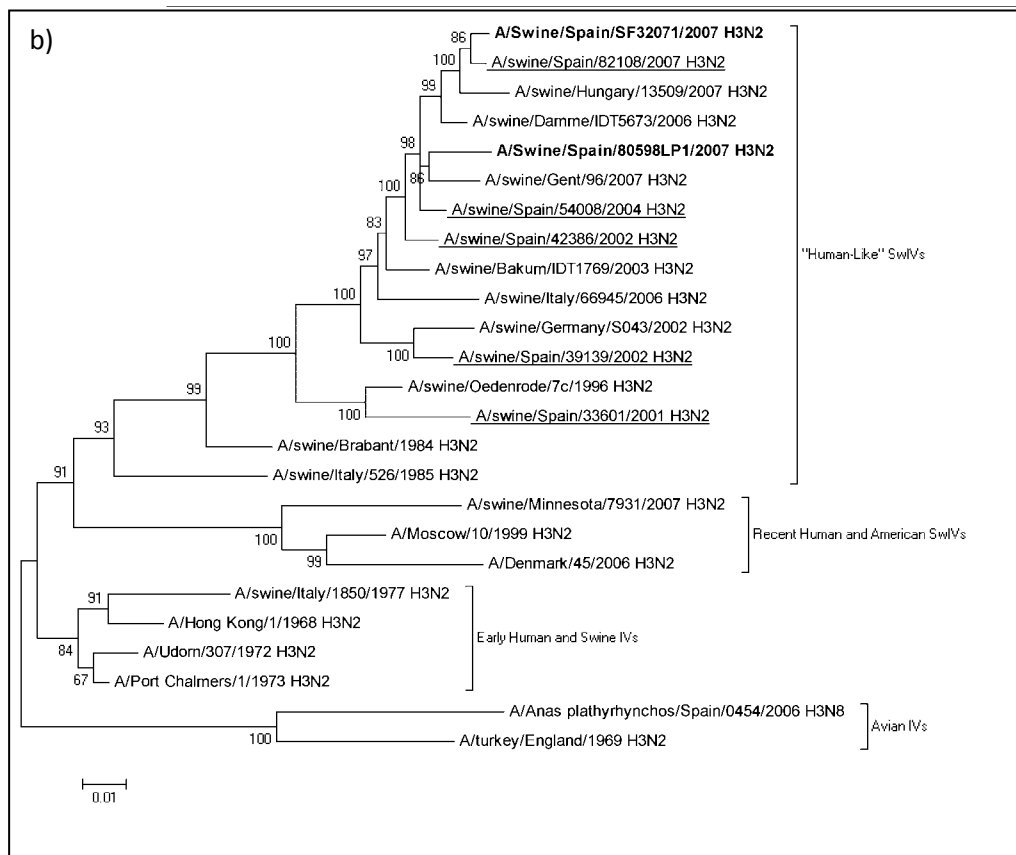


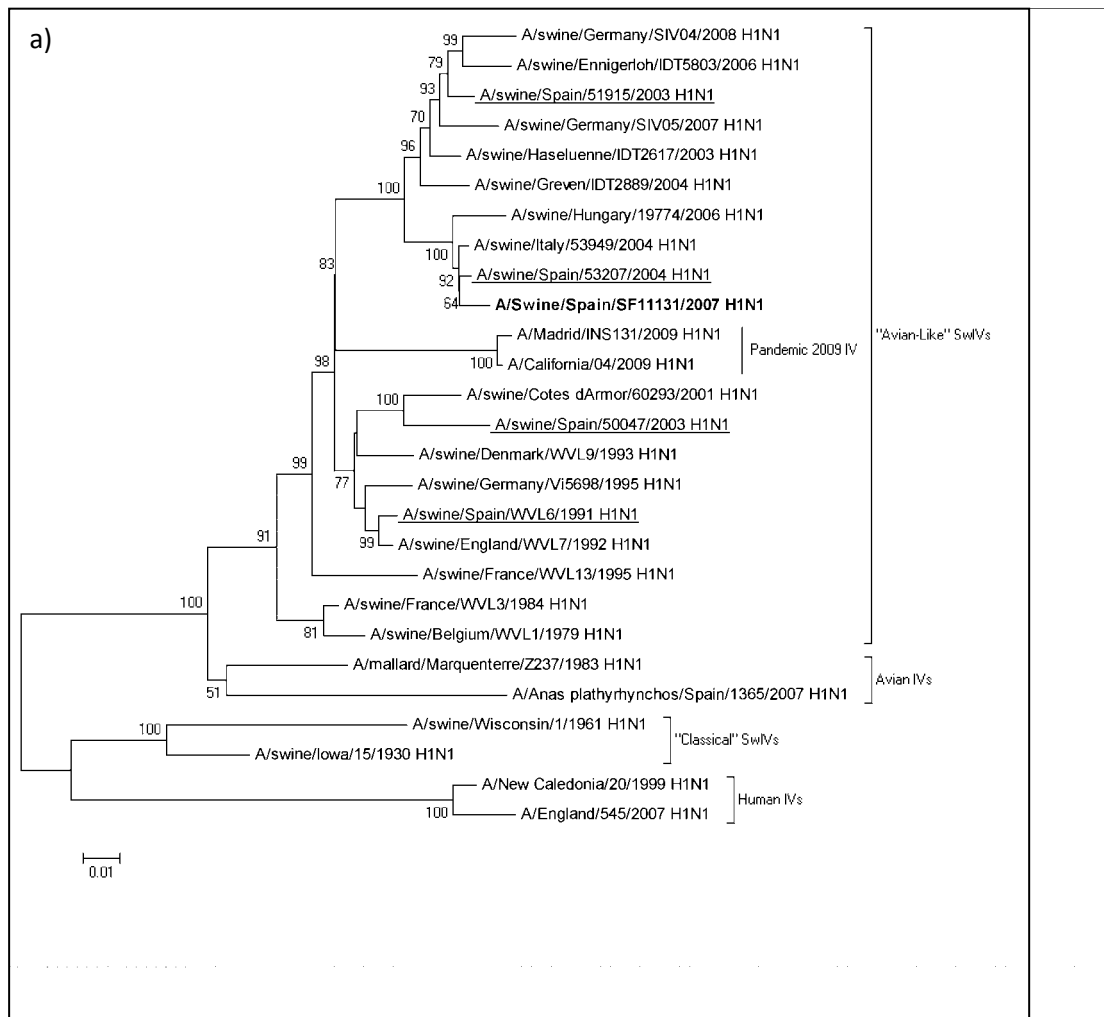
Figure 22. Evolutionary relationships of HA CDS of taxa. The tree is drawn to scale, with branch lengths in the same units as those of the evolutionary distances used to infer the phylogenetic tree. Bootstrap values greater than 50% are shown (1000 replicates). Strains isolated in this study are in boldface and Spanish SwIV strains previously isolated are underlined. (a) H1 HA phylogenetic tree. The analysis involved 38 nucleotide sequences of H₁N₁ and H₁N₂ IV subtypes. There were a total of 1676 positions in the final dataset. (b) H3 HA phylogenetic tree. The analysis involved 25 nucleotide sequences of H₃N₂ IV subtype. There were a total of 1694 positions in the final dataset.

The HA CDS of isolate SF32071 was particularly highly related with A/swine/Spain/82108/2007 (H₃N₂), whereas the NA was highly related with the same strain but also with A/swine/Gent/96/2007 (H₃N₂) (Table 2, figures 22b and 23b). Conversely, the HA CDS of isolate 80598LP1 exhibited a higher phylogenetic distance from SF32071 and the closest neighbour was the European strain A/swine/Gent/96/2007 (H₃N₂). The NA of 80598LP1 showed the same trend as the HA CDS but the closest neighbour was the Spanish strain A/Swine/Spain/54008/2004 (H₃N₂).

H₁N₂ Subtypes

The surface glycoproteins CDSs of the isolates SF12091 and 80598LP4 belonged to the same lineage of SwIVs, the "Human-like" H₁N₂. However, they showed a divergent evolution

between them, which was particularly evident when analysing the NA gene (Figure 23b). The HA CDS of the isolate SF12091 were related to the Spanish strain A/Swine/Spain/40564/2002 (H₁N₂) and strains circulating in north-east Europe. Among them, the strain A/swine/Kitzen/IDT6142/2007 (H₁N₂) was the most closely related one (Table 2, Figure 22b). The NA CDS showed a clustering pattern similar to the HA CDS (Figure 24b). The HA of isolate 80598LP4 was more phylogenetically distant from the other co-circulating H₁N₂ viruses, including the co-isolated SF12091. Besides, the greatest identity found by BLAST was 94%, the lowest compared to the other strains (Table 2, figure 23b). On the contrary, the NA CDS clustered with strains circulating in the 1990s in England and France. However, none of them showed a close relationship in terms of either identity or genetic distance (Table 2, figures 22b and 23b).



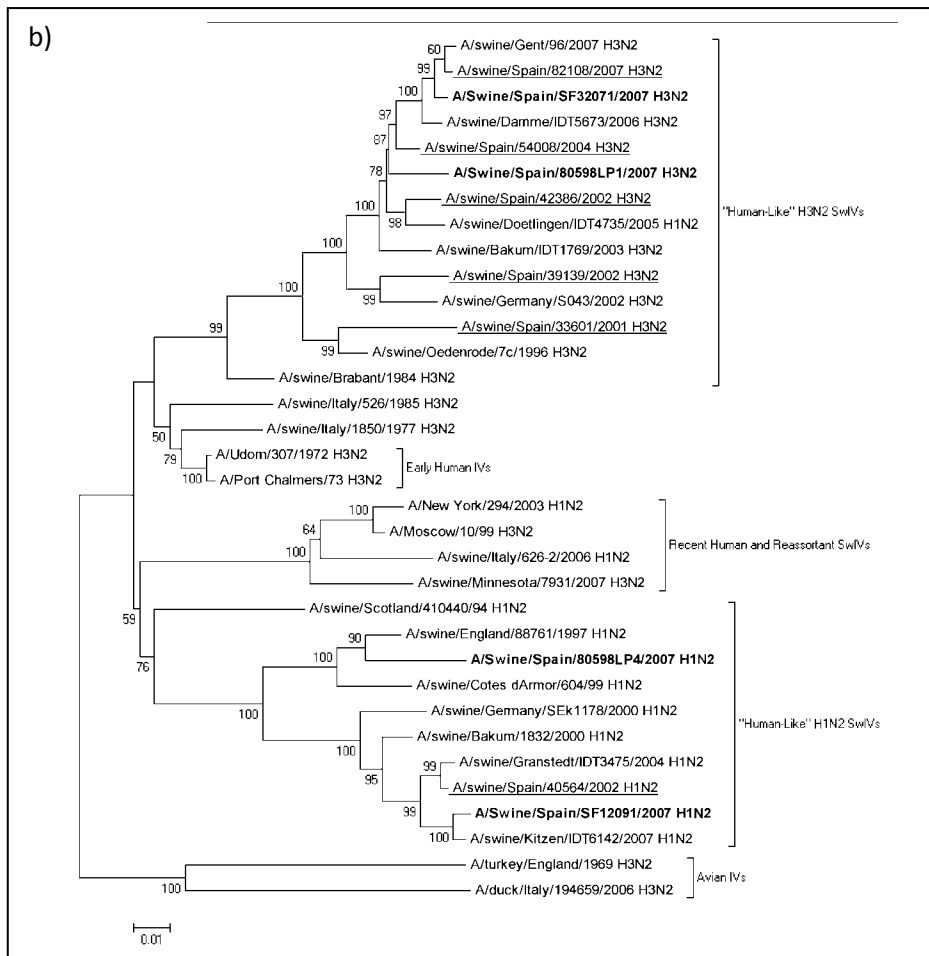


Figure 23. Evolutionary relationships of taxa of NA CDS. The tree is drawn to scale, with branch lengths in the same units as those of the evolutionary distances used to infer the phylogenetic tree. Bootstrap values greater than 50% are shown (1000 replicates). Strains isolated in this study are in boldface and Spanish SwIV strains previously isolated are underlined. (a) N1 NA phylogenetic tree. The analysis involved 27 nucleotide sequences of H_1N_1 IV subtypes. There were a total of 1403 positions in the final dataset. (b) N2 NA phylogenetic tree. The analysis involved 34 nucleotide sequences of H_3N_2 and H_1N_2 IV subtypes. There were a total of 1398 positions in the final dataset.

Molecular characterization

The divergent evolution of the two H_1N_2 isolates SF12091 and 80598LP4 may have changed their antigenic characteristics; hence, amino acid sequences of their HA protein were compared between them and with the vaccine strain A/Swine/Bakum/1832/2000 (H_1N_2) which has a "Human-Like" HA (figure 2 of supplementary files). The antigenic sites of the two field isolates were unidentical with the vaccine strain. Whereas the isolate SF12091 showed few mutations falling into the antigenic sites, isolate 80598LP4 showed more mutations along the entire length of the protein but also in the hypothetical antigenic site Ca (Table 3).

Strains	Antigenic sites			
	Ca	Sa	Cb	Sb
80598LP4-				
SF12091	6	1	0	1
A/Sw/Bakum/1832/00	5	0	0	1
SF12091-				
A/Sw/Bakum/1832/00	2	1	0	0

Table 3. Number of mutations in the antigenic sites of “Human-Like” H1 HA SwIV proteins.

In contrast, the predicted glycosylation pattern was completely conserved among the H₁N₂ strains screened (Table 4), suggesting that masking of the antigenic sites was conserved.

Strain	Glycosylation sites positions
A/Swine/Spain/80598LP4/2007	27, 28, 40, 172, 177, 286 , 304, 498, 557
A/Swine/Spain/SF12091/2007	27, 28, 40, 172, 177, 286 , 304, 498, 557
A/swine/Bakum/1832/2000	27, 28, 40, 172, 177, 286 , 304, 498, 557

Table 4. Glycosylation sites on the HA protein from selected SwIVs. The boldface positions are the glycosylation sites that are different in all strains.

Chapter II: Generation of an *in vitro* assay to characterize binding proprieties of peptides to SLA-I

In vitro MHC binding assays are used to determine binding affinities of peptides to MHC molecules. Experimentally obtained affinities are then used to validate predicted data or to generate prediction softwares. There are several formats of binding assays in human or mice. Those can be divided into cells-based or cells free assays.

In cell-based assays, the MHC expressed on the cell surface, used to titrate peptides, is in a native form and thus the cell naturally folds it. Generally speaking, there are two main types of cell-based assays. The first method is the MHC reconstitution assay^{206,207} that relates the binding proprieties of peptides with their ability to reconstitute pMHC on cells surface (Figure 25). This is performed through denaturalization of the already expressed MHCs by releasing the already bound natural peptides and β 2m which are then reconstituted with target peptides and β 2m; amounts of pMHCs are then detected by specific antibody and by flow cytometry. The second method is the MHC stabilization assay²⁰⁸⁻²¹⁰ that relates the binding propriety of peptides with their ability to stabilize pMHC on cells surface. The particular type of cells used in this assay (TAP⁺) already offers “empty” MHCs (MHCs not bound to peptides) on the cellular surface and thus can be used for peptide titration. The amount of labelled peptide can be also directly established using fluorescent or radioactive labelled peptides which are used instead of antibodies²¹¹.

Cells free binding assays are based on the same principle of cells based assays; they evaluate the ability of peptides to generate a pMHC-I complex. However, they use a recombinant and *in vitro* folded form of MHC-I molecule. There are several different method of detection of the pMHC complex; these can be detected by antibodies enzymatically linked (Enzyme Linked Immunosorbent Assay (ELISA))²¹² or luminescently linked (Luminescent oxygen channelling immunoassay)²¹³. Another method detect radiolabelled pMHC and retained radiolabelled β 2m is used as indirect measure of pMHC complexes (scintillation proximity assay)²¹⁴. Finally, there are some assays in which *in vitro* folded or native purified MHC-I molecules can be used^{215,216}. In those assays, pMHC are separated from unbound MHC by gel filtration or column filtration chromatography or antibody capture. Use of radiolabelled peptides allows quantification of separated pMHC-I complexes.

In pigs, there are just a few formats of *in vitro* assays to test predicted binding propriety of epitopes; those are “cells free” assay which use a recombinant form of *in vitro* folded SLA-I. As mentioned, there are cell-based assays but they have not been developed for SLA-I. A cell-based assay was chosen based on two reasons, firstly because the naturally folded properties

of the SLA-I molecule and secondly to develop a new assay to increase the knowledge in porcine immunology. The next chapter focus on Babrahams inbred pigs alleles SLA-1*es11 and SLA-2*es22; these alleles were studied here with the aim of complementing the *in vivo* information from chapter III. Allele SLA-1*0401 is not present in Babraham pigs but it was chosen here because there were already available some information about its binding preference^{174,175} and therefore it could be used as a reference in our experiments. The aim of this study was to develop an SLA-I reconstitution assay to allow analysis of peptides binding strength to SLA-I alleles SLA-1*es11, SLA-2*es22 and SLA-1*0401. Hence, in a first instance a pipeline to generate transfected cells lines expressing SLA-I was set up using C1R cells due to the fact that they are MHC negative and express little human HLA. Subsequently, SLA-I stably transfected cells were used to set up optimal conditions for SLA-I reconstitution assay.

Materials and methods

Amplification of SLA heavy chain (SLAhc)

Babrahams pigs bear the alleles SLA-1*es11 (EU440342.1) and SLA-2es22 (EU432089.1). PK15 cells (ATCC CCL-33) bears the SLA-1*0401 allele²¹⁷. RNA was extracted from Babrahams pigs lung or PK15 cells by RNeasy Mini Kit (Qiagen) with the on column digestion of DNA by RNase-Free DNase Set (Qiagen). RNA was used as template for two-steps Reverse Transcription Polymerase Chain Reaction (RT-PCR) with home-made SLA-1 primers forward: *CGAGGCTGAGGATCATGG* and reverse: *CCACAAGGCAGTTGTCTCAC* respectively including the start and stop codons of the SLA-1*es11 and SLA-1*0401 CDS. Primers used for the SLA-2*es22 forward: *AGATGCGGGTCAGGGCCCTCAAG* and reverse: *CAGTCCCCACAAGGCAGCTGTCTC* were from *Gao et al. 2006*¹⁷⁶. RT step was performed with MuLV enzyme (Applied Biosystem), RNase Out (Applied Biosystem), Gold Taq Buffer (Applied Biosystem) and reverse primers incubating 60 minutes at 48°C. PCR was performed with the GoTaq Flexi DNA Polymerase kit (Promega) 2 minutes at 95°C for initial denaturation, 50 cycles of 94°C for 45 seconds, annealing at 55°C for 30 seconds, and extension at 72°C for 2 minute followed by a last step of extension at 72° C for 7 minutes. Amplification products were separated by standard agarose gel electrophoresis and purified with NucleoSpin Extract II (Macherey-Nagel).

Cloning SLAhc

Amplified SLA products were ligated into the pGEM-T vector with the kit pGEM-T Easy Vector System I (Promega) and these were used to transform chemiocompetent *E.coli*. Recombinant

clones were selected with Ampicillin (100 µg/ml) and Blue/White screening. Recombinant plasmids pGEM-T-SLA were purified with the SV miniprep DNA purification System (Promega) and those right oriented and non mutated were screened by sequencing. Sequencing reactions were performed using the BigDye Terminator Cycle Sequencing kit v3.1 (Applied Biosystems), and resolved by using the ABI 3730 DNA automatic sequencer (Applied Biosystems).

Generation of a recombinant mammalian expressing vector bearing SLAhc

Genes inserted into pGEM-T-SLA plasmid were excised using *Not I* enzyme (Roche), separated by standard agarose gel electrophoresis and purified. The same process was applied to pCDNA3.1⁺ plasmid (Life technologies); moreover, this was de-phosphorylated with Alkaline Phosphatase CIP (New England Biolabs) and then purified again. pCDNA3.1⁺ plasmid and SLA gene with generated *Not I* sticky ends were ligated with Instant Sticky-end Ligase Master Mix (New England Biolabs). Chemically competent *E.coli* were then transformed with the recombinant plasmid pCDNA3.1⁺-SLA as described above and selected with Kanamycin (50µg/ml). Right oriented, non mutated plasmids were screened by sequencing and purified by EndoFree Plasmid Maxi Kit (Qiagen).

Cell line and transfection

Immortalized human B lymphoblastoid C1R cells (ATCC CRL-1993) were grown in RPMI 1640 (Life technologies) supplemented with 10% Foetal Calf Serum (FCS) (Lonza), 2mM L-Glutamin (Life technologies) and Penicillin/Streptomycin (Life Technologies). Cells were washed twice with Phosphate Buffer Saline (PBS), once with RPMI 1640 and transfected. 9×10^6 cells in 90µl of RPMI 1640 were placed into a Gene Pulser/MicroPulser Cuvettes 0.4 cm gap (BIORAD) and mixed with 10µg of plasmid. C1R cells were then electroporated with Gene Pulser Xcell Electroporation Systems (BIORAD) using Square wave method at 250V and 20 ms. Cells were incubated 24 hours with RPMI 1640 supplemented with 10% FCS; then, media was supplemented with selecting agent G418 (Life Technologies) at 1mg/ml and cells were incubated during 1 week. After that period, cells were diluted to limit in selecting media and incubated during 2 more weeks. This step was repeated once again to increase the purity of recombinant C1R cells.

Flow cytometry staining

Cells were washed with buffer A or B (Table 5); buffer A was used for identification of recombinant cells clones, while buffer B was used during the optimization of denaturalization.

1x10⁶ cells were incubated with the primary antibodies (table 5), washed twice with buffers (A or B) and incubated with the secondary antibodies (listed in table 6). Cells were then washed again and fixed with 1% paraformaldehyde. The staining process was performed on ice until fixation.

Primary Antibody	Antigen	Dilution	Brand
74-11-10	SLA-I	1/400	Kingfisher
4B7/8	SLA-I	-	In house <i>Bullido et al. 1996</i> ²¹⁸
2G1/VAN	SLA-I	-	In house (N/A)
W6/32	HLA	-	In house <i>Barnstable et al. 1978</i> ²¹⁹
BBM.1	human β 2m	-	In house <i>Brodsky et al. 1979</i> ²²⁰
Secondary antibody			
PE Anti mouse IgG		1/50	Jackson Immunology
FITC Anti mouse IgG		1/400	Jackson Immunology
Buffers		Composition	
A		PBS, 2%FCS and 0.2% Sodium Azide	
B		PBS, 1%Bovine Serum Albumin and 0.2% Sodium Azide	

Table 5. Buffer and antibodies used for flow cytometry.

Denaturalization

Cells were washed two times with PBS. Denaturalization was performed incubating cells in elution buffer (Citric Acid – Sodium phosphate dibasic at various pH). Duration of incubation varies depending on requirement and it was stopped by adding RPMI 1640. Cells were washed again in RPMI 1640 and stained for flow cytometry. Denaturalization process was performed on ice (reagents and incubation) or at 37°C. When required, cells were incubated with Brefeldin A Golgi plug (Becton Dickinson) 0.5 μ g per 10⁶ cells before the denaturalization. RPMI 1640 (pH 8.2) was used instead of elution buffer as CTRL.

Results

Optimization of SLA reconstitution assay.

Firstly, specificity of the antibodies was evaluated in flow cytometry on wild type C1R cells (C1R); in particular this was evaluated in denaturalised and untreated C1R cells. Denaturalisation was performed through incubation of cells at pH3 during 90 seconds. Several antibodies used to detect SLA-I (74-11-10 and 4B7/8), class I HLA (W6/32) and human β 2m

(BBM.1). Staining was performed with buffer that did not contain β 2m (buffer B) to avoid reconstitution of the MHC-I and it was performed on ice to avoid re-circulation. Antibodies 74-11-10 and 4B7/8 did not stained C1R cells in all assayed conditions (Figure 24a and 24b) indicating the absence of cross recognising epitopes on these cells before and after denaturalization. C1R cells showed fluorescent signal due to the staining with W6/32 and BBM.1 antibodies before denaturalization. Therefore, those antibodies detected a little amount of HLA (heavy chain and bound β 2m) on C1R cells. Denaturalization decreased C1R cells fluorescence to background levels for staining with W6/32 and BBM.1 (Figure 24c and 24d), indicating elution of β 2m and peptides from HLA. Therefore, reagents used for SLA reconstitution assay did not cross react with HLA or any other unspecific factor.

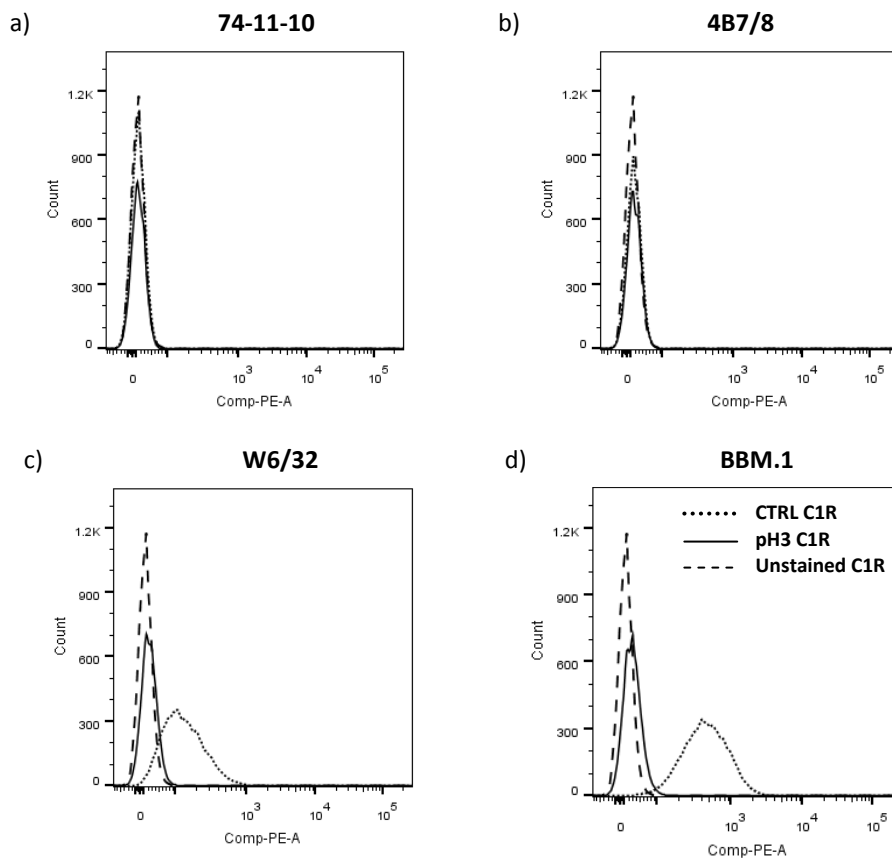


Figure 24. Testing antibodies cross reactivity. C1R cells were denaturalized at pH3 and on ice; then, those were stained with different antibodies: a) 74-11-10, b) 4B7/8, c) W6/32, d) BBM.1. Dotted lines are CTRL C1R treated at physiological pH (RPMI), continuous lines are pH3 treated C1R, slash dotted lines are unstained CTRL C1R.

Generation of C1R expressing SLA-I alleles.

SLA-I alleles were then stably transfected into C1R to be expressed on their cell surface. RNA was extracted from lung tissues of Babraham pigs; SLA-1 specific primers were used to reverse

transcribe and amplify the SLA-1*es11 coding sequence (about 1100 pb) (Figure 25a). This fragment was then ligated into a cloning vector to generate the pGEM-T-SLA-1*es11 plasmid.

The insert was excised by Not I restriction and cloned into a mammalian expression vector to generate the pCDNA3.1⁺-SLA-1*es11 plasmid. This plasmid allowed SLA-1*es11 gene expression into C1R cells after transfection. Screening of transfected clones was performed by flow cytometry using 74-11-10 anti SLA-I antibody based on results from figure 24. This antibody recognised SLA-1*es11 heavy chain and human (from C1R) or bovine (from FCS) β 2m (Figure 25b-c). SLA-I⁺ cells were selected in batch culture and isolated by two limiting dilution steps; in the first limiting dilution, some SLA-I⁻ cells were still present in the culture of transfected cells (Figure 25b). In the second round, C1R cells expressing the SLA-1*es11 were successfully isolated (Figure 25c).

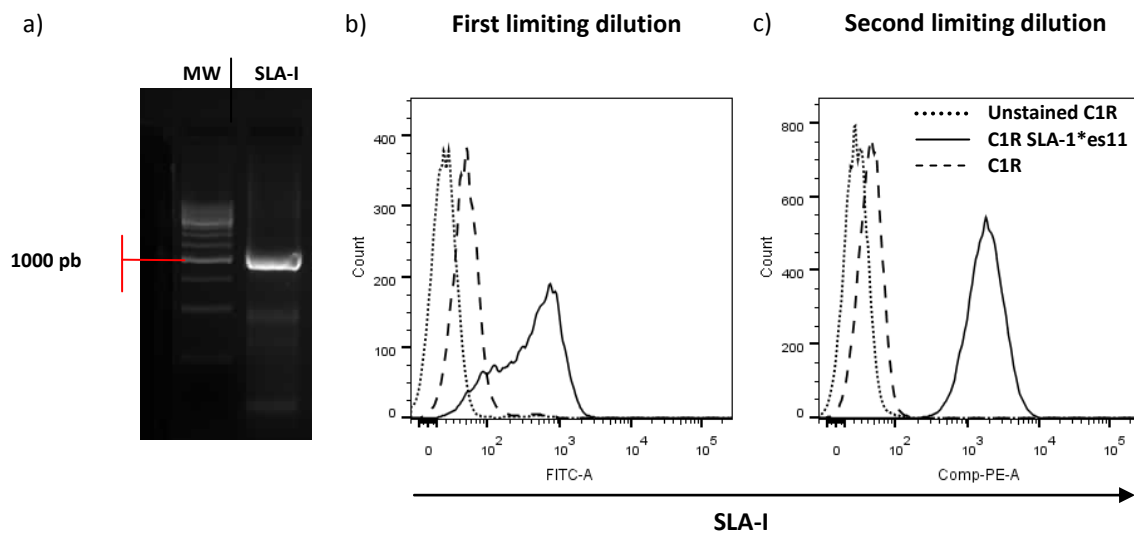


Figure 25. Generation of C1R SLA-1*es11. a) RT-PCR with SLA-1 primers of the RNA of Barbraham pigs lung tissues. C1R cells transfected with pCDNA3.1⁺-SLA-1*es11 plasmid were stained with the antibody 74-11-10 and analyzed by flow cytometry. b) Selection by limiting dilution of the C1R cells transfected with pCDNA3.1⁺-SLA-1*es11 plasmid. c) Second limiting dilution of C1R cells transfected with pCDNA3.1⁺-SLA-1*es11 plasmid. Dotted lines represent unstained cells, slash dotted line are C1R cells, continuous lines are C1R SLA-1*es11 cells. MW stands for molecular weight ladder.

The process for generation a stable C1R cell line expressing SLA-I was also applied to other alleles. SLA-2*es22 coding sequence was amplified by RT-PCR as described above using the SLA-2 primers with RNA extracted from Babraham pig lungs, which was cloned into pGEM-T easy vector and then into the pCDN3.1⁺ (Figure 3 supplementary files).

As mentioned previously, allele SLA-1*0401 was also used. PK15 cells were used as source of allele SLA-1*0401. It was processed as described above to obtain pCDN3.1⁺SLA-1*0401 following the same methods as described in previous sections. C1R cells were transfected with pCDN3.1⁺SLA*10401 plasmid and selected with just one round of limiting dilution. SLA-I⁺ cells were checked by flow cytometry, however, previously used 74-11-10 and 4B7/8 antibodies were not recognising the chimeric structure of SLA-1*0401. In contrast, another anti SLA-I antibody (2G1/VAN) was recognising a small population of transfected cells (Figure 4 supplementary files). Transfection and /or selection of the SLA-2*es22 and SLA-1*0401 were not further continued due to time constrains.

Optimization of the SLA-I reconstitution assay

The SLA reconstitution assay was optimised on C1R cells expressing SLA-1*es11. Conditions to obtain free empty SLA-I heavy chain (denaturalization step) as conditions to elute β 2m and naturally presented peptides, are here optimized. In a first instance, a range of pH was tested by incubating cells during a fixed time (60 seconds). Stability of SLA-I molecules on cell surface was evaluated by staining with antibody 74-11-10 which recognised chimeric SLA-1*es11 structure, based on previous results of figure 25. Re-circularization of newly synthesized MHCs on the cell surface was avoided by working on ice throughout the experiment. Wild type C1R represented background level in the assay (Figure 26). None of the pH conditions used decreased the fluorescence of stained C1R SLA-1*es11, compared to the untreated cells (CTRL), indicating that denaturalization of SLA-I did not happen. In contrast, treatment at pH 3 increased the fluorescence (Figure 26).

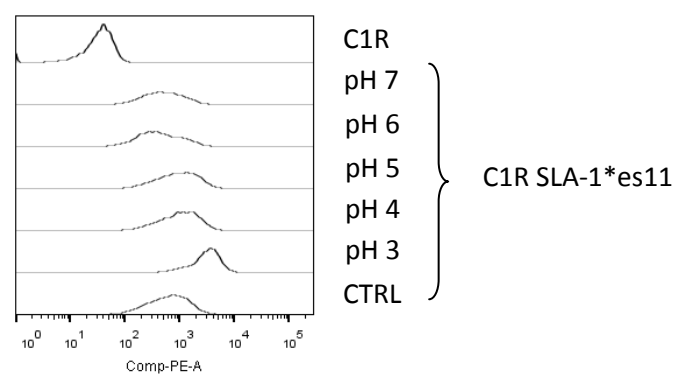


*Figure 26. Detection of chimeric SLA molecules after pH treatment on C1R SLA-1*es11 cells by flow cytometry with antibody 74-11-10. The first line (C1R) represents wild type C1R cells.*

Increasing time of pH treatment might have been helped destabilizing the SLA-I structure. Therefore, 90, 120 and 150 seconds of incubation with elution buffer were also tested,

whereas temperature was maintained constant and pH of the buffer was set up at 3, based on previous results (Figure 24).

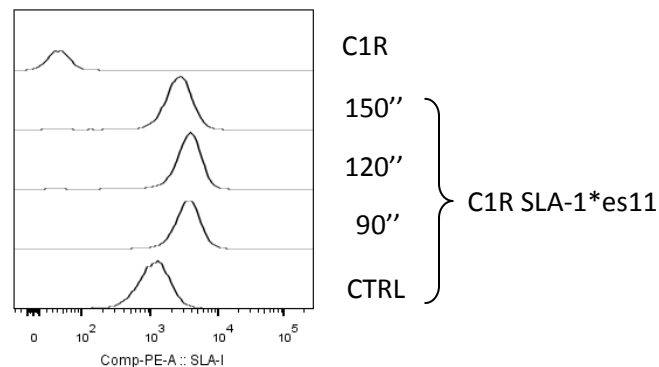


Figure 27. Time dynamic of SLA expression during the denaturalization step at pH 3. Flow cytometry of the cells stained with 74-11-10. CTRL was incubated for 150''.

Wild type C1R represented background levels in the assay (Figure 27). None of the time length used induced any decrease in fluorescence on stained C1R SLA-1es11 cells when pH treated and untreated (CTRL) conditions were compared. In contrast, these treatments increased fluorescence (Figure 27) on transfected cells. This result has been observed in previous experiment (Figure 26) and here again. One possibility would be that 74-11-10 antibody was recognizing the heavy chain instead of the pMHC form of the SLA. Following this hypothesis, denaturalization would increase free heavy chain form of SLA-I and thus C1R SLA-1*es11 fluorescence; this is in line with observed results. To proof this hypothesis, denaturalization experiment was repeated but this time, staining of cells was performed with different anti SLA antibodies (74-11-10 and 4B7/8). Anti HLA (W6/32) and β 2m (BBM.1) antibodies were also used to check that denaturalization was properly performed. Recombinant cells C1R SLA-1*es11 were treated at pH3 during 90 seconds on ice.

74-11-10 antibody staining revealed an increase of fluorescence in C1R SLA-1*es11 cells after denaturalization (Figure 28a) confirming previous results. In contrast, staining with antibody 4B7/8 did not show any mayor change in fluorescence (Figure 28b). Therefore, the effect observed for 74-11-10 could be particular of this antibody. However, this is not due to recognition of SLA-I heavy chain, because 4B7/8 staining indicated that SLA-I was not denaturalized as fluorescence was maintained at the same levels before and after denaturalization. Recombinant cells showed a weak staining with W6/32 antibody, whose fluorescence decreased after denaturalization (Figure 28c). Fluorescence with BBM.1 staining decreased after denaturalization as well. W6/32 and BBM.1 stainings could indicate that the

low levels of HLA in C1R cells could be denaturalised, determining release of β 2m from the cellular surface. However, BBM.1 fluorescence did not reach background levels after denaturalization (Figure 28d) indicating that some β 2m was still retained on the cellular surface, probably by the transfected SLA-I allele.

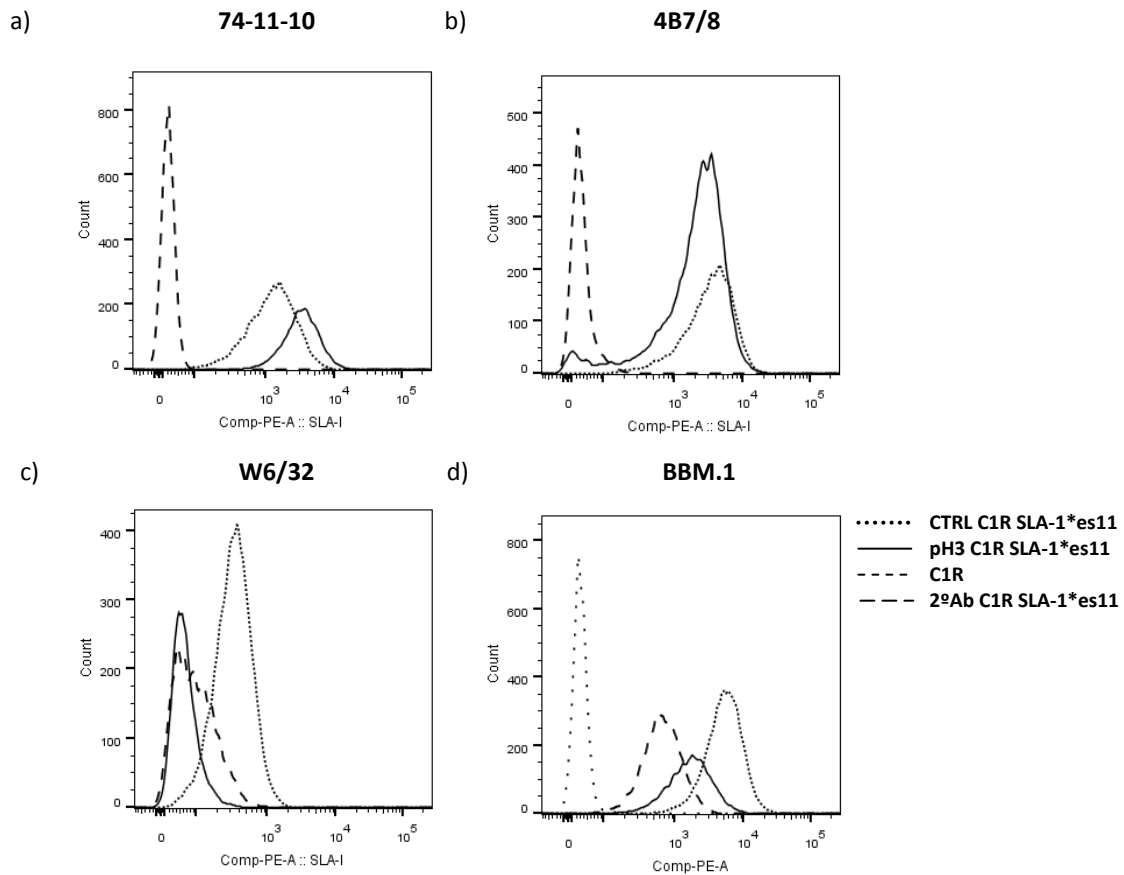


Figure 28. Testing antibody specificity after denaturalization on C1R SLA-1*es11. Cells were denaturalized at pH3 on ice and then stained with different antibodies against SLA-I a) 74-11-10, b) 4B7/8, against HLA-I c) W6/32 and against β 2m d) BBM.1. Dotted lines are CTRL C1R SLA-1*es11, continuous lines are pH3 treated C1R SLA-1*es11, slash dotted lines are C1R, large spaced dotted lines are C1R SLA-1*es11 stained with just the secondary antibody.

These results suggested that HLA was denaturalised while transfected SLA-I was not. To destabilize the chimeric SLA-1*es11 structure and thus achieve its denaturalization, the temperature of the assay was increased up to 37°C. In that case, re-circularization of newly synthesized SLA on cells surface was avoided by pre-incubation of cells with the inhibitor of protein transport Brefeldin A. Staining with antibodies was performed at room temperature. This treatment decreased C1R SLA-1*es11 cells fluorescence in all staining conditions tested using 74-11-10, 4B7/8, W6/32 and BBM.1 (Figure 29).

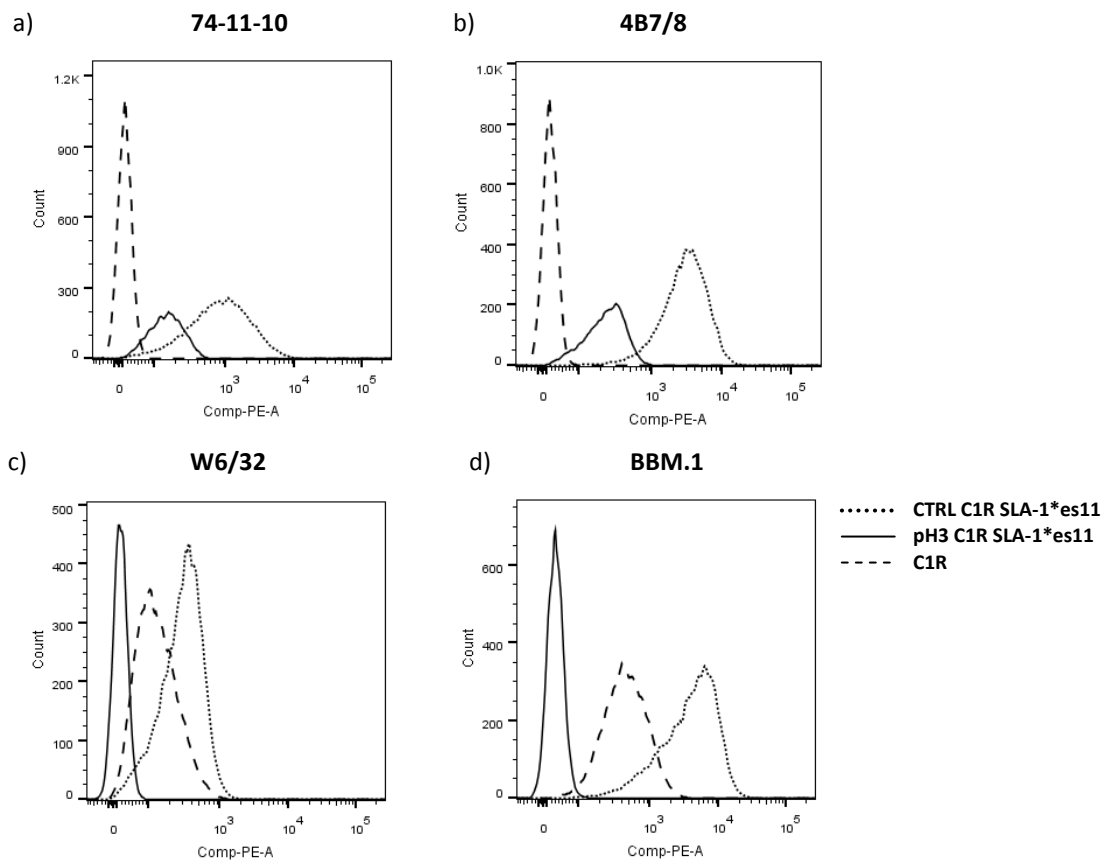


Figure 29. Denaturalization test at 37°C. Cells were denaturalized at pH3, during 90 seconds at 37°C; then, they were stained at room temperature with different antibodies: a) 74-11-10, b) 4B7/8, c) W6/32, d) BBM.1. Dotted lines are CTRL C1R SLA-1*es11, continuous lines are pH3 treated C1R SLA-1*es11 and slash dotted lines are C1R.

Therefore, denaturalization of SLA (measured by 74-11-10 and 4b7/8) and HLA (measured by W6/32) was achieved and thus β 2m (measured by BBM.1) was released. However, a little of SLA-I was still present on cell surface as fluorescence levels of 74-11-10 (Figure 29a) and 4B7/8 (figure 29b) were not brought to background levels (C1R). The behaviour of 74-11-10 staining observed in previous experiments (Figures 26-28) was probably related to performing the experiment on ice, as this effect was not noticed in this experiment performed at 37°C (Figure 29a).

Therefore, denaturalization step of the SLA reconstitution assay was achieved on C1R SLA-I*es11 transfected cells using the following conditions: pH3, incubation of 90 seconds, 37°C and finally staining with the appropriate antibody at room temperature.

Chapter III: Identification of Swine Influenza Virus T cells epitopes in inbred pigs

There is a lack of knowledge around SwIV epitopes recognised by porcine T cells. T lymphocytes are involved in immune responses against SwIV and only few SLA-I epitopes have been identified in just one allele (SLA-1*0401), whereas any SLA-II epitopes have been identified. This situation is partially due to the technologies used for T cells identification. Therefore, knowledge on different SLA epitopes is needed and more evidence supporting the already available tools for their identification is also required. T cells epitopes are generally identified in inbred models, when available. MHC homozygosis allows better definition of epitope restriction²²¹. Inbred lineages are rare in large animals and thus not widely used. Inbred pigs have never been used for T cells epitopes identification. The aim of this work was to apply RV as well as conventional methods to identify T cell epitopes of SwIV in inbred pigs bearing SLA-I alleles SLA-1*es11 and SLA-2*es22. So far, SLA-II alleles in those inbred pigs has not been defined. RV was used to identify SLA-I epitopes through *in silico* prediction followed by *ex vivo* functional assays. Also, SLA epitopes were identified empirically through testing *ex vivo* overlapping peptides representing two SwIV proteins. Another aim of this work was to characterise the identified epitopes, as in their conservation, anchor positions and responding T cells subsets.

Materials and methods

Animals

Babraham pigs were housed at the Greenfield farm (Compton) belonging to The Pirbright Institute. Those are inbred large white pigs syngenic for the allele SLA-1*es11 and SLA-2*es22. Animals were *Mycoplasma Hyopneumoniae* and Porcine Reproductive and Respiratory Syndrome Virus free. They were vaccinated for Glassers Disease (MSD Animal Health), Mites and Parasites Panomec Injection (Merial), Erysipelas Porcillis Ery Injection (MSD Animal Health), Parvo Virus Suvaxyn Parvo/E Injection (Zoetis). Study 1: animals were 25-30 weeks old and around 39-50 Kg of weight; they were labelled B557, B558, B563, B564, B568 and B570. Study 2: animals were 8-9 weeks old and around 5.5-9.5 Kg of weight; they were labelled CTRL, 1 and 2. Study 3: animals were 2-3 years old and around 173-192 Kg of weight; they were labelled B625 and B650. All studies were carried out under UK Home Office Licence number 70/7505 and approved by the ethical review processes at The Pirbright Institute.

Virus propagation and titration

Virus A/Swine/Spain/SF11131/2007 (SpH₁N₁) was isolated and sequenced previously ²²² (Chapter I). Virus was isolated and propagated in embrionated eggs, as described in chapter 1 and then once in MDCKs cells. The latter step is here briefly described. Virus was diluted 1:10 in PBS with 10µg/ml of porcine trypsin type IX from pancreas (Sigma) and incubated 30 minutes at 37°C. MDCKs cells were cultured in flasks until confluent. Treated virus was inoculated to flasks at 0.01 MOI and incubated 1 hour at 37°C and 5% CO₂, for absorption. DMEM (Lonza) media supplemented with 1µg/ml of porcine trypsin and L-Glutamine (Life technologies) was added and then, they were cultured between 2 and 3 days at 37°C and 5% CO₂. Presence of cytopathic effect confirmed replication of the virus. Supernatants were harvested, centrifuged (450g during 10 minutes) and stored at -80°C until further use. Mock treated cells were processed following the same protocol and generated samples labelled as MDCKs sup.

Virus stocks were then titrated as follows. Virus was diluted 1:10 in PBS with 10µg/ml of porcine trypsin type IX from pancreas (Sigma) and incubated 30 minutes at 37°C. MDCKs cells were grown in plain bottom 96 wells plate until confluent. Treated virus was diluted to end point (serial diluted 1:10) in PBS and inoculated to each plate at 20µl per well. Plates were incubated 1 hour at 37°C and 5% CO₂ for absorption. DMEM (Lonza) media supplemented with 1µg/ml of porcine trypsin and L-Glutamine (Life technologies) were distributed at 200µl per well per plate. Plates were then cultured between 5 and 7 days at 37°C and 5% CO₂. Cytopathic effects were read and TCID₅₀ was then calculated by the method of Reed and Muench ²²³.

Generation of the UV inactivated SpH₁N₁

SpH₁N₁ virus (7.36-7.24 logTCID₅₀/ml) was distributed into 6 wells plates generating a layer of 3 mm height. VL-4.C, 4W 254 nm UV lamp (Vilber) was located at 7 cm of distance from the bottom of the plate. Wells were exposed to UV radiation during 20 minutes at room temperature. To determinate virus inactivation the following method was used. The starting volume of inactivated virus to be tested was 500µl; this volume was treated with trypsin as above described and the entire 1:10 solution of virus (5 ml) was tested on MDCK plates at 20µl per well following the standard procedure described above. Absence of any cytopathic effect confirmed virus inactivation with a limit of detection of 0.3 logTCID₅₀/ml. Hemagglutination Units (HAU) were used to evaluate the quality of inactivated virus, as protein integrity. The assay was performed using chicken red blood cells (RBC). Virus was diluted to end point in PBS (1:2 dilution). One volume of 0.5% suspension of RBC in PBS was added to each condition;

then, those were incubated at room temperature up to maximum 45 minutes. The highest dilution of virus that causes complete hemagglutination was considered the HAU titration end point. The HAU units were the reciprocal of titre. HAU were maintained before and after inactivation of the virus at around 512-256 HAU/50 μ l of solution.

Pig immunization

Animals were immunised as described in table 6 and 28 days later they were boosted following the same procedure. Intramuscular immunisation was performed inoculating antigens in the front shoulder. Intranasal immunisations were performed inoculating antigens by a mucous administration device (Wolfe Tory Medical) in nasal cavities. Animals were culled at 28 days post boost (dpb) in study 1 and 2; in contrast, in study 3 animals were culled at 14 dpb. Antigens used to immunise pigs were whole inactivated SwIV (SpH₁N₁ and Gripovac 3) or live attenuated recombinant IAV (S-Flu). S-Flu was used to boost immune response in study 3. This is a recombinant virus constituted by H5 HA subtype and the rest of proteins from the human IAV A/PR/8/34. This virus was generated and attenuated by suppression of HA signal sequence by Dr. Alan Townsend (University of Oxford, UK) as described by Powell *et al.* 2012²²⁴.

Antigen	Adjuvant	Dose TCID ₅₀ *	Brand	Route	Animals
<u>Study 1</u>					
UV inactivated A/Swine/Spain/SF11131/2007 (H ₁ N ₁)	Montanide (Seppic)	10 ⁷	In house	IM	B557 B563 B568
Binary ethyleneimine inactivated A/Swine/Bakum/IDT1769/2003 (H ₃ N ₂) A/Swine/ Haselünne/IDT2617/2003 (H ₁ N ₁) A/Swine/ Bakum/1832/2000 (H ₁ N ₂)	Carbomer 971 P NF	N/A	Gripovac3 (IDT Biologika)	IM	B558 B564 B570
<u>Study 2</u>					
UV inactivated A/Swine/Spain/SF11131/2007 (H ₁ N ₁)	Montanide	2x10 ⁷	In house	IM	1 and 2
None	-	-	-		CTRL
<u>Study 3</u>					
UV inactivated A/Swine/Spain/SF11131/2007 (H ₁ N ₁)	Montanide	3.5x10 ⁷	In house	IM	625
Pseudotyped IAV (S-Flu), H5 HA	-	6x10 ⁷	Powell et <i>al.</i> ²²⁴	IN	650

Table 6. Immunization followed in the three studies. The route of immunization was intramuscular (IM) or intranasal (IN). Live attenuated virus S-Flu was kindly donated by Dr. Alan Townsend (University of Oxford, UK). * in case of inactivated virus the dose corresponded to the titre before inactivation.

Sampling

Samples were collected following the scheme in table 7.

Study 1 dpi	Study 2 dpi	Study 3 dpi
<u>PBMCs</u> 0, 28, 31, 35, 42, 56	0, 28, 35, 42, 49, 56	0, 28, 35, 42
<u>Sera</u> 0, 28, 25, 42, 56	0, 28, 42, 49, 56	0, 28, 35, 42
<u>Spleen</u> 56	-	-
<u>BALc</u> -	-	42

Table 7. Sampling of pigs in each study.

PBMCs

Blood was collected in heparinised tubes by anterior vena cava venepuncture. Peripheral Blood Mononuclear Cells (PBMCs) were obtained by density gradient centrifugation, 1200xg for 30 min over Histopaque 1.083 g/ml (Sigma). RBC were lysed by 5 minutes incubation on ice with Ammonium Chloride buffer (Ammonium Chloride 155mM, Potassium Bicarbonate 10 mM, EDTA disodium salt 0.1mM) and then washed several time with PBS. Cells were counted and frozen at -80°C in FCS (Gemini) with 10% Dimetil Sulfoxid (DMSO). Samples were stored in liquid nitrogen for further use.

Sera

Sera was harvested from centrifuged clotted blood samples maintained at 4°C. Samples were stored at -80°C for further use.

Spleen

Following culling of animals, spleens were harvested and chopped into small pieces. Cells were then passed through a metallic sieve and RBC lysed. Then, cell suspensions were separated in a Histopaque gradient and processed as described for PBMCs.

Broncheo Alveolar Lavage cells (BALc)

Following culling of animals, lungs were removed and washed with 250 ml of cold PBS supplemented with penicillin/streptomycin (Life technologies). The harvested fluids were centrifuged and cells collected. Cells were then separated on Histopaque gradient and processed like the PBMCs.

Culture medium

Culture medium was RPMI-1640 medium with glutamax-I and 25 mM Hepes (Life technologies) supplemented with penicillin/streptomycin (Life technologies), and 10% heat-inactivated pig serum (Life technologies) or FCS (Gemini).

Peptides

Predicted peptides (Table 3 in supplementary files) and those representing the 43 and 44 peptides sequences were synthesized by the Laboratory of Proteomics & Protein Chemistry, Department of Experimental & Health Sciences of the Pompeu Fabra University (Barcelona, Spain). Peptides constituting pools 1-3 represented NP (AFG72805.1) and M1 (AFG72802.1) protein sequences of human IAV strain A/Panama/2007/1999 (H₃N₂) while MSP represented the Malaria Merozoite Surface Protein-1. Those pools were gently donated by Dr. Sarah Gilbert (The Jenner Institute, Oxford, UK). Peptides were resuspended in DMSO and in culture media at the desired concentration. They were conserved at -80°C for further use.

Stimulus

Study 1

Stimulus were diluted in culture media and tested as the following amount per well: predicted peptides (Table 3 of supplementary files) and pools (Table 5 of supplementary files) at 1µg, virus at 10⁵ TCID₅₀, MDCK sup was diluted like virus and Gripovac3 diluted 10 folds. Culture Media was used to determinate background of the assays (Media). Where specified, DMSO was added to the stimulus diluted 500 folds to resemble the amount contained in peptide suspensions.

Study 2-3

Stimulus were diluted in culture media and tested as the follow amount per well: Pools 1-3 and MSP at 1µg, Pools A-D and individual peptides (Table 4 and 5 in supplementary files) at 0.2µg, SpH₁N₁ at 10⁵ TCID₅₀, MDCK sup diluted like the virus, S-Flu at 2x10⁵ TCID₅₀. Culture Media was used to determinate background of the assays (Media).

ELISA assays.

Sera were diluted 1:50 and then serially diluted 1:3 in milk PBST (PBS, 4% dry milk (Marvel) and 0.05% Tween20). Viruses were diluted in carbonate buffer, pH9.6. Falcon 96-Well PVC Plates (Becton Dickinson) were coated with 10⁴ TCID₅₀ per well with diluted virus, incubated 1 hour and washed five time in PBST (PBS and 0.05% Tween20). Plates were blocked 1 hour with milk PBST and washed again five times. Sera dilutions were distributed in each plate at 100µl per well, incubated 1 hour and washed five times. Porcine IgG were labelled with 100µl per well of Goat anti pig IgG(Fc)-HRP (Serotec) diluted 10⁵ folds. Plates were then incubated for 1 hour,

washed five times and then 50µl per well of TMB substrate were added. Finally, adding 50µl per well of 0.1 M sulfuric acid stopped enzymatic reaction. Plates were read at 450nm and 630nm using a PowerWave XS reader (Biotek). Data was analyzed using Excel and Prism software.

IFN γ ELISPOT

Capture antibody Purified Mouse Anti-Pig IFN- γ (Clone P2G10) (Becton Dickinson) was diluted in carbonate buffer (pH9.6). 50ng per well of capture antibody were used to coat MultiScreen-HA ELISPOT plates (Millipore). Plates were incubated for 2 hours and then washed five times with PBS. Blocking was performed distributing 100µl per well of PBS with 4% milk (Marvel), incubating 2 hours and finally washing again five times. Stimuli were distributed at 100 µl per well. Pokeweed mitogen (PWM) 1µg/ml or Concanavalin A (ConA) 10µg/ml (Sigma) were used as positive control. Cells were distributed at 5×10^5 per well for all stimuli except PWM, for which 10^5 cells per well were used. Plates were cultured overnight at 37°C and 5%CO₂. Cells were washed off the plates using PBST (PBS, 0.05% Tween 20). 100 µl per well of biotinylated mouse anti-pig IFN γ (Clone PTC11) (Becton Dickinson) diluted at 0.5 µg/ml, were added to each plate and incubated 2 hours at room temperature. Plates were washed again five times with PBST. 100 µl per well of streptavidin conjugated to alkaline phosphatase diluted 1:1000 (Invitrogen) were added to each plate and incubated 1 hour at room temperature. Plates were washed five times with PBST. 100 µl per well of alkaline phosphatase substrate solution (Biorad) were added to each plate and incubated for 20 min at room temperature. Plates were then rinsed with tap water and allowed to dry overnight at room temperature. Finally, Dark blue-coloured immunospots were counted using the AID ELISPOT reader (AID Autoimmun Diagnostika).

Proliferation assays

[H³] Thymidine incorporation assay

Cells at 2×10^5 per well and each stimulus were plated into a final volume of 200µl in 96 U bottom well plates. PWM at 0.1µg per well was used as positive control. Plates were cultured at 37°C and 5%CO₂ during 5 days. Cells were then pulsed with [H³] Thymidine (Senior RPS) at 1µCi per well and culture for another 16-18 hours. Cells were then harvested onto a glass fibre filter-mat (PerkinElmer) using the semi-automated cells harvester (Tomtec). Scintillation

cocktail (PerkinElmer) was added to the Filtermats and then they were counted with Wallac Trilux Microbeta scintillator counter (PerkinElmer).

CellTrace Violet proliferation assay

Cells were labelled with CellTrace Violet Proliferation Kit (Life technologies), which was used at 2.5 nM following the manufacturer's instructions. Labelled cells were then plated at 5×10^5 per well with stimulus at the above reported conditions. 2 μ g of ConA (Sigma) were used as positive control. Six wells per stimulus were used. Plates were incubated during 5 days at 37°C and 5% CO₂. Cells were then centrifuged and washed with buffer A (above reported). Staining for surface markers CD4, $\gamma\delta$ and isotype controls was performed by incubating cells with reagents in table 8 during 10 minutes at room temperature. Excess of reagents was washed out two times with buffer A and cells were stained with corresponding secondary antibodies (Table 8) during 10-minute incubation at room temperature. Again, the excess of antibody was washed out two times with buffer A and cells were stained with Live/Dead, CD3 and CD8 antibodies during 10 minutes at room temperature. Finally, cells were washed with buffer A and fixed with 1% paraformaldehyd in PBS. Samples were passed through LSR Fortessa II (Beckton Dickinson); at least 1×10^5 events were collected. Data were analyzed with FlowJo v7 (FlowJo). Results were graphed with Prism v5.01 (GraphPad).

	Clone	Subtype	Fluorophore	Brand	
<i>MHC blocking</i>					
<u>1°Antibodies</u>					Amount per 5x10⁵ cells
SLA-I	74-11-10	IgG2a	-	Kingfisher and in house	
SLA-II	MSA-3	IgG2b	-	Kingfisher and in house	
<u>Isotype controls</u>					
	W6/32	IgG2a	-	In house	
<i>IFNγICS</i>					
<u>1°Antibodies</u>					Amount per 10⁶ cells
CD3	BB23-8E6-8C8	IgG2a	Alexa Fluor 647	Becton Dickinson	200ng
CD4	MIL-17	IgG2b	Biotinilated	In house	120ng
CD8 α	MIL-12	IgG2a	FITC	AbD Serotec	100ng
$\gamma\delta$ TCR	PGBL22A	IgG1	-	Kingfisher	40ng
LIVE/DEAD Fixable Near-IR Dead Cell Stain Kit			APC-Cy7	Life Technologies	0.3 μ l
IFN γ	P2G10	IgG1	PE	Becton Dickinson	20ng
<u>2°Antibodies</u>					
Streptavidin			Alexa Fluor	Life technologies	100ng

Anti-IgG1			700 eFluor® 450	eBioscience	20ng
<u>Isotype controls</u>					
-	MOPC-173	IgG2a	Alexa Fluor 647	BD, 558053	0.4µl
-	MPC-11	IgG2b	Biotinilated	AbCam	120ng
-		IgG1	PE	AbCam, ab81200	20ng
-	MRC OX- 34	IgG2a	FITC	AbD Serotec	100ng
-	ICIGG1	IgG1	-	AbCam, ab91353	40ng
<i>Proliferation assay</i>					
<u>1°Antibodies</u>					
γδ	PGBL22A	IgG1	-	Kingfisher	40ng
CD4	MIL-17	IgG2b	Biotinilated	In house	120ng
CD8	76-2-11	IgG2a	PE	Becton Dickinson	80ng
CD3	PPT3	IgG1	PE-Cy5	AbCam	40ng
LIVE/DEAD Fixable Near- IR Dead Cell Stain Kit				Life Technologies	0.3µl
<u>2°Antibodies</u>					
Streptavidin			APC	Southern Biotech	100ng
Anti-IgG1			FITC	Southern Biotech	100ng
<u>Isotype controls</u>					
-	ICIGG1	IgG1	-	AbCam	40ng
-	MPC-11	IgG2b	Biotinilated	AbCam	120ng
-	X39	IgG2a	PE	BD (340459)	80ng
-	15H6	IgG1	PE-Cy5	AbCam	40ng

Table 8. Antibodies used in this chapter.

MHC blocking

Inhibition of class I or class II MHC mediated IFN γ response was performed through co-incubation of cells, stimulus and anti-MHC antibodies. The antibodies used to block SLA-I and SLA-II and the isotype control are listed in table 8. Cells used were from animals of study 2 and 3 at different time points post immunization. Samples were then assayed by IFN γ ELISPOT.

Cells separation by Magnetics Activated Cell Sorting

Cells were labelled with the anti SLA-II antibody MSA-3 (hybridome supernatant diluted 10 fold) and separated by Magnetics Activated Cell Sorting Anti-Mouse IgG MicroBeads (Myltenyi), which are conjugated to goat anti mouse IgG (H+L), following manufacturer instructions. Recall responses to peptides 43 and 44 from SLA positive and negative fractions were then characterized by IFN γ ELISPOT. Viability of cell suspensions was evaluated using LIVE/DEAD Fixable Near-IR Dead Cell Stain Kit (Life Technologies) at 0.3µl per 10⁶ cells. Purity

was evaluated using the anti mouse IgG PE (Jackson Immunology) diluted 50 fold binding to MSA-3 antibody and thus it permitted evaluating presence of SLA-II⁺ cells by flow cytometry in each cell fraction. Reagents used for viability and purity were incubated during 10 minutes at room temperature with samples of SLA-II⁺ and SLA-II⁻ cells fractions. Excess of reagents was washed out two times with PBS, 0.2% Sodium Azide and 2%FCS. Cells were then fixed with 1% paraformaldehyde in PBS and passed through LSR Fortessa II (Beckton Dickinson); at least 2x10⁴ events were collected. Data were analyzed with FlowJo v7 (FlowJo). Results were graphed with Prism v5.01 (GraphPad).

IFN γ Intracellular Cytokine Staining (IFN γ ICS)

Cells were distributed at 5x10⁵ per well in a 96w plate with stimuli. 1ng of Phorbol 12-myristate 13-acetate (PMA) (Sigma) and 20ng of Ionomycin (Sigma) per well were used as positive controls. Six wells for each stimulus were used. After 2 hours of culture at 37°C and 5%CO₂, protein transport was inhibited with 0.25 μ g of Brefeldin A Golgi plug (Becton Dickinson) per well. Plates were cultured again during 6 hours and then stored at 4°C over night. Cells for each stimulus were joined together and stained using the following protocol. Briefly, cells were centrifuged and washed with buffer A (PBS, 0.2% Sodium Azide and 2%FCS). Staining reagents were also diluted in buffer A. Cells were incubated during 10 minutes at room temperature with Live/Dead, isotype controls or cells surface markers CD3, CD4, CD8 and $\gamma\delta$ (Table 8). Excess of reagents was washed out two times with buffer A and then cells were stained with secondary antibodies (Table 8) during 10-minute incubation at room temperature. Excess of reagents was washed out 2 times with buffer A. Cells were fixed and permeabilized with Cytofix/Cytoperm (Becton Dickinson) following manufacturer's instructions and stained with the anti-IFN γ antibody and Isotype control reported in table 8. Finally, samples were passed through LSR Fortessa II (Beckton Dickinson); at least 2x10⁵ events were collected. Data were analyzed with FlowJo v7 (FlowJo). Results were graphed with Prism v5.01 (GraphPad).

Structure of NP protein.

3D structure of NP of A/Panama/2007/1999 IAV strain (AFG72805.1) was built by homology modelling through the automatic ExPasy server Swiss Model (<http://swissmodel.expasy.org/>)²²⁵. The resulting homologous model was visualized and hydrophobicity analyzed with Cn3D (<http://www.ncbi.nlm.nih.gov/Structure/CN3D/cn3d.shtml>)²²⁶.

Conservation analysis of epitopes

Sequences of IAV of different subtype and isolated in swine, human and avian were retrieved from the Influenza Virus Resource (<http://www.ncbi.nlm.nih.gov/genomes/FLU/FLU.html>)¹⁹⁸; at least 500 full length sequences for each group were taken into account. Those belonged to the protein in which epitopes were located. Sequences were aligned with Clustal W implemented in MEGA5; regions corresponding to epitope sequences were used to generate logo by Weblogo Version 2.8.2 (<http://weblogo.berkeley.edu/>).

Statistical analysis

Descriptive statistics including distribution images of results and tables were performed with SAS system V.9.1.3 (SAS institute). Non-parametric statistic analysis were performed with Wilcoxon test implemented from SAS software. Individual pigs were used as experimental unit. The significance level (p) was set at 0.05 with tendencies reported when $p > 0.1$.

Results

Candidate T cell epitopes

SpH₁N₁ epitopes were identified through two main pathways. The first one involved *in silico* prediction of candidate epitopes. Peptides with potential to bind to class I alleles at locus 1 SLA-1*es11 or at locus 2 SLA-2*es22, were predicted using *NetMHCpan v.2.8* software (<http://www.cbs.dtu.dk/services/NetMHCpan-2.8/>). Length from 8 to 10 amino acids was selected as parameter; this respect the minimum and maximum limit for class I MHC binding cleft. The prediction was performed on HA, PB1, M1 and NP proteins of SwIV SpH₁N₁. A total of 49 peptides were predicted (Table 3 in supplementary file). Irrelevant peptide sequence was taken from an irrelevant antigen and used as control.

The second approach empirically identified candidate epitopes through dissection of overlapping pools of peptides representing certain viral proteins. Those representing the sequence of SpH₁N₁ were not generated. However, pools 1 and 2 representing full NP and pool 3 representing M1 proteins (Pool 3) of human IAV strain A/Panama/2007/1999 (H₃N₂). were used (gently donated by Dr. Sarah Gilbert from the Jenner Institute, Oxford, UK). These pools were constituted by peptides between 17 and 20 amino acids and overlapping 10 amino acids (Table 5 in supplementary files). The homology of NP and M1 proteins between that virus and SpH₁N₁ was 90% and 92% respectively. Pool MSP represented an irrelevant antigen and was used as control (gently donated by Dr. Sarah Gilbert from the Jenner Institute, Oxford, UK).

Therefore, some candidates SLA-I epitopes were *in silico* predicted whereas others were empirically tested.

Priming of immune response in Babraham pigs

Antigen specific cells were generated with the desired antigen by immunising and boosting pigs intramuscularly with adjuvated inactive SwIV viruses, either SpH₁N₁ or those composing Gripovac3 (Table 6). Priming of animals was tested by analysing specific antibodies in sera. IgG responses were measured by ELISA and results from studies 1 and 2 are shown in figure 30.

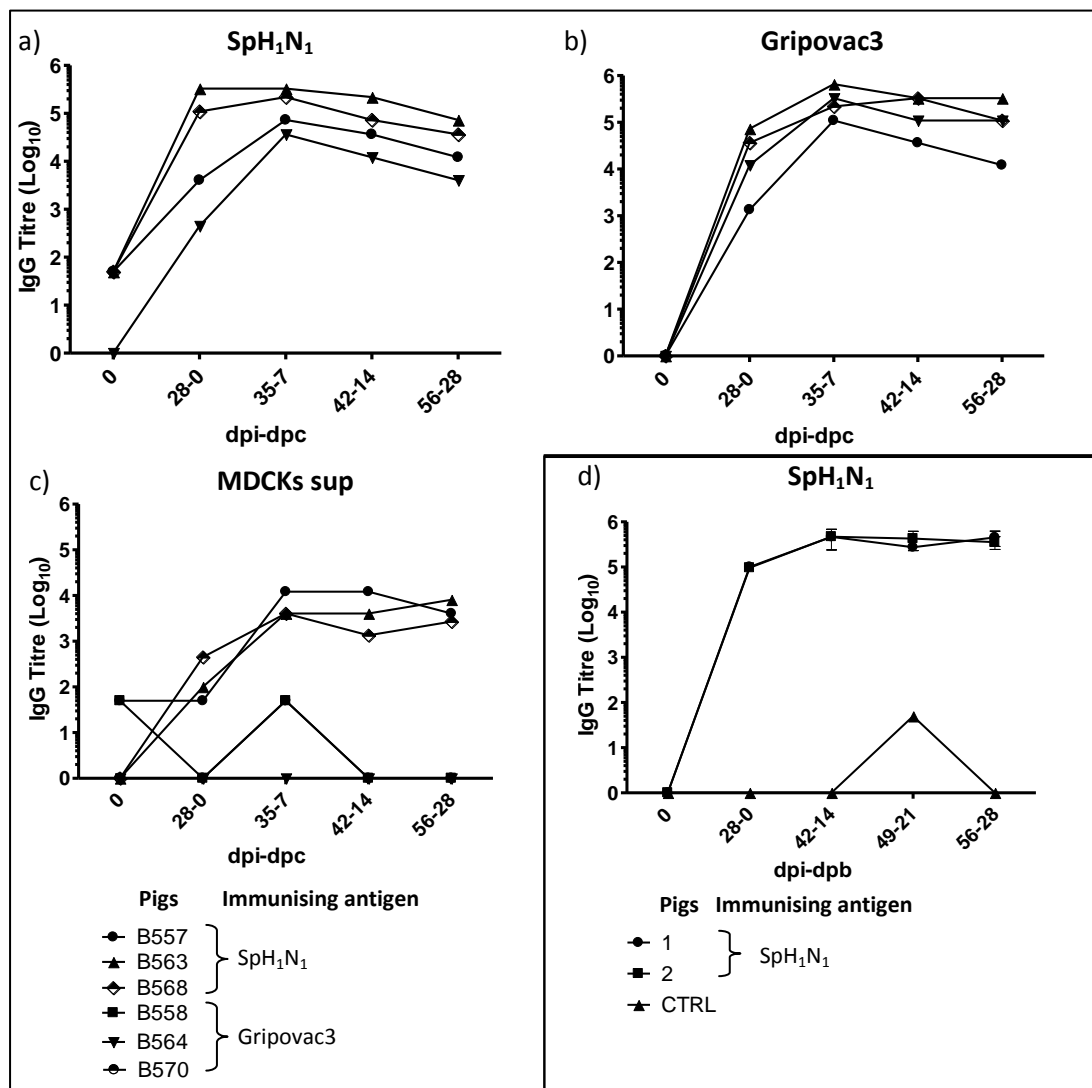


Figure 30. IgG ELISA in sera from study 1 and 2. Sera from study 1 were tested against antigens: a) SpH₁N₁, b) Gripovac3 and c) MDCKs sup. Pigs B557, B563, B568 were immunised with SpH₁N₁; pigs B558, B564, B570 were immunised with Gripovac3. Data are represented as mean of duplicate results. d) Sera from study 2 were tested against SpH₁N₁ antigen. Pigs 1 and 2 were immunised with SpH₁N₁ while pig CTRL was not immunised. Data are represented as mean with standard deviation (sd) of triplicate results.

Specific responses against different antigens were tested. Pigs immunised in study 1 and 2 responded to the homologous antigens used for immunisation and maintained the response during the entire study. In study 1, pigs B557, B563 and B568 responded to SpH₁N₁ (Figure 30a) while B558, B564 and B570 responded to Gripovac3 (Figure 30b); in study 2, pigs 1 and 2 responded to SpH₁N₁, whereas the untreated pigs did not (CTRL) (Figure 30d). Cross-reactive responses in SpH₁N₁ vaccinated animals to Gripovac3 and vice versa were observed. In study 1, B558, B564 and B570 pigs responded to SpH₁N₁ (Figure 30a) whereas B557, B563 and B568 pigs responded to Gripovac3 (Figure 30b). In the same study, immunisation of animals with SpH₁N₁ also generated humoral responses against the vehicle solution (MDCKs sup); this response was not shown when Gripovac3 was used to immunise pigs. IgG response to viral solution SpH₁N₁ was higher than the one against MDCK sup. and thus it was specific for virus antigens. Therefore, pigs showed specific IgG responses against the desired antigens.

Identification of T cells epitope.

Sequences of candidate epitopes were determinate, as explained above, by two approaches: *in silico* peptide prediction and empirical identification. Peptides representing those sequences were tested *ex vivo* on tissues from immunised pigs. Therefore, IFN γ and proliferative recall responses induced by the peptides were evaluated.

Predicted peptides were tested individually by using IFN γ ELISPOT and [³H] Thymidine incorporation assay in PBMCs from immunised pigs of study 1. Descriptive statistic analysis showed that distribution of these responses exhibited high standard deviations (sd) from day 0 and up to the end of the experiment (Figure 31 and figures 5-6 of supplementary files). This observed variability implied that positive responses were identified at each time point as those showing values major than the mean plus two to three times the standard deviation (depending on the assay). Following this approach, only outstanding positive responses were identified, decreasing the type I error of the analysis. However, this approach increased the probability to have a type II error but, at this stage, the most critical point was ensuring positive responses.

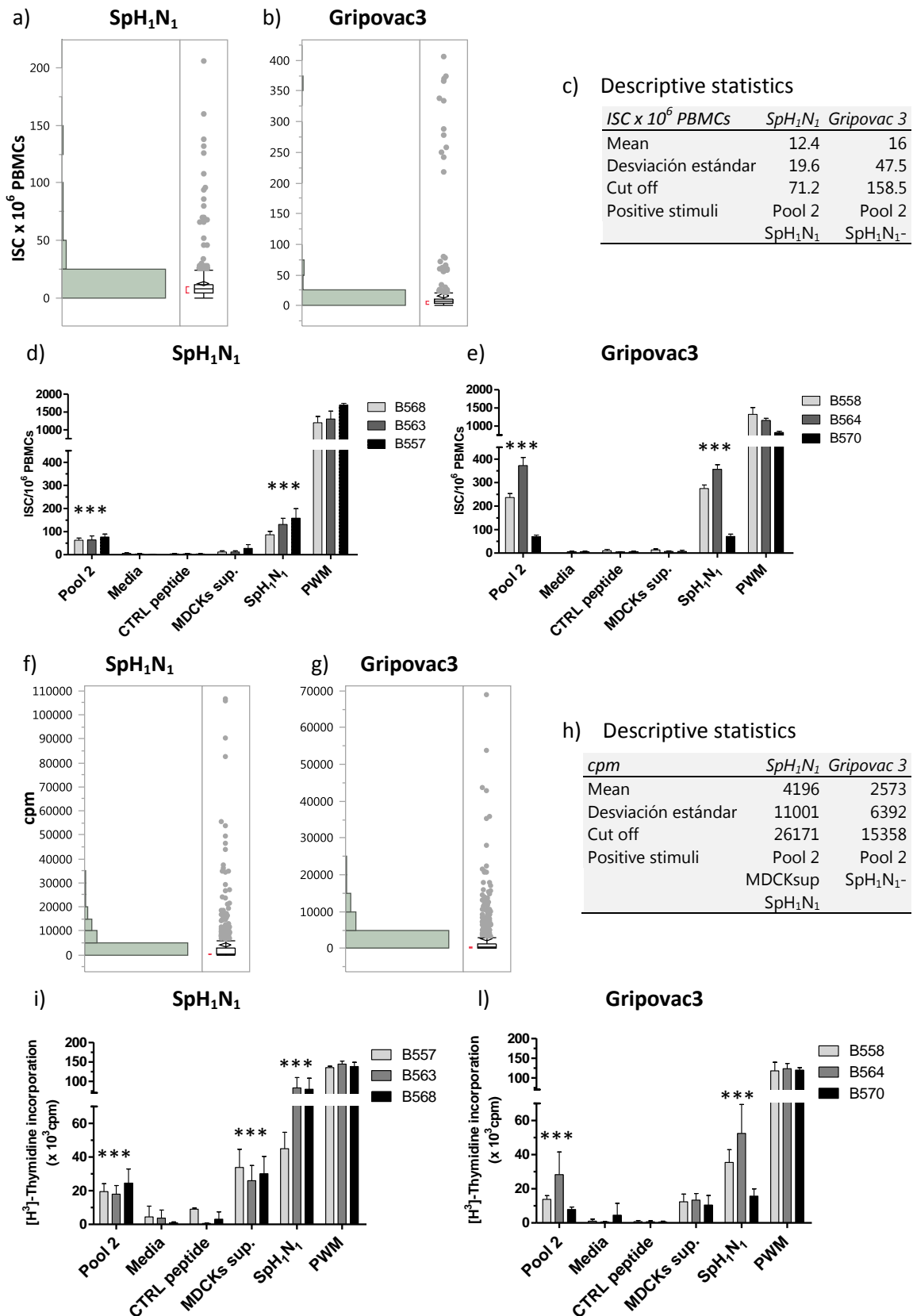


Figure 31. Identification of T cell epitopes in predicted peptides and pools of peptides representing NP, M1 proteins. Predicted peptides and pools 1-3 were tested by a-e) IFN γ ELISPOT or f-l) [3 H] Thymidine incorporation assay with PBMCs from animals immunized with SpH₁N₁ (a, d, f and i) or Gripovac3 (b, e, g and l) in study 1. Distributions (a, b, f and g) and descriptive statistics (c and h) of results are reported;

stimuli showing statistical significant positive results are those having values major than the mean and three times (IFN γ ELISPOT) or two times ([H^3] Thymidine incorporation assay) sd (cut off). Stimuli were tested in triplicate. b) and d) Results of positive identified stimuli; data are represented as mean and sd of IFN γ secreting cells (ISC) per 10^6 PBMCs (ISC/ 10^6 PBMCs) or counts per minute (cpm). Statistically positive stimuli are highlighted by asterisks.

SpH₁N₁ specific responses (IFN γ and proliferation) were generated after the first immunisation and maintained up to the end of the study in PBMCs (Figure 31 and figure 5-6 of supplementary files); those responses were also detected in spleen of animals immunised with Gripovac3 (Figure 5-6d of supplementary files). However, [H^3] Thymidine incorporation results showed that SpH₁N₁ and MDCKs sup recall responses were present even at 0dpi (Figure 6a supplementary files). None of predicted peptides showed a positive response at any tested time point in PBMCs nor spleen (Figure 31 and figure 5-6 of supplementary files). In summary, cellular mediated IFN γ and proliferative responses against SpH₁N₁ were generated and maintained after immunisation to the end of the study but none of the predicted peptides was identified as a SpH₁N₁ T cell epitope using a *in silico* peptide prediction approach.

T cells epitopes were also empirically identified in study 1. Pools 1-3 were tested simultaneously to predicted peptides by using IFN γ ELISPOT and [H^3] Thymidine incorporation assays on PBMCs of 14 dpb. The same statistic approach used for predicted peptides was also used to identify pools inducing positive responses. Pool 2 was giving a positive IFN γ and proliferative recall response (Figure 31) and therefore was selected for further analysis. Pool 1 and 3 were not giving any substantial positive response. Study 2 was performed to identify which peptides from pool 2 were responsible of the observed IFN γ response. Whole virus SpH₁N₁ or in its absence S-Flu, were used in IFN γ ELISPOT to check recall response in pig PBMCs to the antigens used for immunisation (SpH₁N₁). Positive responding stimuli were identified by non-parametric statistics analysis as those showing values major than media or pool MSP and with $p < 0.05$. SpH₁N₁ was tested just at 7dpb and it recalled positive responses in cells from immunised animals (Figure 32). Results using S-Flu were similar to SpH₁N₁ indicating that PBMCs from immunised pigs cross-reacted against S-Flu (Figure 32); however, this response was not positive at any further tested time point (Figure 7 of supplementary files). Peptides composing pool 2 were grouped in pools A-D (Table 5 supplementary file) and they were tested individually by IFN γ ELISPOT on PBMCs from animals in study 2. Pool 2 recalled IFN γ response in cells from all immunised animals (Figure 32). Pools A, B and C were positive at 7 dpb; although pools A and B were not further detected positive at any other time point

whereas pool C was positive also at 21 dpb (Figure 7 supplementary files). Finally, peptides composing pool C (peptides 39-46) were tested individually. Peptide 43 and 44 were inducing positive response at 7 and 14 dpb; at the other time points, they showed a tendency to positive response (figure 7 supplementary files). As expected, cells from CTRL pig were not responding to any pools, sub-pools and or even peptide 43 and 44 (Figure 32). Therefore, these results indicated that peptides 43 and 44 were the mayor inducers of IFN γ responses in pool C and in pool 2.

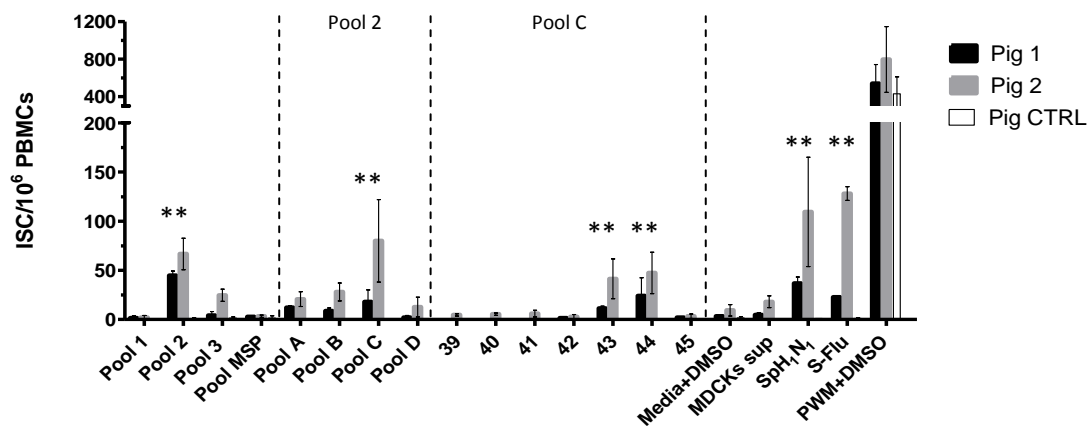


Figure 32. Empirical identification of T cells epitopes in Pool 2. Pool 1-3 and control (MSP), pools A-D and peptides of pool C (39-46) were tested by IFN γ ELISPOT with PBMCs of study 2 at 7 dpi. Pools A-D and individual peptides were not tested on the CTRL pig. DMSO was added to controls at the same concentration as peptides. MDCK sup is the mock infected control or better defined as the vehicle of virus particle of the immunization antigen SpH₁N₁. Results were expressed as IFN γ -producing cells number per 10⁶ stimulated PBMC (ISC/10⁶ PBMCs). Data for each animal was represented in graphs as mean with sd of triplicate results. Non-parametric statistic analysis identified stimuli with difference statistically significant when compared to media+DMSO and pool MSP. Those having a $p < 0.05$ are marked with asterisks (*).

Epitopes were better defined by using a new set of peptides encompassing the 43 and 44 (Table 4 Supplementary files), which were designed hypothesizing that an epitope was located in the overlapping region between peptide 43 and 44. Peptides differed each other by 2 amino acids in length; thus, the importance of amino acids located at the N-terminus and C-terminus of peptide 43 and 44 respectively was sequentially tested by IFN γ ELISPOT assay. Peptide 44 showed some mutations compared to the corresponding region in SpH₁N₁. Therefore, peptide Sp44 was designed without those mutations to evaluate their influence in recall responses. Study 3 was performed to test those peptides. Animals were immunised with the same inactive antigen previously used in previous studies, SpH₁N₁. However, live attenuated virus S-Flu was used for boosting. S-Flu had a high homology in the amino acid sequences of NP and

M1 within pools 1-3 (92% and 96%) and five mutations were falling into the sequences of peptide 43 and 44. As seen above (Figure 32), response to this virus was cross-reacting and thus able to boost epitopes shared by pool 2 and SpH₁N₁. Therefore, peptides were tested by IFN γ ELISPOT assay on PBMCs and positive responding peptides were identified by non parametric statistics analysis as those showing values major than irrelevant peptide or media and with $p < 0.05$. IFN γ recall response of antigens used for immunization was detected from the time of boosting (28 dpi or 0 dpb) and it was maintained up to the end of the study (Figure 33).

Positive response to virus vehicle (MDCKs sup) was also detected, defining non specific responses. Reactivity of PBMCs from immunised pigs from study 3 to pool 2, pool C and peptide 43 and 44 (Figure 33c) was positive and consistent with previous studies (1 and 2). Peptides 43a-d and 44c-e induced IFN γ recall responses (Figure 33). These responses were coherent during all time points tested in study 3.

The results showed that 43d (QISVQPTFSVQR) and 44c (SVQPTFSVQRNLPF) were peptides in which shortening of 2 amino acids at respectively the N terminus (QI) and C terminus (PF) led to lose IFN γ recall responses, suggesting that anchor positions important for SLA presentation were located there (anchor regions). A difference in ISC numbers was noticed when peptides 44c and 44d were compared (non-parametric statistics analysis). Peptide 44d induced more ISC than 44c ($p < 0.05$); this can be interpreted in two ways. On one hand, sequence SVQPTFSVQRNLPF EK (peptide 44d) might contain 2 overlapping epitopes in which the first ended at PF (peptide 44c) and the second ended at EK. Those epitopes might contribute to the observed IFN γ response of peptide 44d; however, losing EK disrupted one of the epitopes in peptide 44d and thus IFN γ response decreased to level of peptide 44c. Thus, the anchor position of the second epitope in 44d could be located in EK. On the other hand, another explanation would be that EK amino acids at the C terminus of epitope SVQPTFSVQRNLPF improve presentation from SLA or TCR recognition and thus increasing IFN γ response generated by that epitope. Finally, peptide Sp44, which had the corresponding sequence of peptide 44e (or peptide 44) but from the SpH₁N₁ virus, showed a response similar to 44e (Figure 33), suggesting that those specific mutations (Table 4 supplementary files) were not located in relevant positions for TCR recognition or SLA presentation.

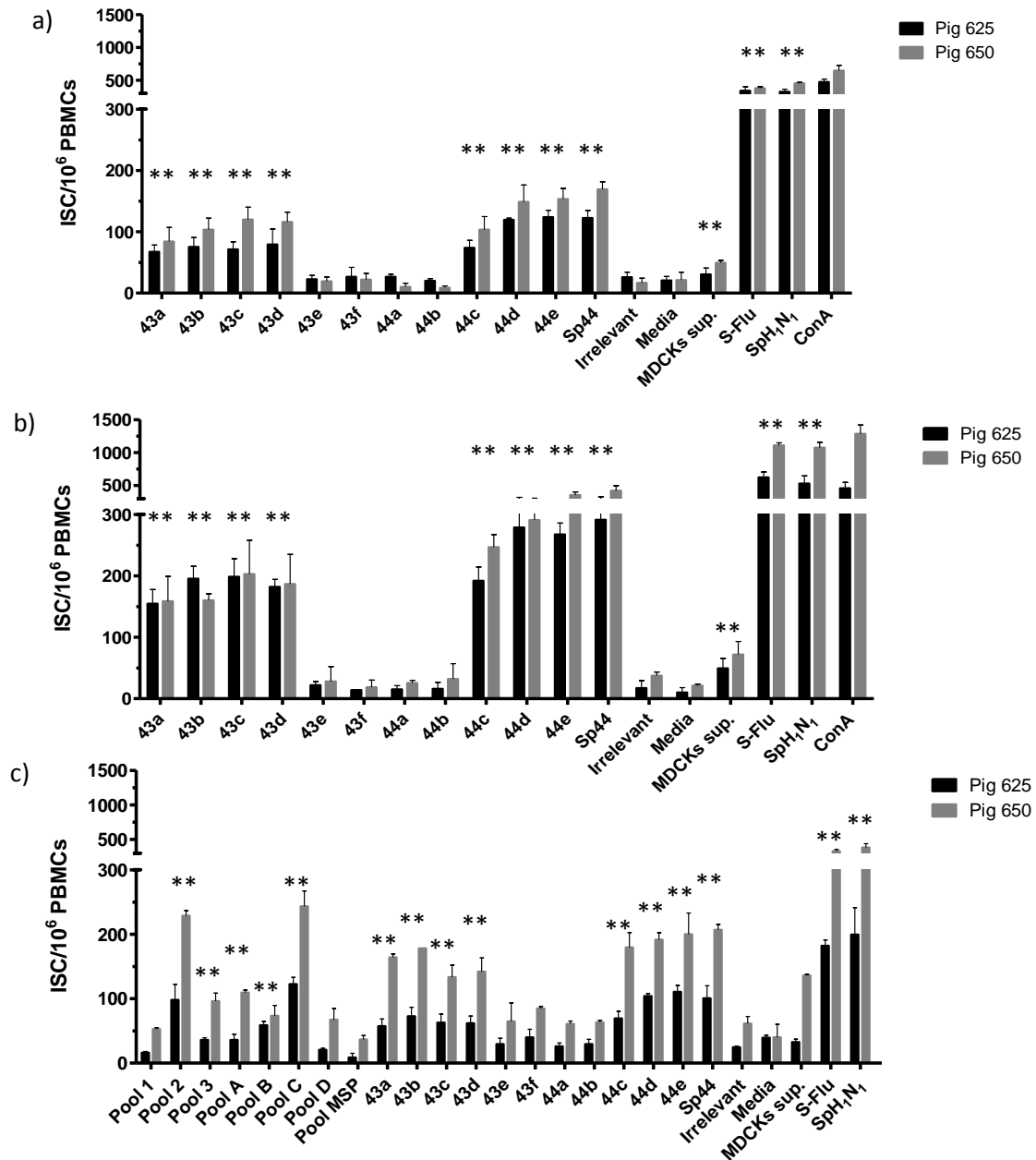


Figure 33. Empirical identification of T cells epitopes in peptide 43 and 44. Pool 1-3 and control (MSP), pools A-D, peptides 43-44, 43a-f, 44a-e and Sp44 were tested by IFN γ ELISPOT with PBMCs of study 3 at a) 28dpi or 0dpb b) 7dpb c) 14dpb. MDCK sup is the mock infected control or better defined as the vehicle of virus particle of the immunization antigen SpH₁N₁. Results were expressed as IFN γ -producing cells number per 10⁶ stimulated PBMC (ISC/10⁶ PBMCs). Data for each animal was represented in graphs as mean with sd of triplicate results. Non-parametric statistic analysis identified stimuli with difference statistically significant when compared to media+DMSO, pool MSP or irrelevant peptide. Those having a p<0.05 are marked with asterisks (*).

Immunisation of pigs in study 3 contributed to induce an antigen specific CMI response also in respiratory tract. SpH₁N₁ and S-Flu showed to recall response in BALc when tested by IFN γ ELISPOT (positive recall response defined as those with showing difference with p<0.05).

Specific IFN γ responses were also recalled when peptides 43 and 44 were tested, although they were observed for just one animal whereas the other one just showed a tendency (Figure 8 in supplementary file). Therefore, responses to virus and peptides 43 and 44 were not only systemic but also local.

Once epitope sequences were defined, the question was whether they were associated to presentation by SLA-I, SLA-II or both. To get insight into the question, PBMCs from immunised pigs were incubated with blocking antibodies against SLA-I and SLA-II. Antibodies treated cells were then tested by IFN γ ELISPOT; antibodies were inhibiting when ISC were compared with untreated control ($p < 0.05$ in non parametric analysis). Results in figure 34a showed that inhibition of IFN γ recall responses from peptides 43 and 44 was accomplished when anti SLA-II antibody was used in the assay. Anti SLA-II antibody inhibition was higher than the one by anti SLA-I antibody every time the experiment was repeated (Figure 34b, $p < 0.05$). This result indicated that IFN γ response induced by peptide 43 and 44 was SLA-II dependent.

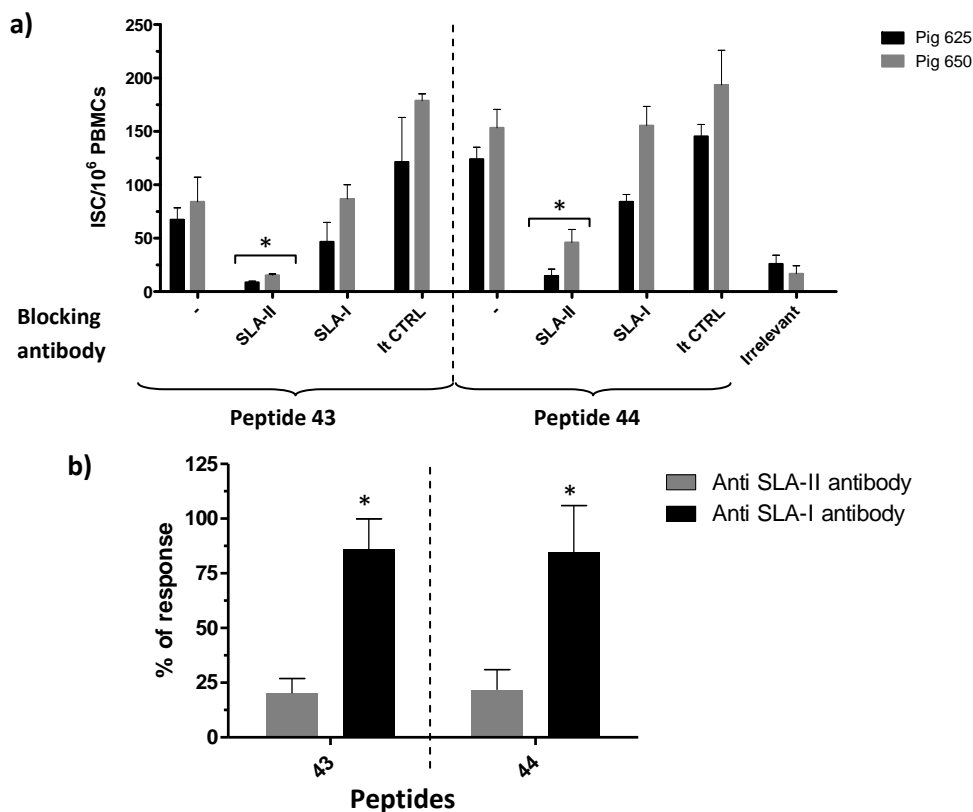


Figure 34. SLA class of the identified T cells epitopes. SLA blocking of IFN γ recall responses of peptides 43 and 44. a) Anti SLA-II and SLA-I antibodies or isotype control (It CTRL) antibody were used to block the response induced by peptides 43 and 44. Responses were recalled in PBMCs of study 3 at 28 dpi and results were tested by IFN γ ELISPOT. Results were expressed as IFN γ -producing cell number per 10⁶ stimulated PBMC (ISC/10⁶ PBMCs). Data for each animal was represented in graphs as mean with sd. Statistical analysis were performed comparing antibodies treated with untreated conditions by non

parametric analysis. b) Percentage of response calculated comparing anti SLA-I or SLA-II antibodies blocked with untreated conditions. PBMCs were stimulated with peptide 43 or 44 and blocked. This experiment was performed at least 4 times for each peptide; mean with sd are represented. Statistical analysis was done using non-parametric comparison between anti SLA-I and anti SLA-II conditions. Those conditions marked by asterisks (*) have at least a $p < 0.05$.

Association to SLA-I or SLA-II in $IFN\gamma$ recall responses induced by both peptides was also evaluated by a complementary method. PBMCs samples at 14 dpb in study 3 were separated using magnetic beads into SLA-II positive and negative populations and viability was evaluated. The purity of those populations was respectively ranging 83.2 to 87.8 % and 93.3 to 94.4 % with viability from 91.2 to 92.4% (Figure 9 in supplementary files). Peptides 43 and 44 were tested by $IFN\gamma$ ELISPOT using SLA-II⁺ and SLA-II⁻ cells (Figure 35).

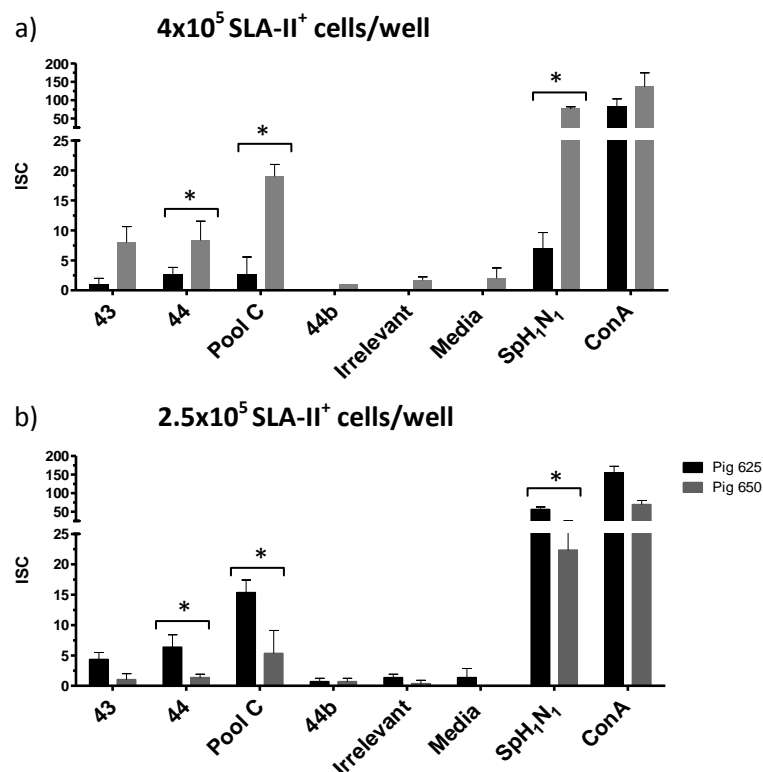


Figure 35. SLA-II⁺ subpopulations responses to peptides 43, 44 and pool C. Purified SLA-II⁺ cells were stimulated and studied by $IFN\gamma$ ELISPOT. Peptide 44b was used as negative control as no recall response was observed previously. In figure a and b, cells were plated respectively at 4×10^5 and 2.5×10^5 per well. Results were expressed as $IFN\gamma$ -producing cell number (ISC). Data for each animal was represented in graphs as mean with sd. Those marked with asterisks (*) had a statistic significant difference compared to media or irrelevant peptide with $p < 0.05$.

Cells were stimulated using two different conditions. In the first condition (Figure 35a), different amount of SLA-II⁺ and SLA-II⁻ cells were exposed to the same amount of stimuli. The relation of the number of cells per stimuli reproduced the condition previously used in $IFN\gamma$ ELISPOT in this work. PBMCs had around 80% of SLA-II⁺ cells in these pigs (data not shown);

therefore, the corresponding amount per well was tested. The same analogy was performed for SLA-II⁻ cells.

Complementary, the experiment was also performed exposing the same amount of cells from each subpopulation (2.5×10^5) to the same amount of stimuli (Figure 35b).

SLA-II⁺ fraction showed similar results in both tested conditions (Figure 35). There was a positive recall response in conditions stimulated by SpH₁N₁, Pool C and peptide 44 ($p < 0.05$). IFN γ response to controls (peptide 44b, irrelevant and media) was negative as expected. SLA⁻ fraction was also tested and it was negative for all stimuli (data not shown). This result indicated that there were no IFN γ competent cells in that subpopulation for the peptides tested. Our results suggested that SLA-II expressing cells are associated with responses to the peptides under study.

In summary, two minimal SLA-II epitopes were defined in NP protein (Figure 36). The first was in peptide 43 and the IFN γ responses were detected up to the sequence QISVQPTFSVQR. The second epitope was in peptide 44 and IFN γ responses were detected up to the sequence SVQPTFSVQRNLPF. Unfortunately, recall responses of the entire sequence QISVQPTFSVQRNLPF were not tested. In those epitopes, QI and PF were supposed to be anchor regions as their deletions disrupt IFN γ responses against those epitopes. Finally, EK amino acids were located at C terminal end of epitope in peptide 44 and two possible hypothesis were formulated about this region, either it could be an anchor position of another possible epitope or it was influencing recall response of the flanking epitope.

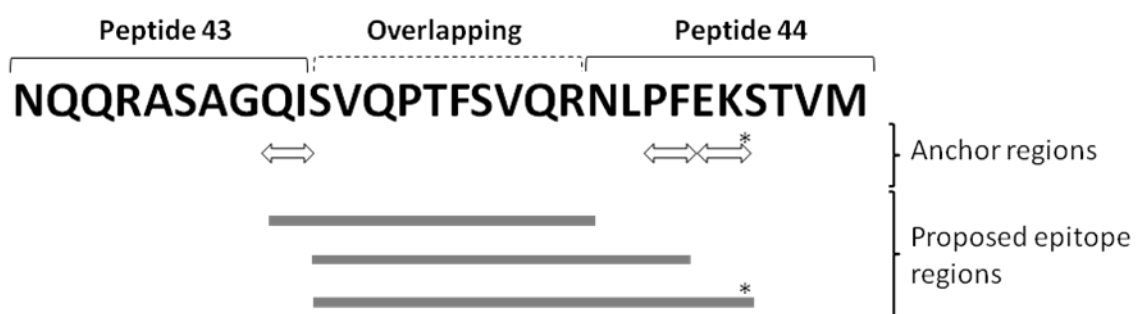


Figure 36. Proposed epitope sequences and their anchor regions. Peptide 43 and 44 exhibited sequence overlapping of 10 amino acids; arrows indicate anchor regions identified in these sequences, whereas grey bars indicate epitopes sequences. Those indicated by asterisks are putative anchor regions.

Cells involved in epitope recognition

Having defined antigenic sequences in peptides 43 and 44 and their dependence to SLA-II binding, the question was to define which cells were responding to this particular SLA-

II/epitope combination. Thus, cells producing $IFN\gamma$ after stimulation by both peptides were identified by flow cytometry through ICS assay on PBMCs at 28 dpb from study 3. Cells were gated following the strategy in figure 37 and both pigs exhibited similar pattern of staining.

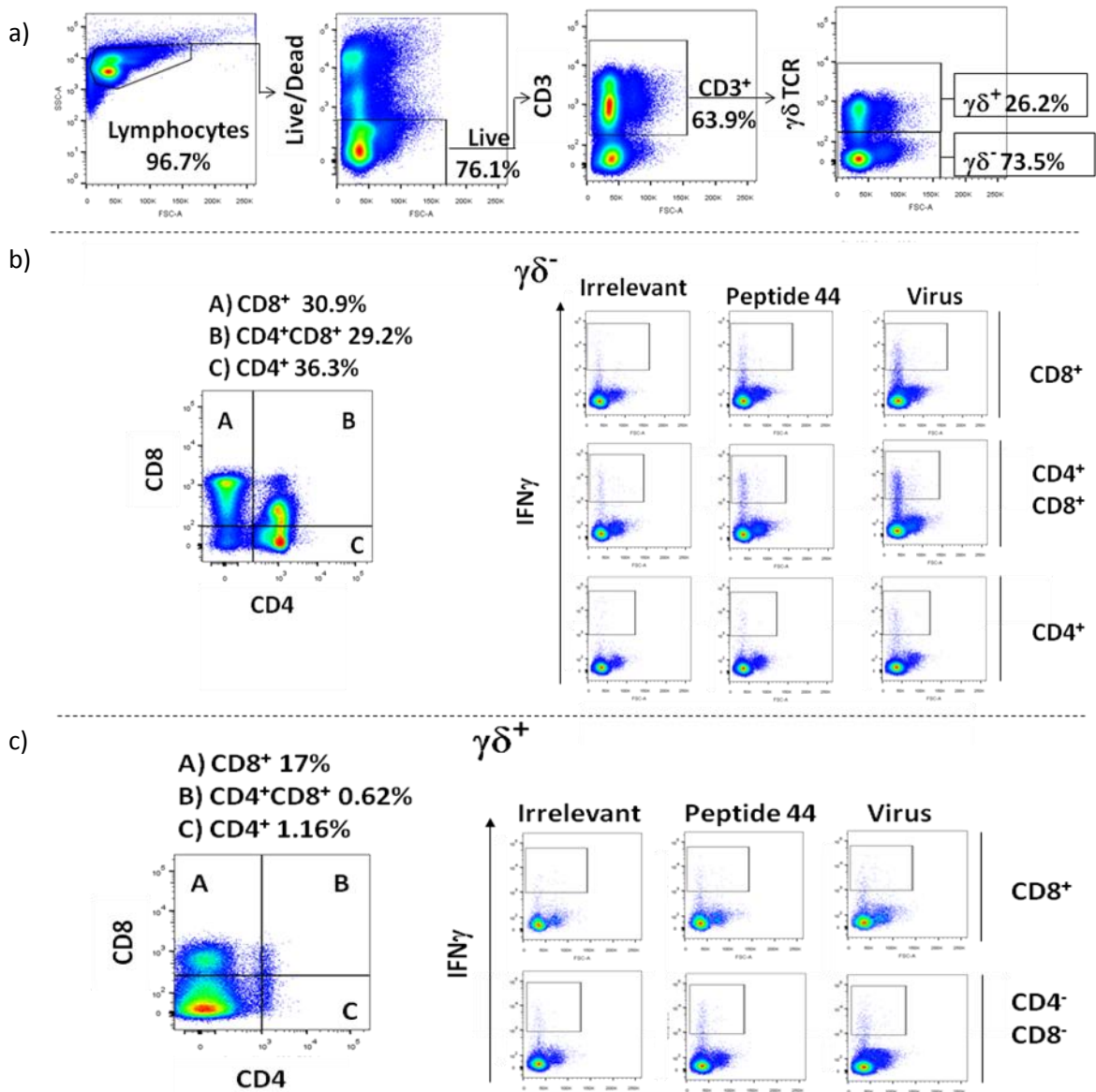


Figure 37. Gating strategy of flow cytometry $IFN\gamma$ ICS assay on PBMCs of pig 650 at 28 dpb (Study 3). a) Live Lymphocytes in T cells ($CD3^+$) were identified; b) $\gamma\delta^-$ and c) positive populations of T cells were then discriminated and further divided into different subpopulation using CD4 and CD8 markers. Single positive CD4 or CD8 and double positive ($CD4^+CD8^+$) cells in $\gamma\delta^+$ or $\gamma\delta^-$ T cells were identified and further analysed to quantify $IFN\gamma^+$ cells. Plots on the right in b and c show some examples of $IFN\gamma^+$ cells gating for irrelevant and 44 peptides and SpH_1N_1 virus (frequencies are showed in figure 38).

Live cells, which constituted a high proportion of lymphocytes (72-76%), were selected for further analysis; T cells ($CD3^+$) were distinguished into $\gamma\delta^-$ and $\gamma\delta^+$ subpopulations (Figure 37a). Also, $\gamma\delta^-$ T cells was the highest proportion of $CD3^+$ cells (67-73%); this population was

further dissected into: CTL ($CD4^+CD8^+$) (31-36%), Th naive ($CD4^+CD8^-$) (27-29%) and Th effector/memory ($CD4^+CD8^+$) (33-36%) (Figure 37b). On the other hand, $\gamma\delta^+$ T cells represented around 26-32% of $CD3^+$ cells and they were dissected into $\gamma\delta^+CD4^-CD8^+$, $\gamma\delta^+CD4^-CD8^-$, $\gamma\delta^+CD4^+CD8^+$ and $\gamma\delta^+CD4^+CD8^-$ cells (Figure 37c). $\gamma\delta^+CD4^-CD8^+$ and $\gamma\delta^+CD4^-CD8^-$ were the highest subpopulations in $\gamma\delta$ T cells (14-17 and 81-83 %); the rest of subpopulations were under 1% and therefore they were not taken into account for further analysis. Isotype controls showed staining frequencies on live cells ranging between 0.01 and 0.26%.

Figure 38 summarizes percentages of $IFN\gamma^+$ cells in each of those subpopulations gating like examples showed in figure 37. Non-parametric analysis showed that the differences observed were not statistically significant, probably due to the low number of animals and repetitions used; therefore, all positive responses were just tendencies. Stimulation with SpH₁N₁ virus induced $IFN\gamma$ responses in CTL, Th effector/memory and $\gamma\delta^+CD4^-CD8^+$ T cells. Cells from pig 625 showed $IFN\gamma$ responses with a frequency around 1.5% in all the cited populations (Figure 38); in contrast, cells from pig 650 showed just a maximum of 1% in Th effector/memory. When MDCKs sup was used as stimuli, frequencies of $IFN\gamma$ positive cells were always lower than 1% in both pigs and therefore, this value was considered background. S-Flu induced a response just in Th effector/memory, with frequencies ranging 0.5 and 1%. Therefore, CTL, Th effector/memory and $\gamma\delta^+CD4^-CD8^+$ T cells in peripheral blood specifically responded with $IFN\gamma$ to stimulation with SpH₁N₁. In contrast, Th effector/memory was the only T cell subpopulation in peripheral blood responding with $IFN\gamma$ to stimulation with S-Flu.

Pool 2 and pool C induced responses in CTL, Th effector/memory and $\gamma\delta^+CD4^-CD8^+$ T cells with frequencies ranging between 0.25 and 1.5%. Peptides 44 induced a response in the same populations cited before; however, frequencies were around 0.5% in the best situation. The rest of peptides 43, 43d, 44c showed frequencies below 0.25%. Peptides 42 and 44b were expected to give negative results as observed previously in $IFN\gamma$ ELISPOT assay (Figure 32 and 33) and thus they were used as additional negative controls; their frequencies were less than 0.25%, similar to all negative controls (Figure 38). In summary, peptide 44 induced $IFN\gamma$ recall responses in CTL, Th effector/memory and $\gamma\delta^+CD4^-CD8^+$ T cells whereas peptide 43 did not induce detectable recall responses in any of the analysed T cells sub populations.

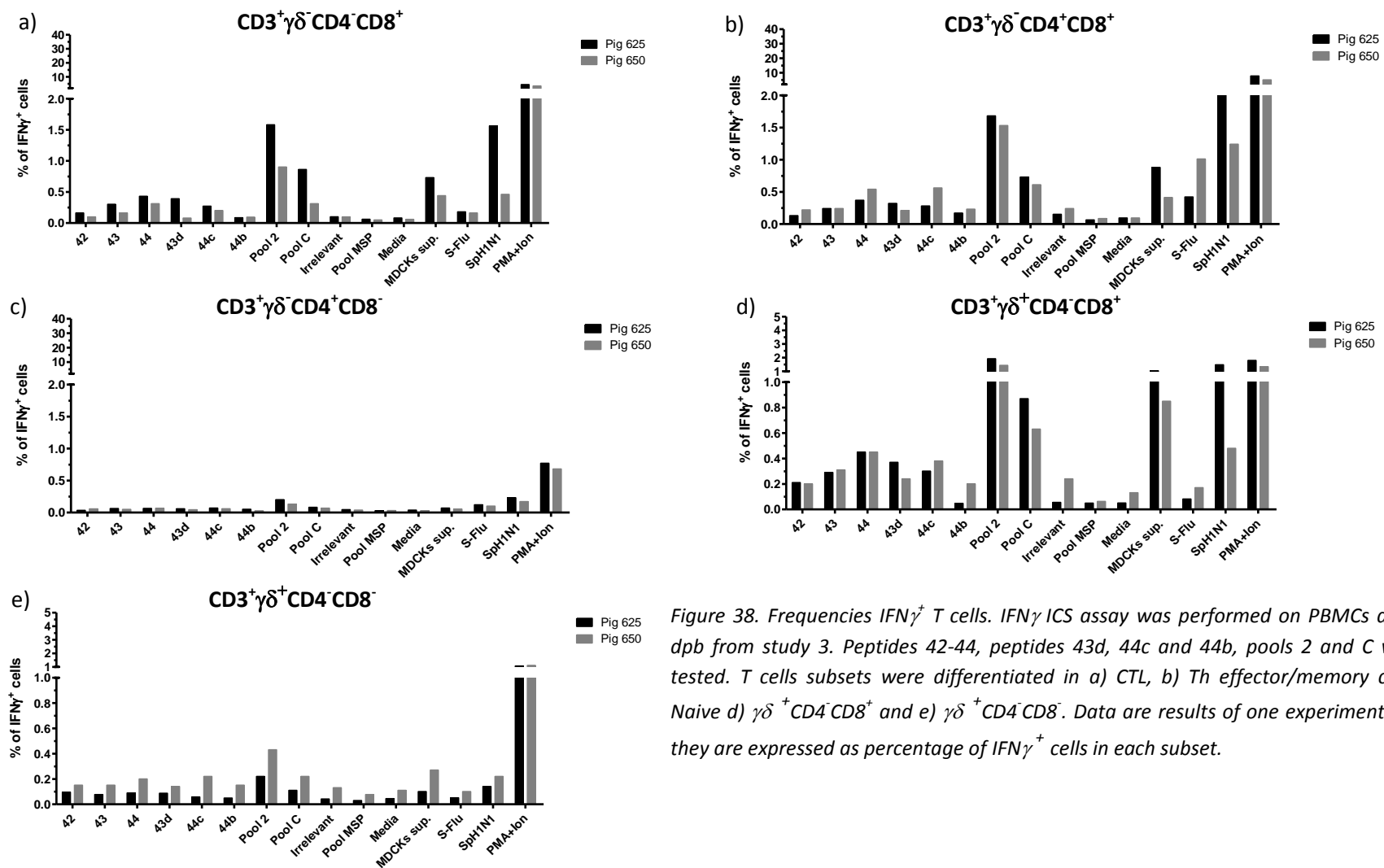


Figure 38. Frequencies IFN γ^+ T cells. IFN γ ICS assay was performed on PBMCs at 28 dpb from study 3. Peptides 42-44, peptides 43d, 44c and 44b, pools 2 and C were tested. T cells subsets were differentiated in a) CTL, b) Th effector/memory c) Th Naive d) $\gamma\delta^+CD4^-CD8^+$ and e) $\gamma\delta^+CD4^-CD8^-$. Data are results of one experiment and they are expressed as percentage of IFN γ^+ cells in each subset.

Cell subpopulations responding to peptides 43 and 44 were also analysed by flow cytometry and cell trace violet. Stimulation was performed on splenocytes at 28 dpb from study 1. Cells were gated following the strategy in figure 39 and results were similar in both analysed pigs. Live cells, which constituted about 43-50% of lymphocytes, were selected for further analysis; T cells ($CD3^+$) were distinguished into $\gamma\delta^-$ and $\gamma\delta^+$ subpopulations (Figure 39a).

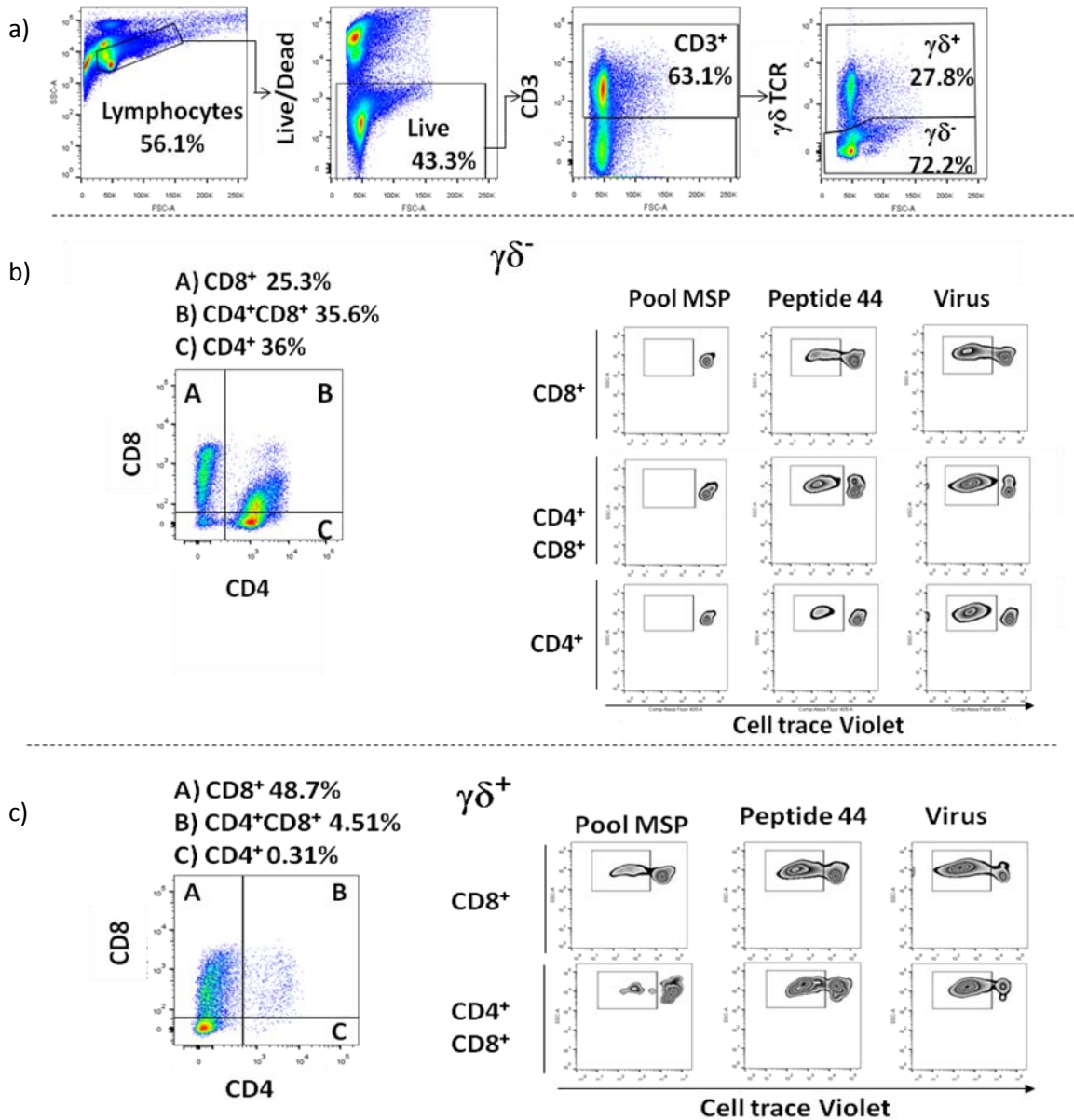


Figure 39. Gating strategy of flow cytometry using Celltrace violet proliferation assay on Splenocytes from pig 564 at 28 dpb (Study 1). a) Live Lymphocytes in T cells ($CD3^+$) were identified; b) $\gamma\delta^-$ negative and c) $\gamma\delta^+$ positive populations of T cells were then discriminated and further divided into different subpopulation using CD4 and CD8 markers. Single positive CD4 or CD8 and double positive ($CD4^+CD8^+$) cells in $\gamma\delta^+$ or $\gamma\delta^-$ T cells were identified and further analysed to quantify cells showing low Celltrace violet staining. Plots on the right in b and c show some examples of low Celltrace violet stained cells gating for irrelevant and 44 peptides and SpH₁N₁ virus (frequencies are showed in figure 40).

$\gamma\delta^-$ T cells were the highest proportion of $CD3^+$ cells (63-72%); this was further dissected into: CTL ($CD4^-CD8^+$) (24-25%), Th naive ($CD4^+CD8^-$) (29-36%) and Th effector/memory ($CD4^+CD8^+$) (36-45%) (Figure 39b). On the other hand, $\gamma\delta^+$ T cells represented around 28-36% of $CD3^+$ cells and they were dissected into $\gamma\delta^+CD4^-CD8^+$, $\gamma\delta^+CD4^-CD8^-$, $\gamma\delta^+CD4^+CD8^+$ and $\gamma\delta^+CD4^+CD8^-$ cells (Figure 39c); $\gamma\delta^+CD4^-CD8^+$ and $\gamma\delta^+CD4^-CD8^-$ populations constituted the highest proportion of $\gamma\delta$ T cells (49 and 35-46 %). $\gamma\delta^+CD4^+CD8^+$ ranged between 4.5-12%. Isotype controls showed staining frequencies of live cells below 0.62%.

Proliferating cells (low Celltrace violet staining) were quantified (Figure 40) for each stimulus, gating like examples showed in figure 39 in CTL, Th naive, Th effector/memory, $\gamma\delta^+CD4^-CD8^+$, $\gamma\delta^+CD4^-CD8^-$, $\gamma\delta^+CD4^+CD8^+$.

Non-parametric analysis showed that differences were not statistically significant, probably due to the low number of animals and repetition used; therefore, all identified positive responses were just tendencies. SpH₁N₁ virus induced proliferation in all analysed subsets and in immunised animals, 564 and 570. In particular, between 70 and 80% of Th effector/memory and $\gamma\delta$ T cells subpopulations ($CD4^-CD8^+$ and $CD4^+CD8^+$) proliferated; the rest of analysed subpopulations showed proliferating cells frequencies between 20 and 50%. MDCKs supernatants induced responses that differed depending on the T cells subsets analysed. In CTL, Th naive and Th effector/memory T cells subsets cells from pig 564 (Figures 40a-c) showed frequencies up to a maximum of 4%, while cells from pig 570 it was about 1%. On the other hand, $\gamma\delta$ subsets (Figures 40d-e) showed proliferation frequencies in response to MDCKs supernatants between 9 and 45% in both pigs. In summary, CTL, Th naive, Th effector/memory T cells but also $\gamma\delta^+$ subsets ($CD4^-CD8^+$ and $CD4^+CD8^+$) proliferated in response to the antigen used for immunisation. Background response to SpH₁N₁ vehicle was also detected, in particular in $\gamma\delta$ subsets; however, it was always less than two times than the response to SpH₁N₁. The T cells subsets Th effector/memory and $\gamma\delta^+$ were responding with the highest frequencies compared to the rest of T cells subsets.

Cells responding to pools A-D were also quantified. Pool C was the only one showing a consistent response among pigs in CTL, Th naive and Th effector/memory; frequencies of proliferating cells in the first two subpopulations were between 7 and 14 % whereas they were about 25-28% in the latter. The rest of pools (A, B and D) induced responses in the those subpopulations with frequencies between 1 and 4% (Figure 40a-c). Pool A gave proliferation

up to about 8%, although just in CTL cells from pig 564. Pool C was also the only one inducing a consistent response in both pigs, particularly in $\gamma\delta^+$ subsets ($CD4^-CD8^+$, $CD4^-CD8^-$ and $CD4^+CD8^+$) with frequencies were between 45 and 65% (Figures 40d-e).

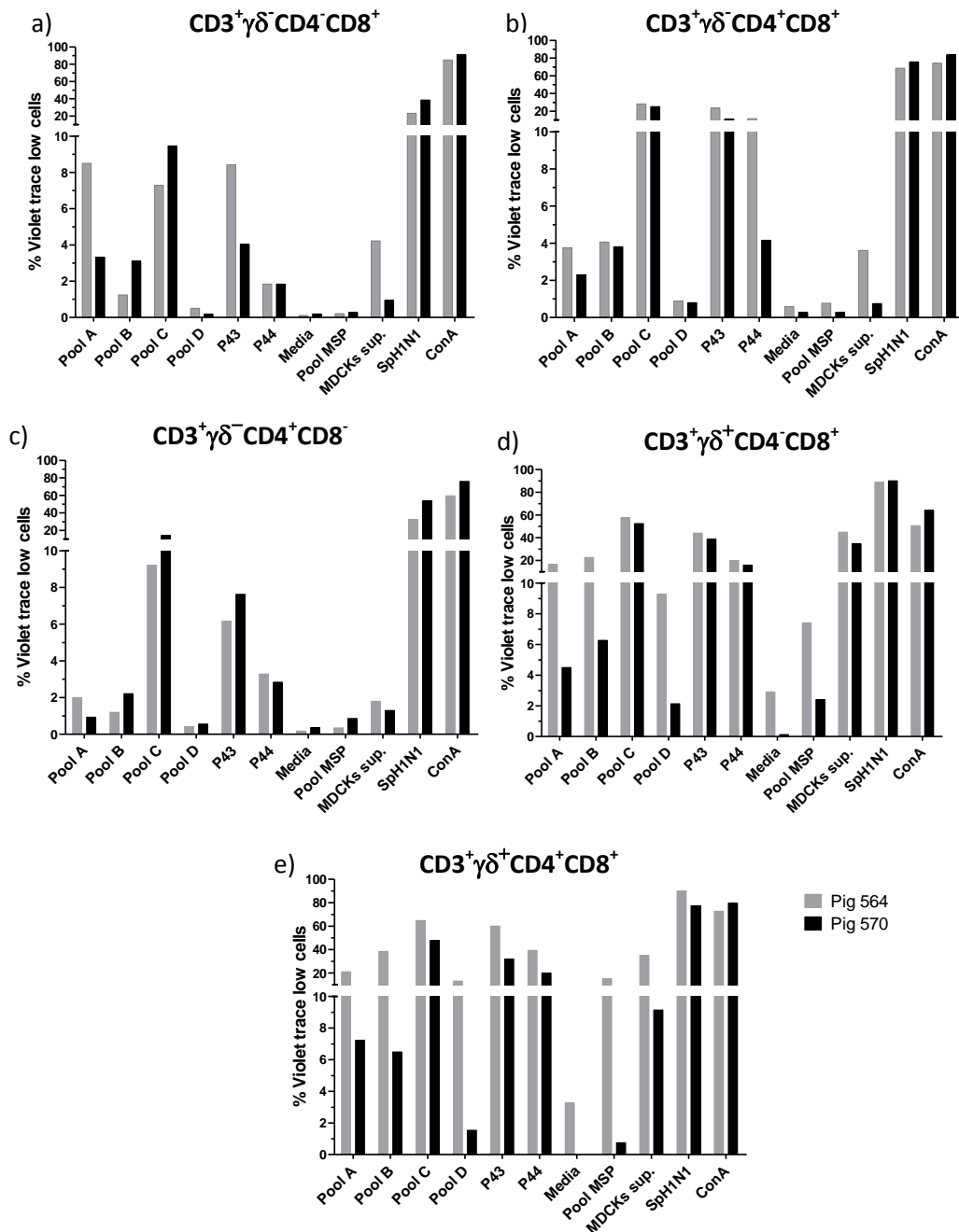


Figure 40. Proliferation frequencies. Results of Celltrace violet assay performed on Splenocytes at 28 dpb of study 1. Response of T cells subsets was differentiated by a) CTL, b) Th effector/memory c) Th Naive d) $\gamma\delta^+CD4^-CD8^+$ and e) $\gamma\delta^+CD4^+CD8^+$. Data are results of one experiment and they are expressed as percentage of low Celltrace Violet cells in each subset.

Pools A and B induced frequencies ranging between 4 and 38% and they were very variable between pigs. Pool D induced proliferating responses just in pig 564. Therefore, CTL, Th naive

and Th effector/memory but also some $\gamma\delta^+$ subsets responded by proliferation to pool C. However, Th effector/memory and $\gamma\delta^+$ subsets were responding with the highest frequencies compared to the rest of T cells subsets.

Proliferating responses were analysed for peptides 43 and 44. Peptide 43 was inducing a response with frequencies between 7 and 14% in CTL and Th naive, and a maximum was observed in Th effector/memory (between 11 and 23%) (Figures 40a-c). Responses to peptides 44 were similar to peptide 43. CTL and Th naive responded with frequencies up to 3%, whereas Th effector/memory responses ranged between 4 and 11 % (Figures 40a-c). On the other hand, $\gamma\delta$ T cells responses exhibited frequencies of proliferating cells between 15 and 60% (Figures 40d-e). Finally, control stimuli like pool MSP and media did not induce any proliferation response in $\gamma\delta^-$ T cells (Figures 40a-c); in contrast, $\gamma\delta^+$ T cells responded to both stimuli (Figures 40d-e). Pig 564 showed frequencies to media up to 3% while responses in the other pig was negative. The same pig responded with frequencies up to 15% to pool MSP while in the other pig a maximum response was 2%. In summary, CTL, Th naive and Th effector/memory but also $\gamma\delta^+$ subsets specifically responded by proliferation to peptides 43 and 44. However, Th effector/memory and $\gamma\delta^+$ subsets were responding with the highest frequencies compared to the rest of T cells subsets.

Proliferative responses were evaluated also in peripheral blood to check consistency of results in different tissues. PBMCs from study 2 were used with the same strategy and method adopted for splenocytes (Figure 39); however, $CD4^+CD8^+$ $\gamma\delta$ T cells were not taken into account as they represented less than 0.1% in PBMCs (Figure 10 of supplementary files). Therefore, low Celltrace cells were quantified (Figure 41). PBMCs cells from immunised pigs (1 and 2) responded to virus SpH₁N₁ as splenocytes did and thus CTL, Th naive, Th effector/memory and $\gamma\delta^+CD8^+$ T cells proliferated; frequencies of Celltrace violet cells ranged between 7 and 10% in the first two T cells subpopulations whereas they were more than 20% in the rest of them (Figure 41). Control MDCKs sup. induced background responses in those T cells subsets, with frequencies ranging between 1 and 8% in $\gamma\delta^-$ T cells subsets (Figures 41a-c) or around 30-40% in $\gamma\delta^+$ T cells subsets (Figure 41d).

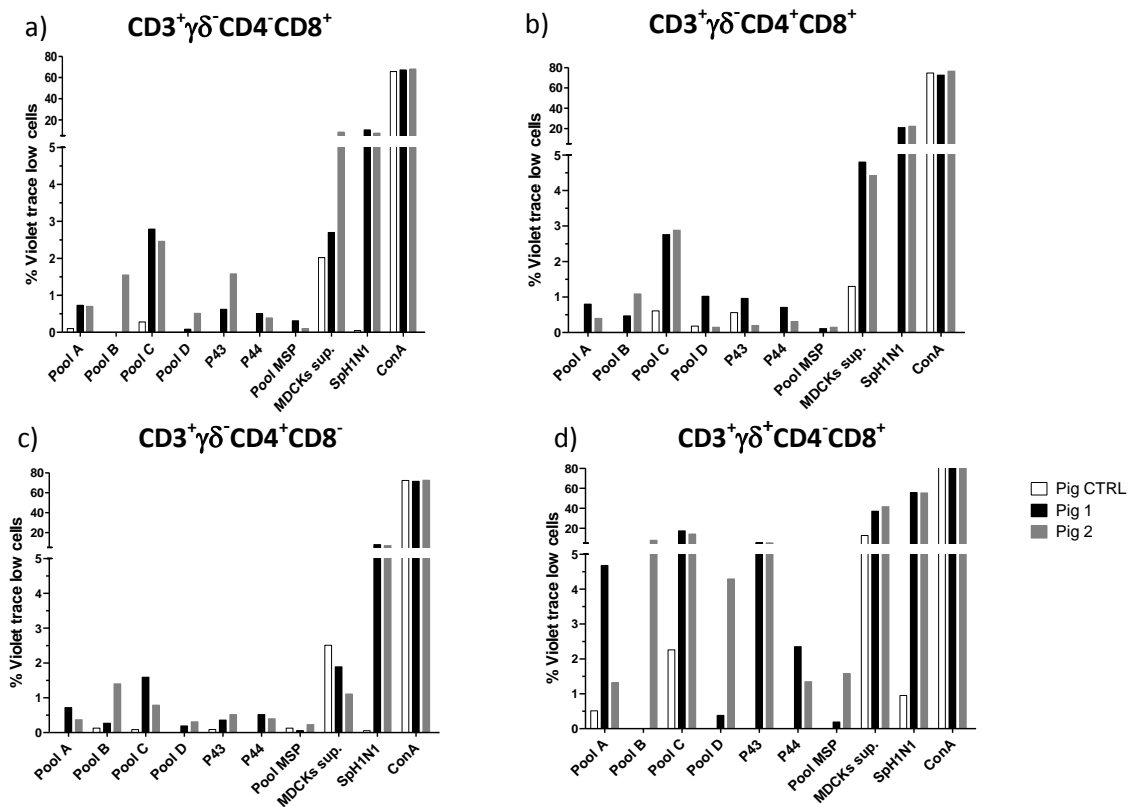


Figure 41. Proliferation frequencies. Results from Celltrace violet assay performed on PBMCs at 28 dpb of study 2. Responses from T cells subsets was differentiated a) CTL, b) Th effector/memory c) Th Naive d) $\gamma\delta^+CD4^-CD8^+$. Data are results of one experiment and they are expressed as percentage of low Celltrace violet cells in each subset.

Therefore, CTL, Th naive, Th effector/memory T cells but also $\gamma\delta^+CD8^+$ T cells proliferated in response to the specific antigen used for immunisation. However, Th effector/memory and $CD8^+\gamma\delta^+$ responded with the highest frequencies compared with the rest of T cells subsets. Proliferative responses to pools A-D were also analysed in PMBCs. Pool C induced responses in CTL, Th effector/memory (2.5 -3%) and $\gamma\delta^+CD8^+$ T cells (14-17%) (Figures 41a, 41b and 41d). The rest of pools exhibited frequencies of proliferating $\gamma\delta^-$ T cells subsets less than 1-1.5% whereas $\gamma\delta^+CD8^+$ proliferating cells ranged between 1 and 8% without consistency between pigs.

Peptides 43 and 44 induced around 0.5-1.5% of proliferating cells in CTL and Th effector/memory (Figures 41a-b). Peptide 43 induced proliferation in $\gamma\delta^+CD8^+$ cells from both immunised animals with frequencies up to 5% (Figure 41d). In contrast, peptide 44 induced proliferation in just 1-2% of cells in that subset (Figure 41d).

Finally, responses to negative sup controls were as follow. Pool MSP induced frequencies of proliferating cells less than 0.5% in $\gamma\delta^-$ T cells subsets and less than 1.5% in $\gamma\delta^+CD8^+$ (Figure

41). Cells from CTRL pig did not respond to any stimuli a part of the positive control; MDCKs sup induced a 2% maximum of proliferating cells in $\gamma\delta^-$ T cells subsets, whereas those were up to 13% in $\gamma\delta^+CD8^+$ in CTRL pig. In summary, peptides 43 and 44 induced proliferation in peripheral blood just in $\gamma\delta^+CD8^+$ T cells subset.

Therefore, different subsets of T cells were involved in $IFN\gamma$ and proliferation recall responses in tissues from immunised animal to the whole virus SpH₁N₁, pool 2 and pool C. Those subsets were CTL, Th helper effector/memory and $\gamma\delta^+CD8^+$ T cells; Th naive cells responded just with proliferation to those stimuli. Th effector/memory and $\gamma\delta^+CD8^+$ T cells were the highest responders when comparing with the rest of T cells subsets. Proliferation responses to SpH₁N₁, pool 2 and pool C were evaluated in PBMCs and spleen; in the latter, a tissue specific responding T cell subpopulation was observed. Between the analysed tissues, just spleen host the $\gamma\delta$ T cells subset $CD4^+CD8^+$ that responded to the stimuli.

Involvement of T cells subsets in $IFN\gamma$ production after stimulation with peptides 43 and 44, was evaluated on PBMCs; CTL, Th helper effector/memory and $\gamma\delta^+CD8^+$ T cells subsets were responding to peptide 44 whereas responses to peptide 43 was not detectable. Proliferation responses to peptides 43 and 44 were evaluated in PBMC and spleen. In the first tissue, the recall responses of peptide 43 involved just $\gamma\delta^+CD8^+$ T cells whereas responses to peptide 44 were not detectable. In contrast, a wide range of T cells subsets in spleen were recalled after stimulation with both peptides; those subpopulations were CTL, Th naive, Th effector/memory, $\gamma\delta^+CD8^+$ and $\gamma\delta^+CD4^+CD8^+$ T cells. Th effector/memory, $\gamma\delta^+CD8^+$ and $\gamma\delta^+CD4^+CD8^+$ T cells were the highest responders when comparing with the rest of T cells subsets. The results indicated that proliferation responses to peptides 43 and 44 were tissue specific.

Characteristics of identified epitopes

The joined sequences of the epitopes found in peptides 43 and 44 were located towards the C-terminal region of the NP protein (Figure 42), particularly between position 405 and 420 (NP₄₀₅₋₄₂₀); therefore, the epitope contained in peptide 43 QISVQPTFSVQR was named NP₄₀₅₋₄₁₆ whereas the epitope contained in peptide 44 SVQPTFSVQRNLPF was named NP₄₀₇₋₄₂₀.

The SLA-II alleles of Brabrahams pigs have not been defined; therefore, prediction of possible anchor position in epitopes NP₄₀₅₋₄₁₆ and NP₄₀₇₋₄₂₀ was roughly based on the hydrophobicity of the amino acids sequence.

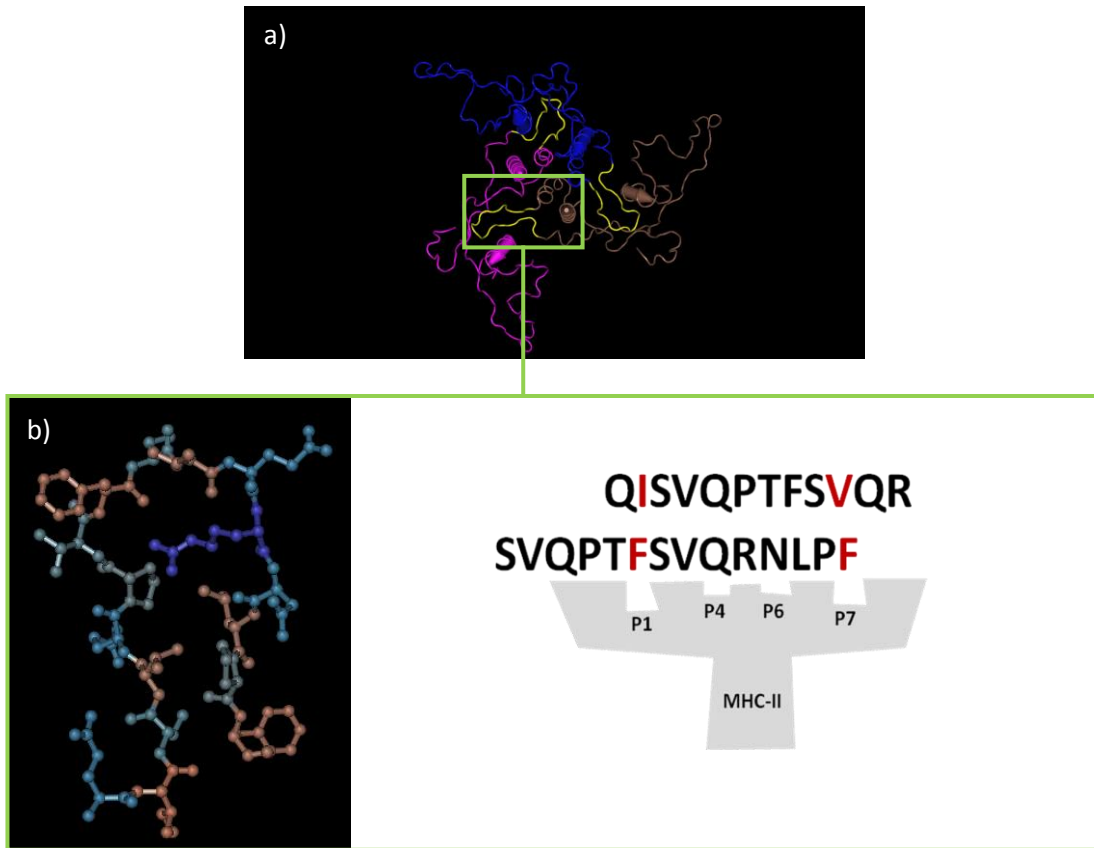


Figure 42. Predicted structure of peptides 43-44 in NP protein. a) The trimeric oligomer structure of the NP protein of A/Panama/2007/1999 was obtained by homology modelling. The best fit model was automatically determined by the server and the one used to generate the image was 4DYS (PDB ID). Each of the monomer are coloured differently whereas the epitope 43-44 sequence is shown in yellow. b) NP₄₀₅₋₄₂₀ sequence QISVQPTFSVQRNLPF is zoomed. On the left side, amino acids are coloured depending the hydrophobicity; colours are shading from brown to blue indicating from hydrophobic to hydrophilic respectively. On the right, predicted anchor positions in epitopes NP₄₀₅₋₄₁₆ and NP₄₀₇₋₄₂₀.

It is generally assumed that the central core of MHC class II epitopes host 2 major anchor positions whose preference is for hydrophobic amino acids²²⁷; those are at epitope position 1 (P1) and 9 (P9). In previous sections the anchor regions QI and PF were suggested respectively in NP₄₀₅₋₄₁₆ and NP₄₀₇₋₄₂₀. Those regions were located at the N terminal and C terminal ends of their respective epitopes and thus they would contain anchor positions 1 and 9. Having established these parameters and taking into account the hydrophobicity of NP₄₀₅₋₄₂₀, it was possible to assume the rest of anchor positions in each peptide. NP₄₀₅₋₄₂₀ shows the presence of at least 6 hydrophobic amino acids (Figure 42b) of which 4 are in NP₄₀₅₋₄₁₆ and 5 are in NP₄₀₇₋₄₂₀. In the anchor region of NP₄₀₅₋₄₁₆ (QI) there was just one hydrophobic amino acid, Isoleucine (I), which could be considered as P1; on the other hand, P9 could correspond to another

hydrophobic amino acid, Valine (V) (Figure 42b). In the anchor region of NP₄₀₇₋₄₂₀ (PF) there was an hydrophobic acid, Phenilalanine (F), which could be considered as P9; thus P1 in this case could be again F. Position 4 (P4) and 6 (P6) could be considered auxiliary anchors and their amino acid preference is considered allele specific²²⁷. If P1 and P9 predictions were right, P4 and P6 would have had preferences for polar uncharged side chains like Glutamine (Q), Asparagine (N) or Threonine (T). Therefore, predicted anchor position in NP₄₀₅₋₄₁₆ would be P1: I, P4: Q, P6: T and P9: V; anchor positions in NP₄₀₇₋₄₂₀ were P1: F, P4: Q, P6: N, P9: F (Figure 42b).

Finally, conservation of epitopes NP₄₀₅₋₄₁₆ and NP₄₀₇₋₄₂₀ was evaluated. Sequences of NP₄₀₅₋₄₂₀ in swine, human and avian IAV were aligned and the frequency of amino acids at each position was plotted in the logo of figure 43.

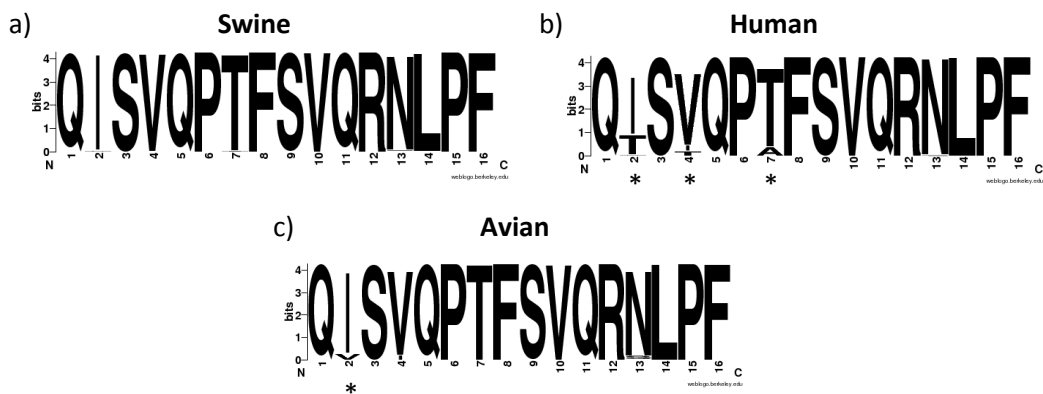


Figure 43. Conservation of NP₄₀₅₋₄₂₀, QISVQPTFSVQRNLPF. Logo was generated using at least 500 sequences of IAV viruses isolated in a) swine b) human or c) avian species. Each letter represent an amino acid and its height is proportional with its frequency. Mutated positions (in which more than one amino acid is showed) are indicated by asterisks.

NP₄₀₅₋₄₂₀ sequence was conserved in swine; however, mutations were detected at position 2 in human and avian IAV and amino acids varied between Isoleucine (I), Threonine (T) or Valine (V). Beside, positions 4 and 7 in human were mutated and amino acids vary between Alanine (A), T or I. Therefore, considering each epitope separately, NP₄₀₅₋₄₁₆ showed mutations at predicted anchor P1 and P6 in human IAV whereas in avian IAV just P1 was mutated. In contrast, none of the mutated positions fall in predicted anchor positions in NP₄₀₇₋₄₂₀.

Chapter IV: identification of Swine Influenza virus class I T cells epitopes in a SLA-I defined pig herd

Methods to identify class I T cell epitopes through RV have been recently introduced for pigs. In particular, a reverse vaccinology pipeline was recently developed and applied by Pedersen *et al.* 2014¹⁷⁸ to identify class I T cell epitopes of SwIV. However, those epitopes are still few and related with just one SLA allele. The aim of this work was to extend that pipeline for allele SLA-1*0702 identifying new SwIV epitopes. For this purpose, the present work was performed in collaboration with the authors of Pedersen *et al.* 2014¹⁷⁸ and several experimental parts were performed by them, which are marked with a sign (#). Hence, *in silico* prediction, *in vitro* testing and tetramers technologies already available for pigs were translated to allele SLA-1*0702 using two strains of SwIV H1N1.

Materials and methods

Animals (#)

Large White x Landrace pigs were typed for their SLA-1 allele by PCR-SPP²²⁸. Four pigs bearing the allele SLA-1*0702 and a miss-matched pig (not bearing the selected SLA allele) were selected and housed at the Lindholm facilities of the Technical Denmark Institute (DTU).

Virus and infection

Viruses were grown and titrated on MDCKs cells as described in previous sections. All animals but one (L12) were intra-nasal infected using a mucosal administration device (Wolfe Tory Medical) with 9.04 log TCID₅₀ of the “avian-like” H₁N₁ SwIV strain A/Swine/Spain/SF11131/2007 (SpH₁N₁)²²²; L12 pig was intra-tracheally infected with 8.2 logTCID₅₀. Animals were intranasal infected at 139 days post primary infection (dpi) with 5.58 logTCID₅₀ of the 2009 pandemic H₁N₁ virus strain A/Swine/Denmark/101310-1/2011 (pdmH₁N₁) and culled at 14 days post challenge (dpc).

Sampling

Blood was collected in EDTA at 0, 8, 139, 144, 146, 148 and 153 dpi and PBMCs were purified as explained in previous sections. Sera samples were harvested as explained in previous sections at 0, 30, 139, 148 and 153 dpi.

*SLA-1*0702 MHC class I protein encoding construct (#)*

The construct encoding the SLA-1*0702 protein was designed as previously described¹⁷⁴. Briefly, a trans-membrane, truncated fragment encompassing the SLA-1*0702 alpha chain

(Genscript) followed by an FXa-BSP-HAT tag (FXa; factor Xa cleavage site comprised of the amino acid sequence IEGR, BSP; biotinylation signal peptide, HAT; histidine affinity tag) was inserted into a pET28a expression vector (Novagen). The construct was transformed into DH5 α cells, and sequenced with ABI Prism 3100Avant (Applied Biosystems)²²⁹. The validated construct of interest was transformed into an *E. coli* production cell line, BL21(DE3), containing the pACYC184 expression plasmid (Avidity) with an IPTG inducible BirA gene to express biotin-ligase leading to almost complete *in vivo* biotinylation of the desired protein product²³⁰.

*Expression and purification of recombinant SLA-1*0702 and human and porcine beta-2 microglobulin (β 2m) (#)*

SLA-1*0702 MHC class I proteins were produced and purified as described elsewhere¹⁷⁴. In brief, *E. coli* BL21(DE3) cells containing the SLA proteins were lysed in a cell-disrupter (Constant Cell Disruptor Systems set at 2300 bar) and the released inclusion bodies were isolated by centrifugation (Sorval RC6, 20 min, 17000 g). Inclusion bodies were washed twice in PBS, 0.5% NP-40 (Sigma), 0.1% deoxycholic acid (Sigma) and extracted into Urea-Tris buffer (8M urea, 25mM Tris, pH 8.0). SLA-1*0401 heavy chain proteins extracted in 8 M urea were previously purified by successive immobilized metal adsorption, hydrophobic interaction, and Superdex-200 size exclusion chromatography¹⁷⁴. Throughout purification and storage, MHC-I heavy chain proteins were dissolved in 8 M Urea to keep them denatured. Recombinant human and porcine β 2m was expressed and purified as described elsewhere^{231,232}.

Peptides (#)

Influenza virus peptide sequences of interest were *in silico* analysed for their potential to bind to SLA-1*0702 using the online available peptide predictor *NetMHCpan* v.2.8 (<http://www.cbs.dtu.dk/services/NetMHCpan-2.8/>). All candidate peptides were purchased from Schafer-N, Denmark (www.schafer-n.com). Briefly, nine and ten amino acid long peptides were synthesized by standard 9-fluorenylmethyloxycarbonyl (Fmoc) chemistry, purified by reversed-phase high-performance liquid chromatography (to at least >80% purity, frequently 95–99% purity), validated by mass spectrometry and quantified by weight.

Epitope binding analysis (#)

Putative peptides were tested for their ability to produce complexes with the SLA-1*0702 molecule using a previously described immunosorbent assay²¹². Complexes of MHC class I heavy chain with human β 2m and peptide were produced in 96 well plates (Thermo Scientific).

All peptides were dissolved in 150µl standard folding (SF) buffer (PBS, 0.1% pluriol (Lutrol F-68, BASF), pH 7.0) using sonication for 5 min. A 5-fold dilution series of peptide in 8 consecutive points was performed in SF buffer. Following a 48-hour incubation (18°C) samples were transferred to streptavidine (SA) coated plates (Nunc) and incubated for 3 hours at 4°C. Plates were washed in wash buffer (PBS, 0.05% Tween-20) and probed with an in-house mouse-anti human β2m mAb²³³, BBM1, (70 nM, final) for 1 hour at room temperature. All wells were washed in wash buffer and detection antibody HRP-conjugated goat-anti-mouse IgG (1.13 nM, final) (Sigma) was added followed by 1 h incubation at room temperature. Plates were washed and TMB substrate (Kirkegaard & Perry Laboratories) was added to all wells. Reactions were stopped using H2SO4 (0.3M) and plates read at 450nm using ELx808 Microplate reader (Biotek). Data was analyzed using Excel and Prism software.

A pre-folded, biotinylated FLPSDYFPSV/HLA-A*02:01²³⁴ complex was used as a standard to convert OD450 values to the amount of complex formed using the second order polynomial ($Y = a + bX + cX^2$) hereby enabling a direct conversion of the assay peptide concentration to the actual concentration of correctly produced pMHC complex. Because the effective concentration of MHC (2–5 nM) used in these assays is below the equilibrium dissociation constant (KD) of most high-affinity peptide–MHC interactions, the peptide concentration, ED50, leading to half-saturation of the MHC is a reasonable approximation of the affinity of the interaction.

Immunoreagents and flow cytometry (#)

SwIV peptides, recombinant SLA-1*0702 and porcine β2m were produced and complexed into tetramers as described previously²³⁵ with minor modifications. Briefly, recombinant β2m and peptides were added to 10-fold and 40-fold excesses, respectively, of SLA-1*0702 in a reaction buffer containing a cocktail of protease inhibitors [0.68 mM EDTA, 4.8 µM pepstatin A, 4.4 µM 1-10 phenanthroline, 0.1 mM Nethylmaleimide, 8.9 µM tosyl-L-lysine chloromethyl ketone (TLCK), 9.3 µM tosyl-L-phenylalanine chloromethyl ketone (TPCK), 66.8 µM phenylmethylsulfonyl fluoride (PMSF), milli-Q H2O]. Following a 48 hour incubation at 18°C streptavidin-BrilliantViolet (Biolegend) was slowly added and mixed thoroughly in a 1:4 ratio with the MHC class I heavy chain final concentration. For tetramer staining, 1×10^6 cells were washed in cold FACS buffer (PBS, 0.5% bovine serum albumin, 0.1% sodium azide) and resuspended in a solution containing BV421-labelled tetramers previously diluted 1:8 with FACS buffer. Tetramer staining was used to identify tetramer positive cells reactive against the

respective influenza epitopes. Cells were incubated at room temperature with rocking for 20 min and washed three times in cold FACS buffer. Cells were resuspended in FACS buffer containing PE-conjugated MAb against porcine CD8 (clone 76-2-11, BD Pharmingen) and FITC-conjugated MAb against porcine CD3 ϵ (clone PPT3, Southern Biologend) and then incubated at room temperature for 20 min. Following washing for three times in FACS buffer, cells were resuspended in cold FACS buffer and analysed on flow cytometer FACSCanto II using DIVA 6 software (BD Pharmingen).

Hemagglutination inhibition (HAI) assay

The assay was performed using chicken RBC. Sera samples were treated overnight with four volumes of Receptor Destroying Enzyme (RDE) (Sigma-Aldrich) solution (100 U/ml) at 37 °C to remove non-specific inhibitors of hemagglutination. Then, five volumes of 1.5% sodium citrate was added and solutions were incubated for 30 min at 56°C. Treated sera were tested by 1:2 titrations in PBS. Finally, 4 hemagglutination units of the viruses and one volume of a 50% suspension of RBC was added and incubated for 1 h at 4°C. HI titers >40 were considered positive. Samples were tested in duplicate.

ELISA anti porcine IgG against IAV.

Sera were diluted 1:50 and then serially diluted 1:3 in Casein PBST (PBS, 1% Casein from Bovine Milk (Sigma) and 0.05% Tween20). 96 wells ELISA plates MICROLON600 (Greiner Bio One) were coated with 10⁴ TCID₅₀ per well with viruses, incubated 1 hour and washed five times in PBST (PBS and 0.05% Tween20). Plates were blocked 1 hour with Casein PBST and washed again five times. 100 μ l per well of sera dilution were distributed in the blocked plates, incubated 1 hour and washed five times. Porcine IgG were labelled with 100 μ l per well of anti-pig IgG (Whole Molecule) Peroxidase Conjugate, Antibody developed in Rabbit (Sigma) diluted 1:50000. Plates were then incubated 1 hour, washed five times and 50 μ l per well of TMB substrate (Sigma) were added. Reaction was stopped by adding 50 μ l per well of 0.1 M Sulfuric acid. Plates were read at 450nm and 630nm using a PowerWave XS reader (Biotek). Data was analysed using Excel and GraphPad (Prism) software.

Conservation analysis

Sequences of IAV from swine, human and avian host were retrieved from the Influenza Virus Resource (<http://www.ncbi.nlm.nih.gov/genomes/FLU/FLU.html>)¹⁹⁸. Strains of H₁N₁ subtype with full length NA protein were selected and thus at least 1400 sequences for each group

were taken into account. Sequences were aligned with Clustal W implemented in MEGA5; region 171-180 (Tet60) was used to generate logo in Weblogo Version 2.8.2 (<http://weblogo.berkeley.edu/>).

Results

In silico prediction

Class I T cell epitopes of SwIV were investigated *in silico* in conserved and non-conserved proteins, respectively M1 and HA, NA. The strains selected were of the same subtype (H₁N₁) but from different lineages: SpH₁N₁ derive from an Avian-Like SwIV lineage, while pdmH₁N₁ derived from a human IAV lineage isolated in pigs. Therefore, class I epitopes conserved but also specific of each of those two strains were expected. Bioinformatics software *NetMHCpan* was used to predict binding propriety of peptides to the allele SLA-1*0702 from M1, HA and NA proteins. However, another *in silico* method was used to further discriminate peptides binders of SLA-1*0702. Nonamer peptide matrix (PSCPL) was used to map SLA-1*0702 binding preferences; those preferences are represented as logo in figure 44.

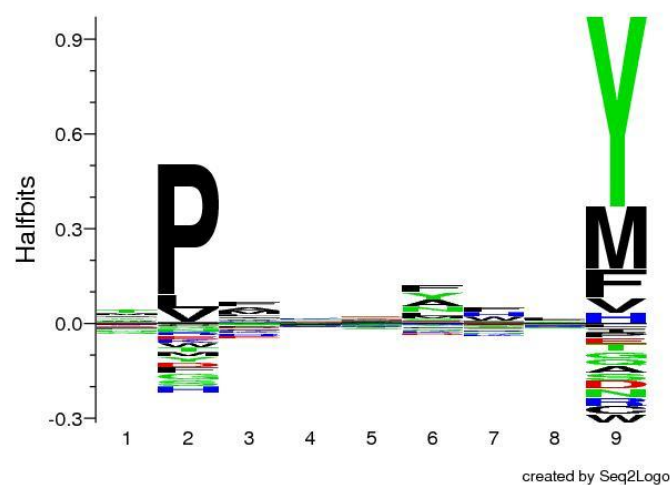


Figure 44. Binding preference of the allele SLA-1*0702. In the sequence logo, each peptide position is represented by a stack of letters indicating its significance for binding (information content) and the height of each letter (amino acid) is proportional to its influence on the binding. The letter located above the X axis have positive impact on the binding; in contrast the letter located below the X axis has the opposite effect. Acidic residues are displayed in red, basic in blue, neutral in green, and hydrophobic in black. Underrepresented amino acids are displayed upside down

Position 2 and 9 of the peptides have the highest impact on the binding performance. Beside, position 2 can tolerate a very restricted variety of amino acids, in which Proline (P) has the highest importance. In contrast, position 9 can tolerate a greater variety of amino acids, in

which Tyrosine (Y), Methionin (M) and Phenylalanine (F) have the highest importance; all of which exhibit hydrophobic side chain. Position 3, 6 and 7 contribute to binding although they were of less importance. Therefore, position 2 and 9 were selected due to their importance as a parameter to predict peptides binders.

Finally, peptides predicted by *NetMHCpan* showing consistency in the amino acid sequence with the binding preference of P2 and P9 of SLA-1*0702 were selected as candidates.

In vitro test

Binding proprieties of putative peptides were tested with an immunosorbent assay to confirm prediction results. 15 peptides predicted *in silico* and meeting the above requirements for binding in positions 2 and 9 in SLA-1*0702 binding groove were identified and subsequently tested *in vitro*. Their Kd are showed in table 9.

Peptide sequence	Viral protein of origin	Position	Virus		Kd (nM)	Tetramer name
			pdmH ₁ N ₁	SpH ₁ N ₁		
NADTLCIGY	HA	16-24	+		1543	
SLSTASSWSY	HA	86-95	+		35	57
TLYQNNHTY	HA	207-215		+	6	66
YVSVGSSKY	HA	215-223		+	987	93
SVKNGTYDY	HA	295-303	+		20000	
GMIDGWYGY	HA	300-308		+	20000	
EIGNGCFEFY	HA	476-485	+	+	132	63
CPVSGWAIY	NA	92-100	+	+	6	55
CPIGEVPSY	NA	171-180	+	+	37	60
GPSNGQASY	NA	245-253	+	+	25	59
SVELNAPNY	NA	266-274		+	20000	
EMNAPNYHY	NA	268-278	+		231	61
NMDRAVKLY	M1	92-100	+	+	293	62
ALASCMGLIY	M1	123-132	+	+	127	56
LASCMGLIY	M1	124-132	+	+	9	64
VSIAAAAAAY	Negative Control					831

Table 9. Peptides binding assay. Peptide were tested in vitro and the resulting binding affinities (Kd) are reported. A name was given to those peptide selected for tetramer synthesis. Protein of origin, location and virus strains having those peptide sequences are also shown.

Observed affinities (Kd) in table 9 could be classified as high affinity (less than 100 nM), intermediate affinity (between 100 and 1000 nM) and low affinity (more than 1000nM). Those peptides showing low affinity were not taken into account for further studies. The rest of peptides (eleven) were used to generate tetramers. Those were exclusive of SpH₁N₁ or pdmH₁N₁ or shared (Table 9).

In vivo test

Pigs bearing the allele SLA-1*0702 were firstly infected with SpH₁N₁ virus and subsequently challenged with pdmH₁N₁. Firstly, priming of animals was tested by determining IAV specific antibodies in sera by ELISA (Figure 45).

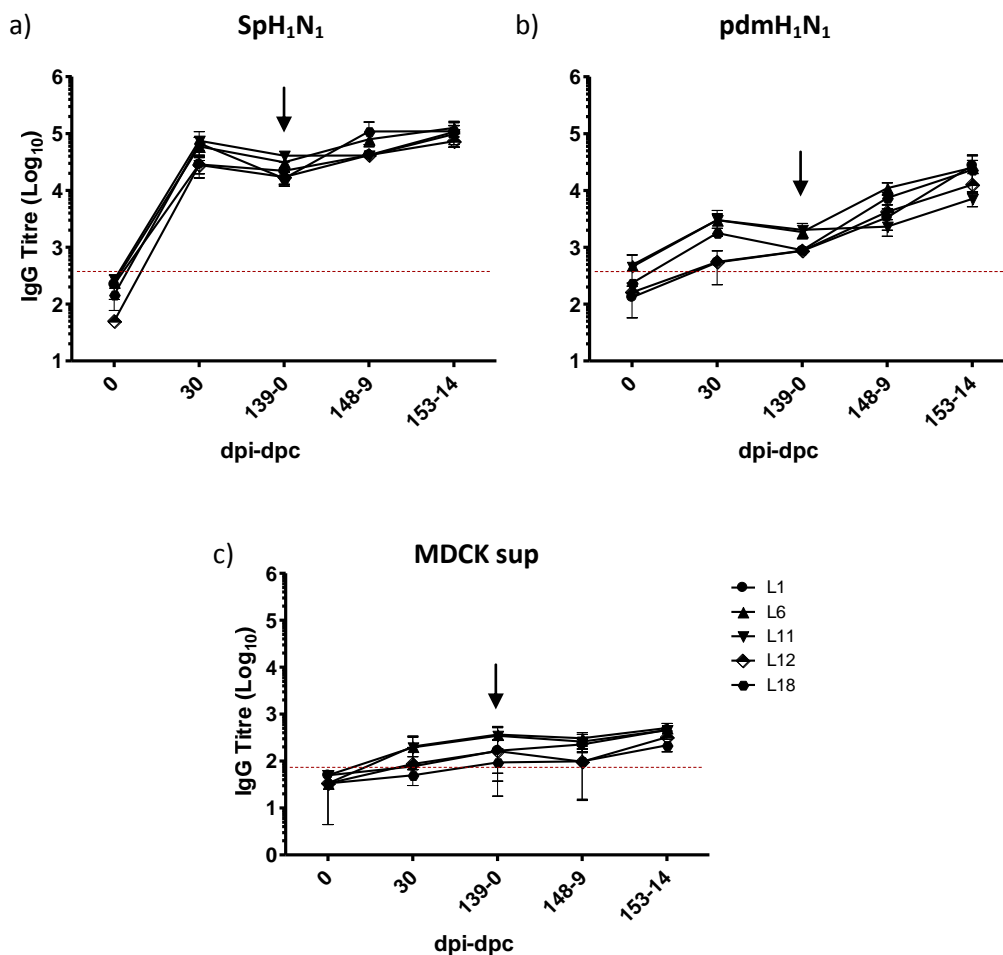


Figure 45. IgG ELISA of sera of infected pigs. Pigs were infected with SpH₁N₁ and challenged with pdmH₁N₁ (arrows). Plates were coated with the following antigens: a) SpH₁N₁, b) pdmH₁N₁ and c) MDCKs sup. Red dotted line is the limit of detection.

Infection with the first virus generated specific humoral responses in all pigs; levels of anti SpH₁N₁ IgG were maintained up to 153 dpi (Figure 45a). Besides, IgG responses were also

cross-reacting with pdmH₁N₁, at least during the pre-challenge period (30 and 139 dpi, figure 44b). Boosting of anti-pdmH₁N₁ IgG was observed after challenge, indicating that pdmH₁N₁ prime and/or boost immune responses. Viruses used in this work were propagated with the previously described method and there could be cross reactivity by their vehicle, MDCKs supernatant (MDCKs sup). Therefore, specific anti-MDCKsup IgG levels were tested by ELISA. Some responses were detected; however, they were close to background levels (Figure 45c).

Virus specific humoral responses were also tested by IAHA. Results confirmed presence of SpH₁N₁ and pdmH₁N₁ specific humoral responses, which also indicated presence of cross-reacting responses before challenge (Figure 11 in supplementary files). In summary, infection and challenge generated humoral responses against SpH₁N₁ and pdmH₁N₁ with cross-reacting properties.

Peptides predicted *in silico* and tested *in vitro* were finally tested *in vivo*. Immunisation of pigs was expected to generate immune response against class I epitopes of viruses used in infection and challenge. Thus, if candidate peptides were class I epitope, peptide specific CTL should be generated and expanded and then detection by specific tetramer constructs would occur. For this purpose, PBMCs from infected animals were stained with anti CD3, CD8 antibodies and tetramers in table 9 (Figure 46).

Two populations of CD3⁺CD8⁺ cells were detected in circulating lymphocytes. One population exhibited the highest CD8 fluorescence (CD8^{high+}) mostly representing CTL cells, and it was analysed for tetramers staining. The other CD8⁺ population were mostly T helper cells and it was excluded from the tetramer analysis. Tetramer staining was performed on PBMCs at all sampling time points. However, tetramer positive specific populations in CD8^{high+} cells were not detectable until 14 dpc (Figure 12 in supplementary files). Tetramers were not staining samples before infection with SpH₁N₁ (0dpi) nor samples of the mismatched pig (L18) after infection with pdmH₁N₁. Similarly, tetramers bearing the irrelevant peptides (Tet 831) were not showing any staining (Figure 46). Results from 14 dpc are shown in table 10 showing frequencies of tetramer positive CTL cells (CD3⁺CD8⁺Tet⁺ cells) ranging from 0.4 to 2.6, depending on each peptide and each animal. Our results identified nine peptides to be T cell epitopes: 3 in M1 (Tet62, Tet56 and Tet64), 3 in NA (Tet55, Tet60 and Tet59) and 3 in HA (Tet93, Tet57 and Tet66).

Figure Y

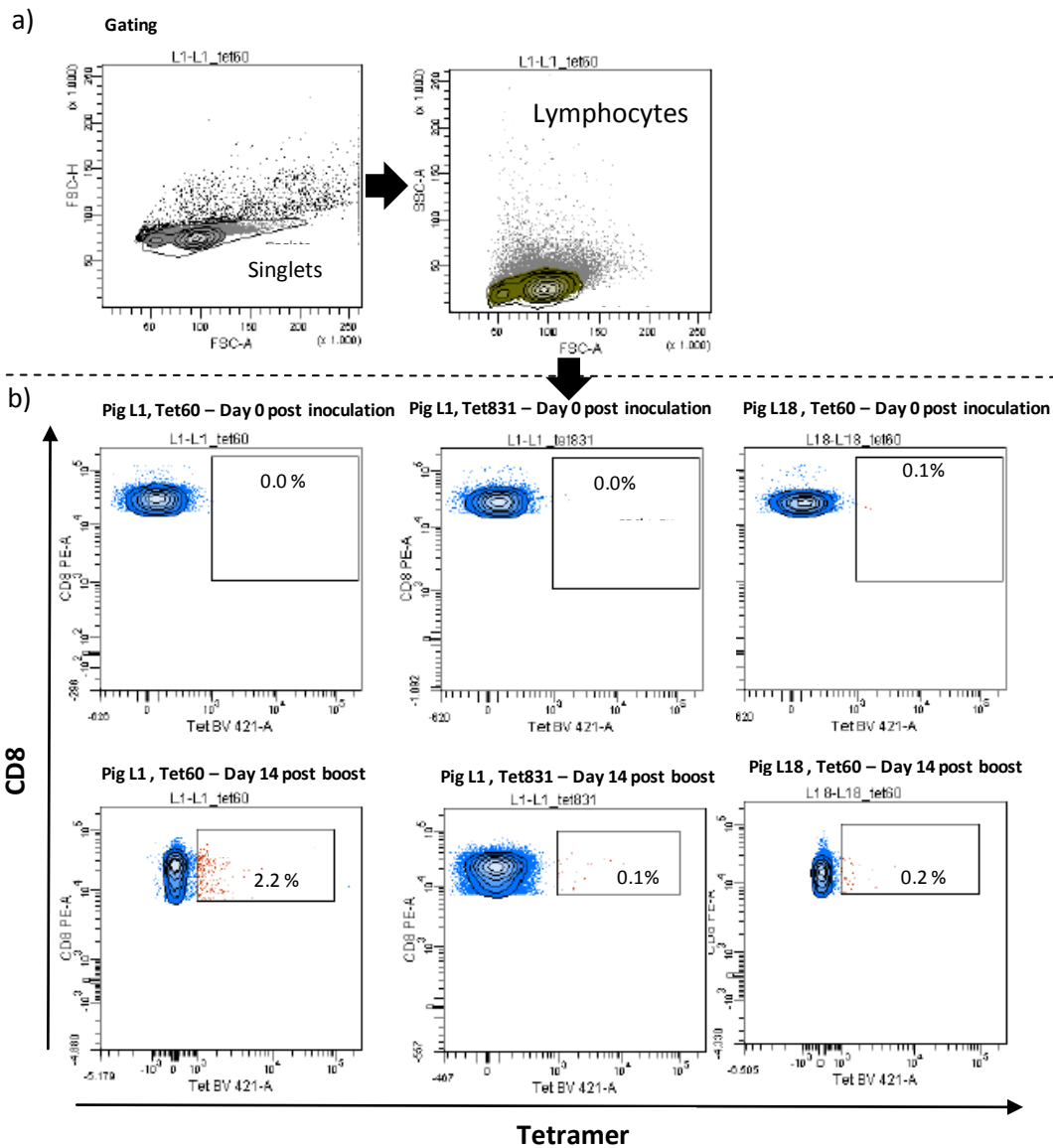


Figure 46. Tetramer staining of PBMCs of infected pigs. Example of gating strategy and staining of cells from pig L1 and pig L18 (mismatched pig) at Day 0 and 153 post infection (14 dpc). a) Singlets and lymphocytes analysis. b) CD3⁺CD8^{high} cells were shown. Tetramer 60 (Tet 60) was shown to stain specifically PBMCs from Pig L1 at 14dpc. The same tetramer and the 381 were not staining PBMCs at 0 dpi nor PBMCs from the mismatched pig at any time point.

Tet60 was reproducibly detected in all animals, being the one with the highest frequency in most of them. Seven tetramers stained positive CTL in Pig L6; in that pig Tet59 (2.1) instead of Tet60 (1.0) had the highest frequency. Therefore, these results indicated that Tet 60 was the immunodominant epitope among all peptides tested and it was taken into account for further analysis.

Pig	Frequency of Tetramers											
	831	93	55	56	57	59	60	61	62	63	64	66
L1	0.1	0.1	0.1	0.7	<u>1.9</u>	0.2	2.2	0.0	0.0	0.1	0.7	0.0
L6	0.1	0.4	1.7	1.2	1.2	2.1	1.0	0.4	0.7	0.1	0.1	1.0
L11	0.7	0.1	0.2	0.0	1.2	1.2	2.6	0.6	1.3	0.1	0.8	0.7
L12	0.3	0.1	0.2	0.1	0.4	0.2	0.7	0.1	0.4	0.6	0.3	0.5
L18	0.1	0.1	0.4	0.5	0.8	0.7	0.2	0.2	0.1	0.1	0.1	0.3

Table 10. Frequencies of CD3⁺CD8⁺Tet⁺ cells at 14 dpb. Numbers in bold show values 2 times higher than background (Negative control or Tetramer 831). Those values that were also 2 times higher than the respective peptide in mismatched pig (L18) are underlined.

Conservation analysis of the immunodominant epitope

Tet60 was located between positions 171 and 180 of NA (NA₁₇₁₋₁₈₀) and it was conserved in both viruses used to infect pigs (Table 9). However, to check the conservation grade in IAV population, strains isolated from swine, human and avian were analysed as reported in material and method. Results were represented as logo in figure 47.

NA₁₇₁₋₁₈₀ sequence was mutated in all three analysed groups. In swine, position 6 varied between Alanine (A) and Valine (V). In humans position 6 showed the same variability as in swine; likewise, position 3 varied among Isoleucine (I), Leucine (L) and Valine (V). In avian, the same positions were mutated, showing respectively Valine (V) at position 3 and Alanine (A) at position 6. Those mutations did not fall into anchor positions 2 and 9; however they fall into anchor positions 3 and 6 (Figure 44).

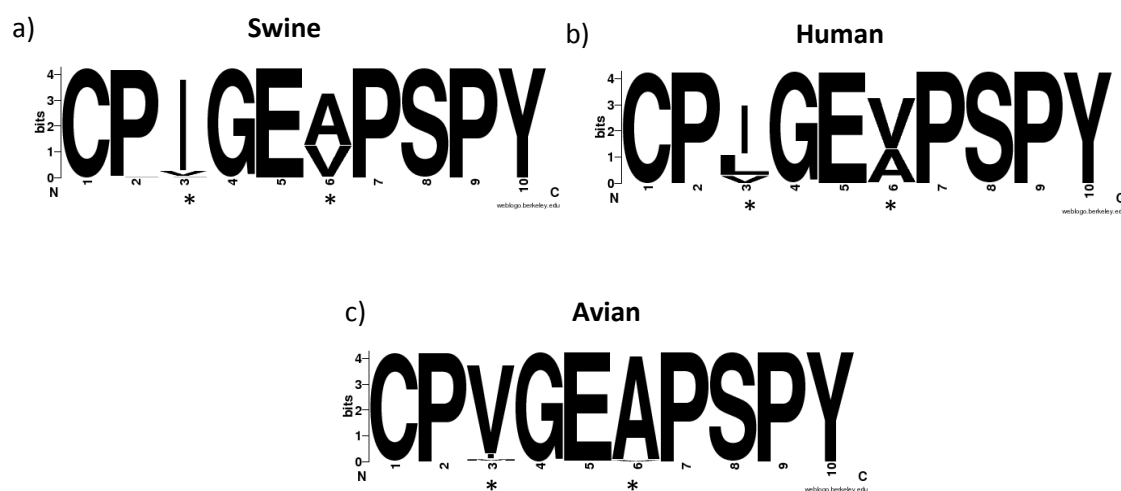


Figure 47. Conservation of NA₁₇₁₋₁₈₀ sequence CPIGEVPSPY. Sequences of IAV H₁N₁ viruses isolated in a) swine b) humans and c) avian were used to generate the logo. Each position represents amino acids found in the analysed group of IAV and its height is proportional with its frequency. Positions mutated compared to NA₁₇₁₋₁₈₀ are indicated by an asterisk.

Discussion

IAV is an important viral pathogen with wide spectra of susceptible host species. In pigs, it already has a stable lineage, SwIV; however, pigs are susceptible also to introduction of new IAV, like the case of pdmH₁N₁. The main concern related to SwIV in the veterinary field is referred to losses in productivity due to an induced disease state; in contrast, the main concern related to SwIV in the human health lays in its zoonotic potential. The control of SwIV is therefore important. Knowledge of IAV ecology is important to design a proper control strategy. Recent pandemic outbreaks showed that there is still a lot to learn; in the 2009 pandemic outbreak, for example, the role of pigs as “mixing vessel” of IAV was further confirmed. This and other findings highlighted the importance of IAV surveillance in other non-human species. Despite the serological data of SwIV circulating in Spain, little was known about their genetic characteristics and thus the epidemiological situation of that country in the European panorama. Therefore, the first chapter of this work contributed to fill this gap.

Updating the epidemiology of SwIV in Spain for RDV (Chapter I).

Field infections of pigs with different SwIV subtypes were detected in Spain in this study during the period 2006–2007. Five strains were isolated from finishing pigs, and their complete genomes were sequenced and analysed. The isolates belonged to the subtypes “Avian-Like” H₁N₁, “Human-Like” H₃N₂ and “Human-Like” H₁N₂. The studied isolates shared a common origin with Spanish strains described previously in each subtype. Notably, the H₁N₁ isolate could be considered drifted from one of them. Additionally, the viruses isolated in this study were also related to SwIV strains circulating in Germany, Hungary and Italy during 2004-2008. Of particular importance were the tight genetic relationship of some strains co-circulating during 2006-2007 (like the isolate SF12091 with the German strain) and the contemporary surge of herds affected by this subtype in Belgium or Italy after the outbreaks in Spain⁵⁵.

Comparisons among European and Spanish strains of SwIVs showed that genetically similar viruses were causing outbreaks contemporarily in different countries, suggesting that they could have been spread across the country in a short period of time. The transboundary movement of live animals may partly explain this finding because other pig pathogens that spread in Spain in the same period showed a similar phylogeographic pattern^{236,237}. Transnational trade of live animals is a relevant factor in the epidemiology of pigs diseases^{236,238-241}, and probably it might also be relevant in the case of SwIV. However, the isolate 80598LP4 was an exception, as the “Human Like” H₁N₂ strains were introduced in Europe from England, with a second wave of introductions in France during ‘90s²⁴². The NA phylogeny

suggests that isolate 80598LP4 might have evolved from the latter. On the other hand, the phylogeny of the HA did not show such clear clustering. Albeit the origin of those genes coding for surface glycoproteins was far from clear and consistent between them, it is noteworthy that they were divergently evolving from the co-circulating H₁N₂ strains, and none of them showed a close relationship. This might suggest that these viruses may have been persistently perpetuated in Spain, evolving divergently than other circulating strains. It cannot be excluded, however, that the isolate 80598LP4 could have been an external introduction from other European countries, and the lack of closely related sequences is due to the limited sampling. As a matter of fact, the persistence or periodical re-introduction of H₁N₂ subtype at regional level has been recently reported by a serological study in five European countries, included Spain⁵⁵.

The “internal genes” of the isolate 80598LP4 could have been evolved differently from the corresponding surface glycoproteins coding genes. They belonged to the “Avian-Like” lineage, as commonly observed in the “Human-Like” H₁N₂ viruses circulating in Europe. However, they were highly related to both co-circulating H₁N₁ and H₁N₂. This particular co-evolution of the 80598LP4 internal genes with the rest of the analysed H₁N₁, H₁N₂ and H₃N₂ viruses, together with the controversial divergent evolution of the genes coding for the surface glycoprotein, suggested that a reassorting event could have been acting to generate a “second generation” of reassortants.

The detection of an H₃N₁ SwIV in Spain during the first half of the 2000s²⁴³ suggested that reassortments were not an uncommon event. A great variety of new reassortants have been described in different European countries, suggesting that reassortment in SwIV is also a common event in other European rearing pig areas in the continent^{56,71,244,245}. The most important finding supporting this hypothesis was that H₁N₁ and H₁N₂ subtype reassortment had the highest rate (every 2-3 years)⁵⁴; thus, the origin of the internal genes of the isolate 80598LP4 could have followed that trend.

A recent study conducted in Spain in a period following this study, between 2010 and 2011, confirms the obtained results²⁴⁶. Notably, the H₁N₂ lineage was shown again to be divergently evolving. Moreover, that study also supports the idea of recent reassorting of SwIV, showing again that SwIV isolates retrieved from respiratory disease cases presented internal genes that clustered differently from HA and NA.

Vaccines against SwIV commercialized in Europe contain inactivated viruses of the subtypes H₁N₂, H₃N₂ and H₁N₁. Antigenic drift is one of the challenges for the control of diseases in pigs using this kind of vaccines^{56,181,190,196,247,248}. However, in comparison with humans, the evolution of SwIV in Europe was slow (see Introduction), supporting the approach that vaccine for pigs update was performed with less frequency. Human vaccines are updated yearly while vaccines for pigs commercially available in Europe have been updated just a few times. A recent study showed that SwIV vaccines for pigs containing old strains offered protection to some more recent strains¹⁸¹. Therefore, the real impact of antigenic drift on SwIV and vaccines in pigs was not yet clear. However, other factors related with the ecology of the virus should be taken into account. Another important finding in chapter I and in another recent publication (Martin-Valls *et al.* 2014²⁴⁶), was that some IAV strains could have been circulating and evolving just in Spain. Those strains evolved divergently making that vaccines designed in other European countries might not have enough efficacies. It is plausible to think that with the novelty of the viruses and the fact that frontiers are open to other European countries, a pandemic potential for pigs might reside in some Spanish SwIV.

Due to the divergent genetic evolution of HA of the H₁N₂ isolated viruses, the antigenic variations were evaluated comparing the most updated commercial vaccine. Isolate 80598LP4 showed a large variation of the HA protein falling into but also outside of the hypothetical antigenic site. However, its glycosylation pattern was the same, suggesting that at least the exposed antigenic sites were conserved. If correct, this idea suggested that there was an on-going divergent evolution that changed the supposed antigenic sites in comparison to some other co-circulating strains; however, those results could not specify the effect on serological recognition.

The antigenic shift is also of great concern. The most important impact of this event on SwIV vaccines is the reduced efficacy due to mismatched virus surface glycoproteins, which are their target. However, that is not a great problem unless there is an introduction of new HA and NA variant excluded from European commercial vaccines. Unfortunately, pigs are susceptible to infection with IAV of different species and moreover they are considered a “mixing vessel” of them; a clear example is the pdmH₁N₁. Therefore, genetic drift of SwIV can be a problem in the latter situation in when non-circulating IAV in pigs were the source of antigenic novelty.

European Surveillance Network for Influenza in Pigs (ESNIP) was recently created (<http://www.esnip3.eu>)²⁴⁹. Surveillance of SwIV circulating in Europe would be able to cope

with this problem allowing, as it was done in human health, to include those divergent strains in the next vaccines generation. However, the combination of surveillance and vaccine design has not been infallible, as seen in the pdmH₁N₁ case in 2009.

Reverse vaccinology: from gene to epitope.

Control of IAV in humans is based on therapeutic or prophylaxis measures; RDV is being applied to develop next generation vaccines which take advantage of the CMI responses against class I or class II T cells epitopes²⁵⁰. In pigs, CMI responses have been just partially described and its importance in control of SwIV infection still to be fully established. Therefore, identification of SwIV T cells epitopes would aid research on CMI responses against SwIV identifying possible targets for RDVs development. This chapter discusses this topic in the light of the results from chapter II to IV using different methodologies including empirical research and RV. RV is a good option to empirical study of T cells identification in human field due to cost and time concerns; however, for pigs there are just few tools and data available. RV works by identifying T cells epitopes starting from genomes of pathogens. The available Spanish SwIV sequences were few and old; therefore, Chapter I provided complete CDSs of SwIVs of the three main subtypes circulating in pigs. Conservation of epitopes is one important quality factor of T cells epitopes, this impact the spectra of SwIV targeted by T cells response. The internal proteins are highly conserved in IAV and thus a good target for development of vaccine with wide strain spectra²⁷; in European SwIV, the internal proteins of all subtypes have common ancestors in “Avian-Like” H₁N₁ lineage (introduction and chapter I) and thus they are highly homologous to it. Therefore, the Spanish strain A/Swine/Spain/SF11131/2007 belonging to the “Avian-Like” H₁N₁ was selected as target for these studies and it was referred as SpH₁N₁.

Porcine T cells epitopes were generally predicted *in silico* through *pan* methods and then they were tested: *in vitro* through binding assay, *ex vivo* through functional assay or *in vivo* through tetramer technology (see Introduction). All the cited methods for identification of class I epitopes but *ex vivo* were recently introduced for pigs; in contrast, for class II epitopes, *in vitro* and *in vivo* assays were not available and the *in silico* ones available were based on a *pan* method which has never been tested in pigs.

Providing new in vitro tools to RV. Development of a cell based SLA binding assay (Chapter II)

In chapter II, an *in vitro* binding assay was developed to allow characterization of class I T cell epitope. The assay used cells as platform for titration of peptides and thus it was referred as “cells based” assay. Reactivity of reagents and all conditions used in this type of assay were set up for humans or mice molecules and they were not previously used in assays for pig molecules; thus they needed to be defined.

There were three main concerns: the availability of immortalised cell lines expressing the desired SLA, the format of the assay and the availability of antibodies to detect pSLA complexes. MHC binding assays using cells as platform for peptides titration need the expression of just one MHC allele to avoid problems of specificity, like the binding of tested peptides to more than one allele on cell surface. There was no commercially available immortalized cell line expressing just one class I SLA allele homozygous²¹⁷. Therefore, the target SLA required to be expressed in a cell line of other specie expressing no or little MHC-I. C1R cells are immortalised human B-lymphoblastoid cells expressing little amount of HLA-Cw4 and no other detectable class I HLA allele at any other locus²⁵¹. This characteristic was also confirmed in this work directly with anti HLA-I antibody (W6/32) or indirectly as retention of human β 2m on C1R cell surface (Figure 24). Therefore, those cells were suitable to express the selected SLA-I alleles. The recombinant cell line expressed human β 2. β 2m is highly conserved among species and *in vitro* folded chimeric β 2m MHC-I molecules (pigs-human) have been shown to be functional without altering binding specificities¹⁷⁴; however, viability of its presentation on the cell surface was unknown.

The second concern referred to the format of the assay. Two main formats of cell based assay were possible, the MHC stabilization assay and the MHC reconstitution assay (See chapter II introduction); format decision was based on the difficulty to generate the corresponding SLA recombinant cell line. Selection of transfected cells was a long process which was complicated by the fact that it was unknown if expression of SLA would have been achieved in cell lines from human. Furthermore, comparing cell based assays, another specific factor was found. MHC stabilization assay requires a particular type of cell which stabilize and thus present MHC on the cell surface just at temperatures below 37°C (TAP⁻ cells)^{208,209}; this made that detection of recombinant SLA molecule in TAP⁻ cells during selection process of transfected cells would have required particular temperature conditions. In contrast, the MHC reconstitution assay used cells which did not require special culture conditions making that selection of

recombinant SLA cells was a more straightforward process. These reasons made to give priority to generation of a MHC reconstitution assay.

The specificity of antibodies used to detect p-SLA complexes constituted the third concern. The main antibody generally used in this kind of assay was W6/32 which is MHC class I specific and pan-reactive, thus, it recognizes a wide spectra of class I alleles. There are few ones described and even less commercially available anti SLA-I antibodies. Furthermore, SLA reactivity is not specified or it is haplotype defined for SLA alleles. Therefore, selection of a porcine pan antibody was a feasible task during this work and reactivity of some anti SLA-I antibodies and antibody W6/32 was tested.

SLA reconstitution assay was designed taking into account the three concerns cited above and developed as follow. Selection of the allele to be expressed in C1R cells was based on the pigs used experimentally. Babraham inbred pigs were used in chapter III to identify class I epitopes due to the fact that their SLA-I was homozygous and results were more reproducible. Therefore, stable C1R cell line expressing SLA-1*es11 or SLA-2*es22 were developed. Allele SLA-1*0401 was also studied because its binding preferences were already described¹⁷⁴ and thus it would have been used as reference to compare data. Stable recombinant C1R cell line expressing SLA heavy chain on cell surface was complete just for SLA-1*es11 and thus these were used to optimize the SLA reconstitution assay. The dynamic of chimeric SLA on cell surface was followed using some specific antibodies, the 74-11-10 and 4B7/8; those were described to recognize the SLA class I^{252,253}. In this work, antibodies 74-11-10 and 4B7/8 recognized the SLA structure in C1R cells surface and they did not recognize HLA; these characteristics made them suitable to be used in the assay. However, those antibodies were not *pan* and thus specific antibodies may be required to detect other transfected alleles in the future. The *pan* W6/32 did not recognise the chimeric SLA structure and thus it was not suitable to be used in the assay.

SLA reconstitution assay was divided into three main steps in which the elution of naturally presented peptides and β 2m from the SLAhc (denaturalization step) was the first one. This is generally achieved through acid treatment of cells on ice (during denaturalization and up to the staining process) to avoid re-circulation of new MHC on the surface of cells^{206,207,254}. Using this method the little amount of HLA expressed on C1R and C1R SLA-1*es11 cells surface was denaturalised and β 2m (tracked by the BBM.1 antibody) was eluted from cells surface. The optimal pH and time of acid treatment is generally allele specific²⁰⁷, thus those factors were

optimized for the SLA-1*es11 allele. Conditions of pH from 3 to 7 and incubation time from 60 to 150 seconds were tested and none of them allowed achieving the expected results. Therefore, denaturalization of SLA-1*es11 was not achieved by translating conditions used for MHC in other species. Noteworthy, a peculiar characteristic of the antibody 74-11-10 was noticed. After denaturalization of C1R SLA-1*es11 on ice and at pH 3, flow cytometry signal after 74-11-10 staining increased instead of decreasing. This could be attributed to 74-11-10 recognition of SLA free heavy chains, which were supposed to increase after denaturalization; however, it was not the case as antibody 4B7/8 and BBM.1 showed that SLA was not denaturalized and thus β 2m was not eluted from SLA heavy chains. 74-11-10 antibody did not show cross reactivity with any form of the HLA. In contrast, the acid treatment on ice may have permeabilised cell membranes and thus exposed intracellular SLA to the 74-11-10. Therefore, a plausible explanation would be that 74-11-10 antibody may have recognised intracellular forms of chimeric SLA-1*es11 structure.

It is known that decreasing temperature below the physiological one (37°C) increases the stability of the MHC structure²⁰⁹. Therefore, the use of physiological temperature should have decreased the stability of the chimeric SLA structure and thus should have allowed its denaturalization. The introduction of this factor allowed achieving denaturalization with the previously used conditions, with acid treatment at pH3 during 90 seconds; however, this procedure implied using an inhibitor of protein transport to avoid MHC recirculation on cell surface. HLA molecule was completely denaturalized as no signal was detected on the C1R SLA-1*es11; in contrast, chimeric SLA-1*es11 was partially denaturalized and thus a little amount of it was still present on the cell surface (Figure 29). This result was confirmed by the little amount of β 2m still present on cell surface after denaturalization. Therefore, a fine tuned optimization will be required to decrease the amount of chimeric SLA-1*es11 after denaturalization to background levels. Due to time restrictions the assay was not further developed.

The second step of the assay is the reconstitution of the SLA with β 2m and peptides. β 2m is an important reagent as it influences the stability of MHC structure; the interaction of MHC with heterologous β 2m can decrease or increase stability of the final MHC complex in an allele specific way as described in human-mice case by Anderson *et al.* 1993²⁵⁵. However, in experimental models with higher homology (human-rhesus macaque) no difference was noticed²⁵⁶. The study of Pedersen *et al.* 2011¹⁷⁴ demonstrated that porcine β 2m could be substituted by the human one in cell-free binding assays using *in vitro* folded chimeric SLA.

They found that interactions with the stalk region of SLA heavy chain of human compared to pig $\beta 2m$ were just slightly different; however, interactions of $\beta 2m$ with the rest of the heavy chain were not taken into account. Interactions of $\beta 2m$ with $\alpha 1\alpha 2$ domain of heavy chain have been suggested to play a central role, in a human-mouse interchange model, to stabilize and to prolong retention of the peptide-receptive conformation of the peptide-binding cleft²⁵⁷. The effect of human and porcine $\beta 2m$ on SLA structure remains an issue requiring further investigations. Finally, the last step of the assay was the analysis by flow cytometry. In this case, optimization of reagents (amount of cells and peptides) depending on the sensitivity of the cytometer would have been needed to reduce the cost of the assay. This step was not performed due to time constraints.

The assay developed in this work will allow in the future testing predicted peptides, to characterize epitopes specificity for SLA alleles (at least for SLA-1*es11) and if the PSCPL was used, the binding preferences of Barbraham pigs class I SLAs.

RV vs. conventional methods. (Chapter III and Chapter IV)

RV was used in this work to identify class I T cells epitope of SwIV in pigs. Those were predicted *in silico* through the *pan* method *NetMHCpan* on three internal proteins (NP, M1, PB1) and one surface glycoprotein (HA) of SpH₁N₁. This method showed in other studies high accuracy of prediction for SLA, although it was combined with *in vitro* assay of SLA binding^{173,178,234}. This combination of methodologies (*in silico-in vitro*) is a normal procedure in RV by means of increasing accuracy of prediction. However, *in vitro* assays were not available for this study.

T cells epitopes were predicted for class I SLAs alleles SLA-1*es11 and SLA-2*es22 as those were syngenic in pigs selected to test prediction results. Therefore, 49 peptides were predicted and then tested for the first time directly *ex vivo* in pigs immunized with the inactivated SpH₁N₁ virus. In the same line, another strategy was complementary adopted. T cells epitopes have been previously empirically discovered in pigs by testing overlapping peptides representing pathogen proteins^{258,259}. Therefore, this approach was used to identify SwIV T cells epitopes in pigs by using pools of overlapping peptides representing NP and M1 sequences belonging to a human seasonal H₃N₂ virus. Peptides and their combinations were tested in animals immunized with the inactivated SpH₁N₁ virus. Those two studies are described in Chapter III.

Inbred animals are generally used to test T cells epitopes as lower allelic variability at the MHC locuses increases the specificity of results. This kind of animals is rare in pigs and we were extremely fortunate to be able to perform these studies with pigs from Babrahams lineage, with defined SLA-I molecules. Babraham pigs are an inbred lineage syngenic for class I SLAs²⁶⁰. Their class I SLAs (SLA-1*es11, SLA2-*es22) showed to be not very common in pig populations as described by the study of Pedersen *et al.* 2014¹⁷⁵; however, it has to be said that this study was restricted to a specific European countries and thus do not reflect the European situation as a whole.

The best way to induce a MHC class I dependent T cell response is expected to be through infection with the target pathogen as its antigens enter to class I epitopes presenting pathway. Unfortunately, due to the unavailability in the license for animal infection, infection studies were not feasible in part of the work. Induction of T cell response was performed through immunization and boost with an UV inactivated form of a SwIV, whose genome was used to predict the class I epitopes, SpH₁N₁. Some animals were also immunized with a commercial vaccine (Gripovac3) constituted by whole killed SwIV; results for testing peptides were equally valid as Gripovac3 contains SwIV with high homology to SpH₁N₁ as shown in chapter 1 Figure 1 supplementary files and Figures 22 and 23. Gripovac3 is an alternative commercial name of Resporc flu3 shown in Table 2 supplementary file. Although immunising with inactivated pathogen is generally associated with class II presentation of antigen; another previous study showed that immunising pigs with inactivated SwIV primed also CTL responses¹⁸⁸. Based on these results, it was expected that the antigen was presented by class II MHC but also by class I through cross-presenting pathway. In the last experiment performed in this part of the work, animals were auxiliary infected with a live attenuated virus (S-Flu) to boost CMI responses. This is a recombinant IAV with defective replication due to deletion of HA signal sequence²²⁴; it is constituted by an H5HA with the rest of genome from the human IAV A/Puerto Rico/8/1934 (H₁N₁). The homology of internal proteins of this virus with SpH₁N₁ was high (PB2, PA, PB1, M1 and NP: 92-96%), thus S-Flu had high probability to share epitopes with SpH₁N₁. Other S-Flu vaccines have previously shown to induce heterosubtypic immunity and protect mice from IAV infection²²⁴, thus H5 S-Flu was used in this study to boost CMI response. In summary, the fact of using inactivated virus for priming responses and a replication deficient S-Flu virus to boost responses in this part of the work would contribute to enhance class II derived immune responses, explaining the reason why epitopes identified in this part of the work were class II dependent.

Immunisation of animals with SpH₁N₁ generated humoral (IgG) and CMI responses against the homologous virus in peripheral blood; CMI responses were detected as recalled IFN γ and proliferative responses. It is interesting to note that the type of antigen used for immunization may have influenced the involvement of spleen in immune responses. Spleen of animals immunised with Gripovac3 showed recall response to SpH₁N₁, whereas animals immunised with the homologous virus did not. Immune responses in immunised animals showed also cross-reacting characteristics. IFN γ response to S-Flu was detected in peripheral blood of animals immunised with SpH₁N₁, although it was weak and of short duration.

The 49 peptides representing predicted class I T cells epitopes were tested by IFN γ and proliferation functional assays. No one of the peptides recalled a positive response neither in peripheral blood nor in spleen. As already cited, *NetMHCpan* demonstrated to be accurate in combination with other methods and the results from these experiments confirmed that it was not accurate when used alone. Also, the data on which the prediction algorithm is trained do not represent the entire variability of MHCs as they contain mainly human and mouse data. Binding preferences of MHC alleles that are not present in the database are therefore extrapolated, showing little accuracy. Porcine alleles SLA-1*es11 and SLA-2*es22 might have been outside the capacity of prediction of *NetMHCpan* as no similar data were included in the database. However, it cannot be excluded that the way of induction of T cell response might have been the cause of negative results. As explained before, immunisation was not the best way to induce class I T cell responses, thus class II response might have been immunodominant. Using positive control epitope for class I presentation would have helped to answer those questions, unfortunately no one has been described so far for the SLA-I alleles under study.

Complementary to prediction methods, T cells epitopes were investigated by testing overlapping epitopes representing NP and M1 protein through IFN γ and proliferative functional assays. NP protein and in particular its second half recalled a positive response in both functional assays. The observed responses were cross-reactive as even though the virus used for immunisation (SpH₁N₁) and the virus whose NP sequence belongs (human IAV) were from far related lineages. Two overlapping peptide (p43 and p44) were identified as dominant for IFN γ responses in the second half of NP (NP₂₀₀₋₄₄₈). Dissection of those peptides allowed identification of two minimum epitope respectively of 12 and 14 amino acids, overlapping 10 amino acids; those were called NP₄₀₅₋₄₁₆: QISVQPTFSVQR and NP₄₀₇₋₄₂₀: SVQPTFSVQRNLPF.

Another possible epitope might have been overlapping NP₄₀₇₋₄₂₀; however, further analyses are required to define whether this peptide is recognised. Length of the identified epitopes suggested that they might be prone to be SLA-II related. Experiments using anti SLA-II antibody showed blocking of IFN γ recall responses with much higher efficacy than in the case of using anti SLA-I antibody for p43 and p44. Complementary, depletion of SLA-II cells also inhibited p43 and p44 IFN γ recall responses further supporting the idea of class II related epitopes. MHC-II is expressed on cells with antigen presenting characteristics, thus their elimination would avoid presentation and thus stimulation of related effector cells. In contrast, class I epitope could be still presented to related effector cells as MHC-I is expressed by all nucleated cells. However, MHC-II is also expressed in a high proportion of CD8⁺ cells^{261,262} and T helper effector/memory cells¹³⁷ in pigs. Therefore, some T cells might have been depleted together with APC. In that way the absence of response in the MHC-II⁺ population might not have depended on the absence of peptides presentation to MHC class II but it might be related to absence of responding T cells. Therefore, these results require further confirmation by characterising the cells subsets within the MHC-II fraction responsible for epitope recognition.

Determination of binding preference of Babraham pigs SLA-II by *pan* method was not feasible, because the allele sequence was unknown. Moreover, there was not sufficient amount of identified epitopes to do it by alignment. However, binding preferences were roughly identified in this study. Regions containing anchor positions were identified at one terminal end at each of p43 and p44. It is generally assumed that MHC-II binding pockets hosting the aminoacids at the extreme end of the peptides have preference for hydrophobic aminoacids²²⁷. Following this line of thought, P1 and P9 were identified as anchor positions and then auxiliary positions (P4 and P6) were deduced. However, it has been reported that anchor positions might not have been the only position influencing antigen presentation as regions flanking P1 and P9 may play a direct role during T cell antigen recognition²⁶³. The C-terminal flanking region of the P9 in p44 (EK) seems to increase antigenicity in the minimal epitope, supporting the role proposed by other authors²⁶³. However, it can also suggest that the observed antigenicity increase could have been due to the presence of another T cell epitope and thus EK might have contained an anchor position. Further analyses are required to establish the role of EK in binding.

Identification of T cell *in silico* by using just *NetMHCpan* failed, whereas those identified empirically were just class II; therefore, another strategy for RV was adopted to identify class I

T cells epitopes, as described in Chapter IV. Recently, a pipeline for identification of class I T cells epitopes in pigs has been developed and applied to SwIV¹⁷⁸. Here, the same pipeline was applied to identify class I T cells epitopes of another allele, SLA-1*0702. This allele was found with high frequency in Danish pigs population¹⁷⁵. *In vitro* characterization showed that SLA-1*0702 has preference for Proline at position 2 while at position 9 three hydrophobic amino acids (Tyrosine, Methionine and Phenylalanine) were preferred. This information was used to discern candidates among some bioinformatically predicted peptides. Peptides were predicted on surface glycoproteins HA and NA and internal protein M1 of two IAV viruses strains. One of these was SpH₁N₁ while the other was a pandemic 2009 IAV isolated in pigs (pdmH₁N₁). *In vitro* testing showed that not all peptide candidates were high binders, therefore intermediate and low binders were found too, suggesting that the use of binding preferences as cut off cannot discriminate the grade of binding affinity, thus other factors rather than just amino acid preference at position 2 and 9 could influence it. Nonetheless, the combination of the two methods used for predictions permitted to narrow possible peptides candidates. Therefore, 11 out of 15 peptides with high to intermediate affinity were selected and used to generate tetramers. Peptide binding was used as pivotal correlate of immunogenicity; however, there are several other factors influencing the final results (for example: original protein amount, naive population frequency) and therefore not all binders may have a detectable CTL population. Presence of peptide specific CTL subpopulations was determined by tetramers staining of PBMCs from animals bearing the allele SLA-1*0702 and infected with IAV. Generation of a T cells response to IAV infection in cited pigs was performed as follow. It was known that CMI response is primed after infection (see introduction) however, the chances to detect peptide specific subpopulations in pigs were unknown. Therefore, to increase those chances, peptide specific T cells should be primed and then boosted. A previous work showed that infection with an “Avian-Like” H₁N₁ Spanish strain was able to induce protection in absence of cross-reacting antibodies against a heterologous virus belonging to the pandemic 2009 H₁N₁ lineage²⁶⁴. The same infection strategy was used to infect with SpH₁N₁ and re-infection with the pdmH₁N₁. In that way, the response against the conserved T cells epitope was expected to be primed and boosted. SpH₁N₁ induced long lasting humoral response in pigs and weak cross-reactions with pdmH₁N₁ were also detected. This contrasts with the above study of Busquets *et al.* 2010²⁶⁴ in which no cross-reacting antibodies were found. pdmH₁N₁ was an IAV strain belonging to the 2009 pandemic lineage but isolated from pigs, which probably passed from humans to pigs and circulated among them. Surface glycoproteins may have adapted to pigs and they could acquire specific mutations; therefore, cross-reacting

antibodies epitopes could be generated due to mutations on surface glycoproteins during adaptation of pdmH₁N₁ to pig. Another possible explanation is that during the study of Busquets *et al.* 2010 the timing used for the experiment was shorter than the one used in this study. Sera were tested for cross-reactivity to a pandemic 2009 IAV only up to 28 days post SwIV infection whereas in this study sera showed cross-reactivity at 139 dpi.

Infection and boosting in pigs by IAV was achieved as indicated by the serological results. Therefore, T cells responses were also expected to be stimulated and subsequently boosted. Presence of peptide specific T cells subsets was evaluated in peripheral blood. Tetramer specific subpopulations were not detected after pdmH₁N₁ infection. Low numbers or low sensitivity of the assay could explain the lack of detection at this time point. However, it cannot be excluded that peptide specific responses picked after the first infection when animals were not sampled. CTL subpopulations specific for 9 out of 11 tetramers were identified; this highlight the high efficiency of the pipeline for class I T cells epitope discovery. NA₁₇₁₋₁₈₀ (CPIGEVSPY) was consistently detected in all pigs and had the highest frequencies of CTL; thus, it can be described as immunodominant. It was noteworthy that most of other T cells epitopes identified in this study were found just in animal L6 in which NA₁₇₁₋₁₈₀ had not the highest frequency and thus was not the dominant. The lack of consistence in positive results among pigs for other peptides might reflect differences in immunodominance hierarchy per pig. Several factors have been suggested to influence immunodominance in other animal models with matched MHC ²⁶⁵. Pigs used in this experiment (Chapter IV) were not inbred; therefore, different levels of SLA might have been expressed in pigs depending on homozygosis in SLA-1*0702. Moreover, different allele interaction influence immunodominance hierarchy ²⁶⁵.

Three consecutive methods were used in this study to identify T cells epitopes of SwIV in pigs. *In silico* methods are known to decrease immunological analysis needed to identify T cells epitopes, with time and cost save. A strategy involving *in silico* prediction (*NetMHCpan*) of class I T cells epitopes and *ex vivo* test by functional assays was used for the first time in this work (Chapter III). This strategy failed to identify any class I T cells epitopes. The same *in silico* prediction was combined with an *in vitro* assay and finally with *in vivo* testing by tetramers (Chapter IV). This strategy was previously used by other authors resulting in high efficiency of identification of class I T cells epitopes ^{173,175} and thus it was also used in this work. A high efficiency of prediction was also detected here as nearly 82% of tested peptides were T cells

epitopes. Therefore, this work supported the previously observed data and showed flexibility of this strategy for more SLA alleles. Tetramer technology was integrated as *in vivo* test of peptides; offering several advantages when compared with other previous testing methods. One of them is that it allowed determination of phenotype as well as studying the amount and dynamic of responding cell populations. Time was another important factor; this method permitted to test just a restricted number of peptides with quick methods.

T cells epitopes were also identified empirically. Use of overlapping peptides was time and cost expensive. Decision of length and overlapping region of peptides, allowed establishing the preferential class of MHC to be investigated. Peptides used in this work were large and overlapping ten amino acids; those characteristics made them suitable to identify class I and II epitopes at the same time²⁶⁶. Therefore, one advantage of this strategy was the possibility to investigate both types of T cells epitopes at the same time. This was important considering that no class II epitope prediction method had been tested or used previously for pigs.

Reverse vaccinology demonstrated to be an alternative to empirical identification of T cells epitopes; however, it was still applicable to just class I epitope as no tool was available to identify class II epitopes. Prediction tools can be improved making available more experimental data about SLA binding preference; however, they were not infallible. Therefore, T cells epitopes still needed to be empirically identified to fill actual gaps in RV for pigs.

T cells subsets involved in SwIV immune response. (Chapter III and IV)

T cells subsets involved in re-stimulation response to SwIV of tissues from immunised animals were evaluated by functional assays coupled to flow cytometry. Results were not statistically significant due to the low number of animals and experiments; however, some discussion about results could be withdrawn.

It has been speculated by other authors that CD4⁺ T cells are naive T helper and they lack proliferative or IFN γ activity after antigen re-stimulation¹³⁷. In contrast, those characteristics were found in CD4⁺CD8⁺ T which were considered T helper effector/memory¹³⁷. Immunisation with SwIV primed both Th and CTL subsets of T cells. Those were able to proliferate and/or secrete IFN γ in response to whole SwIV particle in peripheral blood and even in spleen (Figures 38, 40 and 41). In particular, Th naive were able to just proliferate in response to SwIV re-stimulation. This was in line with previously published work evaluating re-stimulation response

of some vaccinated animals; however, in those studies proliferative response in T cells subpopulations was indirectly detected as up-regulation of CD25 (IL-2 receptor) ^{188,189} and $\gamma\delta$ T cells were not discriminated from other T cells ¹⁹¹. Under infection conditions, Th and CTL have been shown to be involved in immune responses against SwIV, exhibiting multifunctional properties, including secretion of IFN γ ¹⁴⁸.

Importantly, $\gamma\delta$ was another important subset of T cells recently functionally described ¹⁴². In this work, $\gamma\delta$ T cells also contributed to IFN γ secretion and proliferative responses to whole SwIV particle; however, it has to be said that a considerable response was also unspecifically recalled by mock SwIV vehicle (MDCK supernatants). Previous authors did not find $\gamma\delta$ T cells responding with IFN γ to SwIV re-stimulation in immunised pig ¹⁸⁸; however, these studies were performed in infected pigs ¹⁴⁴. In contrast to IFN γ , proliferative responses by porcine $\gamma\delta$ in response to SwIV have been less described. Up-regulation of CD25 in $\gamma\delta$ cells was observed in recall responses induced by SwIV in infected pigs ¹⁴⁴. In species like human and cattle, $\gamma\delta$ T cells did not show surface marker for CD4⁺ and/or CD8⁺ in extratymic population ^{267,268}; in contrast, in pigs, CD8⁺ or CD8⁻ subsets have been described in $\gamma\delta$ T cells ¹⁴¹. In this work, $\gamma\delta^+CD8^+$ T cells of peripheral blood and spleen from immunised pigs were involved in the above described recall responses. Additionally, a non-conventional $\gamma\delta$ subset was found in spleen from immunised Babraham pigs, CD4⁺CD8⁺ ($\gamma\delta$ DP T cells) which proliferated after stimulation with whole SwIV. Those cells have been described to be an intermediate stage in $\gamma\delta$ T cells formation and thus to be confined in primary lymphoid organs in pigs, in particular thymus ^{138,139}. Therefore, an extratymic population of $\gamma\delta$ were known to be either CD8⁺ or CD8⁻. Results in this work showed absence of $\gamma\delta$ DP T cells in peripheral blood but their presence in spleen, a secondary lymphoid organ; therefore, their location and ability to proliferate specifically to stimuli suggested they might be more than just an intermediate stage and thus be involved in immune response to pathogens. However, the ability to respond stimuli requires further studies on purified populations, as the observed responses could have been due to an antigen independent activation (bystander) due to the fact that it was known that cytokine exposure can activate IFN γ and proliferative responses in $\gamma\delta$ T cells in pigs ¹⁴².

On the other hand, immune responses in immunised animals were able to cross-react with heterologous IAV. IFN γ responses to S-Flu were detected by ELISPOT in peripheral blood of animals immunised with SpH₁N₁, although it was weak and of short duration. Cell subsets responding to virus were dissected by flow cytometry. Th effector/memory and CTL were

shown to be involved in IFN γ response in peripheral blood. However, levels of responding CTL were not consistent between experiments. A previous work in immunised pig also showed that re-stimulation with heterologous IAV induced IFN γ response in the cited T cells subsets¹⁸⁸. This point will require further examination in the future.

T cells subsets involved in immune responses generated by immunisation with whole SwIV had been previously described in a few studies. However, functional involvement of T cell subsets in response to single SwIV T cells epitope has never been characterised. T cells subsets involved in recall response induced by NP₃₆₂₋₄₄₆ (corresponding to Pool C) and T cells epitopes NP₄₀₅₋₄₁₆ (contained in p43) and NP₄₀₇₋₄₂₀ (contained in p44) in tissues from immunised Babraham pigs were analysed by flow cytometry. CTL, T helper effector/memory and $\gamma\delta^+$ CD8⁺ T subsets in peripheral blood seemed to respond by IFN γ to NP₃₆₂₋₄₄₆; however, for p43 and p44 no positive population was identified. Proliferative responses were also evaluated by flow cytometry showing that CTL, Th effector/memory, $\gamma\delta^+$ CD8⁺ T and $\gamma\delta^+$ CD4⁺CD8⁺ subsets in spleen proliferated in response to NP₃₆₂₋₄₄₆, p43 and p44. In contrast, in peripheral blood just $\gamma\delta$ T cells proliferated in response to those stimuli. This discrepancy could have been associated to different memory phenotypes in T cells in different locations. The effector phenotype was known to secrete more cytokines and killing proprieties rather than proliferative abilities while the memory phenotype has the opposite characteristics¹³¹. The results obtained here might reflect those differences and therefore peptide specific cells detected in periphery were more like effector cells, secreting cytokines like IFN γ , whereas cells in lymphoid organ were more like memory phenotype. These results were also in line with the generally described tropism preference of those cells¹³¹.

Immune response of immunised pigs to whole SwIV involved multiple T cells subsets dependent on class I or class II SLAs; thus, SwIV might have contained both kinds of epitopes. Previous results in this work showed that NP₃₆₂₋₄₄₆ and in turn T cells epitopes NP₄₀₅₋₄₁₆ and NP₄₀₇₋₄₂₀ were the mayor contributors to IFN γ immune response against NP protein from SwIV in immunised pigs. Functional assays coupled to flow cytometry shown that multiple T cells subsets were involved in recall responses against NP₃₆₂₋₄₄₆. this could be attribute again to the presence of both class I and class II T cells epitopes. When the two class II dependent T cells epitopes (NP₄₀₅₋₄₁₆ and NP₄₀₇₋₄₂₀) were analysed, the main responding subsets were expected to be Th. In contrast, multiple T cells subsets were involved in re-stimulation responses with those two T cell epitopes; including CTL which recognises class I T cells epitopes. Therefore,

reducing the portion of SwIV analysed from whole virus to class II dependent T cells epitopes, did not make class I epitope dependent cells losing their responses. Effector function of T cells can be activated through an antigen independent way (bystander) ^{142,269}. It seems plausible that Th were also re-stimulated by NP₃₆₂₋₄₄₆, NP₄₀₅₋₄₁₆ or NP₄₀₇₋₄₂₀ and in turn activated effector function of other T cells subsets. $\gamma\delta$ were T cells disposing of a peculiar TCR. Its dependence to MHC and reactivity was still largely unknown, particularly in pigs. Therefore, those cells could have been also contributing to re-stimulation by NP₃₆₂₋₄₄₆, NP₄₀₅₋₄₁₆ or NP₄₀₇₋₄₂₀.

In conclusion, re-stimulation responses to whole SwIV in immunised animals involved multiple T cells subsets. Likewise, re-stimulation with SLA-II dependent T cell epitopes involved multiple T cell subsets, including those depending on class I like CTL. Studies on single T cell epitope immune responses might contribute to elucidate immune response mechanisms operating for these epitopes in pigs.

Generation of CTL immune responses with multiple functions during SwIV infection have been recently described ¹⁴⁸. Results in Chapter IV showed that tetramers bearing SwIV class I T cell epitopes were able to stain subpopulations of CD3⁺CD8^{high} T cells (defined as CTL) in peripheral blood of boost-infected pigs. Those subpopulations increased in percentage just after secondary infection (boost infection) with SwIV suggesting their involvement in immune response against that pathogen in pigs (at least after re-infection). Studies of other authors showed that multi functional CTL response could be generated after IAV infection in pigs and results in this work showed that CTL response can be peptide specific. However, functional responses of porcine CTL to SwIV epitopes identified in chapter IV were not characterised and thus their roles in immune response required further investigations. More importantly, implication in protection against SwIV of peptides specific or not, multifunctional or not, porcine CTL has not been fully investigated.

SwIV T cells epitopes. (Chapter III and Chapter IV)

Run for universal vaccines for IAV is recently looking for CTL epitopes instead of focusing the attention to humoral response only. Recently, Th subsets and thus its related epitopes were suggested to be relevant ²⁵⁰. These subsets do not only provide help to B and CTL cells but can also have a direct role in IAV clearance. Therefore, given those important functions and the implication in protection of Th cells in IAV infection, MHC-II epitopes has been suggested to be included together with MHC-I epitopes to generate an optimal vaccine ²⁵⁰.

In pigs, a few SLA-II epitopes were previously identified and none of them were from SwIV. In chapter III two SLA-II epitope (NP₄₀₅₋₄₁₆ and NP₄₀₇₋₄₂₀) of SwIV were identified. Spectra of protection and resistance to IAV escape were important factors to rationally develop a vaccine. Conservation of identified epitopes in IAV lineages was thus an important characteristic to be taken into account. NP₄₀₅₋₄₁₆ and NP₄₀₇₋₄₂₀ were falling into a functionally important region of NP protein which was in charge of oligomerization²⁷⁰. This region had also been described to contain highly conserved and other low variable residues²⁷¹, which could be important to carry out its function. A similar conservation grade was obtained in this work although a less accurate method was used to calculate it. The sequence of the identified epitopes were analysed in different lineages; results showed they were particularly high conserved in SwIV. Most of the variability was observed in human IAV strains and in lesser extent in avian strains. The high conservation exhibited in those epitopes explained the cross-reactivity between the SwIV SpH₁N₁ and NP in human virus A/Panama/2007/1999. This cross reactivity could be extrapolated to other IAV of different lineages. However, there was variability in a few residues being one of them a predicted anchor position (I of NP₄₀₅₋₄₁₆). The influence of mutations at the predicted anchor position should be tested, as it could be the source of viral escape, which can compromise vaccine efficacy. The identified epitopes were not important just in pigs. In humans, it has been shown that CD4⁺ T cells responses focused mainly on two proteins, M1 and NP. Moreover, it was found that epitope NP₄₀₄₋₄₁₆ was among the immunodominant ones²⁷². Importantly, the same epitopes found in this work had a counterpart in humans. Other studies in humans confirmed the antigenic properties of epitope NP₄₀₄₋₄₁₆ and showing their specificity for HLA-II alleles (Reviewed in Chen *et al.* 2014²⁷²).

In Chapter IV one SLA-I epitope was identified as immunodominant. Sequence of NA₁₇₁₋₁₈₀ was falling into NA protein; this is a IAV surface glycoprotein known to be highly variable and no highly conserved sequence was present among all IAV strains²⁷. Due to its high variability, analysis of conservation of NA₁₇₁₋₁₈₀ was performed in this study just on viruses from the H₁N₁ subtype. Sequence was mutated in few positions in swine, human and avian viruses. Notably, mutations did not fall into anchor positions (P2 and P9), which were conserved; however, those were located exactly in two auxiliary anchor positions (P3 and P6). Interestingly, it has been observed by other authors that IAV favoured escape at the residues that anchor epitope peptides to MHC²⁷³. This fact suggested that selecting pressure might have already acted on this epitope to allow viral escape. However, implications of the mutations into TCR recognition should be verified. NA₁₇₁₋₁₈₀ had no counterpart in any other species. More SLA-I epitopes have

been recently identified ¹⁷⁵ and they were located into NP, PB2 and HA protein of SwIV. Surface glycoproteins are highly variable and thus offer restricted spectrum of protection that can be limited to a specific subtype, lineage or even period of time depending on the conservation grade of the sequence and its flexibility to be recognised by TCR. In contrast internal proteins are better choice due to their high grade of conservation.

Knowledge of T cells epitopes is not only fundamental to rationally design vaccines but it is also important to enrich and validate already available database making them more accurate for *in silico* prediction. In humans, epitopes able to bind to multiple allele are being investigated to maximize vaccine efficacy ²⁵⁰. Therefore, it is also important to characterise binding preference of more SLAs and thus to be able identifying shared characteristics; this would allow to design promiscuous T cells epitopes able to bind more than one SLA and thus to protect a wide range of pigs populations. Additionally, understanding IAV evolution is fundamental to design next generation control tools and to predict possible threats to public health. Immune pressure is the mayor contributor to evolution of human IAV; therefore, knowledge of IAV antigenic characteristics would allow understanding evolution and may be to predict next IAV pandemic ⁴⁵.

Conclusions

1. SwIV epidemiological situation circulating in Spain during the period 2006- 2007 was updated. A close relation of those with other European countries was observed through phylogenetic analysis. However, divergently evolving strains were also observed.
2. An *in vitro* and cell based SLA-I reconstitution assay was generated and partially optimised for allele SLA-1*es11.
3. Predicting class I T cells epitopes *in silico* and testing them *ex vivo* was not sufficiently accurate to allow identification of SwIV epitopes in Babraham pigs.
4. SLA-II T cells epitopes NP₄₀₅₋₄₁₆ and NP₄₀₇₋₄₂₀ of SwIV were identified for the first time by using overlapping peptides in Babraham immunised pigs.
5. Multiple T cells subsets were involved in IFN γ and proliferative re-stimulation responses to SwIV as well as to single NP₄₀₅₋₄₁₆ and NP₄₀₇₋₄₂₀ epitopes. Those were T helper, CTL and $\gamma\delta$ subsets $\gamma\delta^+CD8^+$ and $\gamma\delta^+CD4^+CD8^+$.
6. T cells epitopes of SwIV related to SLA-1*0702 were identified by combining *in silico* prediction with *in vitro* testing and *in vivo* analysis by tetramers. An SLA-I immunodominant epitope for SLA-1*0702 was described for the first time in NA protein of SwIV; this was NA₁₇₁₋₁₈₀.

References

- 1 Webster, R. G., Bean, W. J., Gorman, O. T., Chambers, T. M. & Kawaoka, Y. Evolution and ecology of influenza A viruses. *Microbiological reviews* **56**, 152-179 (1992).
- 2 Hutchinson, E. C., von Kirchbach, J. C., Gog, J. R. & Digard, P. Genome packaging in influenza A virus. *The Journal of general virology* **91**, 313-328, doi:10.1099/vir.0.017608-0 (2010).
- 3 Li, X. & Palese, P. Characterization of the polyadenylation signal of influenza virus RNA. *Journal of virology* **68**, 1245-1249 (1994).
- 4 Zheng, H., Palese, P. & Garcia-Sastre, A. Nonconserved nucleotides at the 3' and 5' ends of an influenza A virus RNA play an important role in viral RNA replication. *Virology* **217**, 242-251, doi:10.1006/viro.1996.0111 (1996).
- 5 Firth, A. E. & Brierley, I. Non-canonical translation in RNA viruses. *The Journal of general virology* **93**, 1385-1409, doi:10.1099/vir.0.042499-0 (2012).
- 6 Yewdell, J. W. & Ince, W. L. Virology. Frameshifting to PA-X influenza. *Science* **337**, 164-165, doi:10.1126/science.1225539 (2012).
- 7 Vigerust, D. J. & Shepherd, V. L. Virus glycosylation: role in virulence and immune interactions. *Trends in microbiology* **15**, 211-218, doi:10.1016/j.tim.2007.03.003 (2007).
- 8 Brett, K. *et al.* Site-specific S-acylation of influenza virus hemagglutinin: the location of the acylation site relative to the membrane border is the decisive factor for attachment of stearate. *The Journal of biological chemistry* **289**, 34978-34989, doi:10.1074/jbc.M114.586180 (2014).
- 9 Bertram, S., Glowacka, I., Steffen, I., Kuhl, A. & Pohlmann, S. Novel insights into proteolytic cleavage of influenza virus hemagglutinin. *Reviews in medical virology* **20**, 298-310, doi:10.1002/rmv.657 (2010).
- 10 Vasin, A. V. *et al.* Molecular mechanisms enhancing the proteome of influenza A viruses: An overview of recently discovered proteins. *Virus research* **185C**, 53-63, doi:10.1016/j.virusres.2014.03.015 (2014).
- 11 Richardson, J. C. & Akkina, R. K. NS2 protein of influenza virus is found in purified virus and phosphorylated in infected cells. *Archives of Virology* **116**, 69-80, doi:10.1007/BF01319232 (1991).
- 12 Epstein, S. L. & Price, G. E. Cross-protective immunity to influenza A viruses. *Expert review of vaccines* **9**, 1325-1341, doi:10.1586/erv.10.123 (2010).
- 13 Hutchinson, E. C. & Fodor, E. Transport of the influenza virus genome from nucleus to nucleus. *Viruses* **5**, 2424-2446, doi:10.3390/v5102424 (2013).
- 14 Fodor, E. The RNA polymerase of influenza a virus: mechanisms of viral transcription and replication. *Acta virologica* **57**, 113-122 (2013).
- 15 Bialas, K. M., Bussey, K. A., Stone, R. L. & Takimoto, T. Specific nucleoprotein residues affect influenza virus morphology. *Journal of virology* **88**, 2227-2234, doi:10.1128/JVI.03354-13 (2014).
- 16 Roberts, K. L., Leser, G. P., Ma, C. & Lamb, R. A. The amphipathic helix of influenza A virus M2 protein is required for filamentous bud formation and scission of filamentous and spherical particles. *Journal of virology* **87**, 9973-9982, doi:10.1128/JVI.01363-13 (2013).
- 17 Rossman, J. S. & Lamb, R. A. Influenza virus assembly and budding. *Virology* **411**, 229-236, doi:10.1016/j.virol.2010.12.003 (2011).
- 18 Marcelin, G., Sandbulte, M. R. & Webby, R. J. Contribution of antibody production against neuraminidase to the protection afforded by influenza vaccines. *Reviews in medical virology* **22**, 267-279, doi:10.1002/rmv.1713 (2012).

- 19 Matrosovich, M. N., Matrosovich, T. Y., Gray, T., Roberts, N. A. & Klenk, H. D. Neuraminidase is important for the initiation of influenza virus infection in human airway epithelium. *Journal of virology* **78**, 12665-12667, doi:10.1128/JVI.78.22.12665-12667.2004 (2004).
- 20 Chakrabarti, A. K. & Pasricha, G. An insight into the PB1F2 protein and its multifunctional role in enhancing the pathogenicity of the influenza A viruses. *Virology* **440**, 97-104, doi:10.1016/j.virol.2013.02.025 (2013).
- 21 Hale, B. G., Randall, R. E., Ortin, J. & Jackson, D. The multifunctional NS1 protein of influenza A viruses. *The Journal of general virology* **89**, 2359-2376, doi:10.1099/vir.0.2008/004606-0 (2008).
- 22 Le Goffic, R. *et al.* Influenza A virus protein PB1-F2 exacerbates IFN-beta expression of human respiratory epithelial cells. *J Immunol* **185**, 4812-4823, doi:10.4049/jimmunol.0903952 (2010).
- 23 Zheng, W. & Tao, Y. J. Structure and assembly of the influenza A virus ribonucleoprotein complex. *FEBS letters* **587**, 1206-1214, doi:10.1016/j.febslet.2013.02.048 (2013).
- 24 Domingo, E., Sheldon, J. & Perales, C. Viral quasispecies evolution. *Microbiology and molecular biology reviews : MMBR* **76**, 159-216, doi:10.1128/MMBR.05023-11 (2012).
- 25 Boni, M. F., Zhou, Y., Taubenberger, J. K. & Holmes, E. C. Homologous recombination is very rare or absent in human influenza A virus. *Journal of virology* **82**, 4807-4811, doi:10.1128/JVI.02683-07 (2008).
- 26 Tong, S. *et al.* New world bats harbor diverse influenza A viruses. *PLoS pathogens* **9**, e1003657, doi:10.1371/journal.ppat.1003657 (2013).
- 27 Heiny, A. T. *et al.* Evolutionarily conserved protein sequences of influenza a viruses, avian and human, as vaccine targets. *PloS one* **2**, e1190, doi:10.1371/journal.pone.0001190 (2007).
- 28 Schrauwen, E. J. *et al.* Determinants of virulence of influenza A virus. *European journal of clinical microbiology & infectious diseases : official publication of the European Society of Clinical Microbiology* **33**, 479-490, doi:10.1007/s10096-013-1984-8 (2014).
- 29 Ison, M. G. Antivirals and resistance: influenza virus. *Current opinion in virology* **1**, 563-573, doi:10.1016/j.coviro.2011.09.002 (2011).
- 30 Kay, R. M., Done, S. H. & Paton, D. J. Effect of sequential porcine reproductive and respiratory syndrome and swine influenza on the growth and performance of finishing pigs. *The Veterinary record* **135**, 199-204 (1994).
- 31 W.H.O. *Influenza - Swine influenza in humans*, <http://www.who.int/influenza/human_animal_interface/swine_influenza/en/> (2009).
- 32 Opriessnig, T., Gimenez-Lirola, L. G. & Halbur, P. G. Polymicrobial respiratory disease in pigs. *Animal health research reviews / Conference of Research Workers in Animal Diseases* **12**, 133-148, doi:10.1017/S1466252311000120 (2011).
- 33 Kuntz-Simon G, K. C., Madec F. in *Infectious and parasitic diseases of livestock* (ed Blancou J Lefevre PC, Taylor DW.) 273–285 (Lavoisier, 2010).
- 34 Olsen CW, B. I., Easterday BC, Van Reeth K. in *Diseases of swine* (ed Zimmermann W Straw B, D’Allaire S, Taylor DJ. Ames) 469–482 (Iowa State University Press, 2006).
- 35 Vincent, A. L., Ma, W., Lager, K. M., Janke, B. H. & Richt, J. A. Swine influenza viruses a North American perspective. *Advances in virus research* **72**, 127-154, doi:10.1016/S0065-3527(08)00403-X (2008).
- 36 Rose, N. *et al.* Dynamics of influenza A virus infections in permanently infected pig farms: evidence of recurrent infections, circulation of several swine influenza viruses

- and reassortment events. *Veterinary research* **44**, 72, doi:10.1186/1297-9716-44-72 (2013).
- 37 Janke, B. H. Influenza A virus infections in swine: pathogenesis and diagnosis. *Veterinary pathology* **51**, 410-426, doi:10.1177/0300985813513043 (2014).
- 38 De Vleeschauwer, A. *et al.* Comparative pathogenesis of an avian H5N2 and a swine H1N1 influenza virus in pigs. *PLoS one* **4**, e6662, doi:10.1371/journal.pone.0006662 (2009).
- 39 Janke, B. H. Clinicopathological features of Swine influenza. *Current topics in microbiology and immunology* **370**, 69-83, doi:10.1007/82_2013_308 (2013).
- 40 Lyoo, K. S., Kim, J. K., Jung, K., Kang, B. K. & Song, D. Comparative pathology of pigs infected with Korean H1N1, H1N2, or H3N2 swine influenza A viruses. *Virology journal* **11**, 170, doi:10.1186/1743-422X-11-170 (2014).
- 41 Zell, R., Scholtissek, C. & Ludwig, S. Genetics, evolution, and the zoonotic capacity of European Swine influenza viruses. *Current topics in microbiology and immunology* **370**, 29-55, doi:10.1007/82_2012_267 (2013).
- 42 Gray, G. C. *et al.* Influenza A(H1N1)pdm09 virus among healthy show pigs, United States. *Emerging infectious diseases* **18**, 1519-1521, doi:10.3201/eid1809.120431 (2012).
- 43 Pomorska-Mol, M., Kwit, K., Markowska-Daniel, I., Kowalski, C. & Pejsak, Z. Local and systemic immune response in pigs during subclinical and clinical swine influenza infection. *Research in veterinary science*, doi:10.1016/j.rvsc.2014.06.007 (2014).
- 44 Frank, S. A. in *Immunology and Evolution of Infectious Disease* (2002).
- 45 Smith, D. J. *et al.* Mapping the antigenic and genetic evolution of influenza virus. *Science* **305**, 371-376, doi:10.1126/science.1097211 (2004).
- 46 de Jong, J. C. *et al.* Antigenic and genetic evolution of swine influenza A (H3N2) viruses in Europe. *Journal of virology* **81**, 4315-4322, doi:10.1128/JVI.02458-06 (2007).
- 47 Moreno, A. *et al.* Different evolutionary trends of swine H1N2 influenza viruses in Italy compared to European viruses. *Veterinary research* **44**, 112, doi:10.1186/1297-9716-44-112 (2013).
- 48 Kyriakis, C. S. *et al.* Virological surveillance and preliminary antigenic characterization of influenza viruses in pigs in five European countries from 2006 to 2008. *Zoonoses and public health* **58**, 93-101, doi:10.1111/j.1863-2378.2009.01301.x (2011).
- 49 Vijaykrishna, D. *et al.* Long-term evolution and transmission dynamics of swine influenza A virus. *Nature* **473**, 519-522, doi:10.1038/nature10004 (2011).
- 50 Nelson, M. I. *et al.* Introductions and evolution of human-origin seasonal influenza A viruses in multinational Swine populations. *Journal of virology* **88**, 10110-10119, doi:10.1128/JVI.01080-14 (2014).
- 51 Ninomiya, A., Takada, A., Okazaki, K., Shortridge, K. F. & Kida, H. Seroepidemiological evidence of avian H4, H5, and H9 influenza A virus transmission to pigs in southeastern China. *Veterinary microbiology* **88**, 107-114 (2002).
- 52 Olsen, C. W., Carey, S., Hinshaw, L. & Karasin, A. I. Virologic and serologic surveillance for human, swine and avian influenza virus infections among pigs in the north-central United States. *Arch Virol* **145**, 1399-1419 (2000).
- 53 Yuan, Z. *et al.* Serological surveillance of H5 and H9 avian influenza A viral infections among pigs in Southern China. *Microbial pathogenesis* **64**, 39-42, doi:10.1016/j.micpath.2013.08.001 (2013).
- 54 Lycett, S. J. *et al.* Estimating reassortment rates in co-circulating Eurasian swine influenza viruses. *The Journal of general virology* **93**, 2326-2336, doi:10.1099/vir.0.044503-0 (2012).

- 55 Kyriakis, C. S. *et al.* Influenza A virus infection dynamics in swine farms in Belgium, France, Italy and Spain, 2006-2008. *Veterinary microbiology* **162**, 543-550, doi:10.1016/j.vetmic.2012.11.014 (2013).
- 56 Zell, R. *et al.* Novel reassortant of swine influenza H1N2 virus in Germany. *The Journal of general virology* **89**, 271-276, doi:10.1099/vir.0.83338-0 (2008).
- 57 Pol, M. Pig farming in the EU, a changing sector. (2010). <http://epp.eurostat.ec.europa.eu/portal/page/portal/product_details/publication?product_code=KS-SF-10-008>.
- 58 Neumeier, E., Meier-Ewert, H. & Cox, N. J. Genetic relatedness between influenza A (H1N1) viruses isolated from humans and pigs. *The Journal of general virology* **75 (Pt 8)**, 2103-2107 (1994).
- 59 Lange, J. *et al.* Circulation of classical swine influenza virus in Europe between the wars? *Arch Virol* **159**, 1467-1473, doi:10.1007/s00705-013-1950-x (2014).
- 60 Pensaert, M., Ottis, K., Vandeputte, J., Kaplan, M. M. & Bachmann, P. A. Evidence for the natural transmission of influenza A virus from wild ducts to swine and its potential importance for man. *Bulletin of the World Health Organization* **59**, 75-78 (1981).
- 61 Van Reeth, K. *et al.* Seroprevalence of H1N1, H3N2 and H1N2 influenza viruses in pigs in seven European countries in 2002-2003. *Influenza and other respiratory viruses* **2**, 99-105, doi:10.1111/j.1750-2659.2008.00043.x (2008).
- 62 Brown, I. H., Chakraverty, P., Harris, P. A. & Alexander, D. J. Disease outbreaks in pigs in Great Britain due to an influenza A virus of H1N2 subtype. *The Veterinary record* **136**, 328-329 (1995).
- 63 Lam, T. Y. *et al.* Evolutionary analyses of European H1N2 swine influenza A virus by placing timestamps on the multiple reassortment events. *Virus research* **131**, 271-278, doi:10.1016/j.virusres.2007.08.012 (2008).
- 64 Dawood, F. S. *et al.* Emergence of a novel swine-origin influenza A (H1N1) virus in humans. *The New England journal of medicine* **360**, 2605-2615, doi:10.1056/NEJMoa0903810 (2009).
- 65 Grontvedt, C. A. *et al.* Influenza A(H1N1)pdm09 virus infection in Norwegian swine herds 2009/10: the risk of human to swine transmission. *Preventive veterinary medicine* **110**, 429-434, doi:10.1016/j.prevetmed.2013.02.016 (2013).
- 66 Starick, E. *et al.* Reassorted pandemic (H1N1) 2009 influenza A virus discovered from pigs in Germany. *The Journal of general virology* **92**, 1184-1188, doi:10.1099/vir.0.028662-0 (2011).
- 67 Welsh, M. D. *et al.* Initial incursion of pandemic (H1N1) 2009 influenza A virus into European pigs. *The Veterinary record* **166**, 642-645, doi:10.1136/vr.4851 (2010).
- 68 Vincent, A. *et al.* Review of influenza A virus in swine worldwide: a call for increased surveillance and research. *Zoonoses and public health* **61**, 4-17, doi:10.1111/zph.12049 (2014).
- 69 Juergen Richt, R. J. W. *Swine Influenza*. (Springer-Verlag Berlin Heidelberg, 2013).
- 70 Trebbien, R. *et al.* Genetic and biological characterisation of an avian-like H1N2 swine influenza virus generated by reassortment of circulating avian-like H1N1 and H3N2 subtypes in Denmark. *Virology journal* **10**, 290, doi:10.1186/1743-422X-10-290 (2013).
- 71 Moreno, A. *et al.* Genomic characterization of H1N2 swine influenza viruses in Italy. *Veterinary microbiology* **156**, 265-276, doi:10.1016/j.vetmic.2011.11.004 (2012).
- 72 Maldonado, J. *et al.* Evidence of the concurrent circulation of H1N2, H1N1 and H3N2 influenza A viruses in densely populated pig areas in Spain. *The Veterinary Journal* **172**, 377-381, doi:10.1016/j.tvjl.2005.04.014 (2006).
- 73 Maldonado J., V. L. in *European association of Veterinary Laboratory Diagnosticians congress*.

- 74 Valls, L., Maldonado, J., Riera, P. in *6th International Symposium on Emerging and Re-Emerging Pig Diseases*.
- 75 Worobey, M., Han, G. Z. & Rambaut, A. A synchronized global sweep of the internal genes of modern avian influenza virus. *Nature* **508**, 254-257, doi:10.1038/nature13016 (2014).
- 76 Neumann, G. & Kawaoka, Y. The first influenza pandemic of the new millennium. *Influenza and other respiratory viruses* **5**, 157-166, doi:10.1111/j.1750-2659.2011.00231.x (2011).
- 77 Association, A. V. M. One Health: A New Professional Imperative. (2008). <https://www.avma.org/KB/Resources/Reports/Documents/onehealth_final.pdf>.
- 78 Richard, M., de Graaf, M. & Herfst, S. Avian influenza A viruses: from zoonosis to pandemic. *Future virology* **9**, 513-524, doi:10.2217/fvl.14.30 (2014).
- 79 Herfst, S., Imai, M., Kawaoka, Y. & Fouchier, R. A. Avian Influenza Virus Transmission to Mammals. *Current topics in microbiology and immunology*, doi:10.1007/82_2014_387 (2014).
- 80 Ma, W., Kahn, R. E. & Richt, J. A. The pig as a mixing vessel for influenza viruses: Human and veterinary implications. *Journal of molecular and genetic medicine : an international journal of biomedical research* **3**, 158-166 (2008).
- 81 Freidl, G. S. *et al.* Influenza at the animal-human interface: a review of the literature for virological evidence of human infection with swine or avian influenza viruses other than A(H5N1). *Euro surveillance : bulletin European sur les maladies transmissibles = European communicable disease bulletin* **19** (2014).
- 82 Wei, K. *et al.* Influenza A virus Acquires Enhanced Pathogenicity and Transmissibility After Serial Passages in Swine. *Journal of virology*, doi:10.1128/JVI.01679-14 (2014).
- 83 Meurens, F., Summerfield, A., Nauwynck, H., Saif, L. & Gerdt, V. The pig: a model for human infectious diseases. *Trends in microbiology* **20**, 50-57, doi:10.1016/j.tim.2011.11.002 (2012).
- 84 Iwasaki, A. & Pillai, P. S. Innate immunity to influenza virus infection. *Nature reviews. Immunology* **14**, 315-328, doi:10.1038/nri3665 (2014).
- 85 Cohen, M. *et al.* Influenza A penetrates host mucus by cleaving sialic acids with neuraminidase. *Virology journal* **10**, 321, doi:10.1186/1743-422X-10-321 (2013).
- 86 Bottazzi, B., Doni, A., Garlanda, C. & Mantovani, A. An integrated view of humoral innate immunity: pentraxins as a paradigm. *Annual review of immunology* **28**, 157-183, doi:10.1146/annurev-immunol-030409-101305 (2010).
- 87 Short, K. R., Kroeze, E. J., Fouchier, R. A. & Kuiken, T. Pathogenesis of influenza-induced acute respiratory distress syndrome. *The Lancet. Infectious diseases* **14**, 57-69, doi:10.1016/S1473-3099(13)70286-X (2014).
- 88 Jost, S. & Altfeld, M. Control of human viral infections by natural killer cells. *Annual review of immunology* **31**, 163-194, doi:10.1146/annurev-immunol-032712-100001 (2013).
- 89 Quinones-Parra, S., Loh, L., Brown, L. E., Kedzierska, K. & Valkenburg, S. A. Universal immunity to influenza must outwit immune evasion. *Frontiers in microbiology* **5**, 285, doi:10.3389/fmicb.2014.00285 (2014).
- 90 Short, K. R. *et al.* A Novel Method Linking Antigen Presentation by Human Monocyte-Derived Macrophages to CD8(+) T Cell Polyfunctionality. *Frontiers in immunology* **4**, 389, doi:10.3389/fimmu.2013.00389 (2013).
- 91 Akira, S. Innate immunity and adjuvants. *Philosophical transactions of the Royal Society of London. Series B, Biological sciences* **366**, 2748-2755, doi:10.1098/rstb.2011.0106 (2011).

- 92 Vantourout, P. & Hayday, A. Six-of-the-best: unique contributions of gammadelta T cells to immunology. *Nature reviews. Immunology* **13**, 88-100, doi:10.1038/nri3384 (2013).
- 93 Zeng, X. *et al.* gammadelta T cells recognize a microbial encoded B cell antigen to initiate a rapid antigen-specific interleukin-17 response. *Immunity* **37**, 524-534, doi:10.1016/j.immuni.2012.06.011 (2012).
- 94 Holderness, J., Hedges, J. F., Ramstead, A. & Jutila, M. A. Comparative Biology of $\gamma\delta$ T Cell Function in Humans, Mice, and Domestic Animals. *Annual Review of Animal Biosciences* **1**, 99-124, doi:doi:10.1146/annurev-animal-031412-103639 (2013).
- 95 van Spriel, A. B. & de Jong, E. C. Dendritic cell science: more than 40 years of history. *Journal of leukocyte biology*, doi:10.1189/jlb.0512263 (2012).
- 96 McGill, J., Heusel, J. W. & Legge, K. L. Innate immune control and regulation of influenza virus infections. *Journal of leukocyte biology* **86**, 803-812, doi:10.1189/jlb.0509368 (2009).
- 97 Neyt, K. & Lambrecht, B. N. The role of lung dendritic cell subsets in immunity to respiratory viruses. *Immunological reviews* **255**, 57-67, doi:10.1111/imr.12100 (2013).
- 98 Moyron-Quiroz, J. E. *et al.* Role of inducible bronchus associated lymphoid tissue (iBALT) in respiratory immunity. *Nature medicine* **10**, 927-934, doi:10.1038/nm1091 (2004).
- 99 Andersen, M. H., Schrama, D., Thor Straten, P. & Becker, J. C. Cytotoxic T cells. *The Journal of investigative dermatology* **126**, 32-41, doi:10.1038/sj.jid.5700001 (2006).
- 100 Kapsenberg, M. L. Dendritic-cell control of pathogen-driven T-cell polarization. *Nature reviews. Immunology* **3**, 984-993, doi:10.1038/nri1246 (2003).
- 101 McGill, J., Van Rooijen, N. & Legge, K. L. Protective influenza-specific CD8 T cell responses require interactions with dendritic cells in the lungs. *The Journal of experimental medicine* **205**, 1635-1646, doi:10.1084/jem.20080314 (2008).
- 102 Villadangos, J. A. & Schnorrer, P. Intrinsic and cooperative antigen-presenting functions of dendritic-cell subsets in vivo. *Nature reviews. Immunology* **7**, 543-555, doi:10.1038/nri2103 (2007).
- 103 Mintern, J. D., Macri, C. & Villadangos, J. A. Modulation of antigen presentation by intracellular trafficking. *Current opinion in immunology* **34C**, 16-21, doi:10.1016/j.coi.2014.12.006 (2015).
- 104 Neefjes, J. & Ovaa, H. A peptide's perspective on antigen presentation to the immune system. *Nature chemical biology* **9**, 769-775, doi:10.1038/nchembio.1391 (2013).
- 105 Hubbell, J. A., Thomas, S. N. & Swartz, M. A. Materials engineering for immunomodulation. *Nature* **462**, 449-460, doi:10.1038/nature08604 (2009).
- 106 Bhati, M., Cole, D. K., McCluskey, J., Sewell, A. K. & Rossjohn, J. The versatility of the alphabeta T-cell antigen receptor. *Protein science : a publication of the Protein Society* **23**, 260-272, doi:10.1002/pro.2412 (2014).
- 107 Bernhard, C. A., Ried, C., Kochanek, S. & Brocker, T. CD169+ macrophages are sufficient for priming of CTLs with specificities left out by cross-priming dendritic cells. *Proceedings of the National Academy of Sciences of the United States of America* **112**, 5461-5466, doi:10.1073/pnas.1423356112 (2015).
- 108 Martinez-Pomares, L. & Gordon, S. CD169+ macrophages at the crossroads of antigen presentation. *Trends in immunology* **33**, 66-70, doi:10.1016/j.it.2011.11.001 (2012).
- 109 Cheng, L. *et al.* Mouse gammadelta T cells are capable of expressing MHC class II molecules, and of functioning as antigen-presenting cells. *Journal of neuroimmunology* **203**, 3-11, doi:10.1016/j.jneuroim.2008.06.007 (2008).

- 110 Brandes, M., Willimann, K. & Moser, B. Professional antigen-presentation function by human gammadelta T Cells. *Science* **309**, 264-268, doi:10.1126/science.1110267 (2005).
- 111 Collins, R. A. *et al.* Gammadelta T cells present antigen to CD4+ alphabeta T cells. *Journal of leukocyte biology* **63**, 707-714 (1998).
- 112 Meuter, S., Eberl, M. & Moser, B. Prolonged antigen survival and cytosolic export in cross-presenting human gammadelta T cells. *Proceedings of the National Academy of Sciences of the United States of America* **107**, 8730-8735, doi:10.1073/pnas.1002769107 (2010).
- 113 Wu, Y. *et al.* Human gamma delta T cells: a lymphoid lineage cell capable of professional phagocytosis. *J Immunol* **183**, 5622-5629, doi:10.4049/jimmunol.0901772 (2009).
- 114 Brandes, M. *et al.* Cross-presenting human gammadelta T cells induce robust CD8+ alphabeta T cell responses. *Proceedings of the National Academy of Sciences of the United States of America* **106**, 2307-2312, doi:10.1073/pnas.0810059106 (2009).
- 115 Janeway, C. *Immunobiology Five*. (Garland Pub., 2001).
- 116 Takahashi, Y., Onodera, T., Kobayashi, K. & Kurosaki, T. Primary and secondary B-cell responses to pulmonary virus infection. *Infectious disorders drug targets* **12**, 232-240 (2012).
- 117 Potter, C. W. & Oxford, J. S. Determinants of immunity to influenza infection in man. *British medical bulletin* **35**, 69-75 (1979).
- 118 Mancini, N. *et al.* A potential role for monoclonal antibodies in prophylactic and therapeutic treatment of influenza. *Antiviral research* **92**, 15-26, doi:10.1016/j.antiviral.2011.07.013 (2011).
- 119 Corti, D. & Lanzavecchia, A. Broadly neutralizing antiviral antibodies. *Annual review of immunology* **31**, 705-742, doi:10.1146/annurev-immunol-032712-095916 (2013).
- 120 Strutt, T. M. *et al.* Multipronged CD4(+) T-cell effector and memory responses cooperate to provide potent immunity against respiratory virus. *Immunological reviews* **255**, 149-164, doi:10.1111/jmr.12088 (2013).
- 121 Annunziato, F., Romagnani, C. & Romagnani, S. The 3 major types of innate and adaptive cell-mediated effector immunity. *The Journal of allergy and clinical immunology* **135**, 626-635, doi:10.1016/j.jaci.2014.11.001 (2015).
- 122 Swain, S. L., McKinstry, K. K. & Strutt, T. M. Expanding roles for CD4(+) T cells in immunity to viruses. *Nature reviews. Immunology* **12**, 136-148, doi:10.1038/nri3152 (2012).
- 123 La Gruta, N. L. & Turner, S. J. T cell mediated immunity to influenza: mechanisms of viral control. *Trends in immunology* **35**, 396-402, doi:10.1016/j.it.2014.06.004 (2014).
- 124 McKinstry, K. K. *et al.* Memory CD4+ T cells protect against influenza through multiple synergizing mechanisms. *The Journal of clinical investigation* **122**, 2847-2856, doi:10.1172/JCI63689 (2012).
- 125 Krammer, F. & Palese, P. Influenza virus hemagglutinin stalk-based antibodies and vaccines. *Current opinion in virology* **3**, 521-530, doi:10.1016/j.coviro.2013.07.007 (2013).
- 126 Cerwenka, A., Morgan, T. M., Harmsen, A. G. & Dutton, R. W. Migration kinetics and final destination of type 1 and type 2 CD8 effector cells predict protection against pulmonary virus infection. *The Journal of experimental medicine* **189**, 423-434 (1999).
- 127 Hamada, H. *et al.* Tc17, a unique subset of CD8 T cells that can protect against lethal influenza challenge. *J Immunol* **182**, 3469-3481, doi:10.4049/jimmunol.0801814 (2009).

- 128 Hamada, H. *et al.* Multiple redundant effector mechanisms of CD8+ T cells protect against influenza infection. *J Immunol* **190**, 296-306, doi:10.4049/jimmunol.1200571 (2013).
- 129 Hillaire, M. L., Rimmelzwaan, G. F. & Kreijtz, J. H. Clearance of influenza virus infections by T cells: risk of collateral damage? *Current opinion in virology* **3**, 430-437, doi:10.1016/j.coviro.2013.05.002 (2013).
- 130 McKinstry, K. K., Strutt, T. M. & Swain, S. L. Regulation of CD4+ T-cell contraction during pathogen challenge. *Immunological reviews* **236**, 110-124, doi:10.1111/j.1600-065X.2010.00921.x (2010).
- 131 Farber, D. L., Yudanin, N. A. & Restifo, N. P. Human memory T cells: generation, compartmentalization and homeostasis. *Nature reviews. Immunology* **14**, 24-35, doi:10.1038/nri3567 (2014).
- 132 Crisci, E., Mussa, T., Fraile, L. & Montoya, M. Review: influenza virus in pigs. *Molecular immunology* **55**, 200-211, doi:10.1016/j.molimm.2013.02.008 (2013).
- 133 Mussa, T. *et al.* Swine, human or avian influenza viruses differentially activates porcine dendritic cells cytokine profile. *Veterinary immunology and immunopathology* **154**, 25-35, doi:10.1016/j.vetimm.2013.04.004 (2013).
- 134 Mussa, T. *et al.* Interaction of porcine conventional dendritic cells with swine influenza virus. *Virology* **420**, 125-134, doi:10.1016/j.virol.2011.09.001 (2011).
- 135 Sinkora, M., Butler, J. E., Lager, K. M., Potockova, H. & Sinkorova, J. The comparative profile of lymphoid cells and the T and B cell spectratype of germ-free piglets infected with viruses SIV, PRRSV or PCV2. *Veterinary research* **45**, 91, doi:10.1186/s13567-014-0091-x (2014).
- 136 Allerson, M. *et al.* The impact of maternally derived immunity on influenza A virus transmission in neonatal pig populations. *Vaccine* **31**, 500-505, doi:10.1016/j.vaccine.2012.11.023 (2013).
- 137 Gerner, W. *et al.* Phenotypic and functional differentiation of porcine alphabeta T cells: Current knowledge and available tools. *Molecular immunology* **66**, 3-13, doi:10.1016/j.molimm.2014.10.025 (2015).
- 138 Sinkora, M., Sinkorova, J., Cimburek, Z. & Holtmeier, W. Two groups of porcine TCRgammadelta+ thymocytes behave and diverge differently. *J Immunol* **178**, 711-719 (2007).
- 139 Sinkora, M., Sinkorova, J. & Holtmeier, W. Development of gammadelta thymocyte subsets during prenatal and postnatal ontogeny. *Immunology* **115**, 544-555, doi:10.1111/j.1365-2567.2005.02194.x (2005).
- 140 Stepanova, K. & Sinkora, M. Porcine gammadelta T lymphocytes can be categorized into two functionally and developmentally distinct subsets according to expression of CD2 and level of TCR. *J Immunol* **190**, 2111-2120, doi:10.4049/jimmunol.1202890 (2013).
- 141 Gerner, W., Kaser, T. & Saalmuller, A. Porcine T lymphocytes and NK cells--an update. *Developmental and comparative immunology* **33**, 310-320, doi:10.1016/j.dci.2008.06.003 (2009).
- 142 Sedlak, C., Patzl, M., Saalmuller, A. & Gerner, W. IL-12 and IL-18 induce interferon-gamma production and de novo CD2 expression in porcine gammadelta T cells. *Developmental and comparative immunology* **47**, 115-122, doi:10.1016/j.dci.2014.07.007 (2014).
- 143 Pomorska-Mol, M., Kwit, K., Markowska-Daniel, I., Kowalski, C. & Pejsak, Z. Local and systemic immune response in pigs during subclinical and clinical swine influenza infection. *Research in veterinary science* **97**, 412-421, doi:10.1016/j.rvsc.2014.06.007 (2014).

- 144 Kappes, M. A. *et al.* Vaccination with NS1-truncated H3N2 swine influenza virus primes T cells and confers cross-protection against an H1N1 heterosubtypic challenge in pigs. *Vaccine* **30**, 280-288, doi:10.1016/j.vaccine.2011.10.098 (2012).
- 145 Lange, E. *et al.* Pathogenesis and transmission of the novel swine-origin influenza virus A/H1N1 after experimental infection of pigs. *The Journal of general virology* **90**, 2119-2123, doi:10.1099/vir.0.014480-0 (2009).
- 146 Heinen, P. P., de Boer-Luijtz, E. A. & Bianchi, A. T. Respiratory and systemic humoral and cellular immune responses of pigs to a heterosubtypic influenza A virus infection. *The Journal of general virology* **82**, 2697-2707 (2001).
- 147 Khatri, M. *et al.* Swine influenza H1N1 virus induces acute inflammatory immune responses in pig lungs: a potential animal model for human H1N1 influenza virus. *Journal of virology* **84**, 11210-11218, doi:10.1128/JVI.01211-10 (2010).
- 148 Talker, S. C. *et al.* Magnitude and kinetics of multifunctional CD4+ and CD8beta+ T cells in pigs infected with swine influenza A virus. *Veterinary research* **46**, 52, doi:10.1186/s13567-015-0182-3 (2015).
- 149 Larsen, D. L., Karasin, A., Zuckermann, F. & Olsen, C. W. Systemic and mucosal immune responses to H1N1 influenza virus infection in pigs. *Veterinary microbiology* **74**, 117-131 (2000).
- 150 Pomorska-Mol, M., Markowska-Daniel, I. & Kwit, K. Immune and acute phase response in pigs experimentally infected with H1N2 swine influenza virus. *FEMS immunology and medical microbiology* **66**, 334-342, doi:10.1111/j.1574-695X.2012.01026.x (2012).
- 151 Reutner, K. *et al.* CD27 expression discriminates porcine T helper cells with functionally distinct properties. *Veterinary research* **44**, 18, doi:10.1186/1297-9716-44-18 (2013).
- 152 Carrat, F. & Flahault, A. Influenza vaccine: the challenge of antigenic drift. *Vaccine* **25**, 6852-6862, doi:10.1016/j.vaccine.2007.07.027 (2007).
- 153 Reperant, L. A., Rimmelzwaan, G. F. & Osterhaus, A. D. Advances in influenza vaccination. *F1000prime reports* **6**, 47, doi:10.12703/P6-47 (2014).
- 154 Noh, J. Y. & Kim, W. J. Influenza vaccines: unmet needs and recent developments. *Infection & chemotherapy* **45**, 375-386, doi:10.3947/ic.2013.45.4.375 (2013).
- 155 Broadbent, A. J. & Subbarao, K. Influenza virus vaccines: lessons from the 2009 H1N1 pandemic. *Current opinion in virology* **1**, 254-262, doi:10.1016/j.coviro.2011.08.002 (2011).
- 156 WHO.
<http://www.who.int/influenza/vaccines/virus/characteristics_virus_vaccines/en/> (2014).
- 157 Plotkin, S. History of vaccination. *Proceedings of the National Academy of Sciences of the United States of America* **111**, 12283-12287, doi:10.1073/pnas.1400472111 (2014).
- 158 Rueckert, C. & Guzman, C. A. Vaccines: from empirical development to rational design. *PLoS pathogens* **8**, e1003001, doi:10.1371/journal.ppat.1003001 (2012).
- 159 Choi, E. H. *et al.* Development of a dual-protective live attenuated vaccine against H5N1 and H9N2 avian influenza viruses by modifying the NS1 gene. *Arch Virol*, doi:10.1007/s00705-015-2442-y (2015).
- 160 Rappuoli, R., Pizza, M., Del Giudice, G. & De Gregorio, E. Vaccines, new opportunities for a new society. *Proceedings of the National Academy of Sciences of the United States of America* **111**, 12288-12293, doi:10.1073/pnas.1402981111 (2014).
- 161 Donati, C. & Rappuoli, R. Reverse vaccinology in the 21st century: improvements over the original design. *Annals of the New York Academy of Sciences* **1285**, 115-132, doi:10.1111/nyas.12046 (2013).
- 162 Sela-Culang, I., Kunik, V. & Ofan, Y. The structural basis of antibody-antigen recognition. *Frontiers in immunology* **4**, 302, doi:10.3389/fimmu.2013.00302 (2013).

- 163 Lafuente, E. M. & Reche, P. A. Prediction of MHC-peptide binding: a systematic and comprehensive overview. *Current pharmaceutical design* **15**, 3209-3220 (2009).
- 164 Zhang, L., Udaka, K., Mamitsuka, H. & Zhu, S. Toward more accurate pan-specific MHC-peptide binding prediction: a review of current methods and tools. *Briefings in bioinformatics* **13**, 350-364, doi:10.1093/bib/bbr060 (2012).
- 165 Hoof, I. *et al.* NetMHCpan, a method for MHC class I binding prediction beyond humans. *Immunogenetics* **61**, 1-13, doi:10.1007/s00251-008-0341-z (2009).
- 166 Karosiene, E. *et al.* NetMHCIIpan-3.0, a common pan-specific MHC class II prediction method including all three human MHC class II isotypes, HLA-DR, HLA-DP and HLA-DQ. *Immunogenetics* **65**, 711-724, doi:10.1007/s00251-013-0720-y (2013).
- 167 Villadangos, J. A. *et al.* Proteases involved in MHC class II antigen presentation. *Immunological reviews* **172**, 109-120 (1999).
- 168 York, I. A., Goldberg, A. L., Mo, X. Y. & Rock, K. L. Proteolysis and class I major histocompatibility complex antigen presentation. *Immunological reviews* **172**, 49-66 (1999).
- 169 Rock, K. L., York, I. A. & Goldberg, A. L. Post-proteasomal antigen processing for major histocompatibility complex class I presentation. *Nature immunology* **5**, 670-677, doi:10.1038/ni1089 (2004).
- 170 Doytchinova, I. A., Guan, P. & Flower, D. R. EpiJen: a server for multistep T cell epitope prediction. *BMC bioinformatics* **7**, 131, doi:10.1186/1471-2105-7-131 (2006).
- 171 Larsen, M. V. *et al.* An integrative approach to CTL epitope prediction: a combined algorithm integrating MHC class I binding, TAP transport efficiency, and proteasomal cleavage predictions. *European journal of immunology* **35**, 2295-2303, doi:10.1002/eji.200425811 (2005).
- 172 IEDB. IEDB, <www.iedb.org> (
- 173 Pedersen, L. E. *et al.* Identification of peptides from foot-and-mouth disease virus structural proteins bound by class I swine leukocyte antigen (SLA) alleles, SLA-1*0401 and SLA-2*0401. *Animal genetics* **44**, 251-258, doi:10.1111/j.1365-2052.2012.02400.x (2013).
- 174 Pedersen, L. E. *et al.* Porcine major histocompatibility complex (MHC) class I molecules and analysis of their peptide-binding specificities. *Immunogenetics* **63**, 821-834, doi:DOI 10.1007/s00251-011-0555-3 (2011).
- 175 Pedersen, L. E., Jungersen, G., Sorensen, M. R., Ho, C. S. & Vadekaer, D. F. Swine Leukocyte Antigen (SLA) class I allele typing of Danish swine herds and identification of commonly occurring haplotypes using sequence specific low and high resolution primers. *Veterinary immunology and immunopathology* **162**, 108-116, doi:10.1016/j.vetimm.2014.10.007 (2014).
- 176 Gao, F. S. *et al.* Reconstruction of a swine SLA-I protein complex and determination of binding nonameric peptides derived from the foot-and-mouth disease virus. *Veterinary immunology and immunopathology* **113**, 328-338, doi:10.1016/j.vetimm.2006.06.002 (2006).
- 177 Oleksiewicz, M. B., Kristensen, B., Ladekjaer-Mikkelsen, A. S. & Nielsen, J. Development of a rapid in vitro protein refolding assay which discriminates between peptide-bound and peptide-free forms of recombinant porcine major histocompatibility class I complex (SLA-I). *Veterinary immunology and immunopathology* **86**, 55-77 (2002).
- 178 Pedersen, L. E., Breum, S. O., Riber, U., Larsen, L. E. & Jungersen, G. Identification of swine influenza virus epitopes and analysis of multiple specificities expressed by cytotoxic T cell subsets. *Virology journal* **11**, 163, doi:10.1186/1743-422X-11-163 (2014).

- 179 Franzoni, G. *et al.* Proteome-wide screening reveals immunodominance in the CD8 T cell response against classical swine fever virus with antigen-specificity dependent on MHC class I haplotype expression. *PLoS one* **8**, e84246, doi:10.1371/journal.pone.0084246 (2013).
- 180 Kitikoon, P. *et al.* Swine influenza virus vaccine serologic cross-reactivity to contemporary US swine H3N2 and efficacy in pigs infected with an H3N2 similar to 2011-2012 H3N2v. *Influenza and other respiratory viruses* **7 Suppl 4**, 32-41, doi:10.1111/irv.12189 (2013).
- 181 Kyriakis, C. S., Gramer, M. R., Barbe, F., Van Doorselaere, J. & Van Reeth, K. Efficacy of commercial swine influenza vaccines against challenge with a recent European H1N1 field isolate. *Veterinary microbiology* **144**, 67-74, doi:10.1016/j.vetmic.2009.12.039 (2010).
- 182 Lloyd, L. E. *et al.* Experimental transmission of avian-like swine H1N1 influenza virus between immunologically naive and vaccinated pigs. *Influenza and other respiratory viruses* **5**, 357-364, doi:10.1111/j.1750-2659.2011.00233.x (2011).
- 183 Romagosa, A. *et al.* Vaccination of influenza A virus decreases transmission rates in pigs. *Veterinary research* **42**, 120, doi:10.1186/1297-9716-42-120 (2011).
- 184 Reeth, K. V., Brown, I., Essen, S. & Pensaert, M. Genetic relationships, serological cross-reaction and cross-protection between H1N2 and other influenza A virus subtypes endemic in European pigs. *Virus research* **103**, 115-124, doi:10.1016/j.virusres.2004.02.023 (2004).
- 185 Reynolds, J. J., Torremorell, M. & Craft, M. E. Mathematical modeling of influenza A virus dynamics within swine farms and the effects of vaccination. *PLoS one* **9**, e106177, doi:10.1371/journal.pone.0106177 (2014).
- 186 Gauger, P. C. *et al.* Kinetics of lung lesion development and pro-inflammatory cytokine response in pigs with vaccine-associated enhanced respiratory disease induced by challenge with pandemic (2009) A/H1N1 influenza virus. *Veterinary pathology* **49**, 900-912, doi:10.1177/0300985812439724 (2012).
- 187 Vincent, A. L., Lager, K. M., Janke, B. H., Gramer, M. R. & Richt, J. A. Failure of protection and enhanced pneumonia with a US H1N2 swine influenza virus in pigs vaccinated with an inactivated classical swine H1N1 vaccine. *Veterinary microbiology* **126**, 310-323, doi:10.1016/j.vetmic.2007.07.011 (2008).
- 188 Platt, R. *et al.* Comparison of humoral and cellular immune responses to inactivated swine influenza virus vaccine in weaned pigs. *Veterinary immunology and immunopathology* **142**, 252-257, doi:10.1016/j.vetimm.2011.05.005 (2011).
- 189 Sandbulte, M. R. *et al.* Divergent immune responses and disease outcomes in piglets immunized with inactivated and attenuated H3N2 swine influenza vaccines in the presence of maternally-derived antibodies. *Virology* **464-465**, 45-54, doi:10.1016/j.virol.2014.06.027 (2014).
- 190 Heinen, P. P., van Nieuwstadt, A. P., de Boer-Luijtz, E. A. & Bianchi, A. T. Analysis of the quality of protection induced by a porcine influenza A vaccine to challenge with an H3N2 virus. *Veterinary immunology and immunopathology* **82**, 39-56 (2001).
- 191 Lefevre, E. A. *et al.* Immune responses in pigs vaccinated with adjuvanted and non-adjuvanted A(H1N1)pdm/09 influenza vaccines used in human immunization programmes. *PLoS one* **7**, e32400, doi:10.1371/journal.pone.0032400 (2012).
- 192 Loving, C. L., Vincent, A. L., Pena, L. & Perez, D. R. Heightened adaptive immune responses following vaccination with a temperature-sensitive, live-attenuated influenza virus compared to adjuvanted, whole-inactivated virus in pigs. *Vaccine* **30**, 5830-5838, doi:10.1016/j.vaccine.2012.07.033 (2012).

- 193 Chen, Q., Madson, D., Miller, C. L. & Harris, D. L. Vaccine development for protecting swine against influenza virus. *Animal health research reviews / Conference of Research Workers in Animal Diseases* **13**, 181-195, doi:10.1017/S1466252312000175 (2012).
- 194 Fouchier, R. A. *et al.* Detection of influenza A viruses from different species by PCR amplification of conserved sequences in the matrix gene. *Journal of clinical microbiology* **38**, 4096-4101 (2000).
- 195 Chiapponi, C., Fallacara, F., Foni, E. in *4th International Symposium on Emerging and Re-emerging Pig Diseases*.
- 196 WHO. *Sequencing primers and protocol*, <http://www.who.int/csr/resources/publications/swineflu/GenomePrimers_20090512.pdf> (2009).
- 197 Altschul, S. F., Gish, W., Miller, W., Myers, E. W. & Lipman, D. J. Basic local alignment search tool. *Journal of molecular biology* **215**, 403-410, doi:10.1016/S0022-2836(05)80360-2 (1990).
- 198 Bao, Y. *et al.* The influenza virus resource at the National Center for Biotechnology Information. *Journal of virology* **82**, 596-601, doi:10.1128/JVI.02005-07 (2008).
- 199 Thompson, J. D., Higgins, D. G. & Gibson, T. J. CLUSTAL W: improving the sensitivity of progressive multiple sequence alignment through sequence weighting, position-specific gap penalties and weight matrix choice. *Nucleic acids research* **22**, 4673-4680 (1994).
- 200 Tamura, K. *et al.* MEGA5: molecular evolutionary genetics analysis using maximum likelihood, evolutionary distance, and maximum parsimony methods. *Molecular biology and evolution* **28**, 2731-2739, doi:10.1093/molbev/msr121 (2011).
- 201 Saitou, N. & Nei, M. The neighbor-joining method: a new method for reconstructing phylogenetic trees. *Molecular biology and evolution* **4**, 406-425 (1987).
- 202 Jukes, T. H. & Cantor, C. R. *Evolution of Protein Molecules*. (Academy Press, 1969).
- 203 Joseph, F. Confidence limits on phylogenies: An approach using the bootstrap. *Evolution* **39**, 783-791 (1985).
- 204 Brownlee, G. G. & Fodor, E. The predicted antigenicity of the haemagglutinin of the 1918 Spanish influenza pandemic suggests an avian origin. *Philosophical transactions of the Royal Society of London. Series B, Biological sciences* **356**, 1871-1876, doi:10.1098/rstb.2001.1001 (2001).
- 205 Gupta, R., Jung E., Brunak, S. *Prediction of N-glycosylation sites in human proteins*. (2004).
- 206 Worley, B. S. *et al.* Antigenicity of fusion proteins from sarcoma-associated chromosomal translocations. *Cancer research* **61**, 6868-6875 (2001).
- 207 Zeh, H. J., 3rd *et al.* Flow-cytometric determination of peptide-class I complex formation. Identification of p53 peptides that bind to HLA-A2. *Human immunology* **39**, 79-86 (1994).
- 208 Alvarez, I. *et al.* The Cys-67 residue of HLA-B27 influences cell surface stability, peptide specificity, and T-cell antigen presentation. *The Journal of biological chemistry* **276**, 48740-48747, doi:10.1074/jbc.M108882200 (2001).
- 209 Ljunggren, H. G. *et al.* Empty MHC class I molecules come out in the cold. *Nature* **346**, 476-480, doi:10.1038/346476a0 (1990).
- 210 Sesma, L. *et al.* Qualitative and quantitative differences in peptides bound to HLA-B27 in the presence of mouse versus human tapasin define a role for tapasin as a size-dependent peptide editor. *J Immunol* **174**, 7833-7844 (2005).
- 211 Kessler, J. H. *et al.* Competition-based cellular peptide binding assays for 13 prevalent HLA class I alleles using fluorescein-labeled synthetic peptides. *Human immunology* **64**, 245-255 (2003).

- 212 Sylvester-Hvid, C. *et al.* Establishment of a quantitative ELISA capable of determining peptide - MHC class I interaction. *Tissue antigens* **59**, 251-258 (2002).
- 213 Harndahl, M. *et al.* Peptide binding to HLA class I molecules: homogenous, high-throughput screening, and affinity assays. *Journal of biomolecular screening* **14**, 173-180, doi:10.1177/1087057108329453 (2009).
- 214 Harndahl, M., Rasmussen, M., Roder, G. & Buus, S. Real-time, high-throughput measurements of peptide-MHC-I dissociation using a scintillation proximity assay. *Journal of immunological methods* **374**, 5-12, doi:10.1016/j.jim.2010.10.012 (2011).
- 215 Sidney, J. *et al.* Measurement of MHC/peptide interactions by gel filtration or monoclonal antibody capture. *Current protocols in immunology / edited by John E. Coligan ... [et al.] Chapter 18*, Unit 18 13, doi:10.1002/0471142735.im1803s100 (2013).
- 216 Buus, S., Lise Lauemøller, S., Stryhn, A. & Østergaard Pedersen, L. in *Current Protocols in Immunology* (John Wiley & Sons, Inc., 2001).
- 217 Ho, C. S., Franzo-Romain, M. H., Lee, Y. J., Lee, J. H. & Smith, D. M. Sequence-based characterization of swine leucocyte antigen alleles in commercially available porcine cell lines. *International journal of immunogenetics* **36**, 231-234, doi:10.1111/j.1744-313X.2009.00853.x (2009).
- 218 Bullido, R., Ezquerra, A., Alonso, F., Gómez del Moral, M. & Domínguez, J. Characterization of a new monoclonal antibody (4B7) specific for porcine MHC (SLA) class I antigens. *Investigación Agraria Producción y Sanidad Animales* **11**, 29-37 (1996).
- 219 Barnstable, C. J. *et al.* Production of monoclonal antibodies to group A erythrocytes, HLA and other human cell surface antigens-new tools for genetic analysis. *Cell* **14**, 9-20 (1978).
- 220 Brodsky, F. M., Parham, P., Barnstable, C. J., Crumpton, M. J. & Bodmer, W. F. Monoclonal antibodies for analysis of the HLA system. *Immunological reviews* **47**, 3-61 (1979).
- 221 Flesch, I. E. *et al.* Altered CD8(+) T cell immunodominance after vaccinia virus infection and the naive repertoire in inbred and F(1) mice. *J Immunol* **184**, 45-55, doi:10.4049/jimmunol.0900999 (2010).
- 222 Baratelli, M. *et al.* Genetic characterization of influenza A viruses circulating in pigs and isolated in north-east Spain during the period 2006-2007. *Research in veterinary science* **96**, 380-388, doi:10.1016/j.rvsc.2013.12.006 (2014).
- 223 REED, L. J. & MUENCH, H. A SIMPLE METHOD OF ESTIMATING FIFTY PER CENT ENDPOINTS. *American Journal of Epidemiology* **27**, 493-497 (1938).
- 224 Powell, T. J., Silk, J. D., Sharps, J., Fodor, E. & Townsend, A. R. Pseudotyped influenza A virus as a vaccine for the induction of heterotypic immunity. *Journal of virology* **86**, 13397-13406, doi:10.1128/JVI.01820-12 (2012).
- 225 Biasini, M. *et al.* SWISS-MODEL: modelling protein tertiary and quaternary structure using evolutionary information. *Nucleic acids research* **42**, W252-258, doi:10.1093/nar/gku340 (2014).
- 226 Wang, Y., Geer, L. Y., Chappey, C., Kans, J. A. & Bryant, S. H. Cn3D: sequence and structure views for Entrez. *Trends in biochemical sciences* **25**, 300-302 (2000).
- 227 Ferrante, A. For many but not for all: how the conformational flexibility of the peptide/MHCII complex shapes epitope selection. *Immunologic research* **56**, 85-95, doi:10.1007/s12026-012-8342-2 (2013).
- 228 Ho, C. S., Rochelle, E. S., Martens, G. W., Schook, L. B. & Smith, D. M. Characterization of swine leukocyte antigen polymorphism by sequence-based and PCR-SSP methods in Meishan pigs. *Immunogenetics* **58**, 873-882, doi:10.1007/s00251-006-0145-y (2006).

- 229 Hansen, N. J., Pedersen, L. O., Stryhn, A. & Buus, S. High-throughput polymerase chain reaction cleanup in microtiter format. *Analytical biochemistry* **296**, 149-151, doi:10.1006/abio.2001.5190 (2001).
- 230 Schmidt, E. G. *et al.* Peptide specific expansion of CD8(+) T cells by recombinant plate bound MHC/peptide complexes. *Journal of immunological methods* **340**, 25-32, doi:10.1016/j.jim.2008.09.020 (2009).
- 231 Ferre, H. *et al.* Purification of correctly oxidized MHC class I heavy-chain molecules under denaturing conditions: a novel strategy exploiting disulfide assisted protein folding. *Protein science : a publication of the Protein Society* **12**, 551-559, doi:10.1110/ps.0233003 (2003).
- 232 Ostergaard Pedersen, L. *et al.* Efficient assembly of recombinant major histocompatibility complex class I molecules with preformed disulfide bonds. *European journal of immunology* **31**, 2986-2996, doi:10.1002/1521-4141(2001010)31:10<2986::AID-IMMU2986>3.0.CO;2-R (2001).
- 233 Brodsky, F. M., Bodmer, W. F. & Parham, P. Characterization of a monoclonal anti-beta 2-microglobulin antibody and its use in the genetic and biochemical analysis of major histocompatibility antigens. *European journal of immunology* **9**, 536-545, doi:10.1002/eji.1830090709 (1979).
- 234 Patch, J. R. *et al.* Induction of foot-and-mouth disease virus-specific cytotoxic T cell killing by vaccination. *Clinical and vaccine immunology : CVI* **18**, 280-288, doi:10.1128/CVI.00417-10 (2011).
- 235 Leisner, C. *et al.* One-pot, mix-and-read peptide-MHC tetramers. *PloS one* **3**, e1678, doi:10.1371/journal.pone.0001678 (2008).
- 236 Allepuz, A. *et al.* Descriptive epidemiology of the outbreak of classical swine fever in Catalonia (Spain), 2001/02. *The Veterinary record* **160**, 398-403 (2007).
- 237 Reuter, G. *et al.* Incidence, diversity, and molecular epidemiology of sapoviruses in swine across Europe. *Journal of clinical microbiology* **48**, 363-368, doi:10.1128/JCM.01279-09 (2010).
- 238 Allepuz, A., Saez, M., Solymosi, N., Napp, S. & Casal, J. The role of spatial factors in the success of an Aujeszky's disease eradication programme in a high pig density area (Northeast Spain, 2003-2007). *Preventive veterinary medicine* **91**, 153-160, doi:10.1016/j.prevetmed.2009.06.005 (2009).
- 239 Mortensen, S. *et al.* Risk factors for infection of sow herds with porcine reproductive and respiratory syndrome (PRRS) virus. *Preventive veterinary medicine* **53**, 83-101 (2002).
- 240 Rose, N. & Madec, F. Occurrence of respiratory disease outbreaks in fattening pigs: relation with the features of a densely and a sparsely populated pig area in France. *Veterinary research* **33**, 179-190, doi:10.1051/vetres:2002100 (2002).
- 241 Zepeda, C., Salman, M. & Ruppner, R. International trade, animal health and veterinary epidemiology: challenges and opportunities. *Preventive veterinary medicine* **48**, 261-271 (2001).
- 242 Marozin, S. *et al.* Antigenic and genetic diversity among swine influenza A H1N1 and H1N2 viruses in Europe. *The Journal of general virology* **83**, 735-745 (2002).
- 243 Martinez-Lopez, B., Perez, A. M., De la Torre, A. & Rodriguez, J. M. Quantitative risk assessment of foot-and-mouth disease introduction into Spain via importation of live animals. *Preventive veterinary medicine* **86**, 43-56, doi:10.1016/j.prevetmed.2008.03.003 (2008).
- 244 Moreno, A. *et al.* Novel swine influenza virus subtype H3N1 in Italy. *Veterinary microbiology* **138**, 361-367, doi:10.1016/j.vetmic.2009.04.007 (2009).

- 245 Zell, R., Bergmann, S., Krumbholz, A., Wutzler, P. & Durrwald, R. Ongoing evolution of swine influenza viruses: a novel reassortant. *Archives of virology* **153**, 2085-2092, doi:10.1007/s00705-008-0244-1 (2008).
- 246 Martin-Valls, G. E. *et al.* Phylogeny of Spanish swine influenza viruses isolated from respiratory disease outbreaks and evolution of swine influenza virus within an endemically infected farm. *Veterinary microbiology* **170**, 266-277, doi:10.1016/j.vetmic.2014.02.031 (2014).
- 247 Van Reeth, K., Labarque, G., De Clercq, S. & Pensaert, M. Efficacy of vaccination of pigs with different H1N1 swine influenza viruses using a recent challenge strain and different parameters of protection. *Vaccine* **19**, 4479-4486 (2001).
- 248 Van Reeth, K., Van Gucht, S. & Pensaert, M. Investigations of the efficacy of European H1N1- and H3N2-based swine influenza vaccines against the novel H1N2 subtype. *The Veterinary record* **153**, 9-13 (2003).
- 249 Simon, G. *et al.* European surveillance network for influenza in pigs: surveillance programs, diagnostic tools and Swine influenza virus subtypes identified in 14 European countries from 2010 to 2013. *PloS one* **9**, e115815, doi:10.1371/journal.pone.0115815 (2014).
- 250 Grant, E. J. *et al.* T-cell immunity to influenza A viruses. *Critical reviews in immunology* **34**, 15-39 (2014).
- 251 Zemmour, J. Inefficient assembly limits transport and cell surface expression of HLA-Cw4 molecules in C1R. *Tissue antigens* **48**, 651-661 (1996).
- 252 Haverson, K. *et al.* Summary of workshop findings for porcine adhesion molecule subgroup. *Veterinary immunology and immunopathology* **60**, 351-365 (1998).
- 253 Pescovitz, M. D., Lunney, J. K. & Sachs, D. H. Murine anti-swine T4 and T8 monoclonal antibodies: distribution and effects on proliferative and cytotoxic T cells. *J Immunol* **134**, 37-44 (1985).
- 254 van der Burg, S. H. *et al.* An HLA class I peptide-binding assay based on competition for binding to class I molecules on intact human B cells. Identification of conserved HIV-1 polymerase peptides binding to HLA-A*0301. *Human immunology* **44**, 189-198 (1995).
- 255 Anderson, K. S., Alexander, J., Wei, M. & Cresswell, P. Intracellular transport of class I MHC molecules in antigen processing mutant cell lines. *J Immunol* **151**, 3407-3419 (1993).
- 256 Liu, J. *et al.* Diverse peptide presentation of rhesus macaque major histocompatibility complex class I Mamu-A 02 revealed by two peptide complex structures and insights into immune escape of simian immunodeficiency virus. *Journal of virology* **85**, 7372-7383, doi:10.1128/JVI.00350-11 (2011).
- 257 Achour, A. *et al.* Structural basis of the differential stability and receptor specificity of H-2Db in complex with murine versus human beta2-microglobulin. *J Mol Biol* **356**, 382-396, doi:10.1016/j.jmb.2005.11.068 (2006).
- 258 Armengol, E. *et al.* Identification of T-cell epitopes in the structural and non-structural proteins of classical swine fever virus. *The Journal of general virology* **83**, 551-560 (2002).
- 259 Blanco, E. *et al.* Identification of T-cell epitopes in nonstructural proteins of foot-and-mouth disease virus. *Journal of virology* **75**, 3164-3174, doi:10.1128/JVI.75.7.3164-3174.2001 (2001).
- 260 Signer, E. N. *et al.* DNA profiling reveals remarkably low genetic variability in a herd of SLA homozygous pigs. *Research in veterinary science* **67**, 207-211, doi:10.1053/rvsc.1999.0310 (1999).
- 261 Bilrha, H. *et al.* Effects of gestational and lactational exposure to organochlorine compounds on cellular, humoral, and innate immunity in swine. *Toxicological sciences*

- : an official journal of the Society of Toxicology **77**, 41-50, doi:10.1093/toxsci/kfg240 (2004).
- 262 Lunney, J. K. & Pescovitz, M. D. Phenotypic and functional characterization of pig lymphocyte populations. *Veterinary immunology and immunopathology* **17**, 135-144 (1987).
- 263 Holland, C. J., Cole, D. K. & Godkin, A. Re-Directing CD4(+) T Cell Responses with the Flanking Residues of MHC Class II-Bound Peptides: The Core is Not Enough. *Frontiers in immunology* **4**, 172, doi:10.3389/fimmu.2013.00172 (2013).
- 264 Busquets, N. *et al.* Experimental infection with H1N1 European swine influenza virus protects pigs from an infection with the 2009 pandemic H1N1 human influenza virus. *Veterinary research* **41**, 74, doi:10.1051/vetres/2010046 (2010).
- 265 Yewdell, J. W. Confronting complexity: real-world immunodominance in antiviral CD8+ T cell responses. *Immunity* **25**, 533-543, doi:10.1016/j.immuni.2006.09.005 (2006).
- 266 Li Pira, G., Ivaldi, F., Moretti, P. & Manca, F. High throughput T epitope mapping and vaccine development. *Journal of biomedicine & biotechnology* **2010**, 325720, doi:10.1155/2010/325720 (2010).
- 267 Fahl, S. P., Coffey, F. & Wiest, D. L. Origins of gammadelta T cell effector subsets: a riddle wrapped in an enigma. *J Immunol* **193**, 4289-4294, doi:10.4049/jimmunol.1401813 (2014).
- 268 Telfer, J. C. & Baldwin, C. L. Bovine gamma delta T cells and the function of gamma delta T cell specific WC1 co-receptors. *Cellular immunology*, doi:10.1016/j.cellimm.2015.05.003 (2015).
- 269 Chu, T. *et al.* Bystander-activated memory CD8 T cells control early pathogen load in an innate-like, NKG2D-dependent manner. *Cell reports* **3**, 701-708, doi:10.1016/j.celrep.2013.02.020 (2013).
- 270 Chan, W. H. *et al.* Functional analysis of the influenza virus H5N1 nucleoprotein tail loop reveals amino acids that are crucial for oligomerization and ribonucleoprotein activities. *Journal of virology* **84**, 7337-7345, doi:10.1128/JVI.02474-09 (2010).
- 271 Kukul, A. & Hughes, D. J. Large-scale analysis of influenza A virus nucleoprotein sequence conservation reveals potential drug-target sites. *Virology* **454-455**, 40-47, doi:10.1016/j.virol.2014.01.023 (2014).
- 272 Chen, L. *et al.* Immunodominant CD4+ T-cell responses to influenza A virus in healthy individuals focus on matrix 1 and nucleoprotein. *Journal of virology* **88**, 11760-11773, doi:10.1128/JVI.01631-14 (2014).
- 273 Valkenburg, S. A. *et al.* Acute emergence and reversion of influenza A virus quasispecies within CD8+ T cell antigenic peptides. *Nature communications* **4**, 2663, doi:10.1038/ncomms3663 (2013).

Supplementary Files

Chapter I

Segment	Position	Sequence (5'-3')	Direction
PB2	861	TGAAAAACGACGGCCAGTCATCACTATTGGAGATGTGT	Forward
	1828	CAGGAAACAGCTATGACCGAATAGTGTCTCACAAACC	Reverse
	1919	TGAAAAACGACGGCCAGTATGCAATTCTTTCTCTAAC	Forward
PB1	1855	TGAAAAACGACGGCCAGTCTTAAAATGGGAGCTAATG	Forward
PA	665	TGAAAAACGACGGCCAGTCTTGCCAACCAAAGTCTC	Forward
	1509	CAGGAAACAGCTATGACCTTCCTTCTTTCTGTTCTG	Reverse
H1 HA	338	TGAAAAACGACGGCCAGTAGAGACTTCAAATTCAAAAA	Forward
	490	CAGGAAACAGCTATGACCCCTTTGGTAGTATTTTGATG	Reverse
	830	TGAAAAACGACGGCCAGTCACGGGGAATTTAATAGCAC	Forward
	1259	TGAAAAACGACGGCCAGTCATTCAATTTACTTCAGTGG	Forward
H3 HA	305	CAGGAAACAGCTATGACCTGAGGGTCCCCCAAT	Reverse
	552	TGAAAAACGACGGCCAGTGGGTAACACATATCCGATGC	Forward
	940	TGAAAAACGACGGCCAGTAGCATACCCAATGACAAACC	Forward
	1116	CAGGAAACAGCTATGACCTCCTTCCAACCATTCTCTA	Reverse
	1632	TGAAAAACGACGGCCAGTGATTTCTTTGCCATATC	Forward
NP	1270	TGAAAAACGACGGCCAGTACAACCTACTTTCTCAGTACA	Forward
N2 NA	391	CAGGAAACAGCTATGACCCATGACACATAAGGTTCTCT	Reverse
	757	CAGGAAACAGCTATGACCGCACTTCCATCAGTCA	Forward
	1032	TGAAAAACGACGGCCAGTCGAAATCCTAACAATGAG	Forward
M	647	TGAAAAACGACGGCCAGTGTCAGACTAGGCAGATGG	Forward
NS	481	CAGGAAACAGCTATGACCCGTGAAAGCTCTAAGGAGT	Reverse
	578	TGAAAAACGACGGCCAGTGGACTTGAATGGAATGATAA	Forward

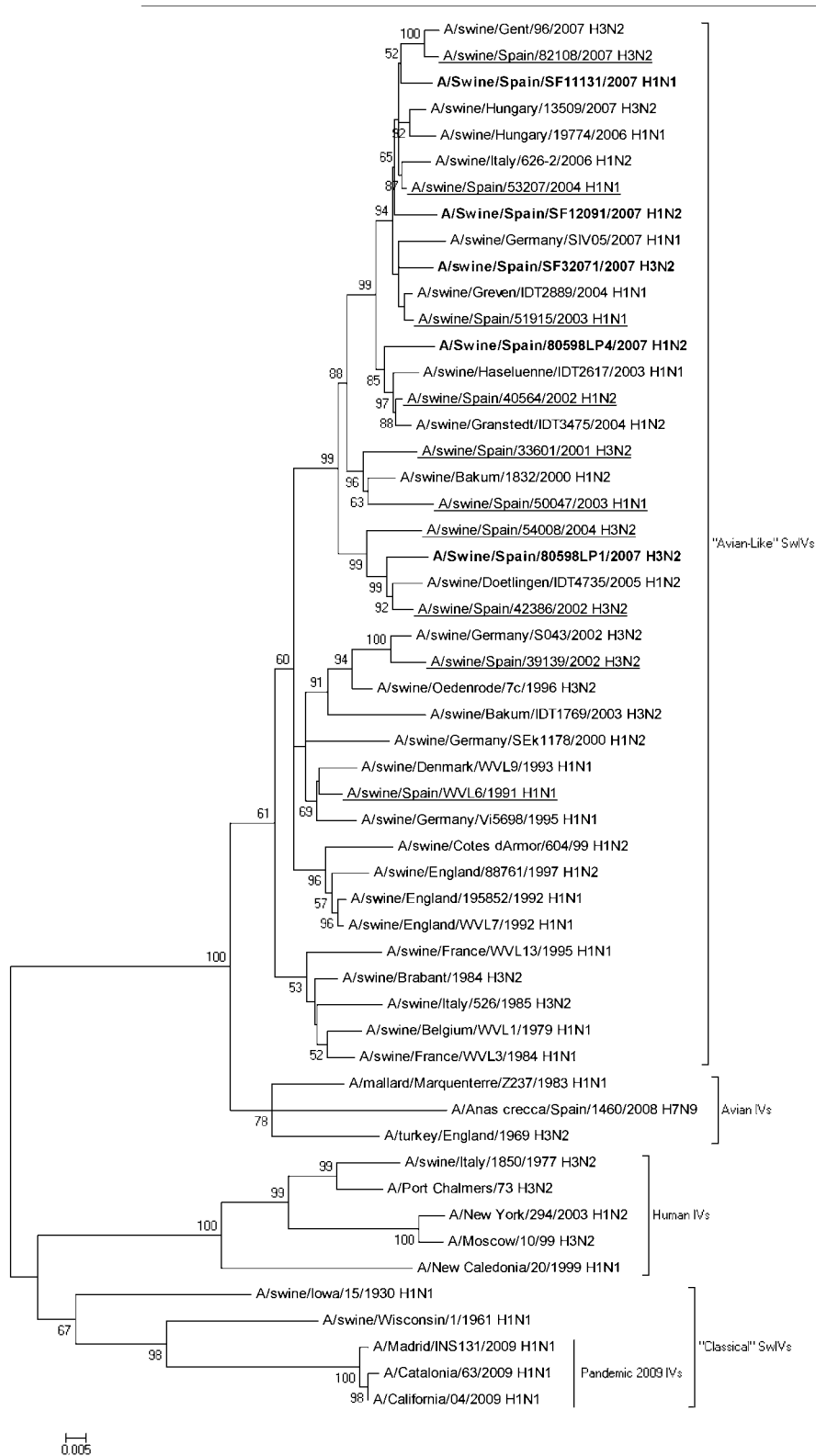
Table 1. Primers designed for amplification of SwIVs under the following conditions: 60 minutes at 42°C for reverse transcription, 2 minutes at 94°C for initial denaturation, 40 cycles of 94°C for 20 seconds, annealing at 50°C for 30 seconds, and extension at 72°C for 1 minute followed by a last step of extension at 72°C for 7 minutes.

Vaccine	Strains	HA Accession
Respiporc flu3	Sw/Haselunne/IDT2617/03 (H ₁ N ₁)	ACR39185.1
	Sw/Bakum/IDT1769/03 (H ₃ N ₂)	ACR39187.1
	Sw/Bakum/1832/00 (H ₁ N ₂)	ABS53372.1

Table 2: Strains in Respiporc flu3 vaccine.

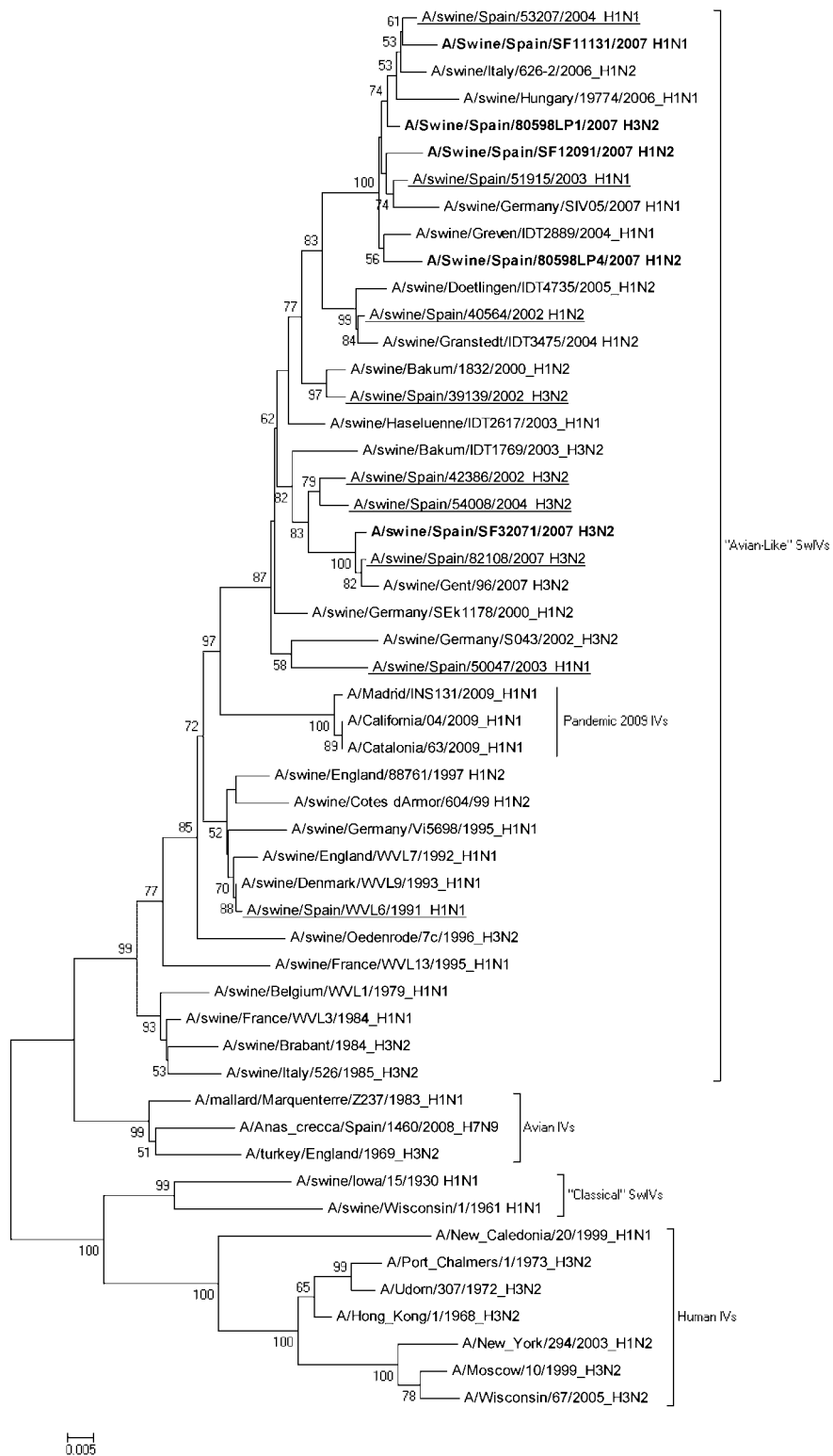
a)

NP



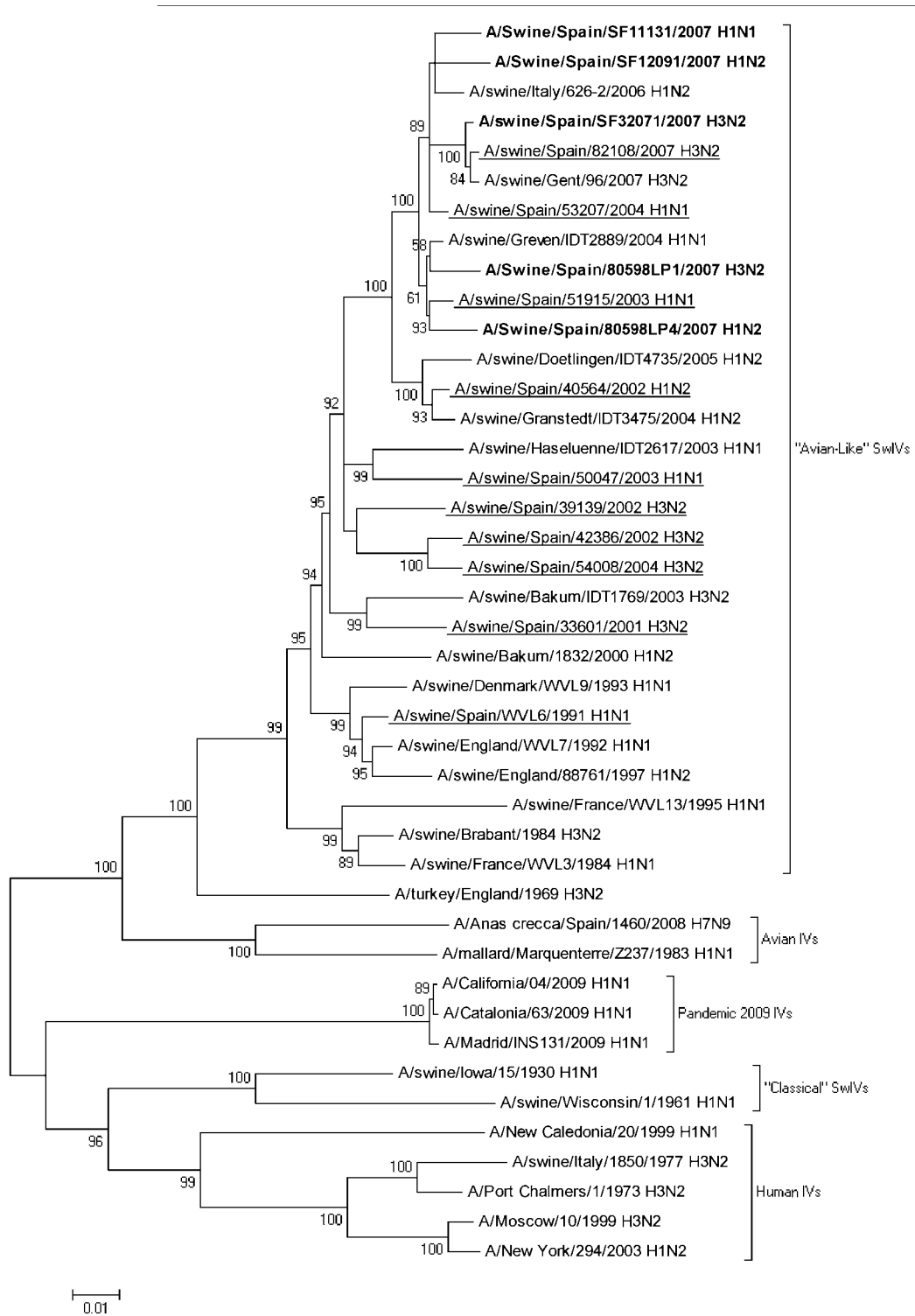
b)

M



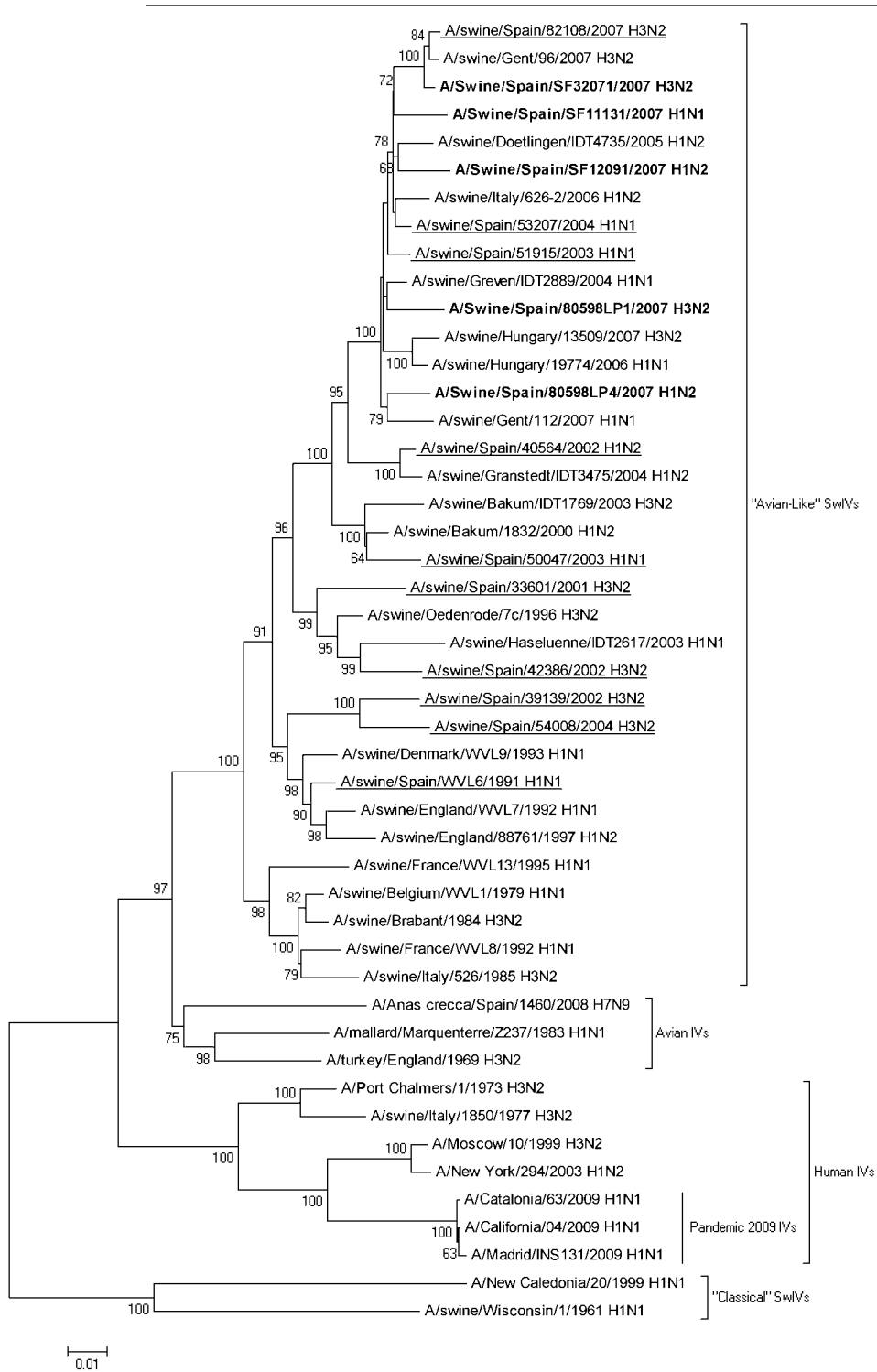
c)

PB2



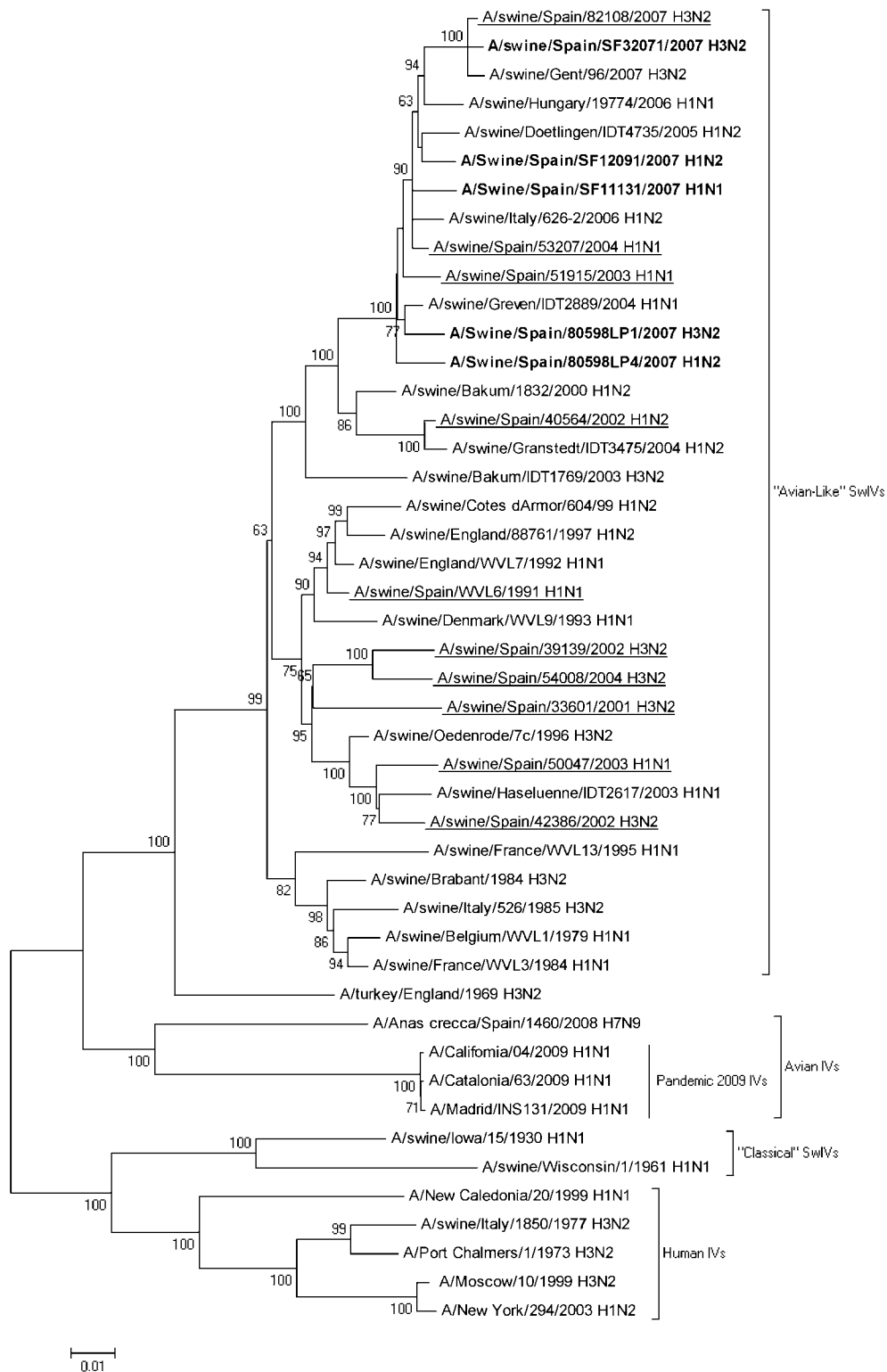
d)

PB1



e)

PA



f)

NS

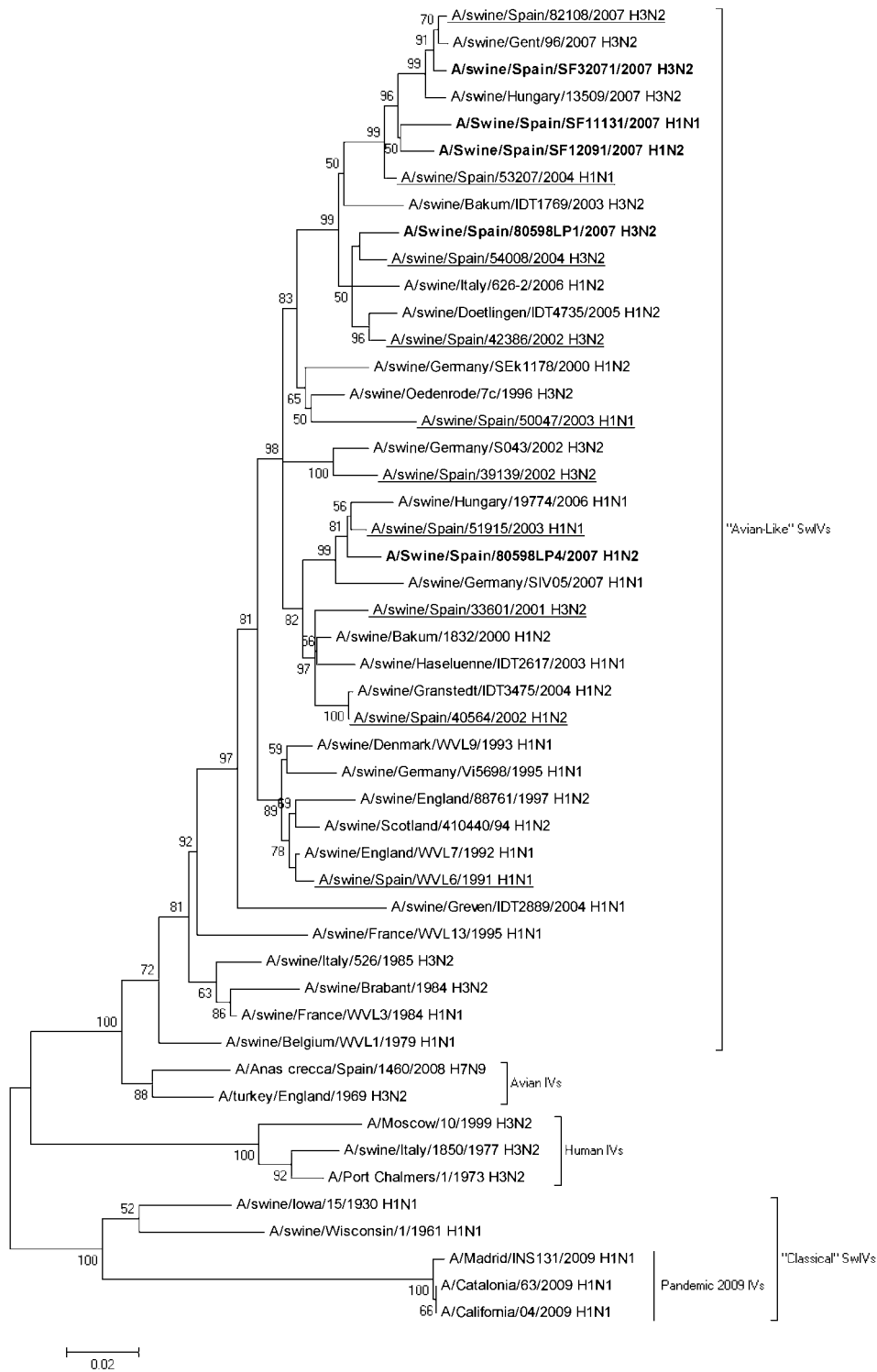


Figure 1. Evolutionary relationships of internal genes of IAV. The tree is drawn to scale, with branch lengths in the same units as those of the evolutionary distances used to infer the phylogenetic tree. Bootstrap values greater than 50% are shown (1000 replicates): a) NP phylogenetic tree. The analysis involved 53 nucleotide sequences. There were a total of 1462 positions in the final dataset; b) M phylogenetic tree. The analysis involved 52 nucleotide sequences. There were a total of 965 positions in the final dataset; c) PB2 phylogenetic tree. The analysis involved 42 nucleotide sequences. There were a total of 2275 positions in the final dataset. d) PB1 phylogenetic tree. The analysis involved 47 nucleotide sequences. There were a total of 2268 positions in the final dataset; e) PA phylogenetic tree. The analysis involved 46 nucleotide sequences. There were a total of 2148 positions in the final dataset; f) NS phylogenetic tree. The analysis involved 49 nucleotide sequences. There were a total of 830 positions in the final dataset.

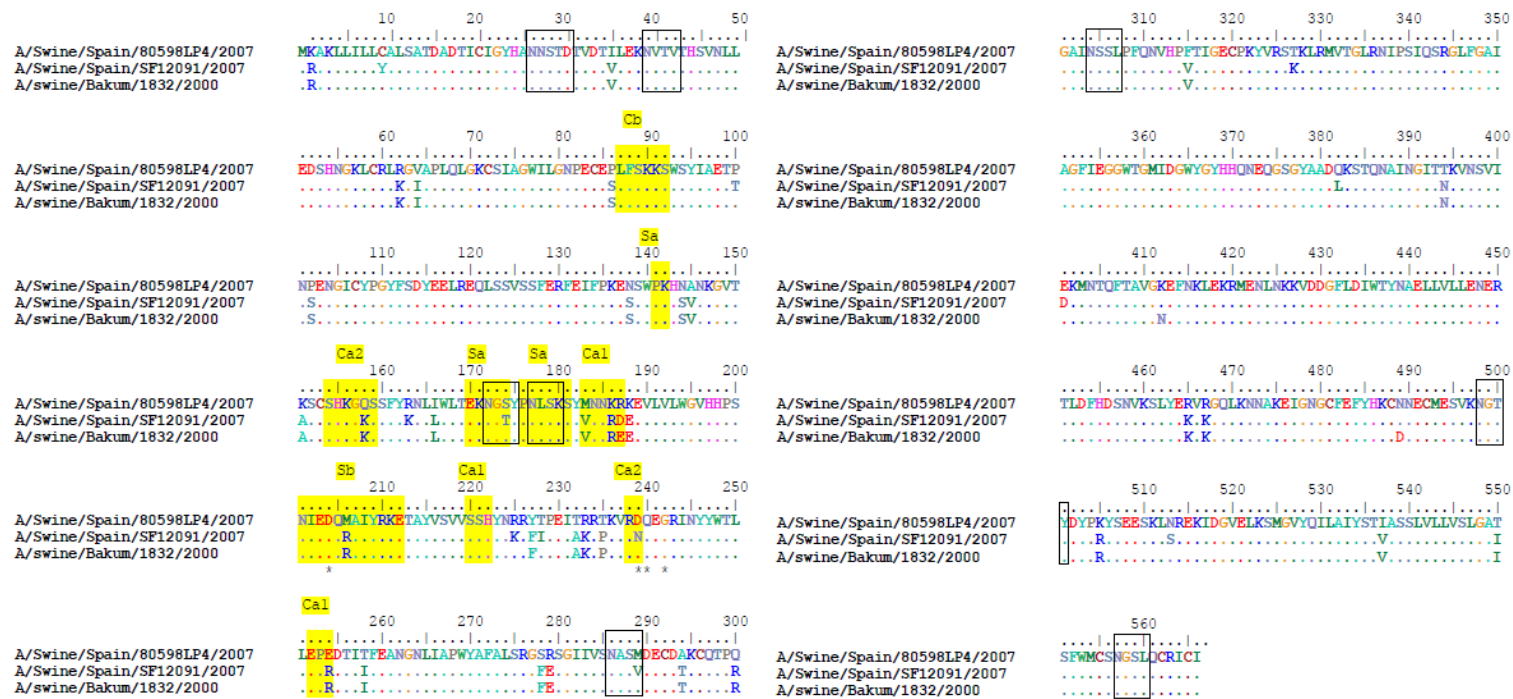


Figure 2. Alignment of the H1HA protein of the H_1N_2 isolates SF12091 and 80598lp4 and the H_1N_2 strain composing the vaccine Resporc flu3. The signal peptide is located at the firsts 16 aminoacid. The post traductional cleavage of the HA0 protein at the site 344 gives rise to the two subunit composing the HA protein: the HA1 (from position 18 to 343) and the HA2 (from position 345 to 566). The globular head of HA protein is located from position 59 to 292 in the HA1 subunit, on the contrary the stalk is located at the flanking regions. The transmembrane region is located from position 529 to 554 at the HA2 subunit. The antigenic sites Cb, Sb, Ca and Sa were identified on the alignment and highlighted in yellow. Relevant signatures in Receptor Binding site were highlighted with asterisks. Glycosylation site were identified at positions 27, 28, 40, 172, 177, 286, 304, 498, 557 (empty squares).

Chapter II

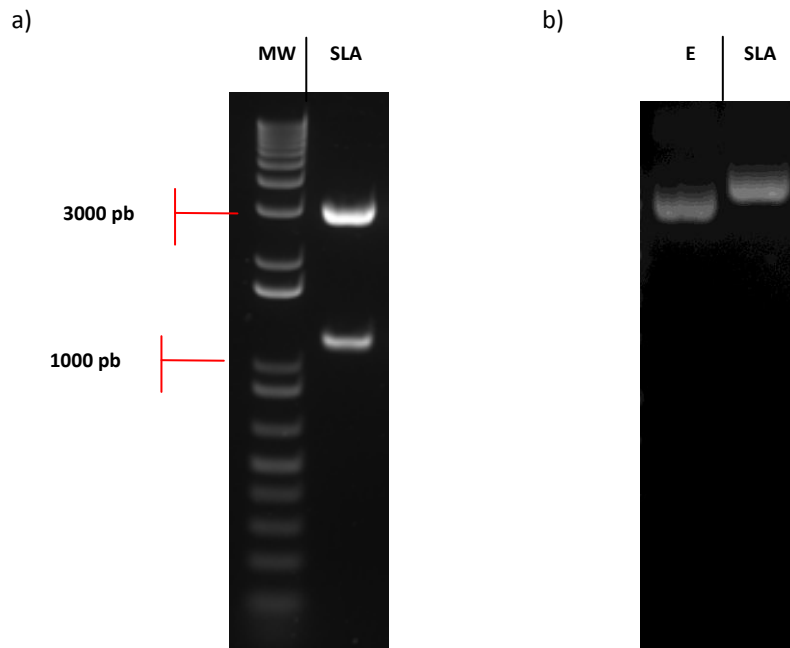


Figure 3. Cloning of SLA-2*es22. a) SLA-2*es22 (low band) was excised by digestion with *NotI* enzyme, leaving an empty pGMET easy vector (high band). b) The excised insert was then ligated into pCDNA3.1⁺ vector; E is the empty vector while SLA represents the ligated vector. MW molecular weight ladder.

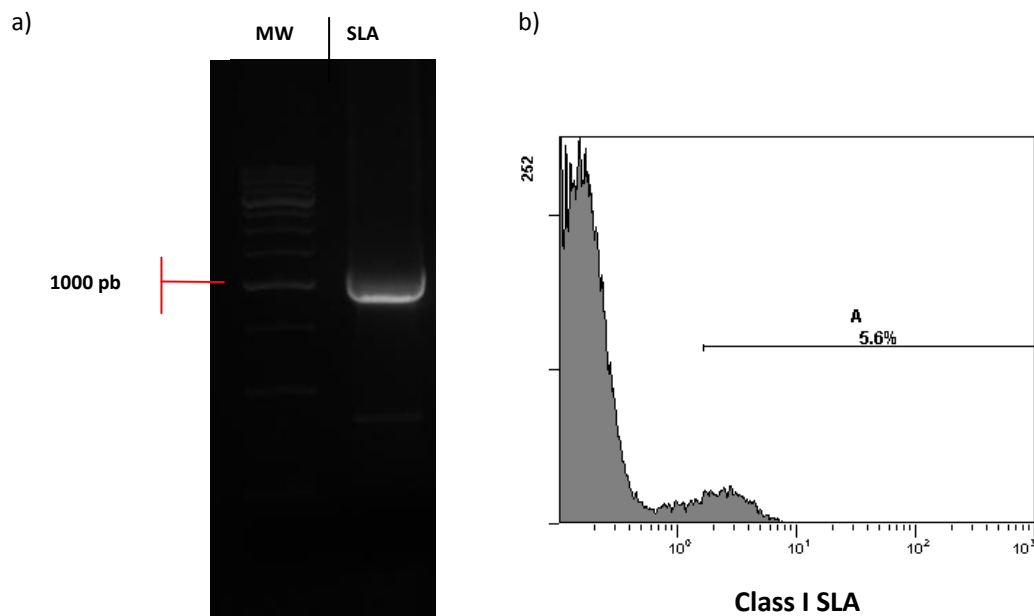


Figure 4. Generation of C1R SLA-1*0401 cells. a) RT-PCR with SLA primers of the RNA of PK15 cells; SLA-1*0401 gene was amplified. C1R cells transfected with pCDNA3.1⁺-SLA-1*0401 plasmid were stained with 2G1/VAN antibody and analysed by Flow cytometry. b) Selection by limiting dilution of the C1R cells transfected with pCDNA3.1⁺-SLA-1*0401 plasmid; SLA⁺ population of C1R (right side) was represent the 5.6% of cells; SLA⁻ cells (left side) were also highly present. MW molecular weight ladder.

Chapter III

Name	Sequence	Name	Sequence	Name	Sequence
1-PB1	YMFESKSMKL	4-HA	SSFERFEIF	6-M1	LASCMGLI
3-PB1	MMMGMFMNM	5-HA	STVASSLVLL	7-M1	RQMVHAMRTI
4-PB1	MMMGMFMNML	6-HA	TANSWSYI	1-NP	FLARSALI
5-PB1	YMFESKSM	7-HA	TANSWSYII	2-NP	FLARSALIL
6-PB1	FSMELPSFGV	8-HA	VASSLVLLV	3-NP	FSVQRNLPF
7-PB1	FSMELPSF	9-HA	VTHSVNLL	4-NP	IAYERMCNIL
8-PB1	FLAMITYI	10-HA	WTYNAELL	5-NP	ITIERMVL
9-PB1	FLKDVIESM	11-HA	YQNNHTYV	6-NP	LMIWHSNL
10-PB1	MGMFMNMLSTV	12-HA	YQRFTPEI	7-NP	NSQVFSLI
11-PB1	FVANFSMEL	13-HA	YSTVASSLVL	8-NP	ETMDSITLEL
12-PB1	YLIRALTL	14-HA	IAPWHAFAL	9-NP	ETMDSITL
13-PB1	MQIRGFVYFV	15-HA	LTANSWSYI	10-NP	MSNEGSYFF
14-PB1	TAQMALQLFI	1-M1	MATTTNPLI	11-NP	IAYERMCNI
15-PB1	LLIDGTASL	2-M1	MVHAMRTI	12-NP	ATAGLTHLMI
1-HA	IMMSDVHV	3-M1	QMATTTNPLI	13-NP	LQNSQVFSLI
2-HA	RMNYYWTL	4-M1	MATTTNPL	Ctrl peptide	SPEMMVTISKT
3-HA	SSFERFEI	5-M1	QMATTTNPL		

Table 3. Predicted peptides.

Name	Sequence	Name	Sequence
43a	NQQRASAGQIS <u>SVQPTFSVQR</u>	44b	<u>SVQPTFSVQR</u> NL
43b	RASAGQIS <u>SVQPTFSVQR</u>	44c	<u>SVQPTFSVQR</u> NLFP
43c	AGQIS <u>SVQPTFSVQR</u>	44d	<u>SVQPTFSVQR</u> NLPFEKS
43d	QIS <u>SVQPTFSVQR</u>	44e	<u>SVQPTFSVQR</u> NLPFEKSTVM
43e	<u>SVQPTFSVQR</u>	Sp44	<u>SVQPTFSVQR</u> NLPFERATIM
43f	<u>VQPTFSVQR</u>	Irrelevant	NIKNESKYSNTFINNAYNMS
44a	<u>SVQPTFSVQ</u>		

Table 4. Peptides of different lengths designed on peptides 43 and 44. Underlined regions are overlapping between peptide 43 and 44. Bolded letter in Sp44 are mutated positions between peptide 44 and the corresponding sequence in SpH₁N₁.

Name	Sequence	Name	Sequence	Name	Sequence
<u>Pool 1</u>		28	LARSALILRGSVAHKSCPLA	54	GGGMSLLTEVETYVLSIV
1	MASQGTKRSYEQMETDGDR	29	SVAHKSCLPACVYGPAVSSG	55	EVETYVLSIVPSGPLKAEIA
2	YEQMETDGDRQNATEIRASV	30	CVYGPAVSSGYDFEKEGYSL	56	PSGPLKAEIAQRLEDVFAGK
3	RQNATEIRASVGKMIDGIGR	31	YDFEKEGYSLVGIDPFKLL	57	AQRLEDVFAGKNTDLEALM
4	VGKMIDGIGRFYIQMCTELK	32	LVGIDPFKLLQNSQVYSLIR	58	GKNTDLEALMEWLKTRPIL
5	FYIQMCTELKLSDYEGRLI	<u>Pool B</u>		59	MEWLKTRPILSPLTKGILGF
6	KLSDYEGRLIQNSLTIEKMV	33	LQNSQVYSLIRPNENPAHK	60	SPLTKGILGFVFTLTPSER
7	IQNSLTIEKMLVSAFDERR	34	IRPNENPAHKSQLVWMACH	61	VFTLTPSERGLQRRRFV
8	MVLSAFDERRNRYLEEHPA	35	KSQLVWMACHSAAFEDLRL	62	ERGLQRRRFVQNALNGNG
9	NRYLEEHPAAGKDPKKTGG	36	SAAFEDLRLLSFIRGTKV	63	FVQNALNGNGDPNNMDKAVK
10	AGKDPKKTGGPIYRRVDGKW	37	LLSFIRGTKVSPRGKLGSTRG	64	DPNNMDKAVKLYRKLKREI
11	PIYRRVDGKWMRELVLVDK	38	SPRGKLGSTRGVQIASNENM	65	KLYRKLKREITFHGAKEIAL
12	WMRELVLVDKEEIRRIWRQA	<u>Pool C</u>		66	TFHGAKEIALSYSAGALA
13	EEIRRIWRQANNGEDATAGL	39	GVQIASNENMDNMGSTLEL	67	ALSYSAGALASCMGLIYNRM
14	NNGEDATAGLTHMMIWHNSL	40	DNMGSTLELRSGYWAIATR	68	SCMGLIYNRMGAVTTEVAFG
15	THMMIWHNSLNDTTYQRTRA	41	RSGYWAIATRSGGNTNQORA	69	GAVTTEVAFGLVCATCEQIA
16	NDTTYQRTRALVRTGMDPRM	42	SGGNTNQORASAGQISV	70	LVCATCEQIADSQHRSHRQM
17	LVRTGMDPRMCSLMQGSTL	43	NQORASAGQISVQPTFSVQR	71	DSQHRSHRQMVATTNPLIKH
18	MCSLMQGSTLPRRSGAAGAA	44	SVQPTFSVQRNLPFEKSTVM	72	VATTNPLIKHENRMVLA
19	PRRSGAAGAAVKGIGTMVM	45	NLPFEKSTVMAAFTGNTEGR	73	IKHENRMVLA STTAKAMEQM
20	AVKGIGTMVMELIRMVVRGI	46	AAFTGNTEGRTSDMRAEIR	74	STTAKAMEQMAGSSEQAAEA
21	ELIRMVVRGINDRNFWRG	<u>Pool D</u>		75	AGSSEQAAEAMEIASQARQM
22	GINDRNFWRGENGRKTRSAY	47	TSDMRAEIRMMEGAKPEEV	76	MEIASQARQMVQAMRTVGTH
23	ENGRKTRSAYERMCNILKGG	48	MMEGAKPEEVSRFRGRGVFEL	77	VQAMRTVGTHPSSTGLR
24	ERM CNILKGGFQTAAQRAMV	49	SFRGRGVFELSDEKATNPV	78	THPSSTGLRDDLLENLQTY
25	FQTAAQRAMVDQVRESRNP	50	SDEKATNPVPSFEMSNEG	79	DDLLENLQTYQKRMGVQMQR
26	DQVRESRNPNAEIEDLIFL	51	VPSFEMSNEGSYFFGDNA	80	QKRMGVQMQRFK
<u>Pool 2 - Pool A</u>		52	EGSYFFGDNAEEYDNGGGPG		
27	NAEIEDLIFLARSALILRG	53	EEYDNGGGPGGGMSLLTEV		

Table 5: Pools of peptides

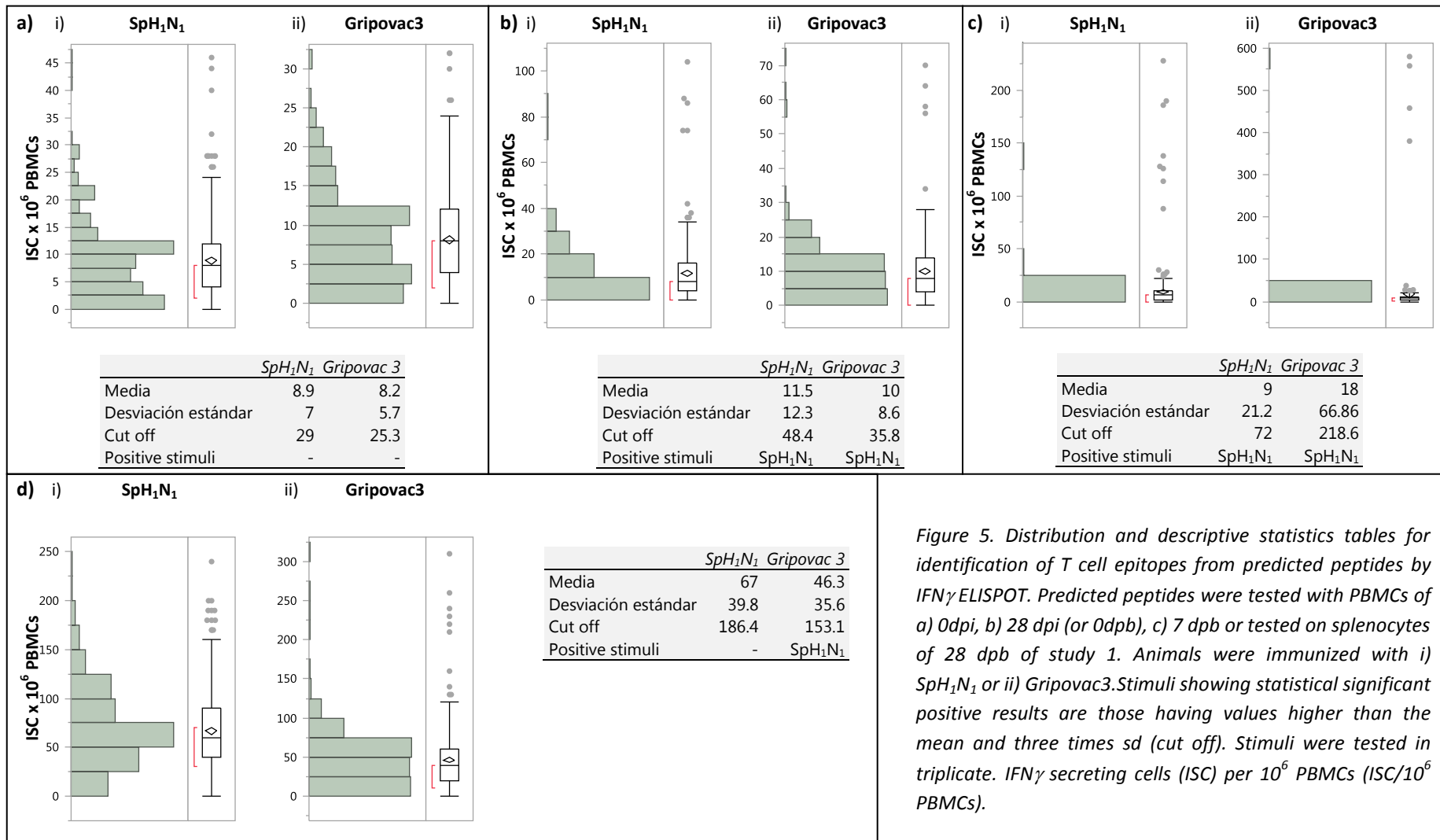


Figure 5. Distribution and descriptive statistics tables for identification of T cell epitopes from predicted peptides by IFN γ ELISPOT. Predicted peptides were tested with PBMCs of a) 0dpi, b) 28 dpi (or 0dpb), c) 7 dpb or tested on splenocytes of 28 dpb of study 1. Animals were immunized with i) SpH₁N₁ or ii) Gripovac3. Stimuli showing statistical significant positive results are those having values higher than the mean and three times sd (cut off). Stimuli were tested in triplicate. IFN γ secreting cells (ISC) per 10⁶ PBMCs (ISC/10⁶ PBMCs).

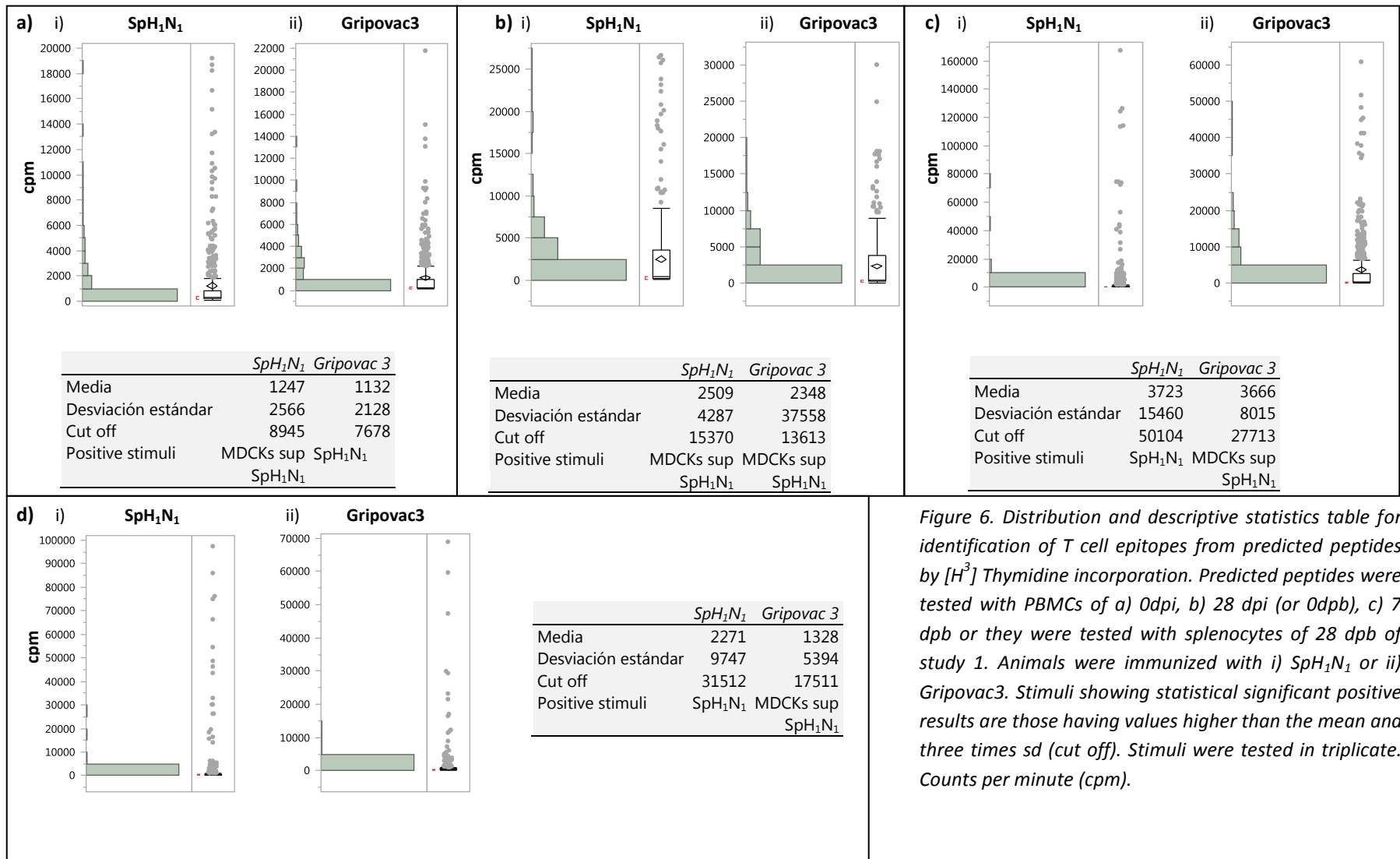


Figure 6. Distribution and descriptive statistics table for identification of T cell epitopes from predicted peptides by [³H] Thymidine incorporation. Predicted peptides were tested with PBMCs of a) 0dpi, b) 28 dpi (or 0dpb), c) 7 dpb or they were tested with splenocytes of 28 dpb of study 1. Animals were immunized with i) SpH₁N₁ or ii) Gripovac3. Stimuli showing statistical significant positive results are those having values higher than the mean and three times sd (cut off). Stimuli were tested in triplicate. Counts per minute (cpm).

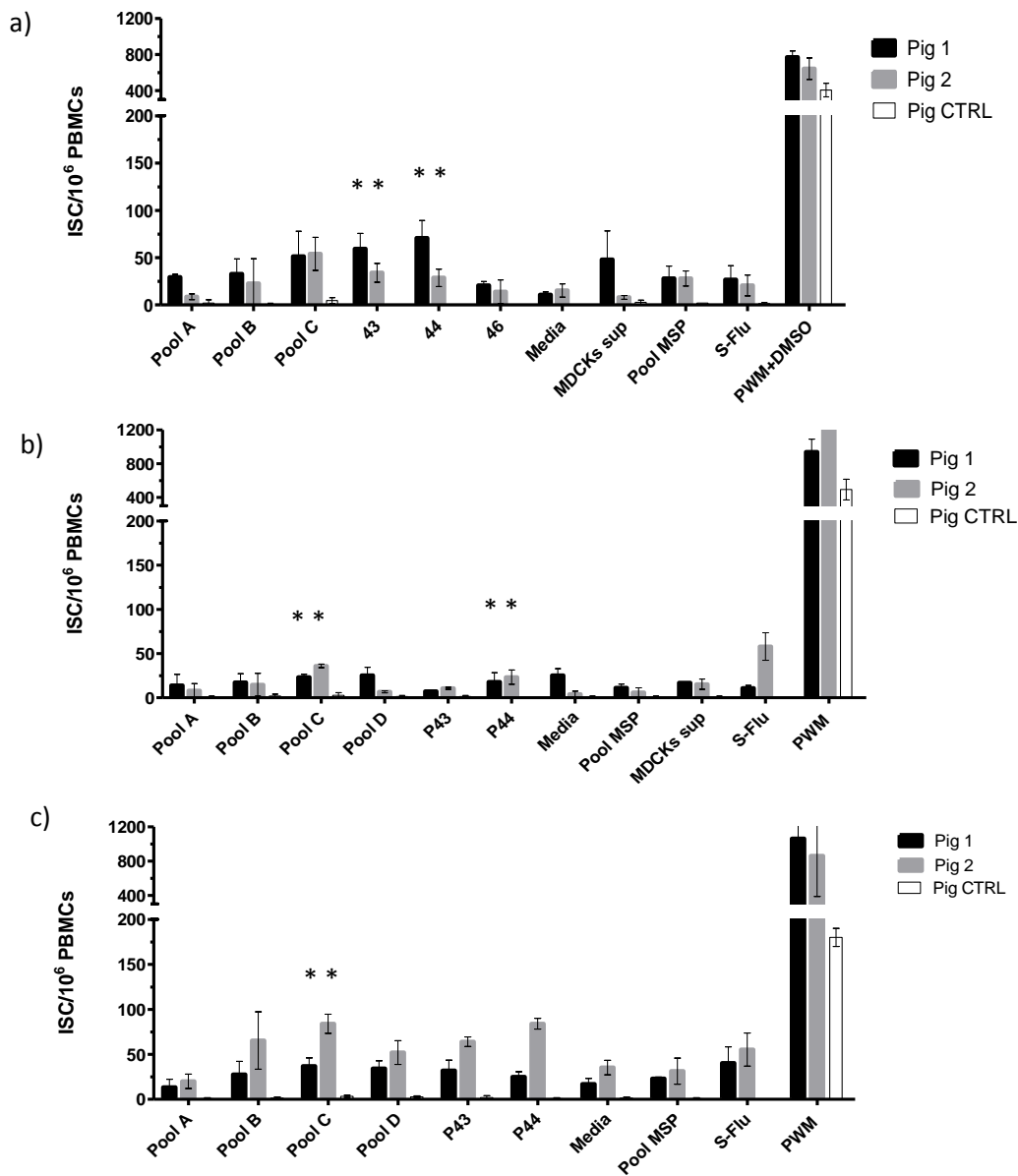


Figure 7. Empirical identification of T cells epitopes in Pool 2. Pool 1-3 and control (MSP), pools A-D and peptides of pool C (39-46) were tested by IFN γ ELISPOT with PBMCs of study 2 at a) 14 dpb, b) 21 dpb and c) 28 dpb. Pools A-D and individual peptides were not tested on CTRL pig. DMSO was added to PWM at the same concentration as in peptide solutions. MDCK sup is the mock-infected control. Results were expressed as IFN γ -producing cells number per 10⁶ stimulated PBMC (ISC/10⁶ PBMCs). Data for each animal was represented in graphs as mean with sd of triplicate results. Non-parametric statistical analysis identified stimuli with statistically significant differences when compared to media+DMSO and pool MSP. Those having a $p < 0.05$ are marked with asterisks (*).

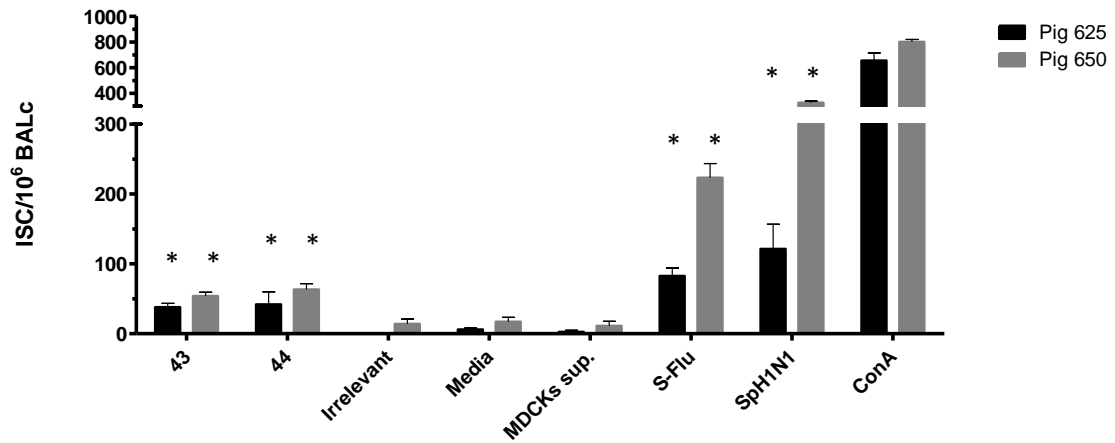


Figure 8. IFN γ ELISPOT at 28 dpi from study 3. Peptide 43-44 and irrelevant peptide were tested on BALc. Results were expressed as IFN γ -producing cell number per 10⁶ stimulated BALc (ISC/10⁶ BALc). Data for each animal was represented in graphs as mean with sd of triplicate results. Non-parametric statistical analysis identified stimuli with statistically significant differences when compared to media+DMSO and pool MSP. Those having a p<0.05 are marked with asterisks (*).

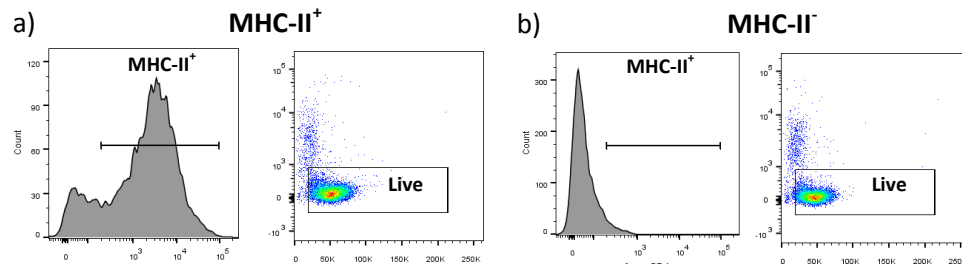


Figure 9. Purity and viability of MHC-II^{+/−} separated fractions of PBMCs. Those are two examples of a) MHC-II⁺ and b) MHC-II[−] populations. In each of those MHC-II⁺ are gated on the image on the left; live cells are gated on the image on the right. Plots showed are samples from Pig 625.

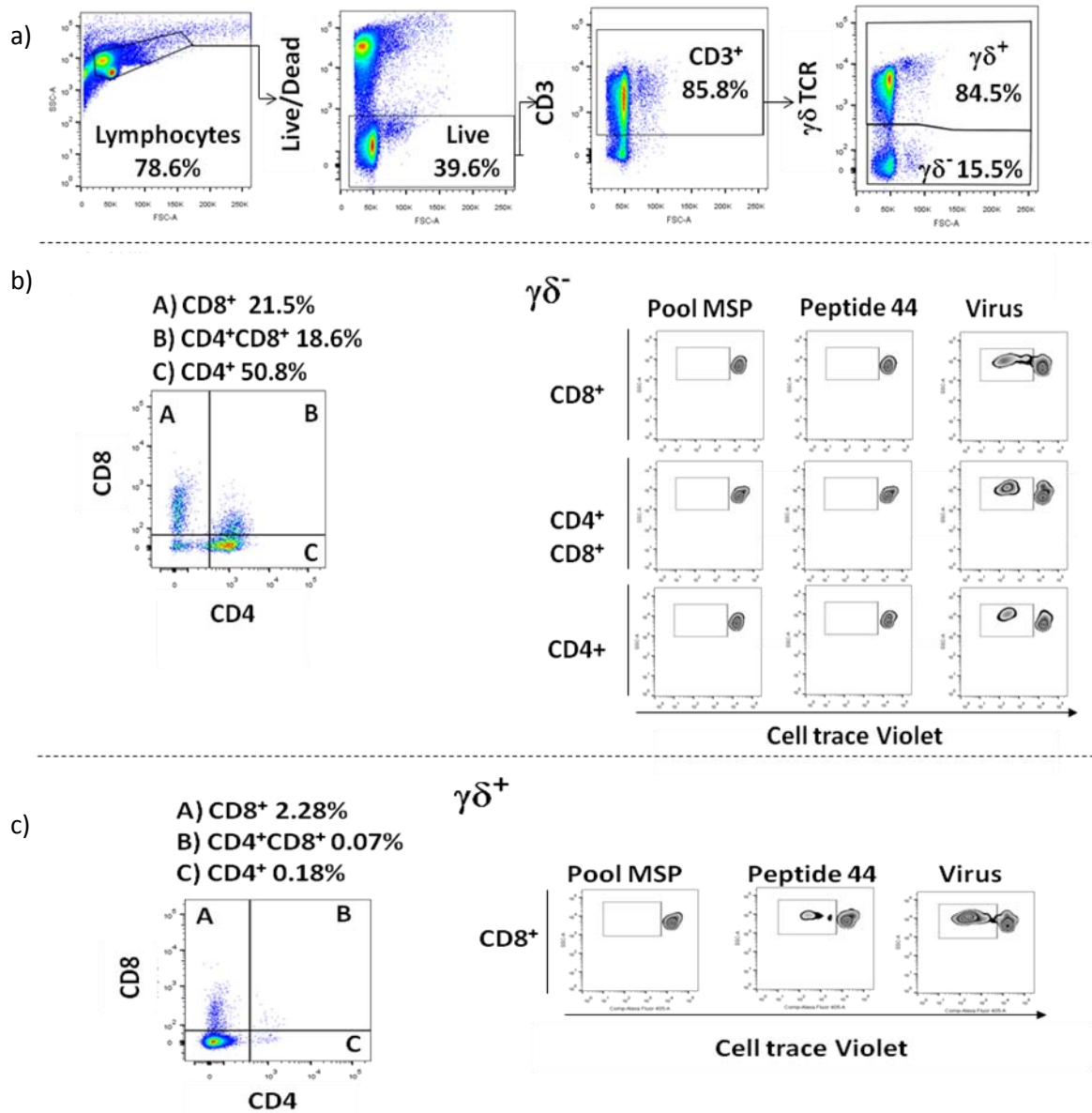


Figure 10. Gating strategy of flow cytometry from Celltrace violet proliferation assay on PBMCs from pig 1 at 28 dpb (Study 2). a) Live Lymphocytes in T cells ($CD3^+$) were identified; b) $\gamma\delta^-$ negative and c) positive populations of T cells were then discriminated and further divided into different subpopulation using CD4 and CD8 markers. Single positive CD4 or CD8 and double positive ($CD4^+CD8^+$) cells in $\gamma\delta^+$ or $\gamma\delta^-$ T cells were identified and further analysed to quantify cells showing low Celltrace violet staining. Plots on the right in b and c show some examples of low Celltrace violet stained cells gating for irrelevant and 44 peptides and SpH₁N₁ virus (frequencies are showed in figure 41).

Chapter IV

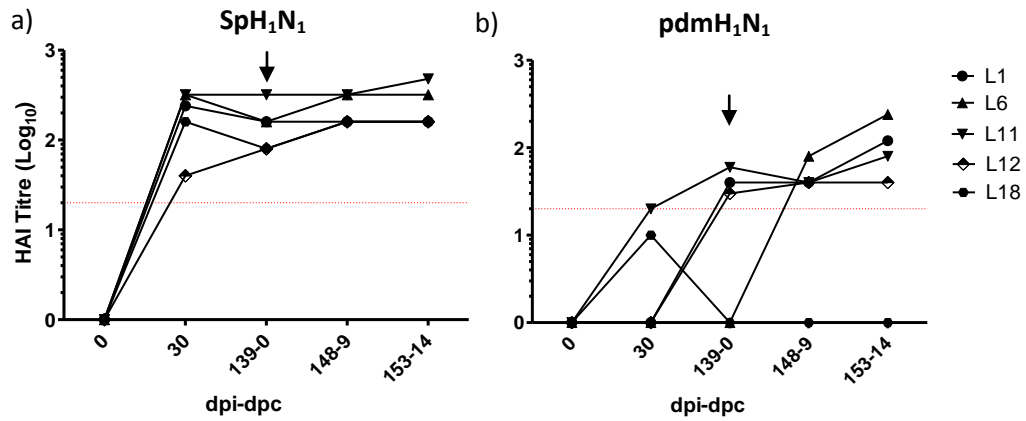


Figure 11. IHA of sera from infected pigs. Pigs were infected with SpH₁N₁ and challenged with pdmH₁N₁ (arrows). Viruses tested were: a) SpH₁N₁ and b) pdmH₁N₁. Results are the average of duplicate. Red dotted line is the limit of detection.

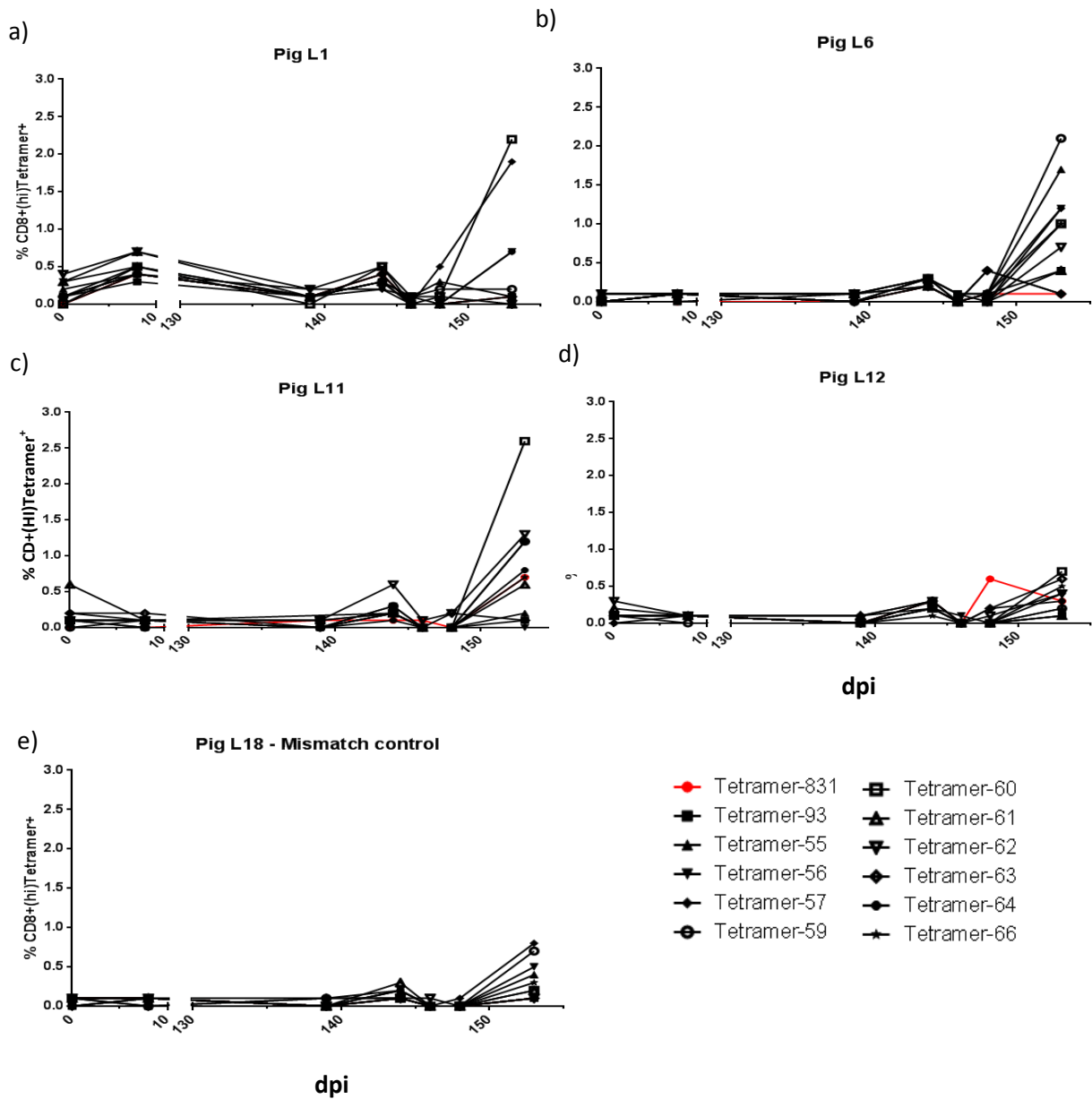


Figure 12. Dynamics of tetramer specific CTL responses in PBMCs of SwIV infected pigs. All time points were taken into account. Tetramer 381 contained the irrelevant peptide. a) pig L1, b) pig L6, c) pig L11, d) pig L12 and e) pig L18 (or mismatched control).

Publications
